Small-Scale Quasi-Static Tests on Non-Slender Piles Situated in Sand

Sørensen, Søren Peder Hyldal; Ibsen, Lars Bo

Publication date:
2011

Document Version
Publisher's PDF, also known as Version of record

Small-scale quasi-static tests on non-slender piles situated in sand – Test results

Søren Peder Hyldal Sørensen
Lars Bo Ibsen

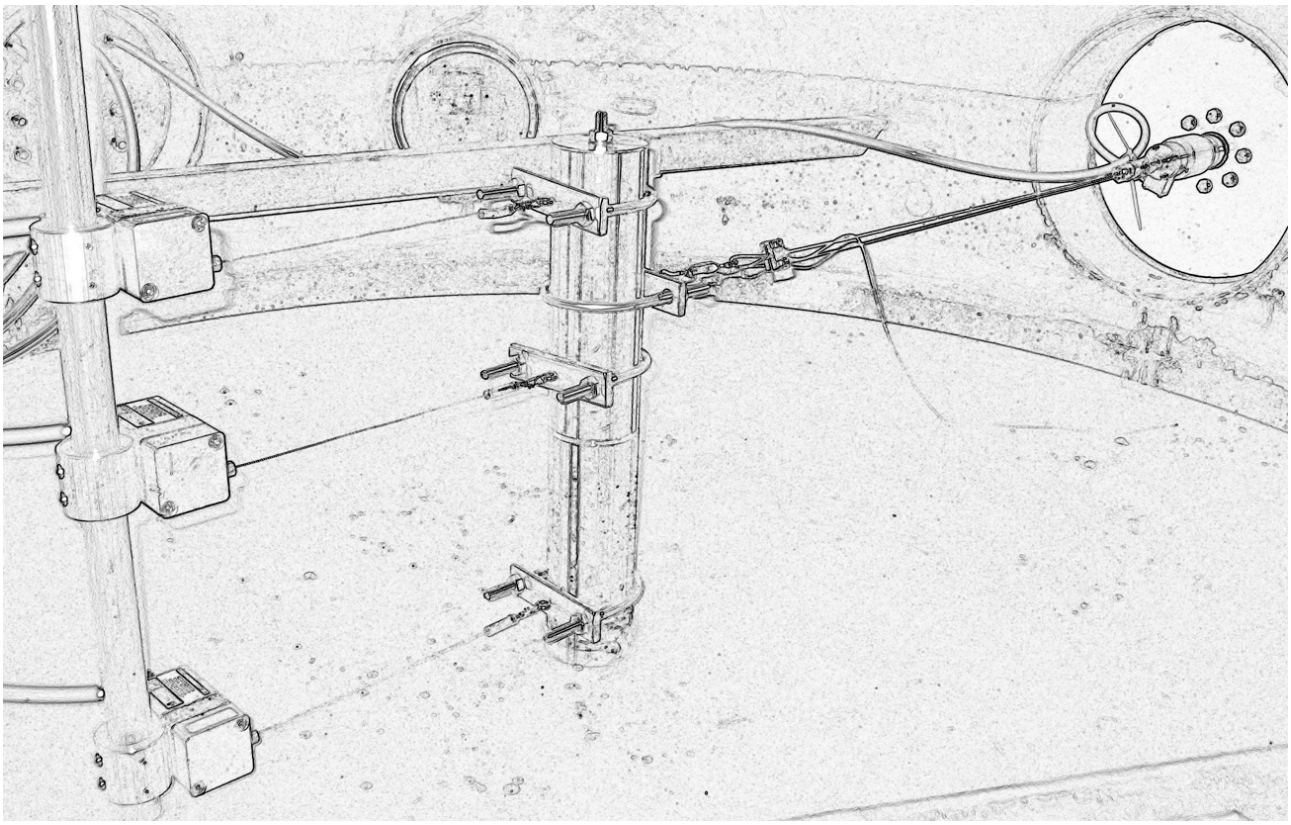

ISSN 1901-726X
DCE Technical Report No. 112

AALBORG UNIVERSITY
Department of Civil Engineering

Aalborg University
Department of Civil Engineering
Geotechnical Engineering Research Group

DCE Technical Report No. 112

Small-scale quasi-static tests on non-slender piles situated in sand – Test results

by

Søren Peder Hyldal Sørensen
Lars Bo Ibsen

July 2011

Scientific Publications at the Department of Civil Engineering

Technical Reports are published for timely dissemination of research results and scientific work carried out at the Department of Civil Engineering (DCE) at Aalborg University. This medium allows publication of more detailed explanations and results than typically allowed in scientific journals.

Technical Memoranda are produced to enable the preliminary dissemination of scientific work by the personnel of the DCE where such release is deemed to be appropriate. Documents of this kind may be incomplete or temporary versions of papers—or part of continuing work. This should be kept in mind when references are given to publications of this kind.

Contract Reports are produced to report scientific work carried out under contract. Publications of this kind contain confidential matter and are reserved for the sponsors and the DCE. Therefore, Contract Reports are generally not available for public circulation.

Lecture Notes contain material produced by the lecturers at the DCE for educational purposes. This may be scientific notes, lecture books, example problems or manuals for laboratory work, or computer programs developed at the DCE.

Theses are monograms or collections of papers published to report the scientific work carried out at the DCE to obtain a degree as either PhD or Doctor of Technology. The thesis is publicly available after the defence of the degree.

Latest News is published to enable rapid communication of information about scientific work carried out at the DCE. This includes the status of research projects, developments in the laboratories, information about collaborative work and recent research results.

Published 2011 by
Aalborg University
Department of Civil Engineering
Sohngaardsholmsvej 57,
DK-9000 Aalborg, Denmark

Printed in Aalborg at Aalborg University

ISSN 1901-726X
DCE Technical Report No. 112

Small-scale quasi-static tests on non-slender piles situated in sand – Test results

Contents

Test setup

In the period from February 2009 till March 2011 a series of small-scale tests on pile foundations has been conducted at Aalborg University. In all the tests the piles have been exposed to quasi-static loading and all the tests have been conducted in a pressure tank. The objective of the tests has been to investigate the effect of pile diameter and length to diameter ratio on the soil response in sand for non-slender piles. Further, the tests have been conducted to calibrate a three-dimensional numerical model in the commercial program *FLAC*^{3D}.

Piles with outer diameters, D, varying between 40 and 100 mm, pile embedment lengths, L_p, between 200 and 500 mm and length to diameter ratios (slenderness ratios), L_p/D, from 3 to 6 have been tested. Hereby, the scales of the tested piles are approximately between 1:40 and 1:150 of a full-scale monopile foundation for an offshore wind turbine.

One of the significant uncertainties when conducting small-scale tests is that the stresses in the soil are small when comparing to a full-scale pile. As the soil parameters depend on the stress level this leads to uncertainties when trying to scale the small-scale tests to a full-scale monopile foundation. Further, the determination of the soil parameters is uncertain for low stress levels. When conducting the tests in a pressure tank it is possible to add an excess pressure (overburden pressure), P_0. In order to increase the effective stresses in the soil, and not the pore pressure, a membrane have been placed on top of the soil for the tests conducted with overburden pressure. The overburden pressure has been varied between 0 and 100 kPa. An overburden pressure of 100 kPa corresponds to the effective vertical stress in the soil at a depth of approximately 10 m.

Pressure tank

Six aluminium piles have been tested in the pressure tank; one closed-ended pile with a pile diameter of 40 mm with no strain gauges attached; one closed-ended pile with a pile diameter of 60 mm with strain gauges attached in 5 levels of the pile; one open-ended pile with a pile diameter of 80 mm with no strain gauges attached; one closed-ended pile with a pile diameter of 80 mm with strain gauges attached in 5 levels of the pile; one closed-ended pile with a pile diameter of 80 mm with strain gauges attached in 11 levels of the pile; one closed-ended pile with a pile diameter of 100 mm with no strain gauges attached. All the piles have a wall thickness, wt, of 5 mm.

Typically monopile foundations for offshore wind turbines are open-ended piles, which make installation by means of pile driving possible. In contrast, five of the six tested piles have closed ends. Otherwise it would be difficult to increase the effective stresses in the soil. Further the strain gauges are protected against water and sand when closed-ended piles are employed. As the piles are loaded laterally the effect of closed pile ends are expected to be minor. To check this, tests are performed on both closed-ended and open-ended piles with a diameter of 80 mm. Monopile foundations for offshore wind turbines are traditionally made of steel. However, the difference between the stiffness and strength of aluminium and steel is not expected to have any influence on the soil response. The employed wall thickness for the test piles is rather

large compared to the tested pile diameters. Hence, the piles might behave slightly stiffer than the full-scale piles employed for offshore wind turbines nowadays. In contrast the choice of using aluminium instead of steel as pile material leads to a more flexible pile behaviour.

The tests are carried out in the pressure tank shown in Figure 1. The pressure tank is manufactured by Bergla Maskinfabrik in Brønderslev, Denmark, and has a height and diameter of approximately 2.5 and 2.1 m, respectively. The pressure tank is mounted on a load-frame resting on a reinforced foundation independent of the remaining floor in the laboratory. A platform is constructed on top of the pressure tank making it possible to access the pressure tank from the top. Trap doors are attached on the sides of the pressure tank making access into the tank possible. The tank contains openings for the wiring from the measurement devices placed inside the tank, cf. Figure 2. The pressure in the tank can be increased by means of a compressor. To increase the pressure in the tank both air and water can be used. When air is led into the tank the pressure is allowed to be increased to 2 bar/200 kPa. When using water pressure a pressure of 10 bar/1000 kPa is allowed due to water being almost incompressible ensuring a significantly improved safety for the personal working in the laboratory. In this test programme air pressure has been employed to create the wanted overburden pressure. Hereby, the preparation time for each test is minimised significantly.

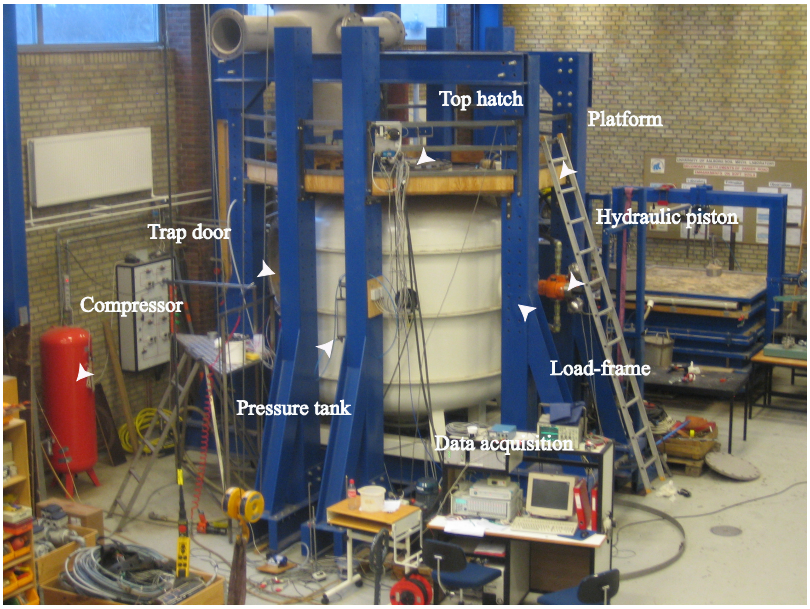

FIGURE 1. PRESSURE TANK AT AALBORG UNIVERSITY.

The test setup is shown in Figure 3. At the bottom of the pressure tank a highly permeable layer of gravel is placed. Water can be led into the tank/drained from the tank through a water inlet/drain pipe located at the bottom of the pressure tank. The gravel layer therefore has the purpose of distributing the water inlet from the bottom evenly inside the tank. On top of the gravel layer fully saturated sand is placed. For test 4 to 6 and test 14, 17 and 20 the thickness of the sand layer is approximately 0.69 m, while the thickness was approximately 580 for the remaining tests.

The lateral loading of the piles is done by means of a hydraulic piston connected to the pile by means of a steel wire. The horizontal hydraulic piston can both apply a specified load and a specified displacement. For

all the tests the loading of the pile has been displacement controlled. A force transducer is connected in series located between the hydraulic piston and the loading wire. When loading with a wire the weight of the wire subjects the pile to a horizontal load. The size of this load depends on the weight of the wire and the vertical deflection of the wire. It has therefore been desired to employ a wire with a low weight; especially for the tests without overburden pressure conducted on the 40 and 60 mm pile. Since the force transducer is connected in series with the wire the load caused by the weight of the wire can be monitored. Through the test programme the wire has been replaced a few times as the wire was too weak for the tests with overburden pressure on the 100 mm pile. The pile displacement is measured in three levels above the soil.

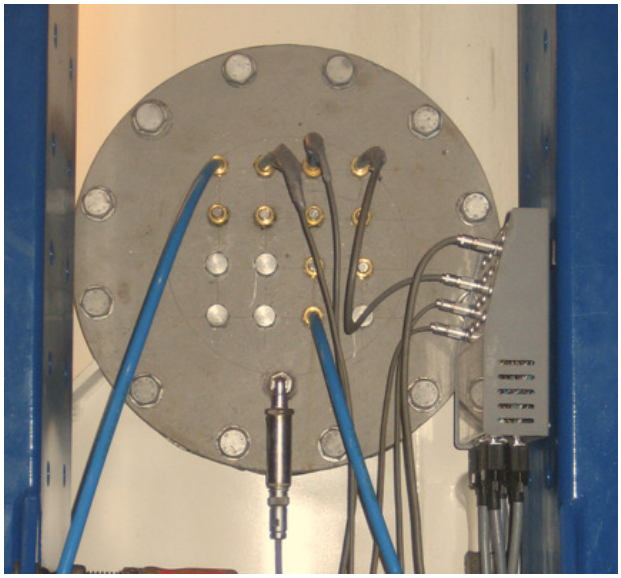

FIGURE 2. OPENINGS FOR WIRING.

The piles are installed in the centre of the pressure tank. When installing the pile a vertical hydraulic piston attached to the top hatch has been employed.

Above the soil a membrane is placed for the tests conducted with overburden pressure. The purpose of the membrane is to seal the air above the soil from the voids in the soil. Hereby, it is possible to increase the effective stresses in the soil when increasing the pressure within the pressure tank. A picture of the membrane is shown in Figure 4. The membrane is made of rubber material. Rubber mouldings are attached to the sides of the membrane in order to ensure a sealing between the wall of the pressure tank and the membrane. The membrane is pressed against the wall of the pressure tank by means of an inflated fire hose, cf. Figure 5. Similarly, a retainer clamp is used to press the membrane against the pile wall.

In the middle of the test programme a new membrane was prepared as the first membrane had started to leak too much. Similarly the joint between the membrane and the pile wall has been improved through the test programme. It has not been possible to hermetically seal the joints between the membrane and respectively the pile wall and the wall of the pressure tank. Water has therefore been placed on top of the

membrane. The dynamic viscosity of water is approximately 50 times bigger than for air at a temperature of 20 ˚C. Hence, the flow through possible leaks in the membrane and the joints with the pile wall and the wall of the pressure tank are minimised significantly when placing water above the membrane. Further, it is hereby ensured that the sand is always fully saturated in spite of leakage through possible gaps.

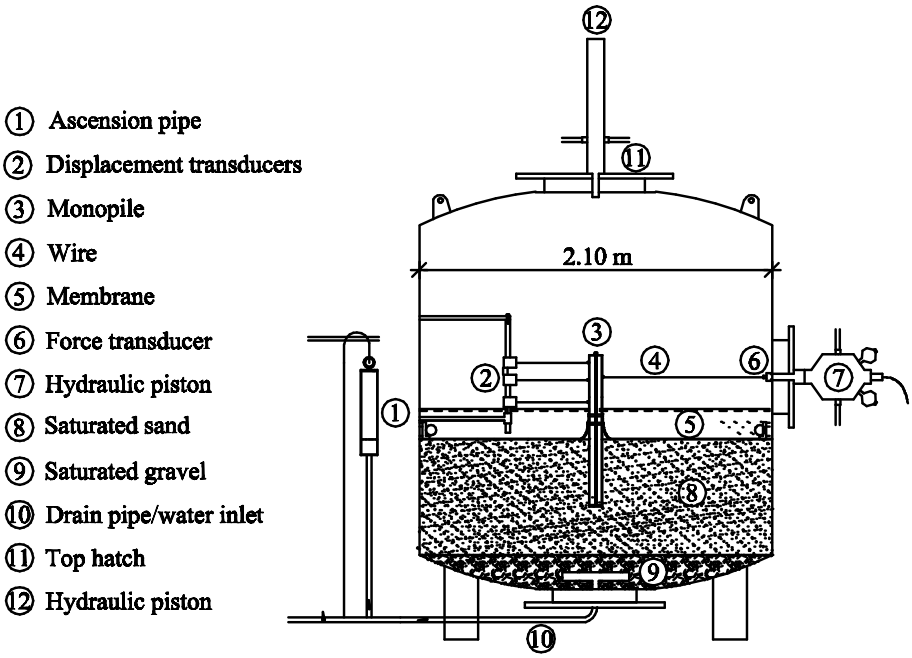

FIGURE 3. CROSS-SECTIONAL VIEW OF THE TEST SETUP.

When applying overburden pressure the soil will compact slightly and hereby the pore pressure in the soil will initially increase. To prevent this increase in pore pressure an ascension pipe is connected to the bottom of the pressure tank, cf. Figure 6. When using the ascension pipe it is possible to maintain a hydrostatic pore pressure in the tank. As there is a small water flow through the membrane the water level in the ascension pipe is regulated during the tests. For most of the tests the water flow through the membrane has been between 15 and 50 L/hour which are considered to be reasonable.

FIGURE 4. MEMBRANE PLACED ON TOP OF THE SOIL.

FIGURE 5. INFLATED FIRE HOSE PRESSURING THE MEMBRANE AGAINST THE PILE WALL.

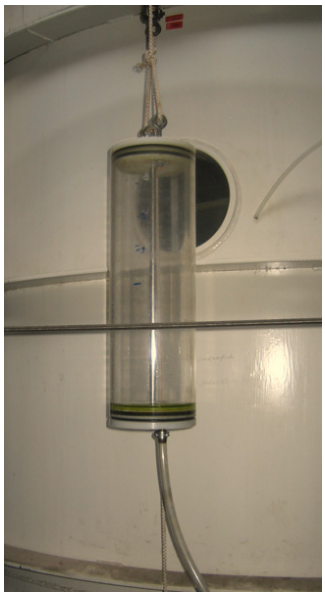

FIGURE 6. ASCENSION PIPE.

Measuring system

The six piles employed in the tests are made from aluminium pipes with a wall thickness of 5 mm. The piles with D = 40 and 100 mm are both closed-ended piles with no strain gauges attached. The pile with D = 60 mm has strain gauges attached in 5 levels of the pile. Three piles with D = 80 mm have been tested; one open-ended pile without strain gauges; one closed-ended pile with strain gauges attached in 5 levels and one closed-ended pile with strain gauges attached in 11 levels. The strain gauges that are attached are from HBM and of the type K-LY43-3/120. The positions of the strain gauges on the 3 piles with strain gauges attached are shown in Figure 7 and Figure 8. The strain gauges are installed in milled grooves as shown in Figure 9. The gauges are sealed with a protective coating in order to protect them from water. The depth, width, and length of the mill outs are approximately 2, 6, and 10 mm, respectively at each gauge. The wiring for the gauges is drawn inside the piles.

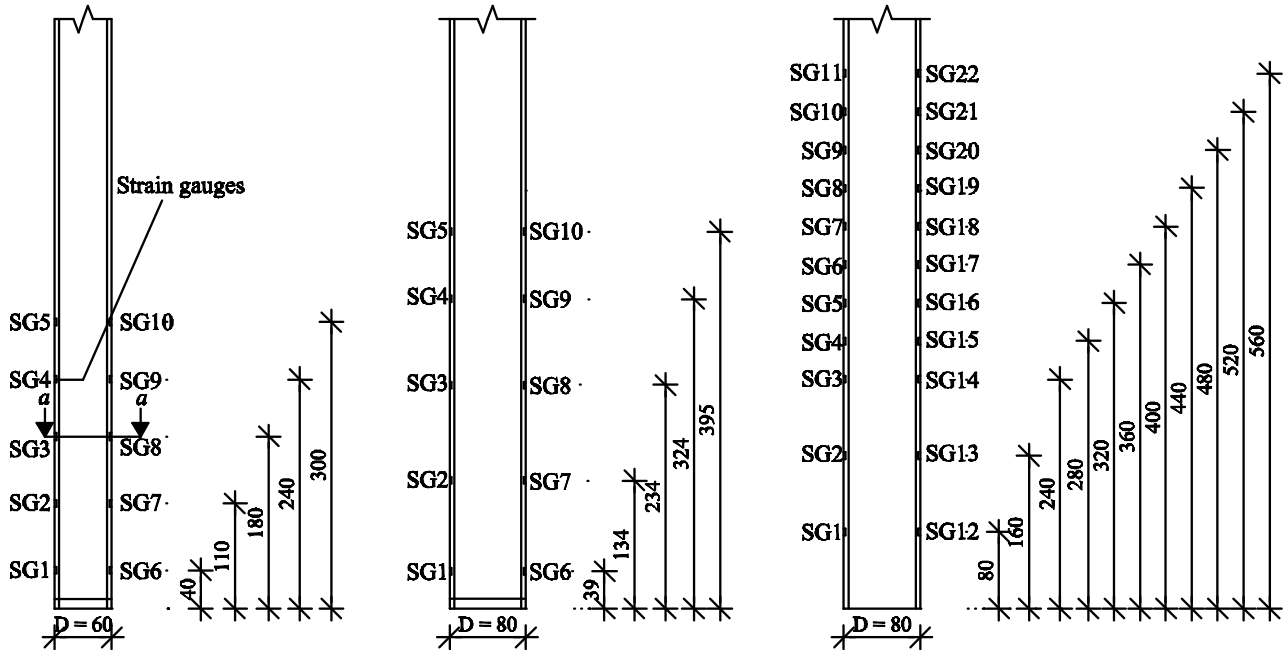

FIGURE 7. STRAIN GAUGE DISTRIBUTION FOR THE THREE PILES WITH STRAIN GAUGES ATTACHED.

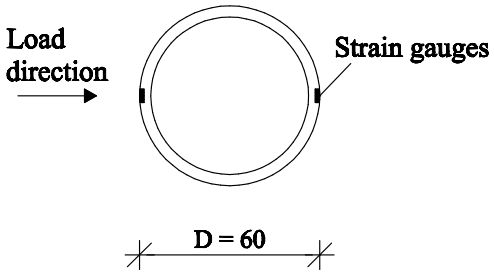

FIGURE 8. CROSS-SECTIONAL VIEW (A-A) OF A PILE WITH STRAIN GAUGES ATTACHED.

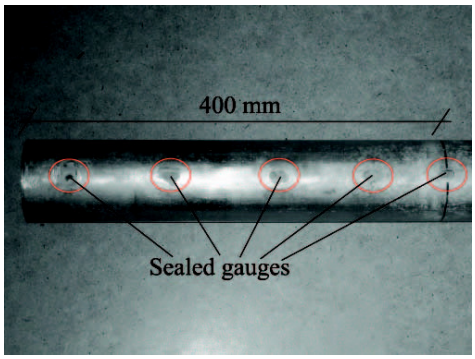

FIGURE 9. STRAIN GAUGES INSTALLED ON THE 80 MM PILE WITH STRAIN GAUGES ATTACHED IN 5 LEVELS. THE GAUGES ARE INSTALLET IN MILLED GROOVES.

For the tests in which the piles with 5 strain gauge levels are employed the strain gauges are setup as half-bridges in which the second active strain gauge in the circuit is a compensation gauge installed in a compensation box. For the tests with the pile with 11 strain gauges the strain gauges are setup as quarter-bridges, i. e. the signal is not compensated for temperature changes. This is however not considered to be a problem as the temperature during the tests has been rather constant as the pressure tank is positioned

indoors. All the strain gauges are positioned in the vertical direction making it possible to determine the pile curvature based on the measured strains.

The lateral pile displacement is measured at three levels above the soil surface, cf. Figure 10. To measure the pile displacement, displacement transducers of the type WS10-1000-R1K-L10 from ASM GmbH have been used. The piles are loaded laterally by means of a displacement controlled hydraulic piston connected to the pile with a steel wire. To measure the horizontal load a force transducer of the type HBM U2B 10 kN is connected in series with the hydraulic piston and the wire. For some of the tests the load exceeded 10 kN and for these tests a force transducer of the type HBM U2B 20 kN was employed. For all the tests the loading eccentricity has been 370 mm above the soil surface. The middle displacement transducer has been attached at the same level as the force transducer. The top displacement transducer has been attached at a height of 480 mm above the soil surface. For test 7, 8, 9, 13, 16, 18, 19, 21, 24 and 25 the bottom displacement transducer has been attached 265 mm above the soil surface. For the remaining tests the bottom displacement transducer has been attached 200 mm above the soil surface.

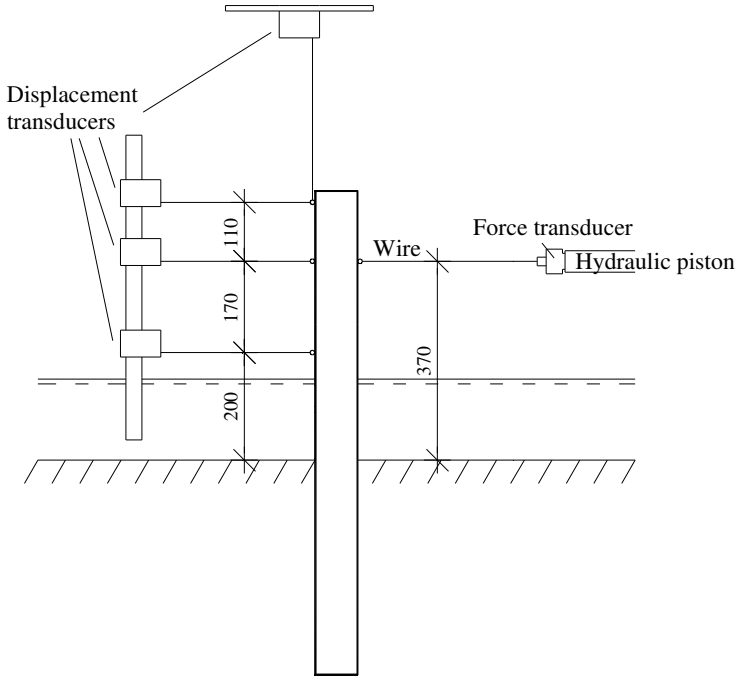

FIGURE 10. POSITIONING OF THE THREE HORIZONTAL DISPLACEMENT TRANSDUCERS AND THE HORIZONTAL FORCE TRANSDUCER. MEASURES IN MM.

For the tests with D = 60 mm a displacement transducer measuring the vertical pile displacement have also been attached. The type of the displacement transducer is similar to the displacement transducers measuring the lateral pile displacement. The displacement transducer measuring the vertical displacement was attached to the side of the pile. Hence, the pile rotation affects the measured vertical displacement, cf. Figure 11. By means of geometric relations the effect of the pile rotation has been deducted from the measured displacement.

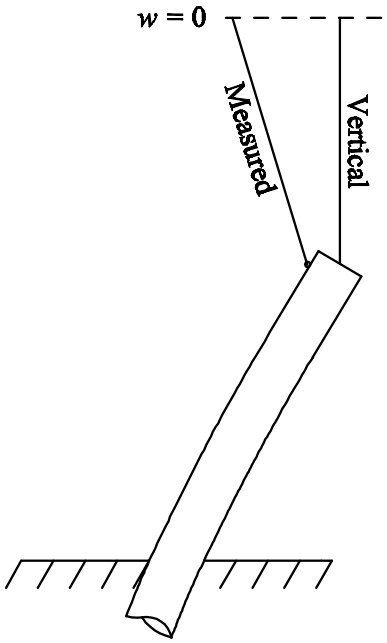

FIGURE 11. MEASURING OF THE VERTICAL PILE DISPLACEMENT.

The pressure in the pressure tank was for the first tests in the test programme measured by a pressure transducer of the type HBM P6A 10 bar. In the middle of the test programme the pressure transducer was changed to a transducer of the type HBM P3MBA 5 bar as the other transducer stopped working properly.

The data acquisition is similar to the data acquisition used for triaxial testing at Aalborg University, cf. Pedersen and Ibsen (2009). However, the transducers employed are not of the same type.

Soil characteristics

All the tests have been conducted with Aalborg University Sand No. 1 (Baskarp Sand no. 15). The sand is homogeneously packed in the pressure tank. Aalborg University Sand No. 1 is graded sand in which the largest grains are round and the smallest grains have sharp edges. The properties of Aalborg University Sand No. 1 are well-known due to previous laboratory tests at Aalborg University, cf. Larsen (2008). A sieve test of the soil material is shown in fig. and the material properties are summarized in Table 1.

TABLE 1. MATERIAL PROPERTIES FOR AALBORG UNIVERSITY SAND NO. 1, AFTER LARSEN (2008).

Specific grain density, d_s	2.64
Maximum void ratio, e_{max}	0.858
Minimum void ratio, e_{min}	0.549
d_{50}, 50 % - quantile	0.14 mm
$U = d_{60}/d_{10}$	1.78

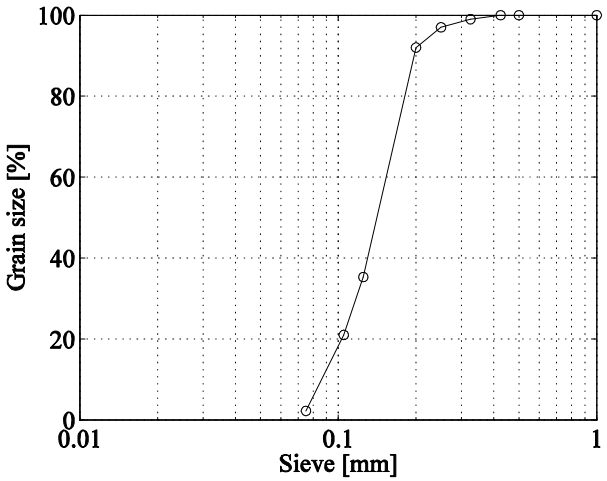

FIGURE 12. SIEVE TEST FOR AALBORG UNIVERSITY SAND NO. 1, AFTER LARSEN (2008).

Calibration of test piles

The strain gauges on the three piles with strain gauges attached have been calibrated in order to make sure that the strain gauge output is correct. The calibrations of the piles have been conducted by loading the piles as simply supported beams, cf. Figure 14 and Figure 13. For all the piles a known load has been applied at several positions along the pile. For all loadings of the pile the applied load has been increased in steps of 10 kg up to a maximum load of 120 kg.

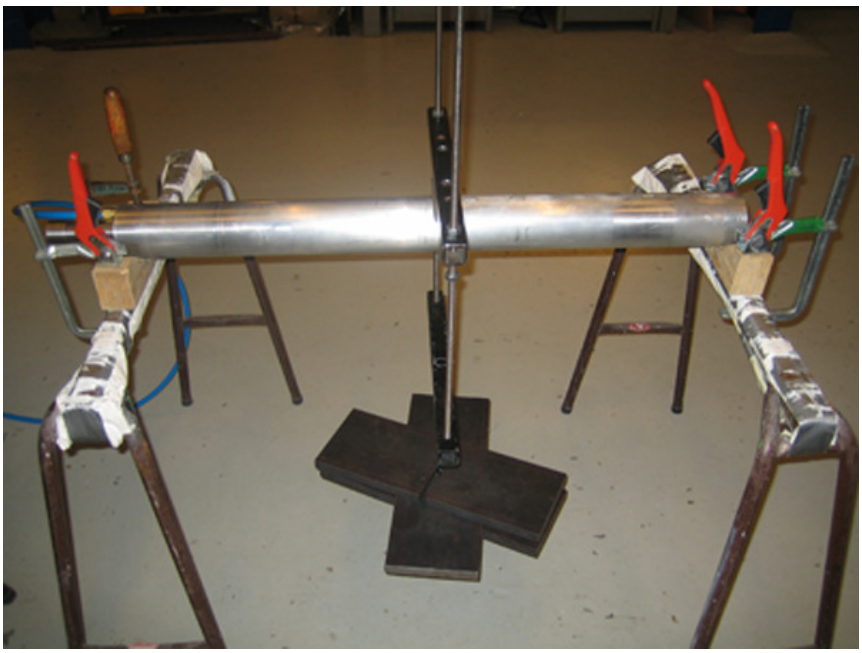

FIGURE 13. CALIBRATION OF STRAIN GAUGES IN THE 80 MM PILE WITH STRAIN GAUGES ATTACHED IN 5 LEVELS.

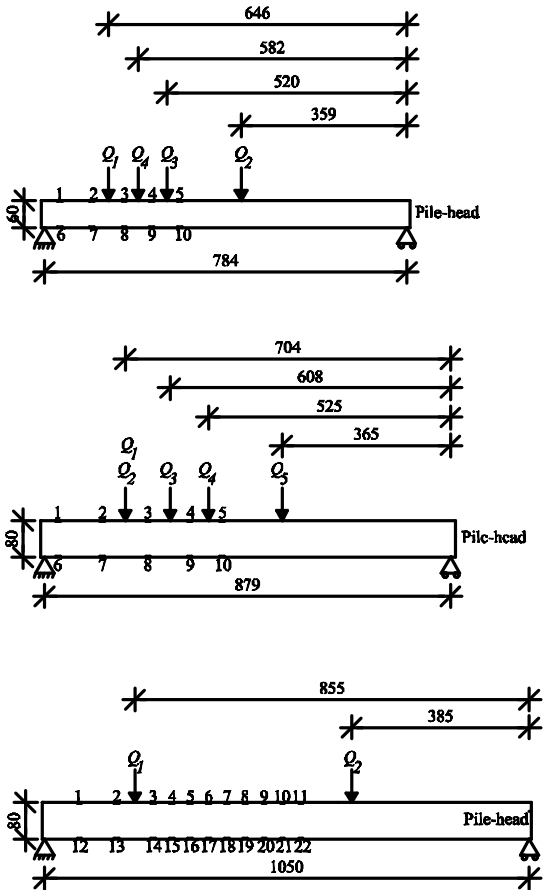

FIGURE 14. CALIBRATION OF STRAIN GAUGES. MEASURES ARE IN MM. TOP: *D* = 60 MM, 5 SG LEVELS – MIDDLE: *D* = 80 MM, 5 SG LEVELS – BOTTOM: *D* = 80 MM, 11 SG LEVELS.

Based on equilibrium conditions the expected bending moments, M_{exp}, can be calculated along the test piles. The expected pile curvature, κ_{exp}, has been determined by:

$$\kappa_{exp} = \frac{M_{exp}}{E_p I_p} \tag{1}$$

where E_p is Young's modulus for the pile material and I_p is the second moment of inertia of a cross-section of the pile. Assuming that Bernoulli-Euler theory is valid the expected strain in the pile, ε_{exp}, can be estimated from:

$$\varepsilon_{exp} = \kappa_{exp} \cdot y = \frac{M_{exp} \cdot y}{E_p I_p} \tag{2}$$

where y is the distance from the center of gravity of the pile to the position of the strain gauge. The strain gauge output from the strain gauges, ε_{SG}, can hereby be compared with the expected value. Generally the strain determined directly from the strain gauge measurements, ε_{SG}, fit well with the strain determined from the applied load, ε_{exp}. Correction factors, k_{SG}, correcting the measured strain to match the expected strain have been used when interpreting the test results:

$$k_{SG} = \frac{\varepsilon_{exp}}{\varepsilon_{SG}} \quad \Leftrightarrow \quad \varepsilon_{exp} = k_{SG} \cdot \varepsilon_{SG} \tag{3}$$

In Table 2 the correction factors are shown for all the attached strain gauges.

TABLE 2. CORRECTION FACTORS FOR THE STRAIN GAUGE MEASUREMENTS.

	D = 60 mm (5 SG levels)	*D* = 80 mm (5 SG levels)	*D* = 80 mm (11 SG levels)
SG 1	1.00	0.72	0.92
SG 2	1.09	0.90	1.14
SG 3	1.09	0.92	0.90
SG 4	1.09	0.89	0.98
SG 5	1.04	0.89	0.99
SG 6	1.00	0.72	0.99
SG 7	1.09	0.90	0.91
SG8	1.09	0.92	0.99
SG 9	1.09	0.89	0.97
SG 10	1.04	0.89	1.00
SG 11	-	-	0.95
SG 12	-	-	0.92
SG 13	-	-	1.13
SG 14	-	-	0.94
SG 15	-	-	0.95
SG 16	-	-	0.93
SG 17	-	-	0.93
SG 18	-	-	0.94
SG 19	-	-	0.98
SG 20	-	-	0.98
SG 21	-	-	1.00
SG 22	-	-	1.00

Interpretation of strain gauge measurements

The strain in the three piles with strain gauges attached is measured with a frequency of 10 Hz. The measured strain is corrected by means of a correction factor, cf. Equation 3. A strain gauge is positioned in both the side of the pile exposed to compression and the side exposed to tension. Hereby, the curvature and bending moment in the pile can be calculated by Equation 4 and 5.

$$\kappa = \frac{\left(\text{abs}\left(\varepsilon_c\right) + \text{abs}\left(\varepsilon_t\right)\right)/2}{y} \tag{4}$$

$$M = E_p \cdot I_p \frac{\left(\text{abs}\left(\varepsilon_c\right) + \text{abs}\left(\varepsilon_t\right)\right)/2}{y} \tag{5}$$

ε_c and ε_t denotes respectively the strain of the strain gauge in compression and in tension. If assuming Bernoulli-Euler theory the following relationships are valid between the pile displacement, *y*, the pile rotation, d*y*/d*x*, the pile curvature, κ, the bending moment, *M*, and the soil resistance, *p*:

$$y = \iint \kappa(x)\, \mathrm{d}x\mathrm{d}x \tag{6}$$

$$\frac{\mathrm{d}y}{\mathrm{d}x} = \int \kappa(x)\, \mathrm{d}x \tag{7}$$

$$M(x) = E_p \cdot I_p \cdot \kappa(x) \tag{8}$$

$$p(x) = -\frac{\mathrm{d}^2 M(x)}{\mathrm{d}x^2} = -E_p \cdot I_p \cdot \frac{\mathrm{d}^2 \kappa(x)}{\mathrm{d}x^2} \tag{9}$$

The variation with depth, *x*, of the curvature measurements at and below the soil surface are fitted with a fifth order polynomial. As an extra point of known curvature it is assumed that the curvature is 0 at the pile toe. The variation of pile displacement with depth can hereby be determined by double integration of the function for the curvature. Hence, two constants needs to be determined based on boundary conditions. The pile displacement is measured in three levels above the soil surface and these can therefore be employed as boundary conditions. However, a minor error in the vertical position of one of these displacement transducers can lead to big errors in the pile displacement at the pile toe. Klinkvort et al. (2010) determined the point of zero displacement for laterally loaded piles loaded in a centrifuge to be in a depth of approximately 0.78 times the embedded pile length. The slenderness ratio of the tested piles was 6. Hence, the point of zero pile displacement can be expected to be at a similar depth for the tested piles. The pile displacement is therefore fixed to be zero at a depth of 0.78 times the embedded pile length, and hereby one of the two constants is determined. The second constant when determining the pile displacement along the pile is determined by fitting the expression to the three measured displacements above the soil surface by means of the least square method.

When differentiating a function fitted to discrete measurements minor discrepancies between the fitted curve and the discrete measurements are amplified. Small uncertainties in the strain gauge measurements are therefore heavily amplified when determining the soil resistance by double differentiation. Yang and Liang (2006) suggest several methods for the double differentiating of the curvature measurements. Both the so-called piecewise polynomial curve fitting method and the high order global polynomial curve fitting method have been employed. The high order global polynomial curve fitting method in which a polynomial on the form given in Equation 10 is fitted to the discrete measurements was found to produce the most reliable results. The soil resistance is then determined by double differentiating the fitted function.

$$\kappa(x) = a + b \cdot x + c \cdot x^{2.5} + d \cdot x^3 + e \cdot x^4 + f \cdot x^5 \tag{10}$$

The uncertainties of the strain gauge measurements have unfortunately been of a high magnitude. Therefore it has not been possible to predict the soil resistance accurately. The inaccurate strain gauge measurements are assumed to arise from stress concentrations due to the mill outs in the aluminium pile. The soil resistance interpreted from the strain gauge measurements are shown in the test results, even though the limited accuracy.

Test programme

The test programme is shown in Table 3.

TABLE 3. TEST PROGRAMME. SG DENOTES STRAIN GAUGES. CLOSED AND OPEN DENOTE CLOSED-ENDED AND OPEN-ENDEN PILES, RESPECTIVELY.

Test	Pile diameter, D [mm]	Embedded pile length, L [mm]	Pile slenderness ratio, L/D [-]	Overburden pressure, P_0 [kPa]	Pile type
1	40	200	5	0	Closed, 0 SG
2	40	200	5	50	Closed, 0 SG
3	40	200	5	100	Closed, 0 SG
4	60	300	5	0	Closed, 5 SG
5	60	300	5	50	Closed, 5 SG
6	60	300	5	100	Closed, 5 SG
7	80	240	3	0	Closed, 0 SG
8	80	240	3	50	Closed, 0 SG
9	80	240	3	100	Closed, 0 SG
10	80	320	4	0	Open, 0 SG
11	80	320	4	0	Closed, 11 SG
12	80	320	4	50	Closed, 11 SG
13	80	320	4	100	Closed, 11 SG
14	80	400	5	0	Closed, 5 SG
15	80	400	5	0	Closed, 11 SG
16	80	400	5	25	Closed, 11 SG
17	80	400	5	50	Closed, 5 SG
18	80	400	5	50	Closed, 11 SG
19	80	400	5	75	Closed, 11 SG
20	80	400	5	100	Closed, 5 SG
21	80	400	5	100	Closed, 11 SG
22	80	480	6	0	Open, 0 SG
23	80	480	6	0	Closed, 11 SG
24	80	480	6	50	Closed, 11 SG
25	80	480	6	100	Closed, 11 SG
26	100	500	5	0	Closed, 0 SG
27	100	500	5	50	Closed, 0 SG
28	100	500	5	50	Closed, 0 SG
29	100	500	5	100	Closed, 0 SG

References

Klinkvort, R. T. & Hededal, O. 2010. Centrifuge modelling of offshore monopile foundation. *Proceedings of the 2nd international symposium on frontiers in offshore geotechnics, Perth, Australia, 8-10 November 2010.*

Larsen, K. A. 2008. Static behavior of bucket foundations. *DCE Thesis no. 7, Department of Civil Engineering, Aalborg University, Denmark.*

Pedersen, T. S. & Ibsen, L. B. 2009. Manual for Dynamic Triaxial Cell. *DCE Technical Report no. 75, Department of Civil Engineering, Aalborg University, Denmark*.

Yang, K. & Liang, R. 2006. Methods for deriving p-y curves from instrumented lateral load tests. *Geotechnical testing journal*, **30**(1), pp. 31-38.

Preparation before testing

For each test it is important that the soil is homogeneously packed and that the relative density, I_D, of the soil material does not change from test to test. In order to do so a standard procedure has been used to prepare the sand before each test. The standard procedure has been developed by Kristensen and Pedersen (2007). They used the procedure to prepare the soil inside the tank for tests on small-scale bucket foundations.

Mechanical vibration has been employed to compact the soil material and to ensure a homogeneous compaction. Further, an upward gradient has been applied to loosen the soil. After the standard procedure to prepare the soil, cone penetration tests (CPT) have been conducted before each tests in order to determine the soil parameters and to ensure that a homogeneous compaction of the soil has been achieved. The procedure for preparing the tests is described in this chapter.

Pile installation

The pile is installed by means of a hydraulic piston mounted in the vertical direction on the top hatch of the pressure tank. Hereby, it is ensured that the pile is vertical after installation. Further, a displacement transducer attached to the top hatch measures the embedded pile length during installation ensuring that the desired embedded pile length is obtained. During installation of the pile, water is poured into the pressure tank from the bottom with an upward gradient of 0.9. This minimises the end and skin resistance along the pile. The size of the gradient has been determined such that water channels do not form in the sand and so that the soil is effectively loosened.

Soil preparation

The soil preparation can be described in four stages:

- Preparation prior to all testing.
- Re-compaction of the soil near the pile after pile installation.
- Re-compaction of the soil material between two tests without removing the pile.
- Re-compaction of the soil material between two tests after removing the pile

In all four stages the sand is loosened by applying an upward gradient and compacted by mechanical vibration. An upward gradient of 0.9 is used as it has been found that this value is sufficient to loosen up the soil and that water channels in the soil can form if a higher gradient is used. The soil is vibrated mechanically by means of a vibrator of a type which typically is employed for concrete. To ensure that the mechanical vibration is conducted similarly for each test a wooden plate with holes fitting the mechanical vibrator is placed above the soil, cf. Figure 15. During vibration of the soil the water table has been at least

5 cm above the soil surface for all the tests. Hereby, air is prevented from coming into the voids of the soil material.

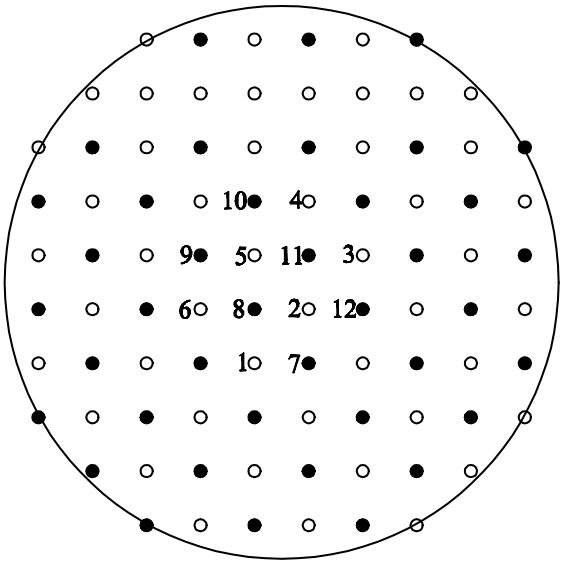

FIGURE 15. PLATE WITH HOLES FITTING THE MECHANICAL VIBRATOR. THE SOLID CIRCLES ARE VIBRATED FIRST AND SECONDLY THE NON-SOLID HOLES ARE VRBRATED. THE NUMBERS INDICATE THE HOLES VIBRATED AFTER PILE INSTALLATION TO ENSURE AN ADEQUATE COMPACTION OF THE SOIL NEAR THE PILE.

In general the following six-point procedure is employed when preparing the soil:

- The soil is loosened by an upward gradient in 5 minutes.
- Vibration of the solid circles, cf. Figure 15.
- Vibration of the non-solid circles, cf. Figure 15.
- The soil is loosened by an upward gradient in 5 minutes.
- Vibration of the solid circles, cf. Figure 15.
- Vibration of the non-solid circles, cf. Figure 15.

Prior to all the tests, the soil in the pressure tank was dry and a more extensive preparation of the soil was therefore needed. The six-point procedure was repeated seven times in order to free all the captured air inside the soil and ensure a homogeneous compaction. After each repetition of the six-point procedure CPT's were carried out.

After pile installation the 12 holes near the pile, cf. the numbered holes shown in Figure 15, was vibrated. The reason for this is that the pile installation creates a failure in the region near the pile. After vibration of these 12 holes the six-point procedure is completed. During vibration the pile is fixed by the vertical hydraulic piston. Hence, horizontal pile displacements are prevented.

Between two tests conducted on the same test pile the pile is brought back to its original position and fixed by the vertical hydraulic piston. The soil is then prepared by first vibrating the 12 numbered holes and afterwards by completion of the six-point procedure.

Between two tests conducted on different test piles the soil near the centre of the pressure tank is vibrated randomly after having removed the first tested piles. Afterwards the new pile is installed and the normal procedure after a pile installation is followed.

References

Kristensen, L. K. & Pedersen, T. S. 2007. Strength and deformation abilities of suction caissons subjected to cyclic loading. *Master thesis, Department of Civil Engineering, Aalborg University, Denmark.*

Cone penetration tests

CPT-tests are conducted prior to each test in order to ensure that a homogeneous compaction of the soil has been obtained and to determine the soil properties. A laboratory CPT-cone which is able to measure the tip resistance, q_c, and the total resistance has been used. Four strain gauges are attached to the tip of the CPT mounted in a full bridge in order to measure the tip resistance. The total resistance can be measured as the sum of three weight cells mounted at the top of the CPT. Hence, the skin friction can be determined by subtraction of the cone tip resistance from the total resistance. However, only the tip resistance is measured as the soil material is sand and the skin friction therefore is expected to be small. A picture of the laboratory CPT-cone and the test setup for the CPT is shown in Figure 16. A cross-sectional view of the CPT is shown in Figure 17. A displacement transducer attached to the top hatch of the pressure tank measures the penetration depth of the tip of the CPT-cone. When conducting the CPT's it is ensured that the CPT penetrates the soil with a velocity of 5 mm/s.

FIGURE 16. PICTURE FROM A CPT-TEST.

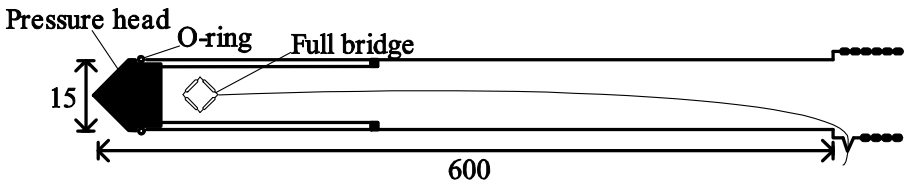

FIGURE 17. CROSS-SECTIONAL VIEW OF THE LABORATORY CPT-CONE. MEASURES IN MM.

Before each test a total of six CPT's have been conducted, cf. Figure 18. Four of the CPT's are taken in a distance of approximately 50 cm from the centre of the pressure tank. The remaining two CPT's are taken approximately 16 cm from the centre. These two CPT's are conducted on the neutral sides of the test piles such that the failure caused by the CPT's does not affect the results when loading the piles laterally afterwards.

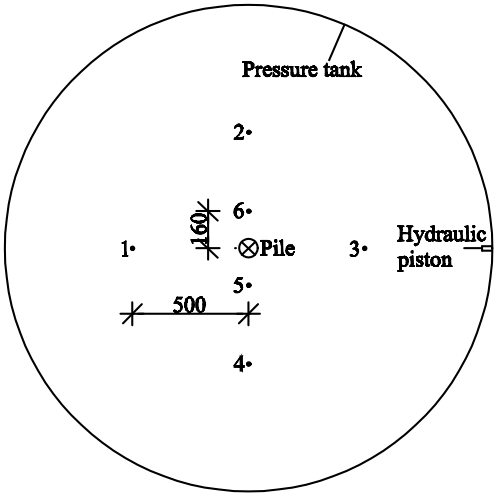

FIGURE 18. CONDUCTED CPT'S PRIOR TO EACH TEST. MEASURES IN MM.

Calibration of tip resistance of the CPT

The tip resistance measured by the laboratory CPT-cone has regularly been calibrated. The setup for the calibration of the CPT is shown in Figure 19. A load increasing stepwise with 10 kg up to a total of 120 kg has been applied for the calibration. In the CPT's taken on the soil the tip resistance, q_c, reaches a value in the order of 150 kg. Hereby the load employed in the calibration covers most of the load range the CPT-cone is exposed to when testing the soil. To avoid the CPT to be exposed to instability during the calibration a bar made of wood is used to fix the CPT-bar horizontally, cf. Figure 19.

FIGURE 19. SETUP FOR THE CALIBRATION OF THE TIP RESISTANCE OF THE CPT-CONE.

The results of one of the calibrations of the tip resistance are shown in Figure 20. The rubber O-ring attached near the tip of the CPT was found to crack after a few tests. These cracks changed the calibration factor of the CPT's tip resistance with approximately 15 %. Therefore, the rubber O-ring was regularly inspected for cracks and calibrations of the tip resistance were performed regularly.

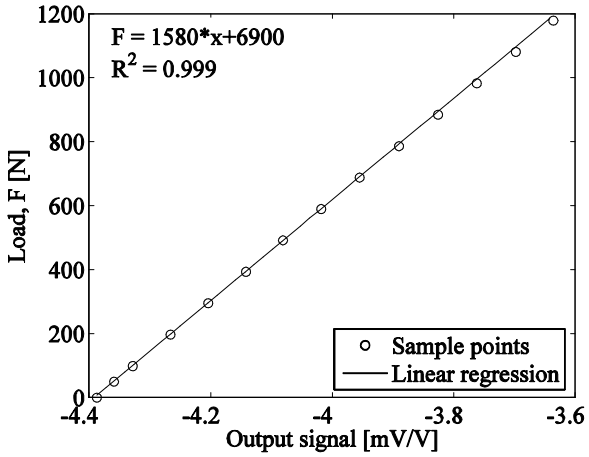

FIGURE 20. RESULTS FROM ONE THE CPT-CALIBRATIONS.

Derivation of soil parameters based on CPT's

The cone penetration tests have been conducted with the purpose of ensuring a homogeneous compaction of the soil in the pressure tank and to determine the soil parameters. A homogeneous compaction of the soil is verified by inspecting the variation of tip resistance with depth for the six CPT's conducted before each test. Further, the variation of tip resistance, q_c, with depth, x, is compared to reference curves conducted prior to the first lateral pile test.

Prior to this test programme the measured tip resistance from the laboratory CPT-cone has been calibrated against the relative density determined by soil samples, cf. Ibsen et al. (2009). Ibsen et al. found the following relation between the tip resistance of the CPT and the relative density of the soil, I_D:

$$I_D = c_2 \cdot \left(\frac{\sigma'_1}{(q_c)^{c_1}} \right)^{c_3} \tag{11}$$

where σ'_1 is the effective vertical stress and c_1, c_2 and c_3 are constants with a value of 0.75, 0.0514 and 0.42, respectively. These constants are valid for Aalborg University Sand No. 1 when using this specific laboratory CPT-cone with a penetration velocity of 5 mm/s. The effective vertical stress and the tip resistance should be inserted in kPa in Equation 11.

When the CPT has penetrated less than approximately 100 mm into the soil the failure in the soil caused by the CPT reaches the soil surface. In contrast, the soil moves around the tip of the CPT for larger penetration depths. Therefore, a change in failure mechanism takes place at a penetration depth of approximately 100 mm. Equation 11 is only valid for penetration depths larger than 100 mm.

The effective vertical stress depends on the effective unit weight of the soil, γ'. Further, the effective unit weight of the soil depends on the in situ void ratio of the soil, $e_{\text{in situ}}$, and the relative density is again correlated with the in situ void ratio:

$$\sigma'_1 = \gamma' \cdot x \tag{12}$$

$$\gamma' = \frac{d_s - 1}{1 + e_{\text{in situ}}} \gamma_w \tag{13}$$

$$I_D = \frac{e_{\max} - e_{\text{in situ}}}{e_{\max} - e_{\min}} \tag{14}$$

In Equation 13 and 14 d_s denote the specific grain density, $e_{\max}$ the void ratio for the loosest possible soil compaction and $e_{\min}$ the void ratio for the densest possible compaction of the soil. The relative density of the soil is determined by iteration by means of Equation 11 to 14.

A series of triaxial tests with varying confining pressure, σ'_3, and varying relative density have been conducted on Aalborg University Sand No. 1 at Aalborg University. The confining pressure has been set to values of 5, 10, 20, 40, 80, 160, 320, 640 and 800 kPa and for each confining pressure a relative density of approximately 51 and 80 % has been tested. Based on these triaxial tests equations for the internal triaxial friction angle, φ_{tr}, the triaxial dilatancy angle, ψ_{tr}, and the secant Young's modulus of elasticity for the soil at a stress level of 50 %, E_{50}, have been determined by cf. Ibsen et al. (2009):

$$\varphi_{tr} = 0.152 \cdot I_D + 27.39 \cdot \sigma'^{-0.2807}_3 + 23.21[°] \tag{15}$$

$$\psi_{tr} = 0.195 \cdot I_D + 14.86 \cdot \sigma'^{-0.09764}_3 - 9.946[°] \tag{16}$$

$$E_{50} = \left(0.6322 \cdot I_D^{2.507} + 10920\right) \cdot \left(\frac{c \cdot \cos(\varphi_{tr}) + \sigma'_3 \cdot \sin(\varphi_{tr})}{c \cdot \cos(\varphi_{tr}) + \sigma'^{ref}_3 \cdot \sin(\varphi_{tr})} \right)^{0.58} \tag{17}$$

The linear relationship between the internal triaxial friction angle and the relative density originates from Schmertmann (1978). In Equation 15-17 the relative density should be inserted in percent and the confining pressure should be inserted in kPa. From Equation 15 and 16 it can be observed that the internal triaxial friction angle and the triaxial dilatancy angle approaches infinity for confining pressures approaching 0. Hence, Equation 15 and 16 are not valid for low stress levels. For the tests without overburden pressure the confining pressure varies from 0 kPa at the soil surface to approximately 2 kPa at the bottom of the sand in the pressure tank. Hereby, the stress level is lower than the equations range of validity. The internal triaxial friction angle and the triaxial dilatancy angle have therefore been determined by assuming a confining pressure of 5 kPa corresponding to the smallest confining pressure used in the triaxial tests. Similarly, large uncertainties are present when determining E_{50} for the lateral pile tests without overburden pressure.

The tangential Young's modulus of elasticity of the soil, E_0, is determined as E_{50} multiplied by a factor as shown in Equation 18, cf. Brinkgreve et al. (2008).

$$E_0 = \frac{2}{2 - R_f} \cdot E_{50} \tag{18}$$

R_f denotes the ratio between the ultimate deviatoric stress and the asymptotic deviatoric stress. A value of 0.9 is recommended by Brinkgreve et al. (2008) and is therefore employed in this project.

References

Brinkgreve, R. B. J., Broere, W. & Waterman, D. 2008. *Plaxis 2D version 9.0, Material models manual.*

Ibsen, L. B., Hanson, M., Hjort, T. H. & Thaarup, M. 2009. MC parameter calibration for Aalborg University Sand No. 1. DCE Technical Report no. 62, Department of Civil Engineering, Aalborg University, Denmark.

Schmertmann, J. H. 1978. Guidelines for cone penetration test, performance and design. Report, FHWA-TS-78-209, 145, US Federal Highway Administration, Washington, DC.

Numerical modelling of test results

The experimental tests have been modelled by means of a three-dimensional model in the commercial programme *FLAC*^{3D}, cf. FLAC^{3D} 3.1 manual (2006). *FLAC*^{3D} employs an explicit finite difference solver able to solve the behaviour of a continuous three-dimensional medium numerically.

The mechanical behaviour of the medium is derived from the laws of motion, the definitions of strain and furthermore the use of constitutive equations to describe the stress-strain relationship for the employed materials. The program solves the problem dynamically. Hence, all variables are time dependent. To solve the set of equations, boundaries and initial conditions are applied.

To describe the kinematic relations the Lagrange formulation is implemented in *FLAC*^{3D}. All components in the kinematic relations are determined at the current positions and as a consequence of this a description of large-strain deformations can be used in which the mesh is updated.

To solve the set of partial differential equations *FLAC*^{3D} uses a method characterised by the following three approaches:

- The continuous medium is replaced of a finite number of elements with forces concentrated at the nodes.
- The finite difference approach is employed to solve the equations. Hence, all first-order space and time derivatives are approximated by finite differences.
- A dynamic solution approach is used in which the program steps forward until equilibrium is reached for all nodes.

To provide valid results the numerical scheme to solve the differential equations must be stable. Hence, the employed time step must be smaller than a critical time step corresponding to the minimum eigenperiod of the total system. In *FLAC*^{3D} this is done by employing a constant time step of 1 and instead to adjust the nodal masses to fulfil a stable condition.

The medium is in *FLAC*^{3D} discretised into hexahedral zones consisting of elements of tetrahedral shape. It is possible to divide each hexahedral zone into two different configurations of tetrahedral elements. *FLAC*^{3D} determines the nodal forces as the average value determined from these two configurations. Hence, a symmetric zone response is ensured. In Figure 21 an element of tetrahedral shape is shown and a hexahedral zone discretised into five tetrahedral elements can also be observed.

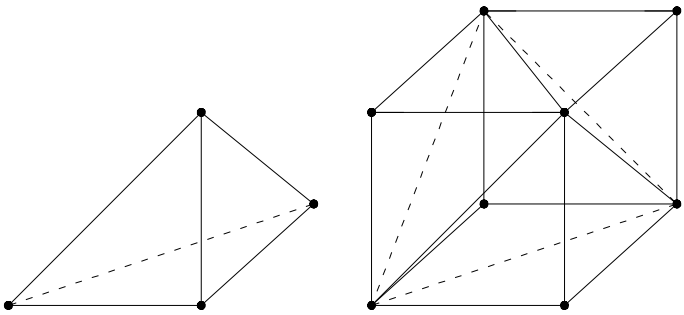

FIGURE 21. LEFT: ELEMENT OF TETRAHEDRAL SHAPE – RIGHT: HEXAHADRAL ZONE DIVIDED INTO FIVE ELEMENTS OF TETRAHEDRAL SHAPE. SOLID CIRCLES ILLUSTRATE ZONE/ELEMENT NODES.

Construction of numerical model

When constructing the numerical model only a half model is modelled due to symmetry. The mesh of one of the numerical simulations is shown in Figure 22. The diameter of the pressure tank has been employed as the outer boundary for the soil and similarly the position of the gravel layer has been employed as the lower boundary of the numerical model.

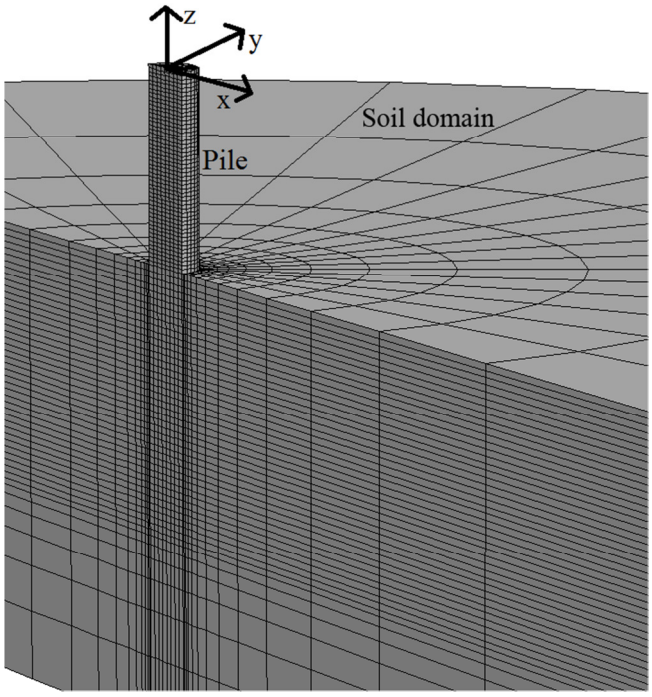

FIGURE 22. EXAMPLE OF THE MESH EMPLOYED IN THE NUMERICAL SIMULATIONS.

Both the soil and the piles are modelled by hexahedral zones. Hence, the piles are modelled as solid piles. Young's modulus of elasticity and the density of the pile elements have been scaled such that the bending stiffness, E_pI_p, and the total pile weight employed in the model are similar to the bending stiffness and total pile weight of the model piles. The Poisson's ratio employed for the pile elements in the numerical model is similar to the real value of Poisson's ratio for the test piles. Hence, the shear stiffness, A_pG_p, of the pile is

not modelled correct in the numerical simulations. The error in not modelling the piles shear stiffness's correct is however assumed to be small as the test piles primarily are exposed to bending.

The soil is modelled by means of the Mohr-Coulomb material model employing the soil parameters determined directly from the CPT's conducted prior to each lateral pile test. To model the interface between the piles and the soil a linear Coulomb shear-strength criterion is employed. The interface is constructed of triangular elements attached to the soil material. To govern the interface strength a wall friction angle, δ, is set:

$$\tan(\delta) = \frac{2}{3} \cdot \varphi_{tr} \tag{18}$$

Similarly, a shear and a normal stiffness have to be applied to the interface elements. These stiffness should not be set too low as interpenetration otherwise can occur and further the stiffness does not represent a physical property. In contrast, a high value increases the calculation time. A value corresponding to 100 times the stiffness of the surrounding soil has been chosen.

At the outer boundary of the soil the elements are fixed in the horizontal directions and are allowed to move in the vertical direction. At the bottom of the numerical model the elements are fixed in all directions. Further, when only modelling half a model due to symmetry the elements at the line of symmetry, cf. $y = 0$ at Figure 22, are fixed horizontally in the outwards direction, $y = 0$.

To apply the horizontal loading a velocity in the x-direction has been applied to the centre nodes of the piles, x = 0, cf. Figure 22, at the height of the hydraulic piston. In order to obtain a stable solution the velocity is set to $1 \cdot 10^{-10}$ initially and the ramped up to a value of $4 \cdot 10^{-9}$ over the first 100000 load steps.

As *FLAC*^{3D} is a dynamic explicit finite difference solver it is necessary to employ damping in the model. This is done by means of the so-called combined damping which is recommended for uniform motions, cf. FLAC^{3D} 3.1 manual (2006).

The numerical simulations are executed in four steps. At first the initial stresses in the soil are generated by means of the K_0-procedure. Hence, the horizontal stresses are determined as the vertical stresses multiplied by the coefficient of horizontal earth pressure at rest, K_0, which is set to:

$$K_0 = 1 - \sin(\varphi_{tr}) \tag{19}$$

Secondly equilibrium is calculated in which the pile is given similar properties as the soil. Thirdly a new equilibrium the pile is given the correct properties and a new equilibrium is determined. Finally the lateral load is applied.

Convergence

Numerical simulations have been conducted for various numbers of elements in order to ensure the convergence of the numerical model. In Figure 23 load-displacement relationships for test 28 can be observed for varying number of elements. Convergence of the numerical model takes place when using

approximately 9000 zones each consisting of 5 tetrahedral elements. Therefore, approximately 9000 zones have been employed for all the numerical simulations.

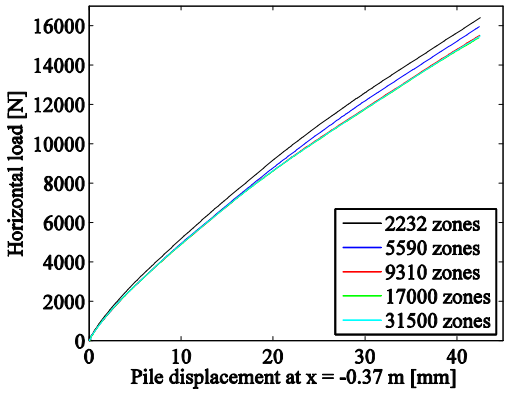

FIGURE 23. HORIZONTAL LOAD VS. PILE HEAD DISPLACEMENT FOR TEST 28 DETERMINED BY MEANS OF FLAC^{3D}. THE SIMULATION HAVE BEEN CARRIED OUT FOR 5 DIFFERENT MESH DENSITIES.

Calculation of pile bending moment and soil resistance acting against the pile wall

The pile bending moment, M, has been determined for several cross-sections in the pile by means of the Navier equation relating normal stresses with bending moment:

$$\sigma = \sigma_M + \sigma_N = -\frac{M}{I_p} y + \frac{N}{A_p} \tag{20}$$

$$M = -\frac{\sigma_M \cdot I_p}{y} \tag{21}$$

where σ_M and σ_N is the normal stress due to bending moments, M, and axial forces, N, respectively, I_p is the second moment of inertia and A_p is the cross-sectional area. The total normal stress, σ, in the pile is determined at $(x,y) = (-D/2,0)$ and $(D/2,0)$ for each cross-section. The normal stress due to bending is then determined as the mean value of the absolute values of the total normal stress in these points. In Equation 20 and 21 the values for I_p and A_p corresponds to a solid pile.

The soil resistance acting on the pile wall, p, has likewise been determined for several cross-sections along the pile. To calculate the soil resistance the interface stresses, σ'_{xx}, σ'_{xy} and σ'_{xz}, have been integrated along the circumference of the pile, cf. Fan and Long (2005):

$$p = \int \sigma'_{xx} n_x + \sigma'_{xy} n_y + \sigma'_{xz} n_z dL \tag{22}$$

L denote the circumference of the interface and n_x, n_y ad n_z denote the x-, y- and z-component of the unit normal:

$$n_x = \frac{x_i}{\sqrt{x_i^2 + y_i^2}} \tag{23}$$

$$n_y = \frac{y_i}{\sqrt{x_i^2 + y_i^2}} \tag{24}$$

$$n_x = 0 \tag{25}$$

x_i and y_i denote the *x*- and *y*-coordinate of an interface node, respectively.

References

Fan, C. C. & Long, J. H. (2005). Assessment of existing methods for predicting soil response of laterally loaded piles in sand. *Computers and Geotechnics* **32**, 274-289.

FLAC^{3D} 3.1 manual (2006). Fast langrangian analysis of continua in 3 dimensions. Itasca Consulting Group Inc., Minneapolis, Minnesota, USA.

Soil parameters and test results

In the following the test results for the 29 conducted tests are presented. The results and interpretation of the conducted CPT's prior to each test is presented. Further, the direct measurements from the tests are presented. For the tests with strain gauges attached the distribution of pile displacement, pile rotation, pile curvature, pile bending moment and soil resistance with depth and furthermore *p-y* curves determined based on the direct measurements are shown.

Test 1: D = 40 mm, L_p = 200 mm and P_0 = 0 kPa (Closed-ended)

Pile type: Closed-ended	**Completed:** Spring 2010
Pile diameter (mm): 40	**No. of strain gauge levels:** 0
Embedded pile length (mm): 200	**Overburden pressure (kPa):** 0
Slenderness ratio, L/D: 5	**Load eccentricity (mm):** 370
Pile wall thickness (mm): 5	**By:** H. R. Roesen and K. Thomassen
Comments: During preparation of the test, the wire connecting the pile with the horizontal hydraulic piston was tightened while the pile was still fixed by the vertical horizontal piston. This caused a minor displacement of the pile when unfixing the pile from the vertical hydraulic piston. Further, the pile got stuck in the joint connecting the pile and the vertical hydraulic piston causing disturbances in the soil around the pile when removing the piston. Due to the small pile diameter these issues might have a rather large impact on the test results.	

Soil parameters:

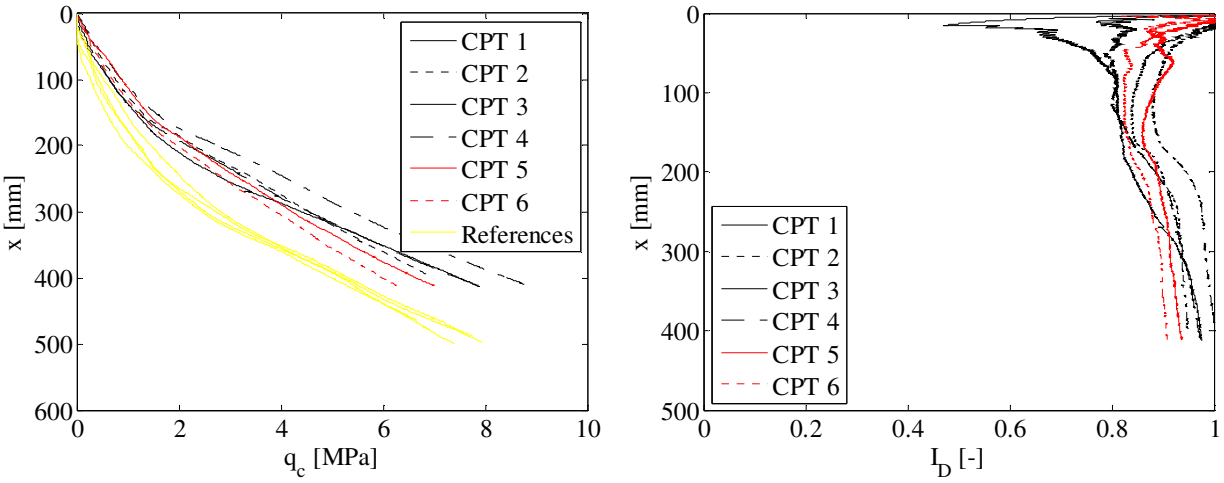

FIGURE 24. CPT-RESULTS FROM TEST 1. LEFT: TIP RESISTANCE VERSUS DEPTH – RIGHT: RELATIVE DENSITY VERSUS DEPTH.

TABLE 4. ESTIMATED SOIL PARAMETERS FOR TEST 1.

Relative density, I_D	Internal friction angle, φ_{tr}	Dilatancy angle, ψ_{tr}	Effective unit weight, γ'	Tangential Young's modulus of elasticity, E_0	Poisson's ratio, ν
[-]	[◦]	[◦]	[kN/m^3]	[MPa]	[-]
0.91	54.4	20.4	10.4	-	0.23

Test results:

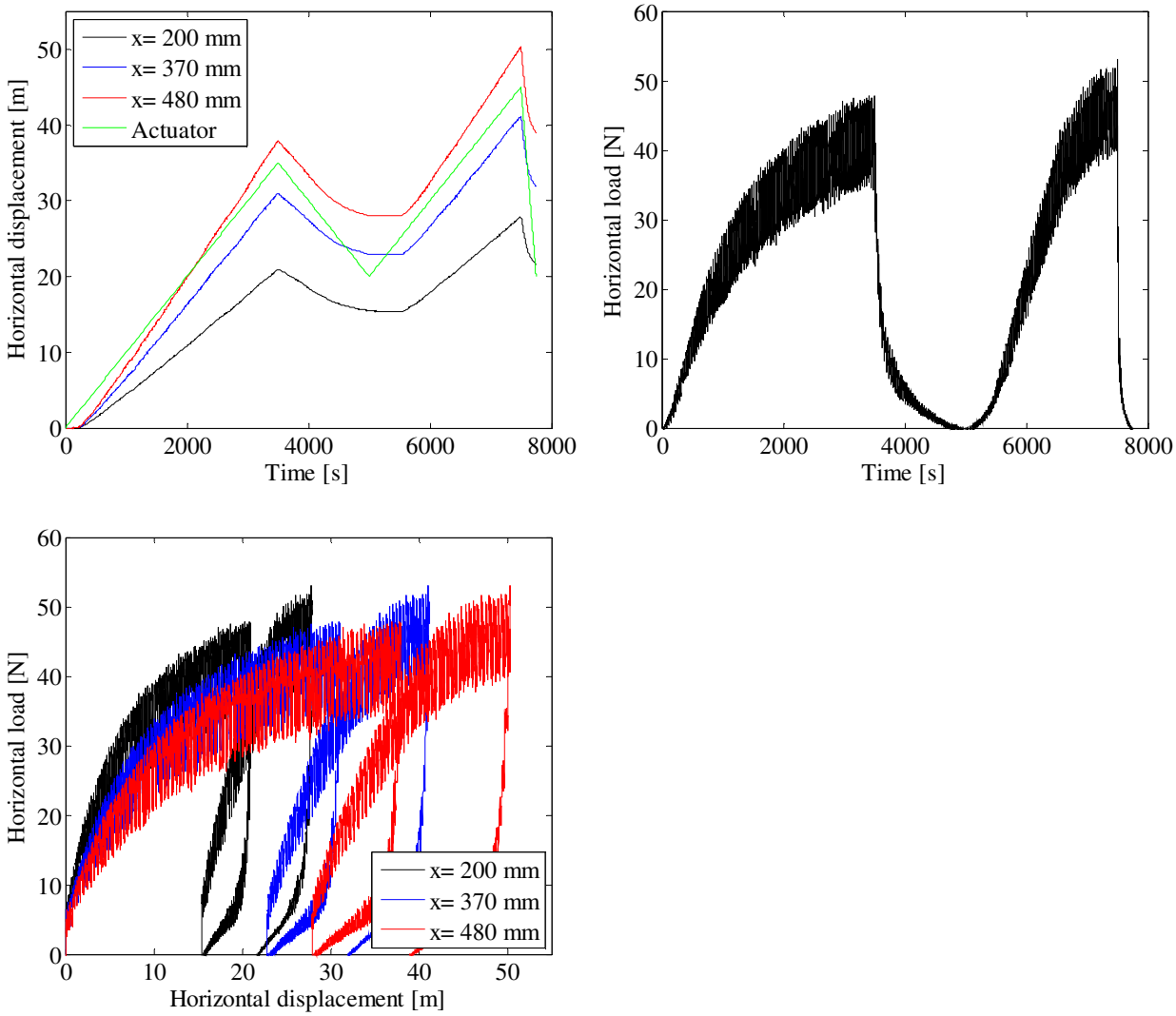

FIGURE 25. TOP LEFT: PILE DISPLACEMENT VERSUS TIME – TOP RIGHT: HORIZONTAL LOAD VERSUS TIME – BOTTOM LEFT: HORIZONTAL LOAD VERSUS PILE DISPLACEMENT.

Test 2: D = 40 mm, L_p = 200 mm and P_0 = 50 kPa (Closed-ended)

Pile type: Closed-ended	**Completed:** Spring 2010
Pile diameter (mm): 40	**No. of strain gauge levels:** 0
Embedded pile length (mm): 200	**Overburden pressure (kPa):** 50
Slenderness ratio, *L*/*D*: 5	**Load eccentricity (mm):** 370
Pile wall thickness (mm): 5	**By:** H. R. Roesen and K. Thomassen
Comments: During preparation of the test, the wire connecting the pile with the horizontal hydraulic piston was tightened while the pile was still fixed by the vertical horizontal piston. This caused a minor displacement of the pile when unfixing the pile from the vertical hydraulic piston. The metal frame holding the CPT device fell down on the soil on the passive side of the pile. The frame landed near the side of the pressure tank and is therefore not expected to have disturbed the soil near the pile. Minor drainage of the soil might have taken place as the water tab securing hydrostatic water pressure was held open for approximately one minute after having emptied the ascension pipe. At the end of the test the leaking of the water through the membrane increased from 30 L/hour to 80 L/hour.	

Soil parameters:

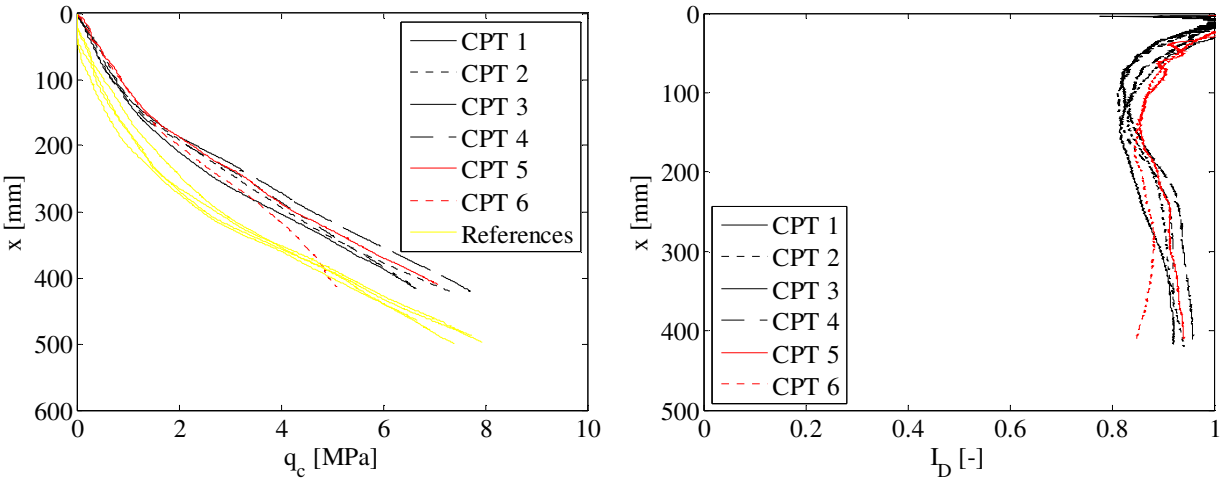

FIGURE 26. CPT-RESULTS FROM TEST 2. LEFT: TIP RESISTANCE VERSUS DEPTH – RIGHT: RELATIVE DENSITY VERSUS DEPTH.

TABLE 5. ESTIMATED SOIL PARAMETERS FOR TEST 2.

Relative density, I_D	Internal friction angle, φ_{tr}	Dilatancy angle, ψ_{tr}	Effective unit weight, γ'	Tangential Young's modulus of elasticity, E_0	Poisson's ratio, ν
[-]	[◦]	[◦]	[kN/m^3]	[MPa]	[-]
0.89	50.4	19.1	10.4	30.9	0.23

Test results:

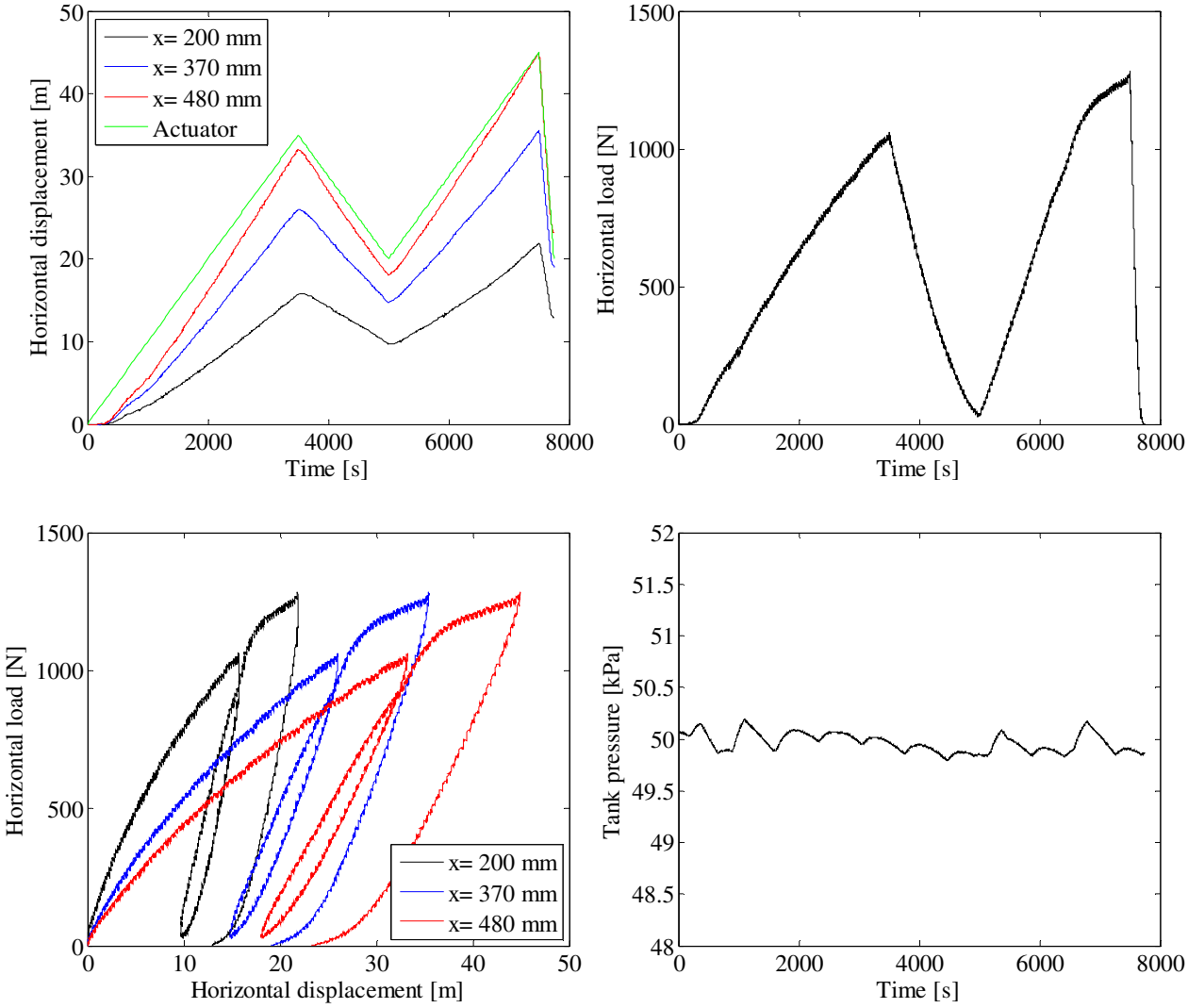

FIGURE 27. TOP LEFT: PILE DISPLACEMENT VERSUS TIME – TOP RIGHT: HORIZONTAL LOAD VERSUS TIME – BOTTOM LEFT: HORIZONTAL LOAD VERSUS PILE DISPLACEMENT – BOTTOM RIGHT: TANK PRESSURE VERSUS TIME.

Test 3: D = 40 mm, L_p = 200 mm and P_0 = 100 kPa (Closed-ended)

Pile type: Closed-ended	**Completed:** Spring 2010
Pile diameter (mm): 40	**No. of strain gauge levels:** 0
Embedded pile length (mm): 200	**Overburden pressure (kPa):** 100
Slenderness ratio, *L*/*D*: 5	**Load eccentricity (mm):** 370
Pile wall thickness (mm): 5	**By:** H. R. Roesen and K. Thomassen
Comments: When preparing the tests too much water was drained from the tank resulting in a water level approximately 20 mm below the soil surface. Water was therefore carefully poured in to the tank. The pile was stuck in the vertical hydraulic piston resulting in disturbances of the soil surrounding the pile.	

Soil parameters:

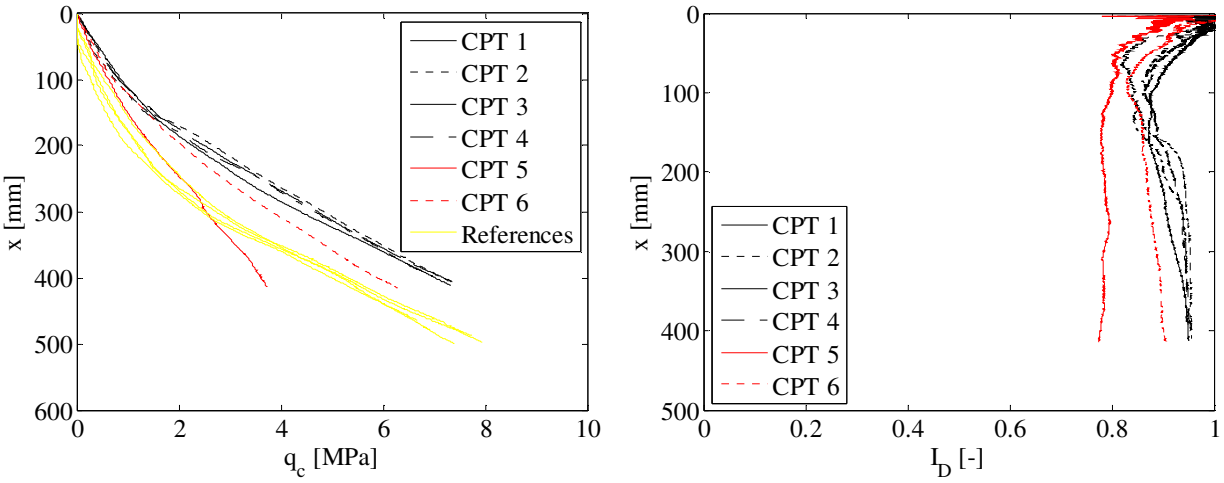

FIGURE 28. CPT-RESULTS FROM TEST 3. LEFT: TIP RESISTANCE VERSUS DEPTH – RIGHT: RELATIVE DENSITY VERSUS DEPTH.

TABLE 6. ESTIMATED SOIL PARAMETERS FOR TEST 3.

Relative density, I_D	Internal friction angle, φ_{tr}	Dilatancy angle, ψ_{tr}	Effective unit weight, γ'	Tangential Young's modulus of elasticity, E_0	Poisson's ratio, ν
[-]	[◦]	[◦]	[kN/m^3]	[MPa]	[-]
0.91	48.0	18.6	10.4	51.7	0.23

Test results:

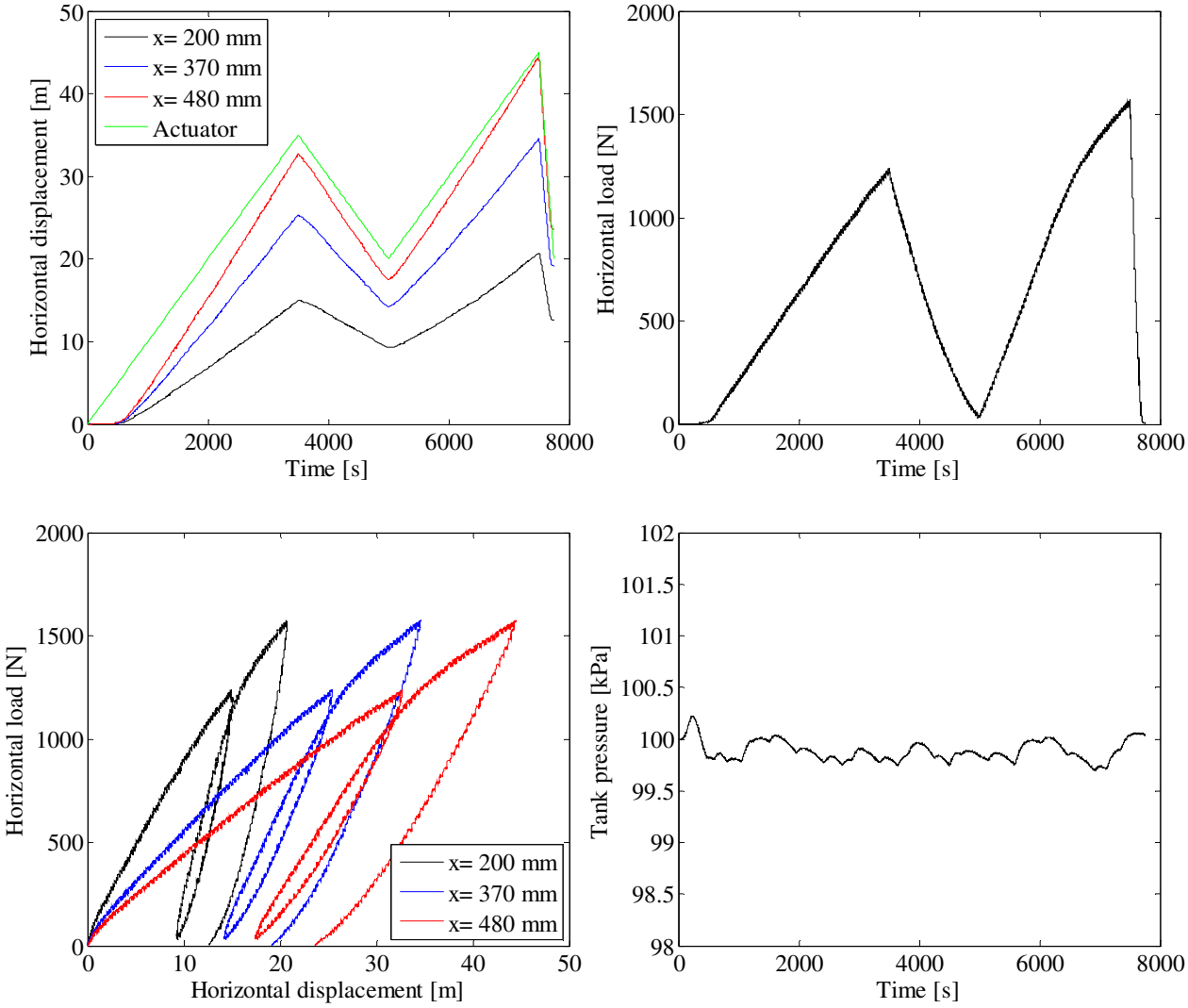

FIGURE 29. TOP LEFT: PILE DISPLACEMENT VERSUS TIME – TOP RIGHT: HORIZONTAL LOAD VERSUS TIME – BOTTOM LEFT: HORIZONTAL LOAD VERSUS PILE DISPLACEMENT – BOTTOM RIGHT: TANK PRESSURE VERSUS TIME.

Test 4: D = 60 mm, L_p = 300 mm and P_0 = 0 kPa (Closed-ended)

Pile type: Closed-ended	**Completed:** Spring 2009
Pile diameter (mm): 60	**No. of strain gauge levels:** 5 (All below soil surface)
Embedded pile length (mm): 300	**Overburden pressure (kPa):** 0
Slenderness ratio, L/D: 5	**Load eccentricity (mm):** 370
Pile wall thickness (mm): 5	**By:** S. P. H. Sørensen, K. T. Brødbæk and M. Møller
Comments: The strain gauge exposed to compression at a depth of 120 mm did not produce reliable results and has therefore not been included in the interpretation of the test results.	

Soil parameters:

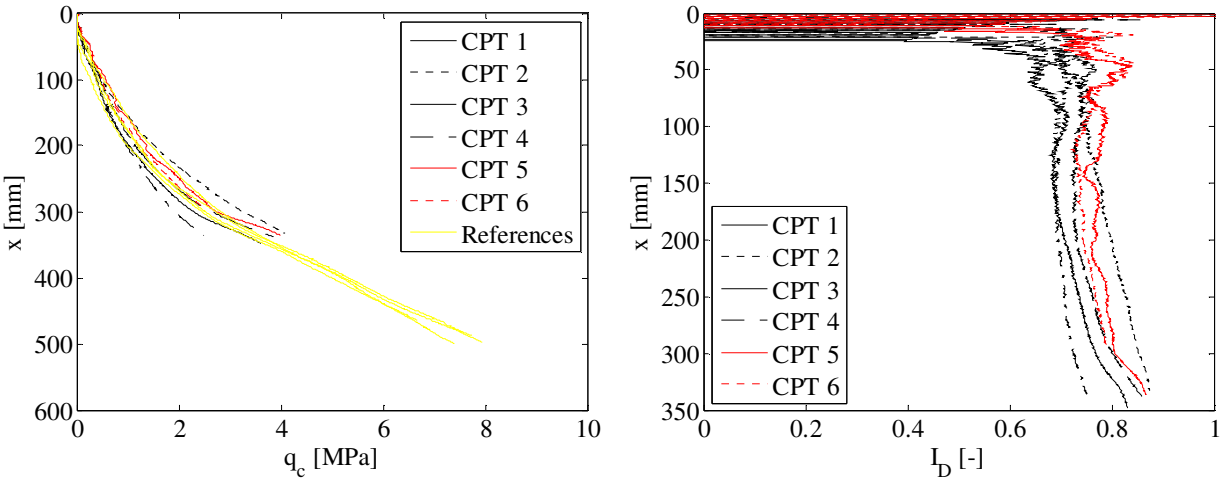

FIGURE 30. CPT-RESULTS FROM TEST 4. LEFT: TIP RESISTANCE VERSUS DEPTH – RIGHT: RELATIVE DENSITY VERSUS DEPTH.

TABLE 7. ESTIMATED SOIL PARAMETERS FOR TEST 4.

Relative density, I_D	Internal friction angle, φ_{tr}	Dilatancy angle, ψ_{tr}	Effective unit weight, γ'	Tangential Young's modulus of elasticity, E_0	Poisson's ratio, ν
[-]	[◦]	[◦]	[kN/m^3]	[MPa]	[-]
0.80	52.2	18.1	10.1	-	0.23

Test results:

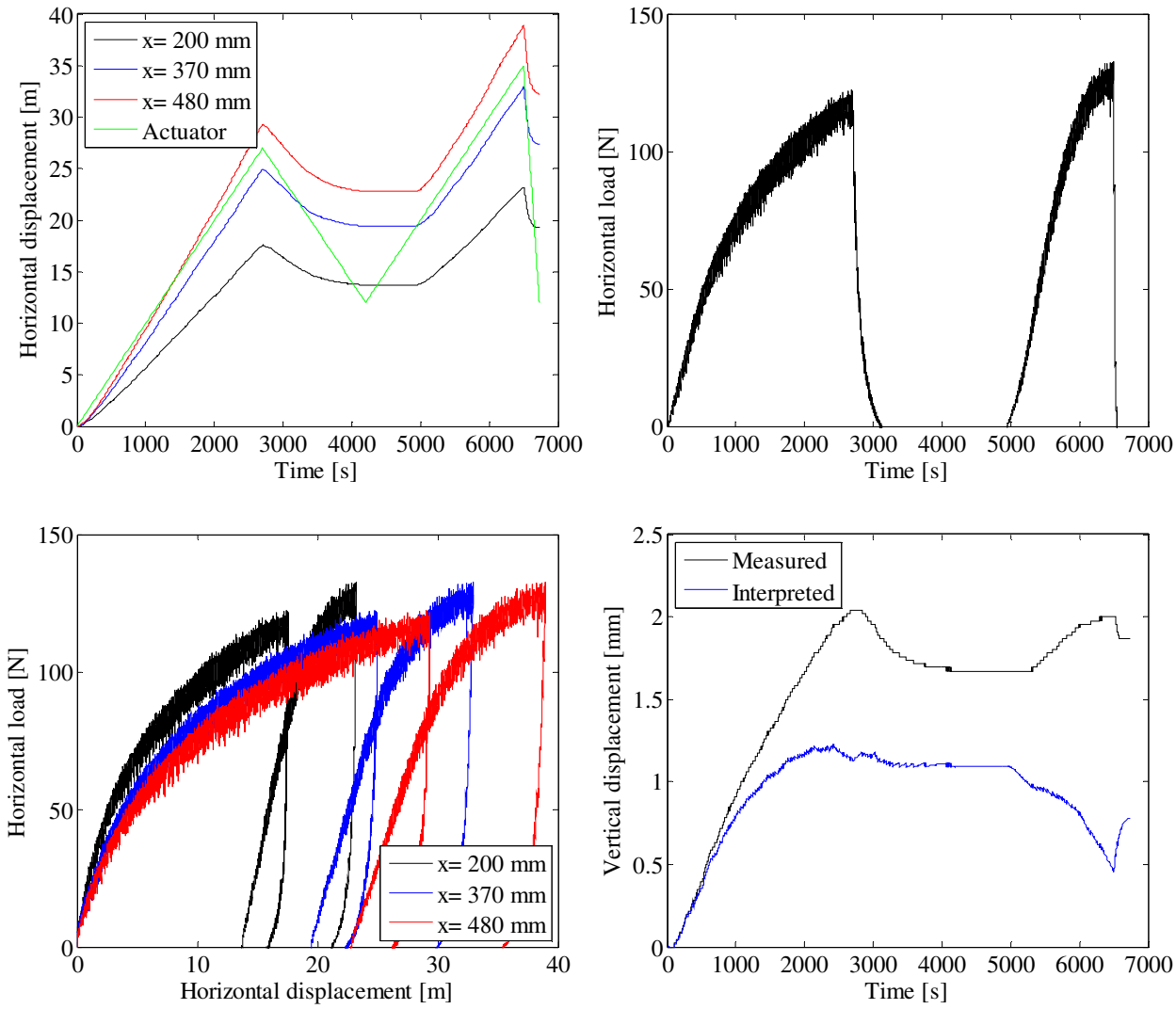

FIGURE 31. TOP LEFT: PILE DISPLACEMENT VERSUS TIME – TOP RIGHT: HORIZONTAL LOAD VERSUS TIME – BOTTOM LEFT: HORIZONTAL LOAD VERSUS PILE DISPLACEMENT – BOTTOM RIGHT: VERTICAL PILE DISPLACEMENT VERSUS TIME .

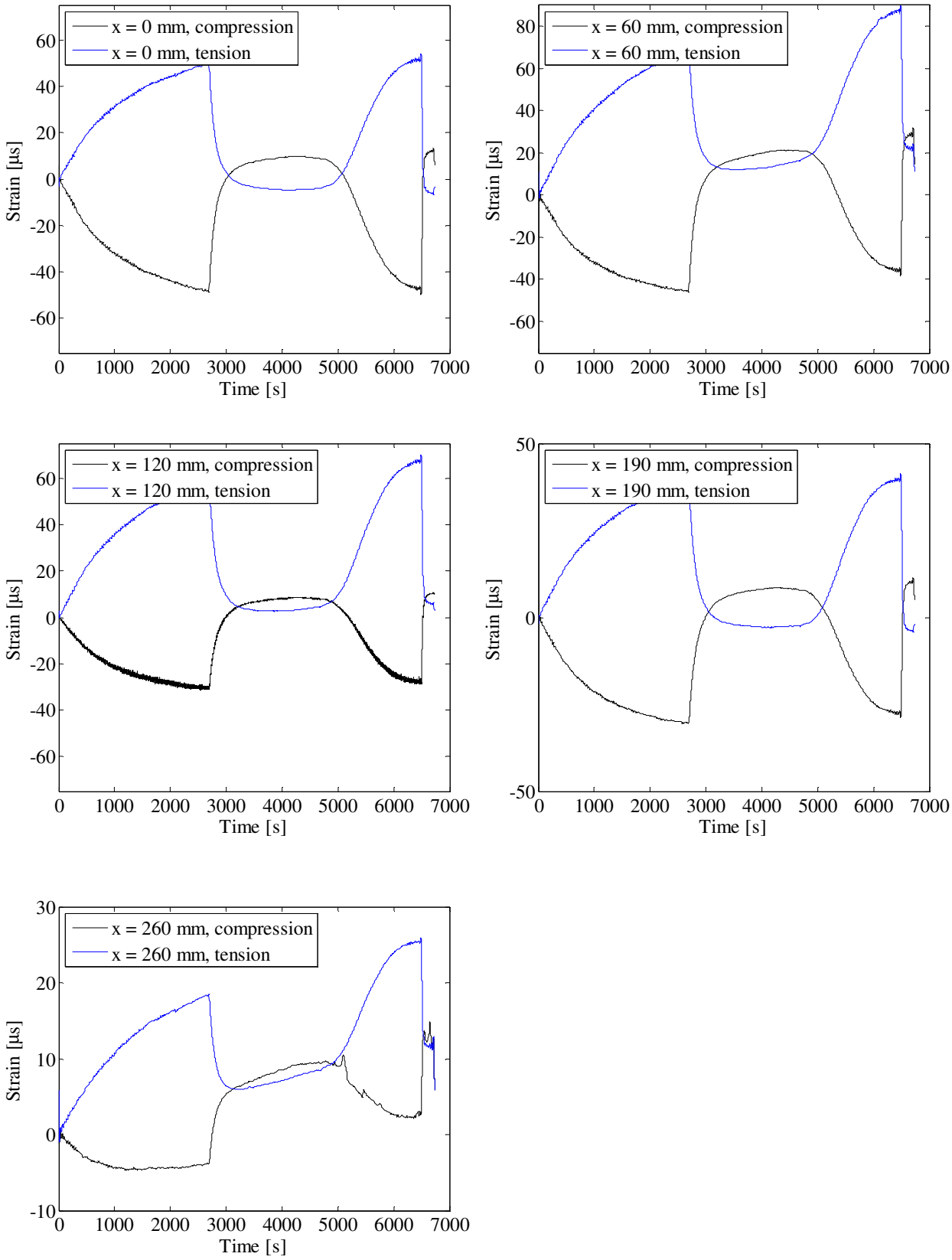

FIGURE 32. STRAIN GAUGE MEASUREMENTS.

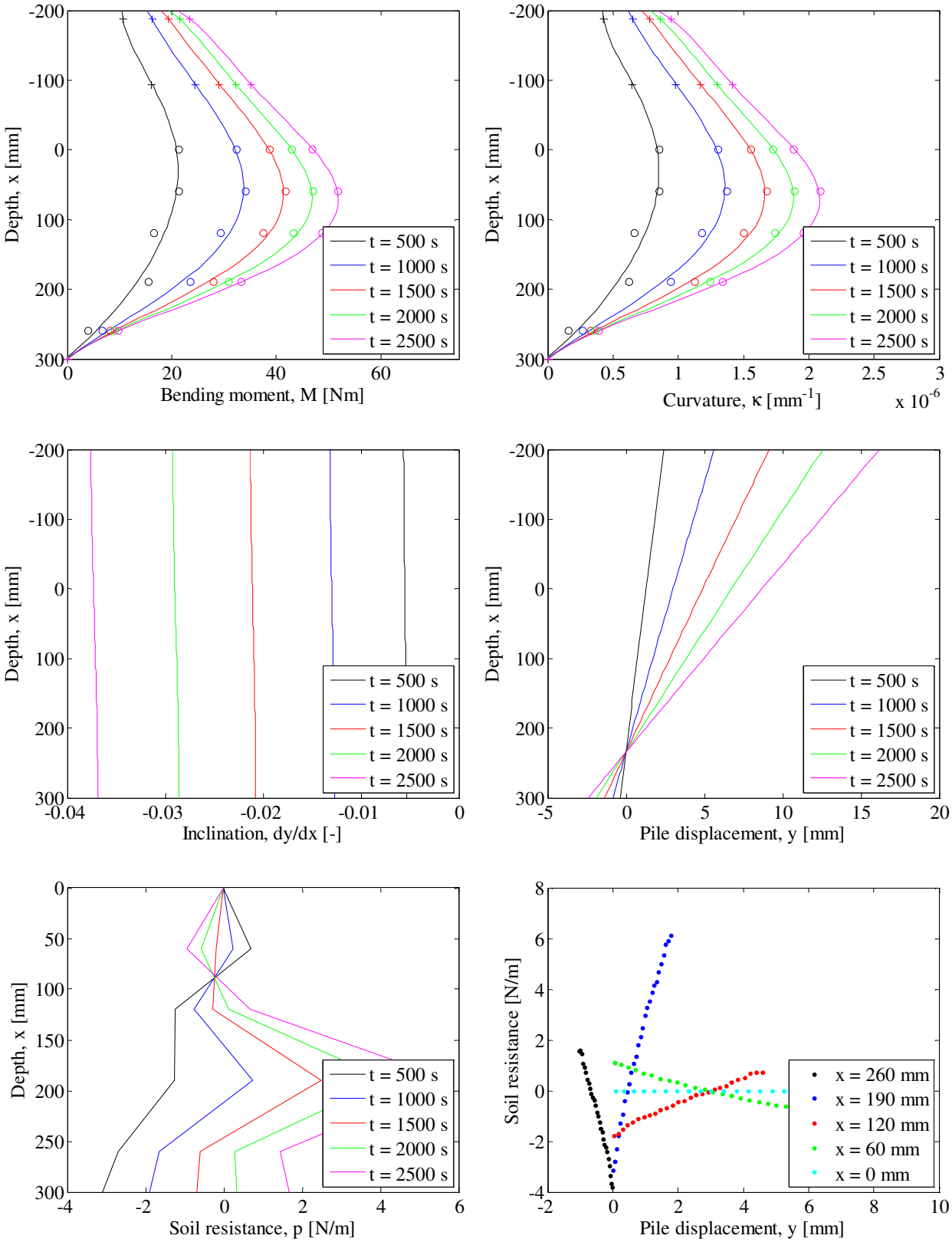

FIGURE 33. INTERPRETATION OF STRAIN GAUGE MEASUREMENTS. TOP LEFT: PILE BENDING MOMENT VERSUS DEPTH – TOP RIGHT: PILE CURVATURE VERSUS DEPTH – CENTER LEFT: PILE INCLINATION VERSUS DEPTH – CENTER RIGHT: PILE DISPLACEMENT VERSUS DEPTH – BOTTOM LEFT: SOIL RESISTANCE VERSUS DEPTH – BOTTOM RIGHT: P-Y CURVES.

Test 5: D = 60 mm, L_p = 300 mm and P_0 = 50 kPa (Closed-ended)

Pile type: Closed-ended	**Completed:** Spring 2009
Pile diameter (mm): 60	**No. of strain gauge levels:** 5 (All below soil surface)
Embedded pile length (mm): 300	**Overburden pressure (kPa):** 50
Slenderness ratio, *L*/*D*: 5	**Load eccentricity (mm):** 370
Pile wall thickness (mm): 5	**By:** S. P. H. Sørensen, K. T. Brødbæk and M. Møller
Comments:	

Soil parameters:

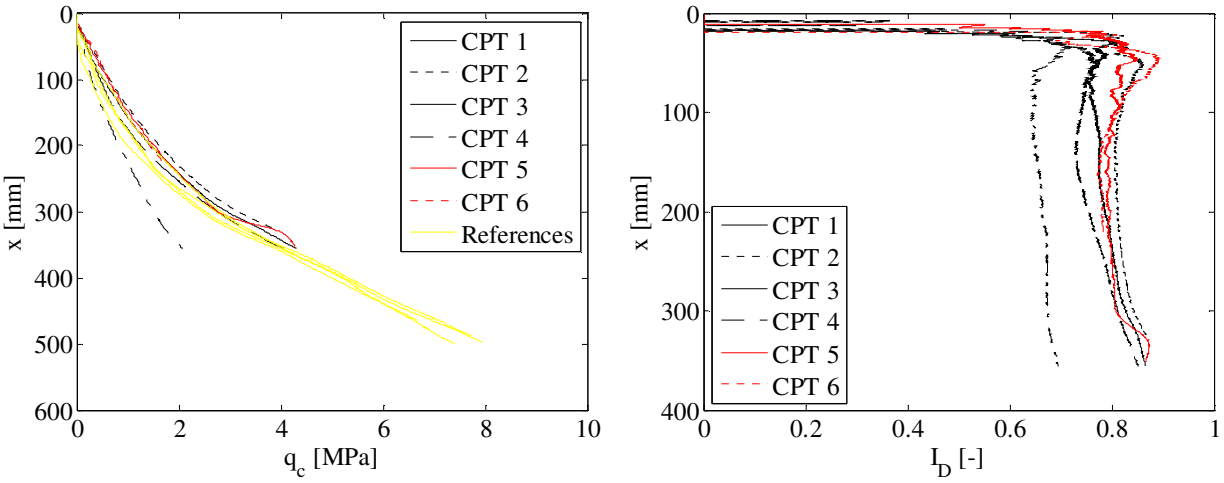

FIGURE 34. CPT-RESULTS FROM TEST 5. LEFT: TIP RESISTANCE VERSUS DEPTH – RIGHT: RELATIVE DENSITY VERSUS DEPTH.

TABLE 8. ESTIMATED SOIL PARAMETERS FOR TEST 5.

Relative density, I_D	Internal friction angle, φ_{tr}	Dilatancy angle, ψ_{tr}	Effective unit weight, γ'	Tangential Young's modulus of elasticity, E_0	Poisson's ratio, ν
[-]	[◦]	[◦]	[kN/m^3]	[MPa]	[-]
0.78	48.3	16.9	10.1	24.9	0.23

Test results:

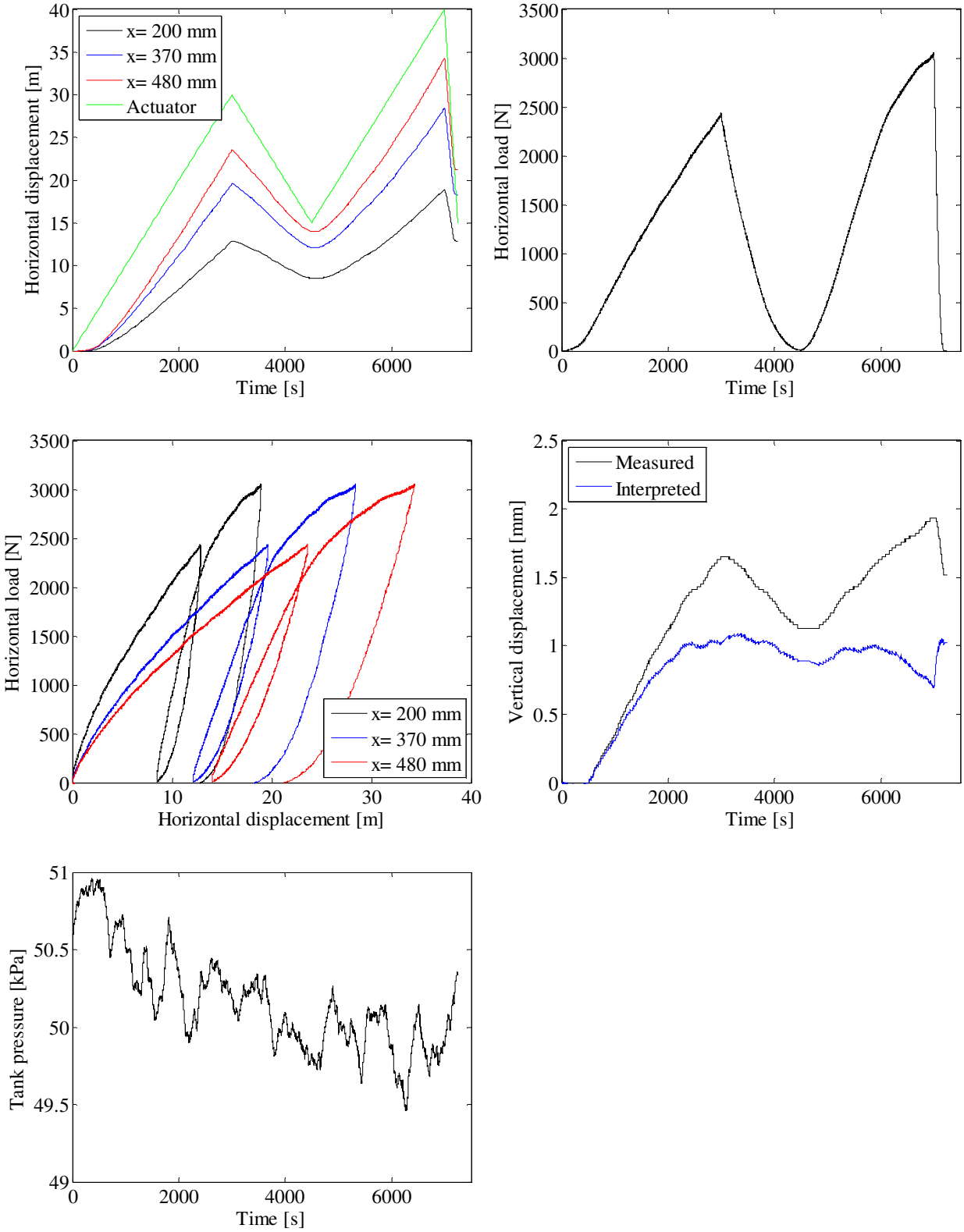

FIGURE 35. TOP LEFT: PILE DISPLACEMENT VERSUS TIME – TOP RIGHT: HORIZONTAL LOAD VERSUS TIME – CENTER LEFT: HORIZONTAL LOAD VERSUS PILE DISPLACEMENT – CENTER RIGHT: VERTICAL PILE DISPLACEMENT VERSUS TIME – BOTTOM LEFT: TANK PRESSURE VERSUS TIME.

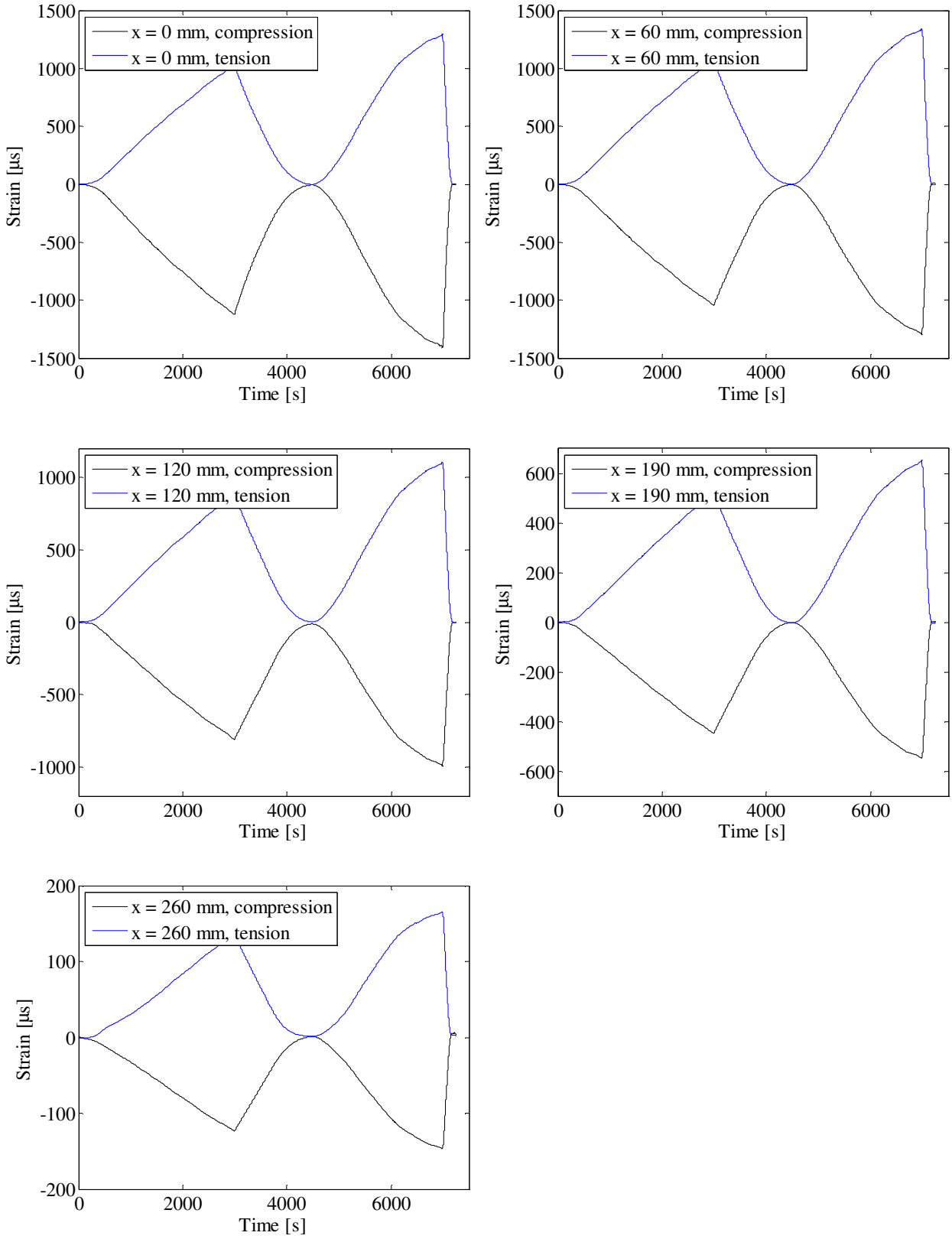

FIGURE 36. STRAIN GAUGE MEASUREMENTS.

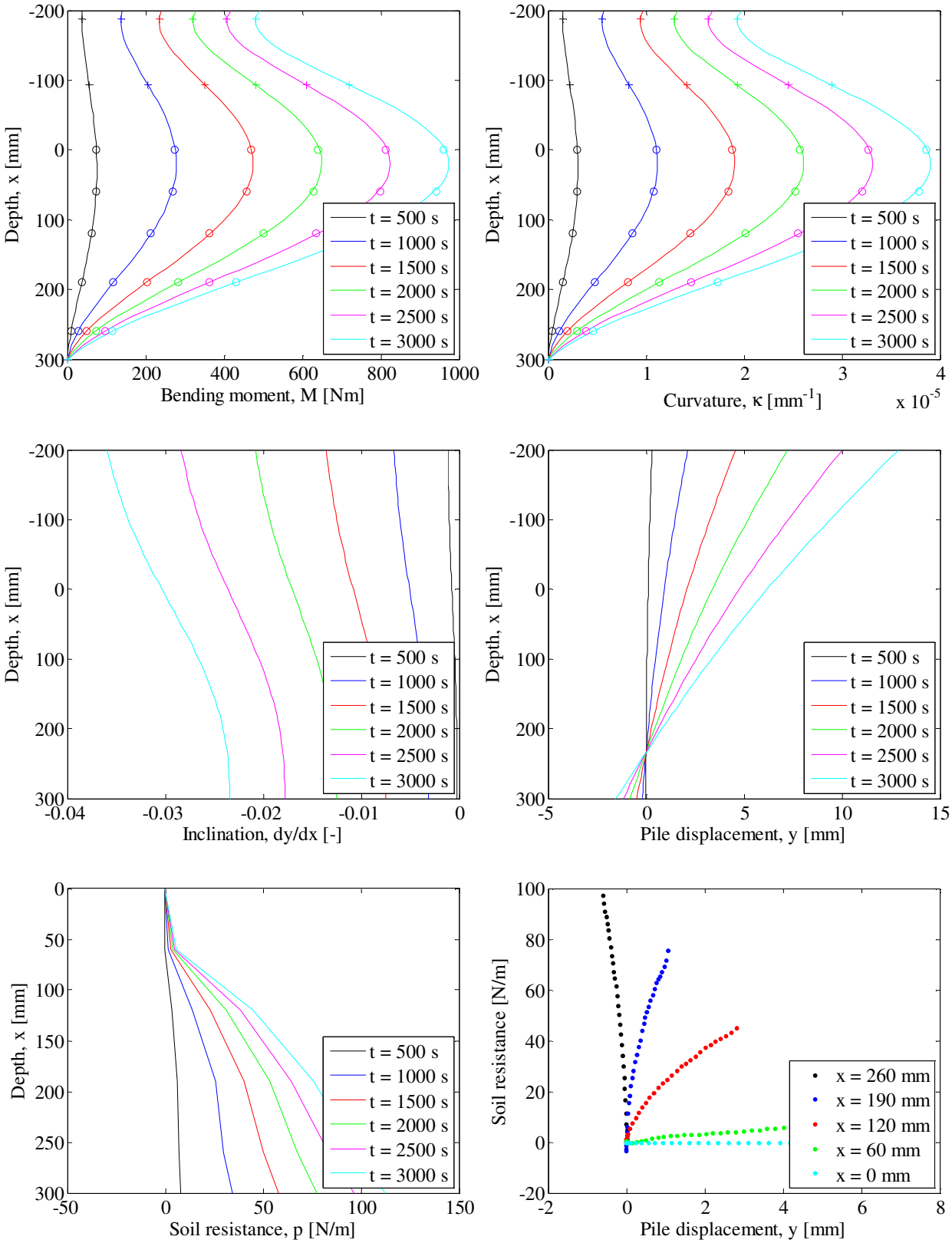

FIGURE 37. INTERPRETATION OF STRAIN GAUGE MEASUREMENTS. TOP LEFT: PILE BENDING MOMENT VERSUS DEPTH – TOP RIGHT: PILE CURVATURE VERSUS DEPTH – CENTER LEFT: PILE INCLINATION VERSUS DEPTH – CENTER RIGHT: PILE DISPLACEMENT VERSUS DEPTH – BOTTOM LEFT: SOIL RESISTANCE VERSUS DEPTH – BOTTOM RIGHT: P-Y CURVES.

Test 6: D = 60 mm, L_p = 300 mm and P_0 = 100 kPa (Closed-ended)

Pile type: Closed-ended	**Completed:** Spring 2009
Pile diameter (mm): 60	**No. of strain gauge levels:** 5 (All below soil surface)
Embedded pile length (mm): 300	**Overburden pressure (kPa):** 100
Slenderness ratio, L/D: 5	**Load eccentricity (mm):** 370
Pile wall thickness (mm): 5	**By:** S. P. H. Sørensen, K. T. Brødbæk and M. Møller
Comments: The strain gauge loaded in tension at a depth of 60 mm was in overflow for strains larger than 1270 µm/m. When the strain gauge is not in overflow both the strain gauge in compression and tension is considered for that level, while the strain gauge in compression is considered to be representative when the gauge loaded in tension is in overflow.	

Soil parameters:

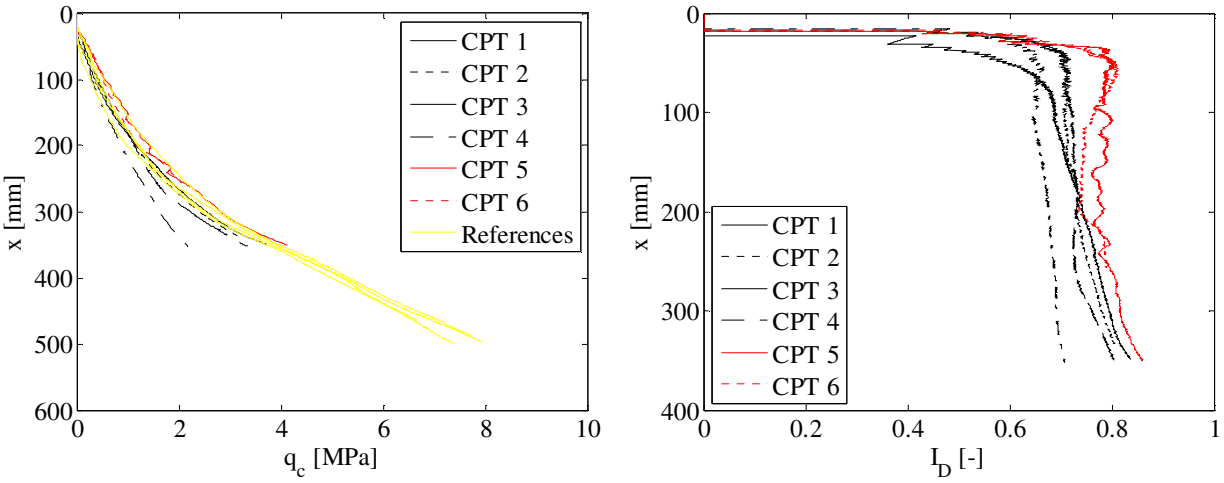

FIGURE 38. CPT-RESULTS FROM TEST 6. LEFT: TIP RESISTANCE VERSUS DEPTH – RIGHT: RELATIVE DENSITY VERSUS DEPTH.

TABLE 9. ESTIMATED SOIL PARAMETERS FOR TEST 6.

Relative density, I_D	Internal friction angle, φ_{tr}	Dilatancy angle, ψ_{tr}	Effective unit weight, γ'	Tangential Young's modulus of elasticity, E_0	Poisson's ratio, ν
[-]	[◦]	[◦]	[kN/m^3]	[MPa]	[-]
0.75	45.1	16.2	10.1	37.4	0.23

Test results:

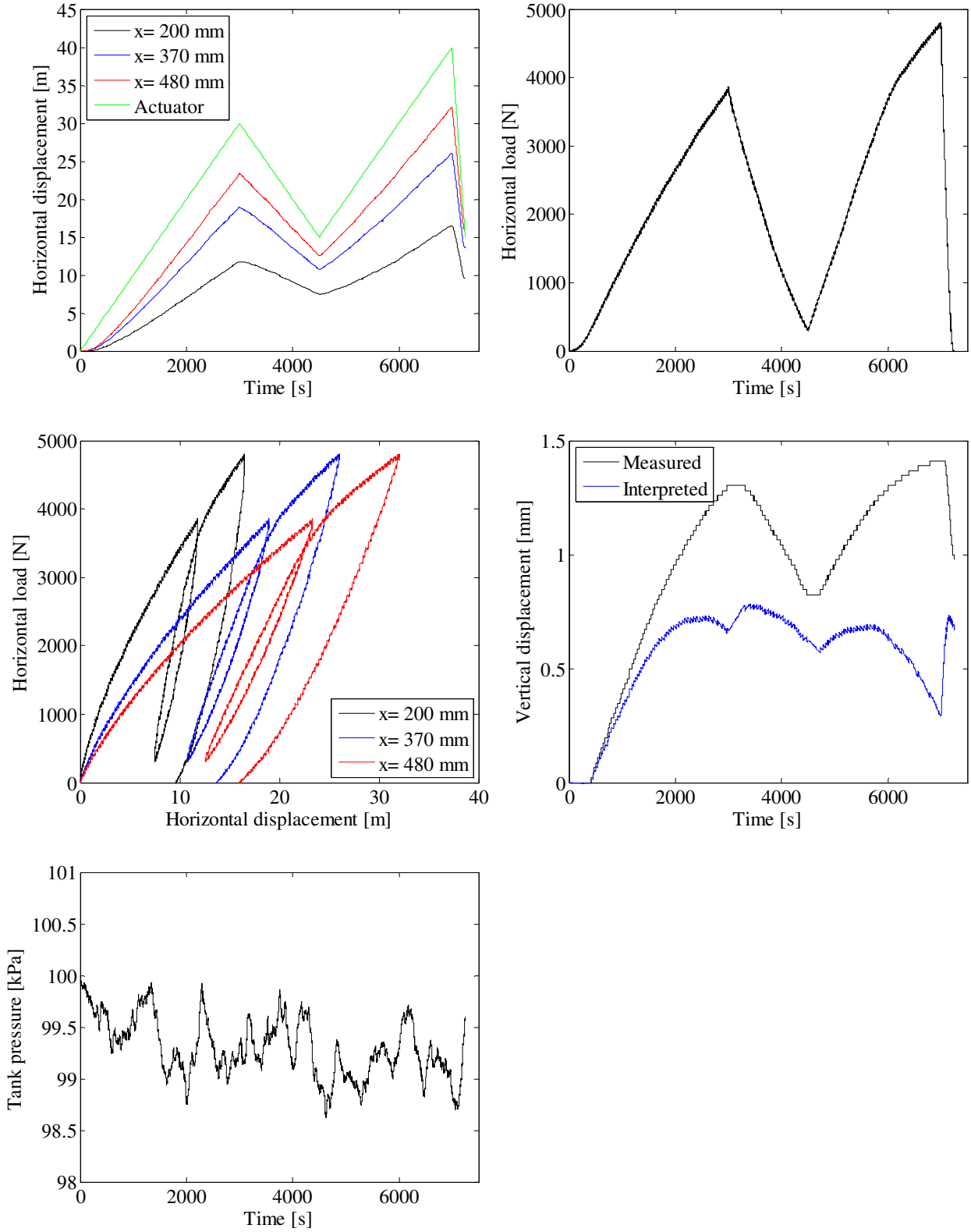

FIGURE 39. TOP LEFT: PILE DISPLACEMENT VERSUS TIME – TOP RIGHT: HORIZONTAL LOAD VERSUS TIME – CENTER LEFT: HORIZONTAL LOAD VERSUS PILE DISPLACEMENT – CENTER RIGHT: VERTICAL PILE DISPLACEMENT VERSUS TIME – BOTTOM LEFT: TANK PRESSURE VERSUS TIME.

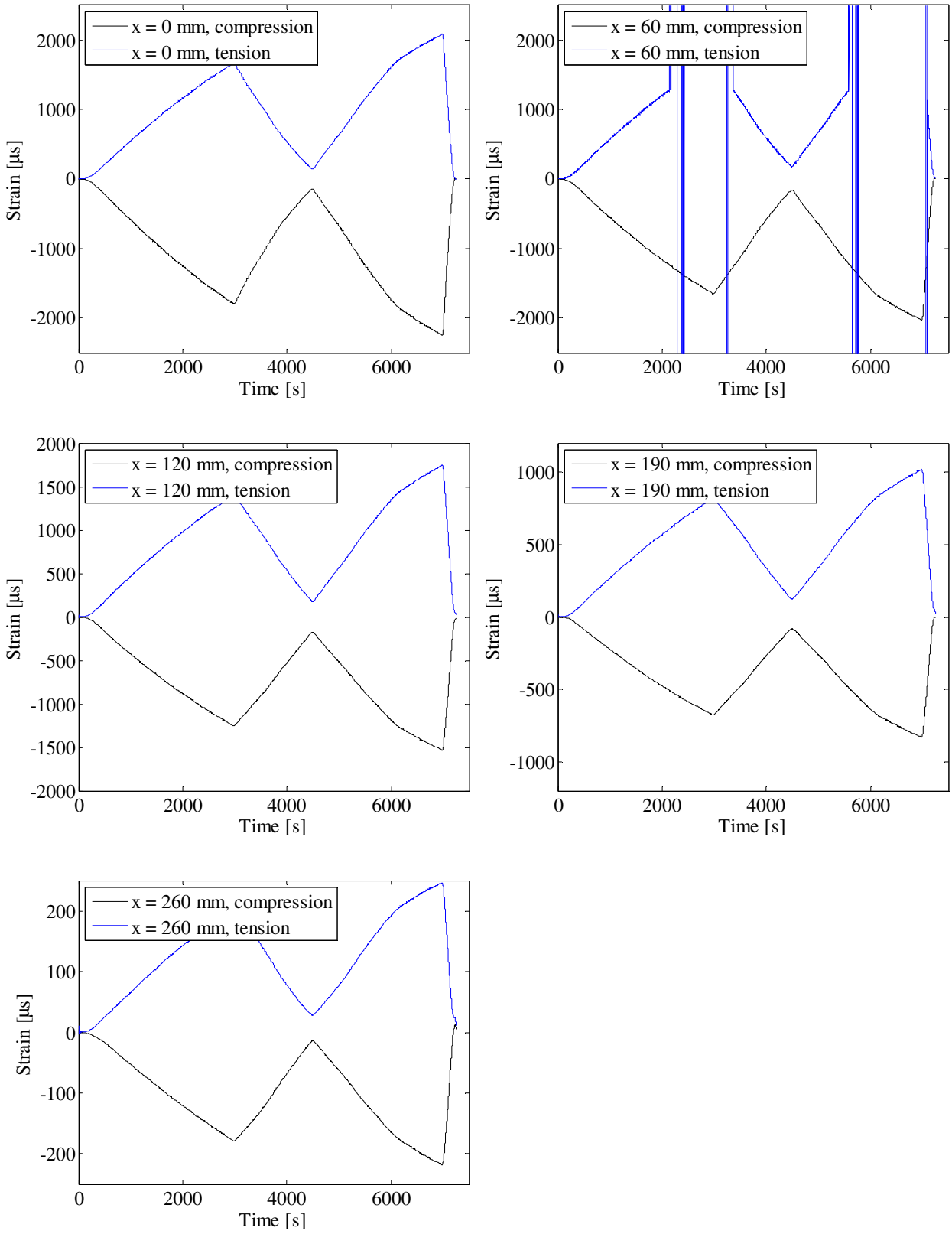

FIGURE 40. STRAIN GAUGE MEASUREMENTS.

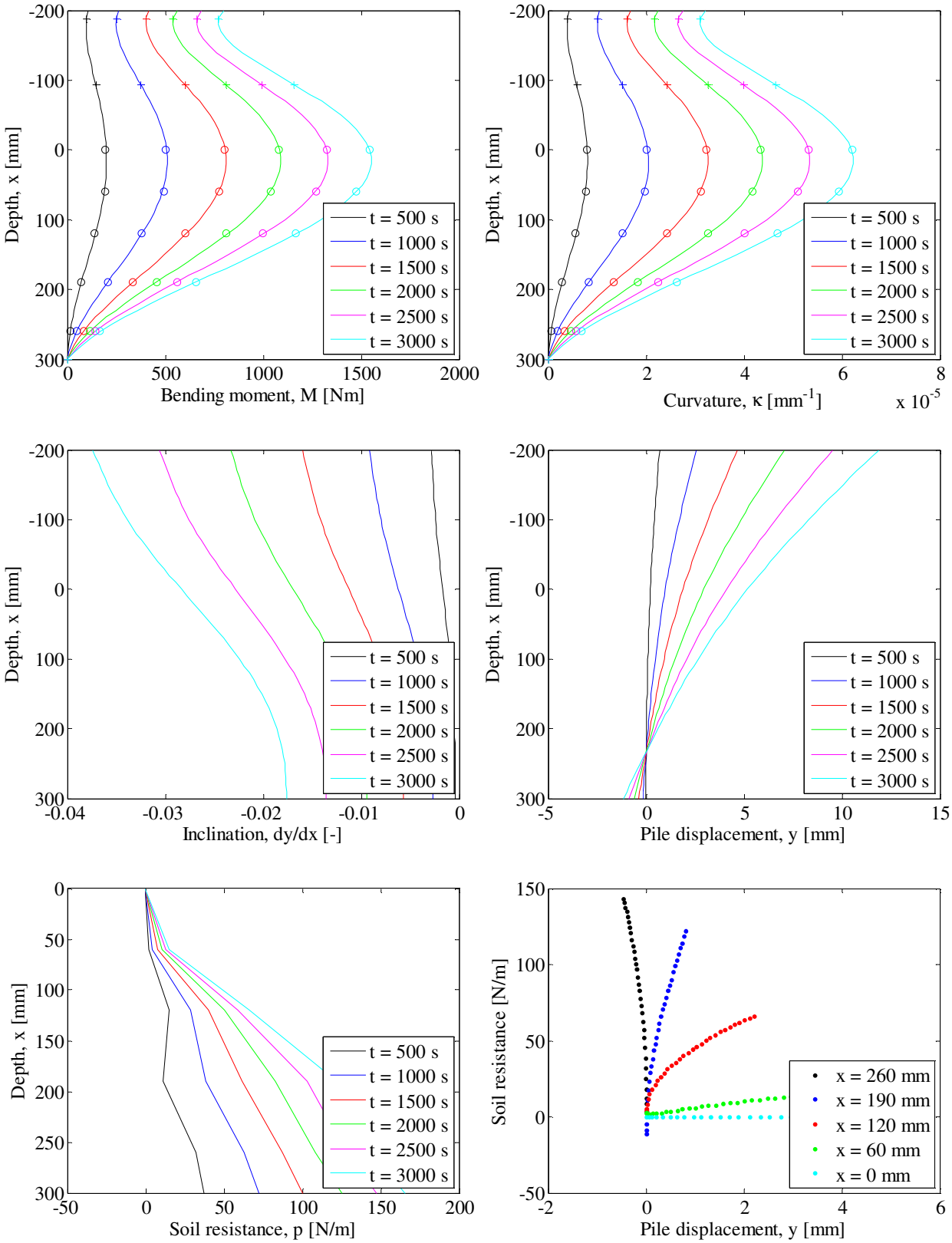

FIGURE 41. INTERPRETATION OF STRAIN GAUGE MEASUREMENTS. TOP LEFT: PILE BENDING MOMENT VERSUS DEPTH – TOP RIGHT: PILE CURVATURE VERSUS DEPTH – CENTER LEFT: PILE INCLINATION VERSUS DEPTH – CENTER RIGHT: PILE DISPLACEMENT VERSUS DEPTH – BOTTOM LEFT: SOIL RESISTANCE VERSUS DEPTH – BOTTOM RIGHT: P-Y CURVES.

Test 7: D = 80 mm, L_p = 240 mm and P_0 = 0 kPa (Closed-ended)

Pile type: Closed-ended	**Completed:** Spring 2011
Pile diameter (mm): 80	**No. of strain gauge levels:** 0
Embedded pile length (mm): 240	**Overburden pressure (kPa):** 0
Slenderness ratio, *L*/*D*: 3	**Load eccentricity (mm):** 370
Pile wall thickness (mm): 5	**By:** A. B. Moreno, L. Mikalauskas and J. L. T. Diaz
Comments: For this test the pile extends 820 mm above the soil surface and the pile hereby blocks for the CPT-equipment. Therefore, it was not possible to conduct CPT's after the pile installation. It is assumed that the relative density of the soil is homogenous and of similar value compared with the previously conducted tests. Hereby, a relative density between 0.75 and 0.91 is expected. The soil parameters has therefore been estimated based on a relative density between 0.75 and 0.91. Due to the small pile embedment length only 3 strain gauges are positioned at the soil surface and below. Hence, p-y curves cannot be derived based on strain gauge measurements. Therefore, it was chosen not to measure the strain in the pile.	

Soil parameters:

TABLE 10. ESTIMATED SOIL PARAMETERS FOR TEST 7.

Relative density, I_D	Internal friction angle, φ_{tr}	Dilatancy angle, ψ_{tr}	Effective unit weight, γ'	Tangential Young's modulus of elasticity, E_0	Poisson's ratio, ν
[-]	[◦]	[◦]	[kN/m^3]	[MPa]	[-]
0.75-0.91	52.0-54.5	17.4-20.5	10.1-10.4	-	0.23

Test results:

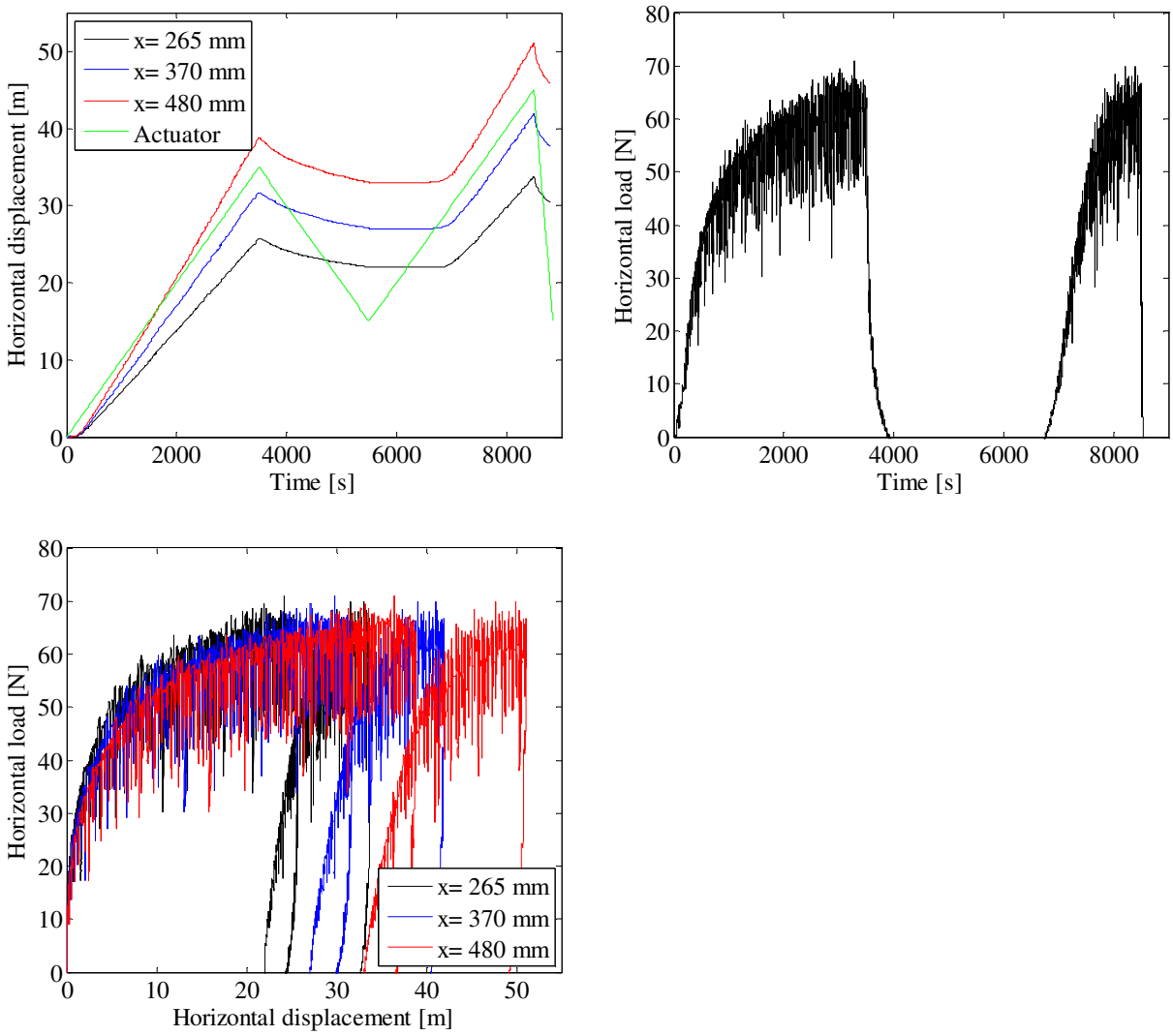

FIGURE 42. TOP LEFT: PILE DISPLACEMENT VERSUS TIME – TOP RIGHT: HORIZONTAL LOAD VERSUS TIME – BOTTOM LEFT: HORIZONTAL LOAD VERSUS PILE DISPLACEMENT.

Test 8: D = 80 mm, L_p = 240 mm and P_0 = 50 kPa (Closed-ended)

Pile type: Closed-ended	**Completed:** Spring 2011
Pile diameter (mm): 80	**No. of strain gauge levels:** 0
Embedded pile length (mm): 240	**Overburden pressure (kPa):** 50
Slenderness ratio, *L*/*D*: 3	**Load eccentricity (mm):** 370
Pile wall thickness (mm): 5	**By:** A. B. Moreno, L. Mikalauskas and J. L. T. Diaz

Comments:

For this test the pile extends 820 mm above the soil surface and the pile hereby blocks for the CPT-equipment. Therefore, it was not possible to conduct CPT's after the pile installation. It is assumed that the relative density of the soil is homogenous and of similar value compared with the previously conducted tests. Hereby, a relative density between 0.75 and 0.91 is expected. The soil parameters have therefore been estimated based on a relative density between 0.75 and 0.91.

Due to the small pile embedment length only 3 strain gauges are positioned at the soil surface and below. Hence, p-y curves cannot be derived based on strain gauge measurements. Therefore, it was chosen not to measure the strain in the pile.

The displacement transducer situated at 480 mm above the soil surface did not function.

After approximately 2500 s the water flow through the membrane increased suddenly to approximately 170 L/hour. This increase in the water causes the horizontal load to decrease by approximately 10 %. The results can therefore only be trusted for the first 2500 s of the test.

Soil parameters:

TABLE 11. ESTIMATED SOIL PARAMETERS FOR TEST 8.

Relative density, I_D	Internal friction angle, φ_{tr}	Dilatancy angle, ψ_{tr}	Effective unit weight, γ'	Tangential Young's modulus of elasticity, E_0	Poisson's ratio, ν
[-]	[◦]	[◦]	[kN/m^3]	[MPa]	[-]
0.75-0.91	48.0-51.0	16.3-19.5	10.1-10.4	23.6-31.8	0.23

Test results:

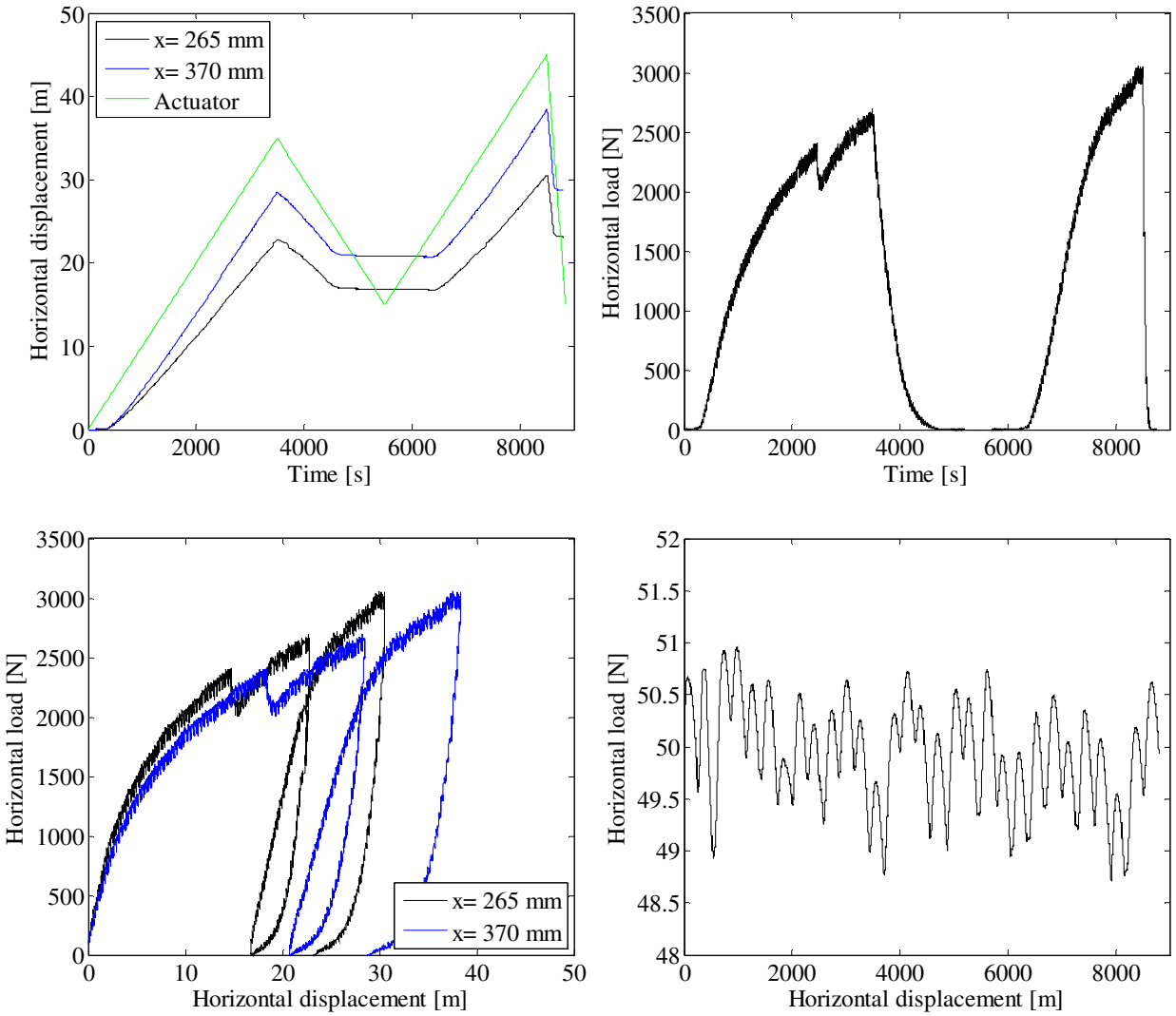

FIGURE 43. TOP LEFT: PILE DISPLACEMENT VERSUS TIME – TOP RIGHT: HORIZONTAL LOAD VERSUS TIME – BOTTOM LEFT: HORIZONTAL LOAD VERSUS PILE DISPLACEMENT – BOTTOM RIGHT: TANK PRESSURE VERSUS TIME.

Test 9: D = 80 mm, L_p = 240 mm and P_0 = 100 kPa (Closed-ended)

Pile type: Closed-ended	**Completed:** Spring 2011
Pile diameter (mm): 80	**No. of strain gauge levels:** 0
Embedded pile length (mm): 240	**Overburden pressure (kPa):** 100
Slenderness ratio, *L*/*D*: 3	**Load eccentricity (mm):** 370
Pile wall thickness (mm): 5	**By:** A. B. Moreno, L. Mikalauskas and J. L. T. Diaz
Comments: For this test the pile extends 820 mm above the soil surface and the pile hereby blocks for the CPT-equipment. Therefore, it was not possible to conduct CPT's after the pile installation. It is assumed that the relative density of the soil is homogenous and of similar value compared with the previously conducted tests. Hereby, a relative density between 0.75 and 0.91 is expected. The soil parameters has therefore been estimated based on a relative density between 0.75 and 0.91. Due to the small pile embedment length only 3 strain gauges are positioned at the soil surface and below. Hence, p-y curves cannot be derived based on strain gauge measurements. Therefore, it was chosen not to measure the strain in the pile.	

Soil parameters:

TABLE 12. ESTIMATED SOIL PARAMETERS FOR TEST 9.

Relative density, I_D	Internal friction angle, φ_{tr}	Dilatancy angle, ψ_{tr}	Effective unit weight, γ'	Tangential Young's modulus of elasticity, E_0	Poisson's ratio, ν
[-]	[◦]	[◦]	[kN/m^3]	[MPa]	[-]
0.75-0.91	45.3-48.1	15.4-18.6	10.1-10.4	37.8-51.5	0.23

Test results:

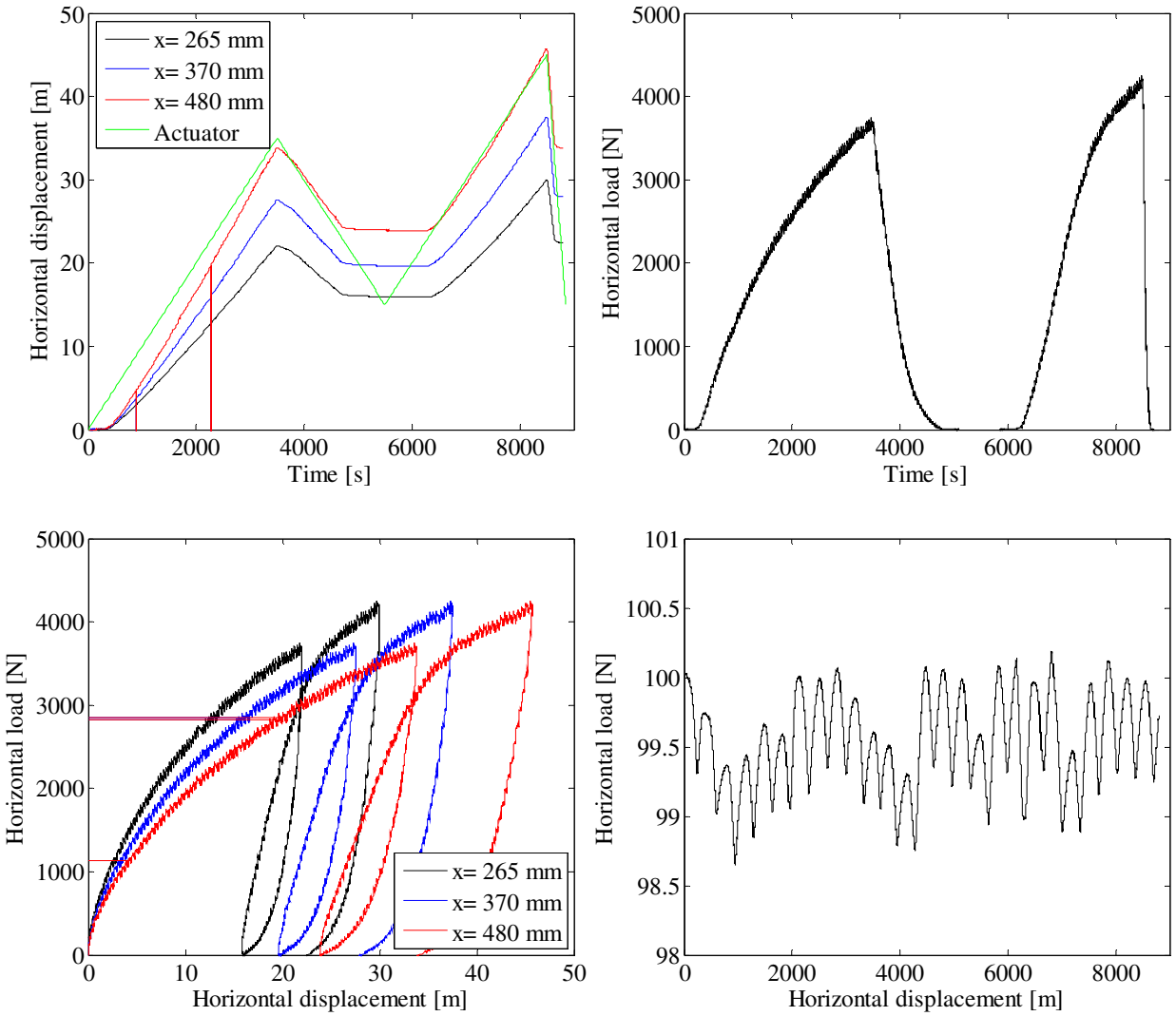

FIGURE 44. TOP LEFT: PILE DISPLACEMENT VERSUS TIME – TOP RIGHT: HORIZONTAL LOAD VERSUS TIME – BOTTOM LEFT: HORIZONTAL LOAD VERSUS PILE DISPLACEMENT – BOTTOM RIGHT: TANK PRESSURE VERSUS TIME.

Test 10: D = 80 mm, L_p = 320 mm and P_0 = 0 kPa (Open-ended)

Pile type: Open-ended	**Completed:** Summer 2010
Pile diameter (mm): 80	**No. of strain gauge levels:** 0
Embedded pile length (mm): 320	**Overburden pressure (kPa):** 0
Slenderness ratio, *L*/*D*: 4	**Load eccentricity (mm):** 370
Pile wall thickness (mm): 5	**By:** S. P. H. Sørensen
Comments:	

Soil parameters:

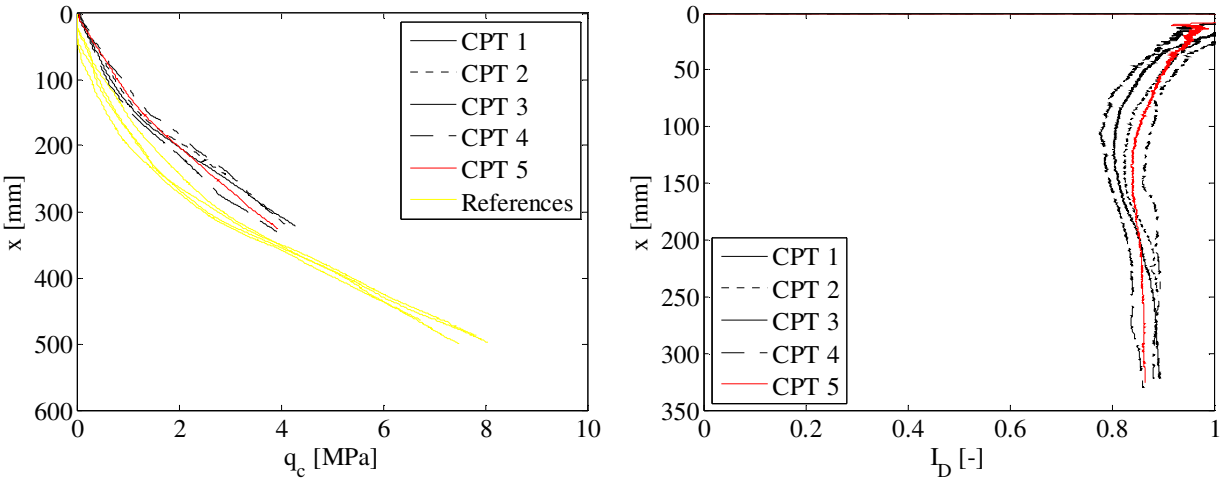

FIGURE 45. CPT-RESULTS FROM TEST 10. LEFT: TIP RESISTANCE VERSUS DEPTH – RIGHT: RELATIVE DENSITY VERSUS DEPTH.

TABLE 13. ESTIMATED SOIL PARAMETERS FOR TEST 10.

Relative density, I_D	Internal friction angle, φ_{tr}	Dilatancy angle, ψ_{tr}	Effective unit weight, γ'	Tangential Young's modulus of elasticity, E_0	Poisson's ratio, ν
[-]	[◦]	[◦]	[kN/m^3]	[MPa]	[-]
0.85	53.6	19.4	10.3	-	0.23

Test results:

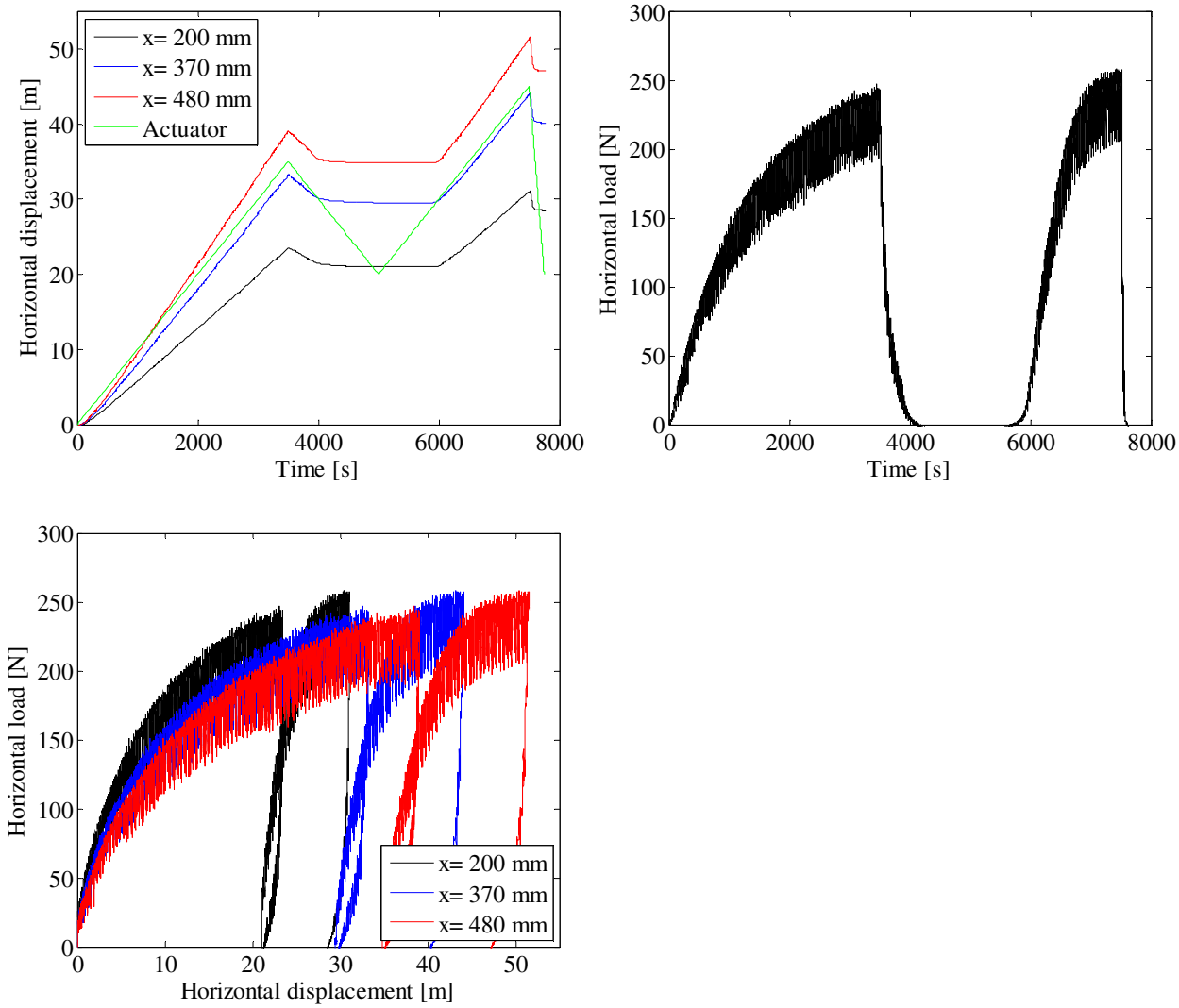

FIGURE 46. TOP LEFT: PILE DISPLACEMENT VERSUS TIME – TOP RIGHT: HORIZONTAL LOAD VERSUS TIME – BOTTOM LEFT: HORIZONTAL LOAD VERSUS PILE DISPLACEMENT.

Test 11: D = 80 mm, L_p = 320 mm and P_0 = 0 kPa (Closed-ended)

Pile type: Closed-ended	**Completed:** Summer 2010
Pile diameter (mm): 80	**No. of strain gauge levels:** 11 (5 below soil surface)
Embedded pile length (mm): 320	**Overburden pressure (kPa):** 0
Slenderness ratio, L/D: 4	**Load eccentricity (mm):** 370
Pile wall thickness (mm): 5	**By:** S. P. H. Sørensen
Comments: No signal was received from strain gauge 2, 5, 12, 16 and 17. In the interpretation of the strain gauge measurements strain gauge 1, 4 and 13 are therefore assumed to be representative for the curvature at these depths.	

Soil parameters:

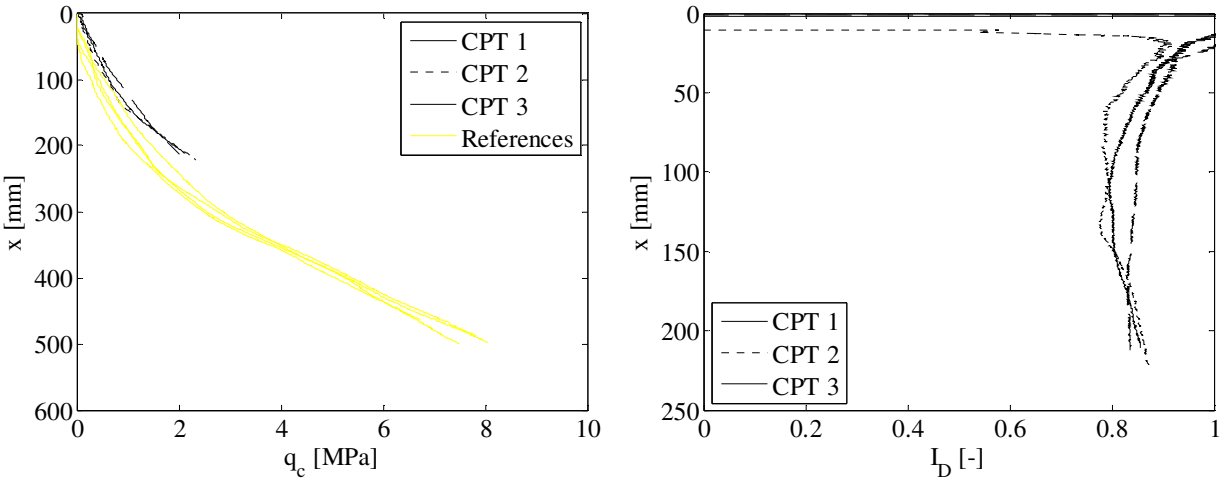

FIGURE 47. CPT-RESULTS FROM TEST 11. LEFT: TIP RESISTANCE VERSUS DEPTH – RIGHT: RELATIVE DENSITY VERSUS DEPTH.

TABLE 14. ESTIMATED SOIL PARAMETERS FOR TEST 11.

Relative density, I_D	Internal friction angle, φ_{tr}	Dilatancy angle, ψ_{tr}	Effective unit weight, γ'	Tangential Young's modulus of elasticity, E_0	Poisson's ratio, ν
[-]	[◦]	[◦]	[kN/m^3]	[MPa]	[-]
0.83	53.2	18.6	10.2	-	0.23

Test results:

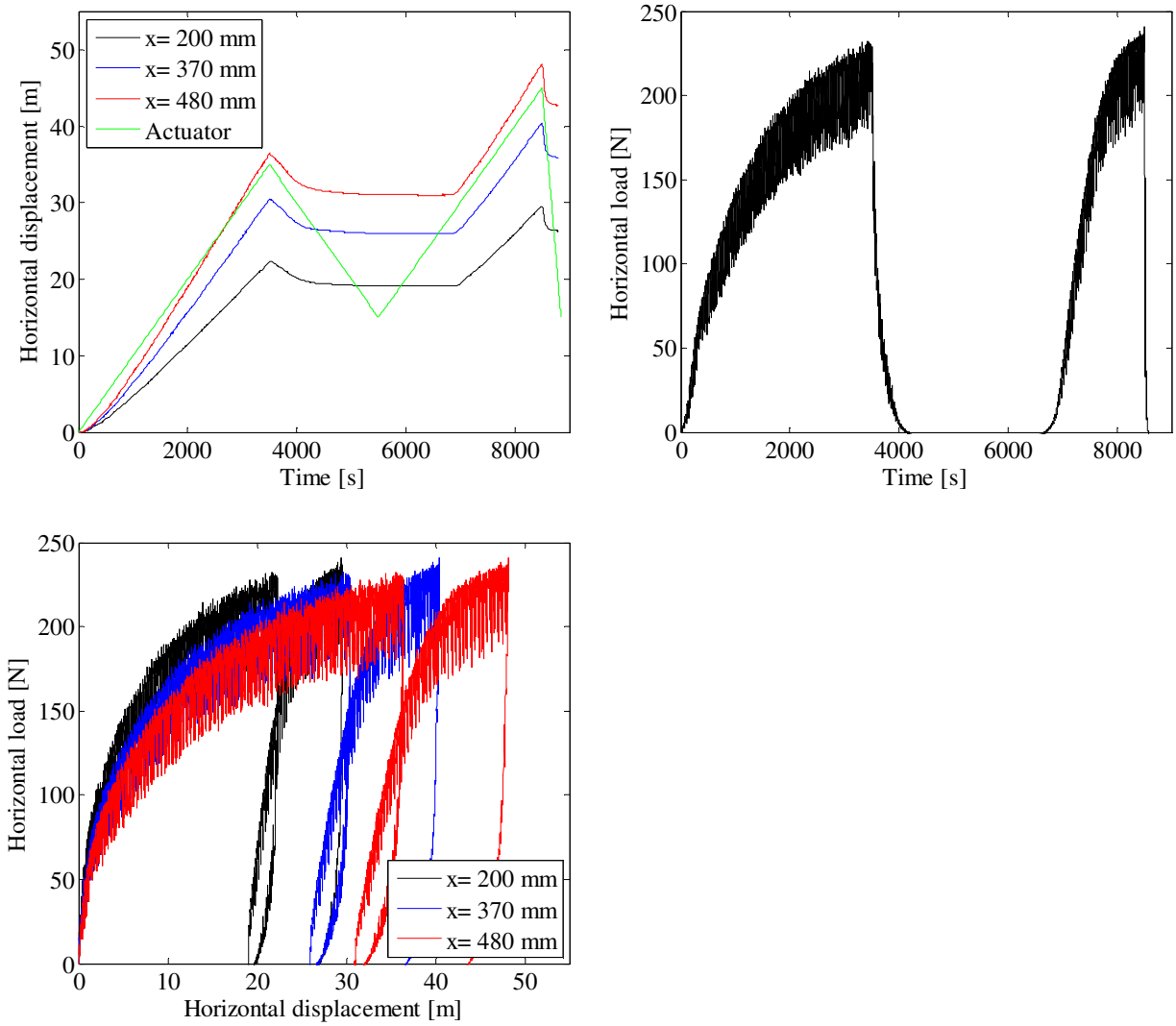

FIGURE 48. TOP LEFT: PILE DISPLACEMENT VERSUS TIME – TOP RIGHT: HORIZONTAL LOAD VERSUS TIME – BOTTOM LEFT: HORIZONTAL LOAD VERSUS PILE DISPLACEMENT.

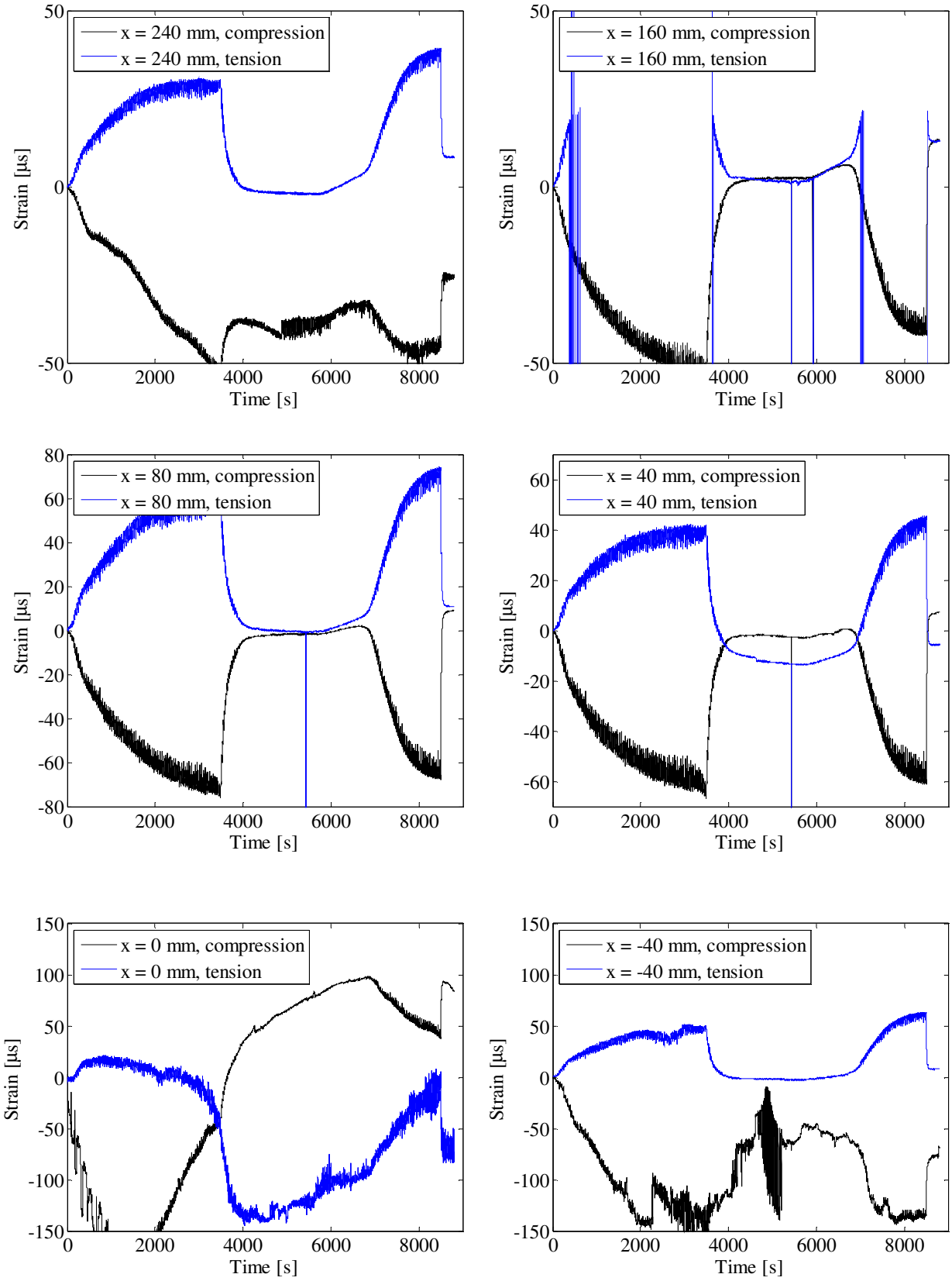

FIGURE 49. STRAIN GAUGE MEASUREMENTS.

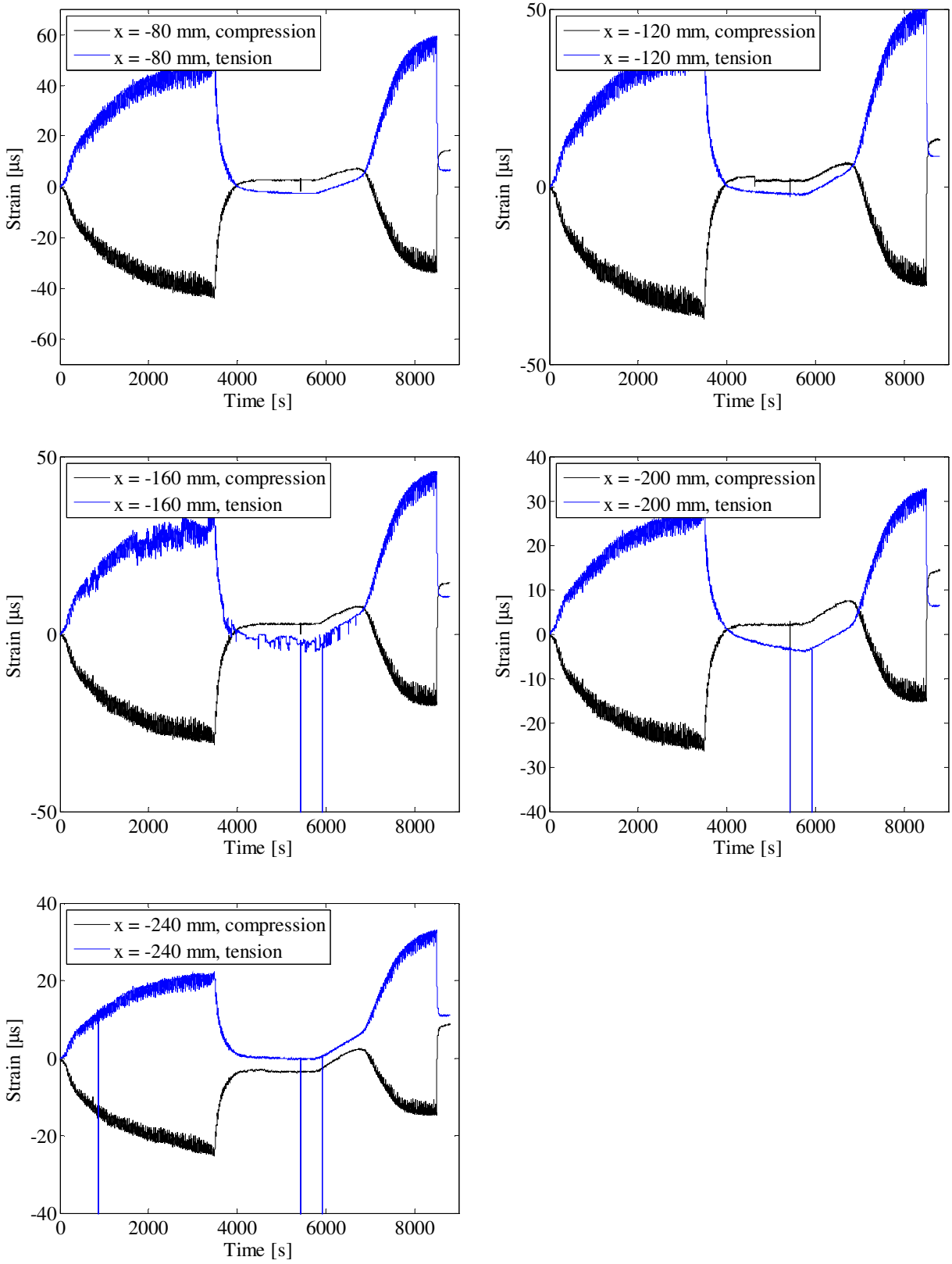

FIGURE 50. STRAIN GAUGE MEASUREMENTS.

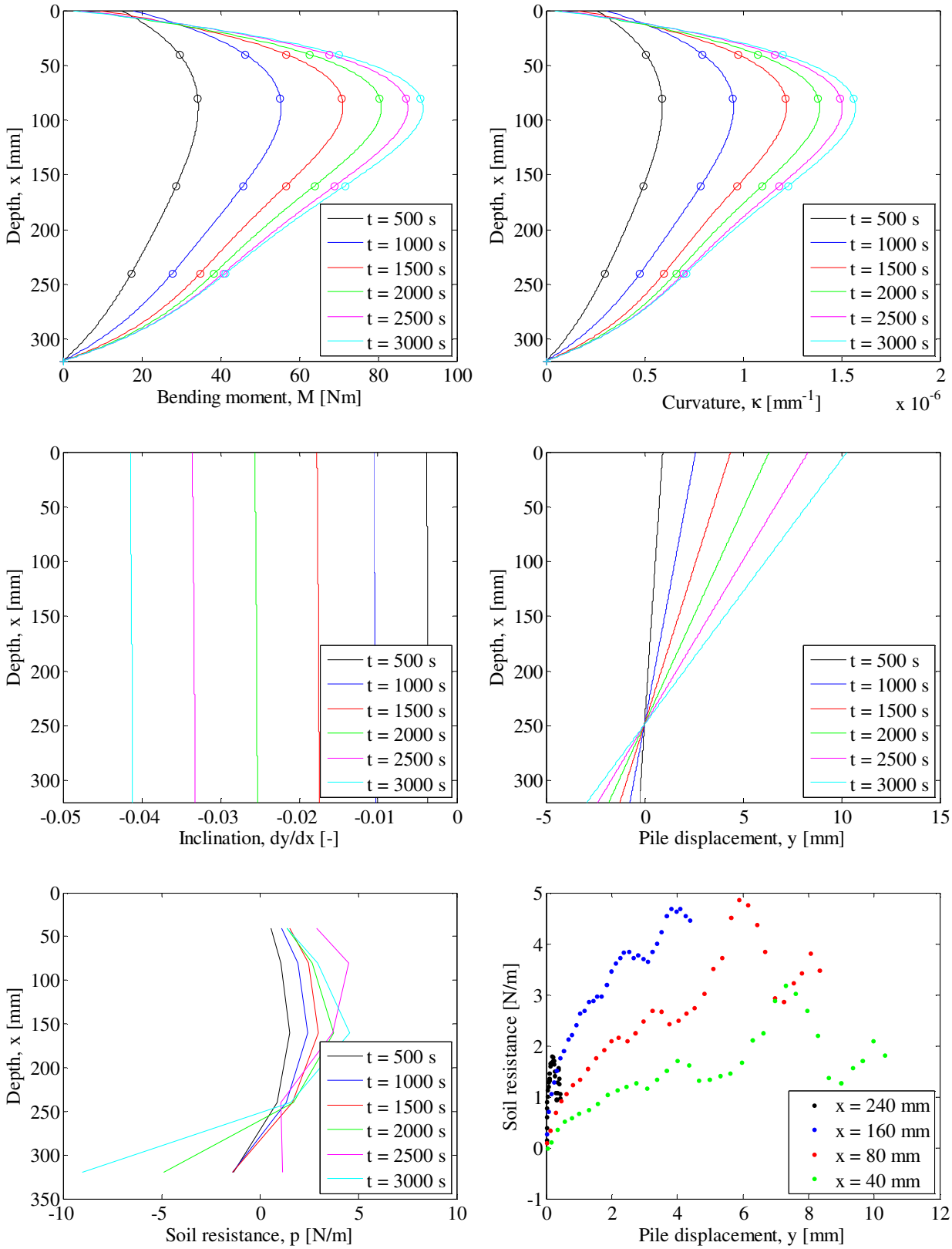

FIGURE 51. INTERPRETATION OF STRAIN GAUGE MEASUREMENTS. TOP LEFT: PILE BENDING MOMENT VERSUS DEPTH – TOP RIGHT: PILE CURVATURE VERSUS DEPTH – CENTER LEFT: PILE INCLINATION VERSUS DEPTH – CENTER RIGHT: PILE DISPLACEMENT VERSUS DEPTH – BOTTOM LEFT: SOIL RESISTANCE VERSUS DEPTH – BOTTOM RIGHT: P-Y CURVES.

Test 12: D = 80 mm, L_p = 320 mm and P_0 = 50 kPa (Closed-ended)

Pile type: Closed-ended	**Completed:** Summer 2010
Pile diameter (mm): 80	**No. of strain gauge levels:** 11 (5 below soil surface)
Embedded pile length (mm): 320	**Overburden pressure (kPa):5** 0
Slenderness ratio, *L*/*D*: 4	**Load eccentricity (mm):** 370
Pile wall thickness (mm): 5	**By:** S. P. H. Sørensen
Comments: No signal was received from strain gauge 4, 15 and 21. In the interpretation of the strain gauge measurements strain gauge 10 is therefore assumed to be representative for the curvature at these depths.	

Soil parameters:

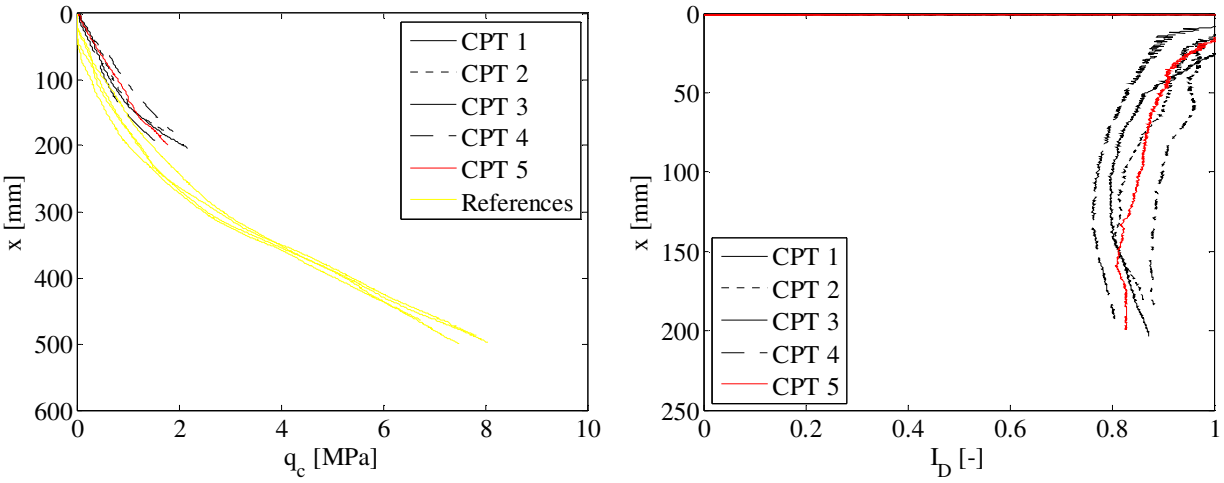

FIGURE 52. CPT-RESULTS FROM TEST 12. LEFT: TIP RESISTANCE VERSUS DEPTH – RIGHT: RELATIVE DENSITY VERSUS DEPTH.

TABLE 15. ESTIMATED SOIL PARAMETERS FOR TEST 12.

Relative density, I_D	Internal friction angle, φ_{tr}	Dilatancy angle, ψ_{tr}	Effective unit weight, γ'	Tangential Young's modulus of elasticity, E_0	Poisson's ratio, ν
[-]	[◦]	[◦]	[kN/m^3]	[MPa]	[-]
0.83	49.3	17.8	10.2	27.7	0.23

Test results:

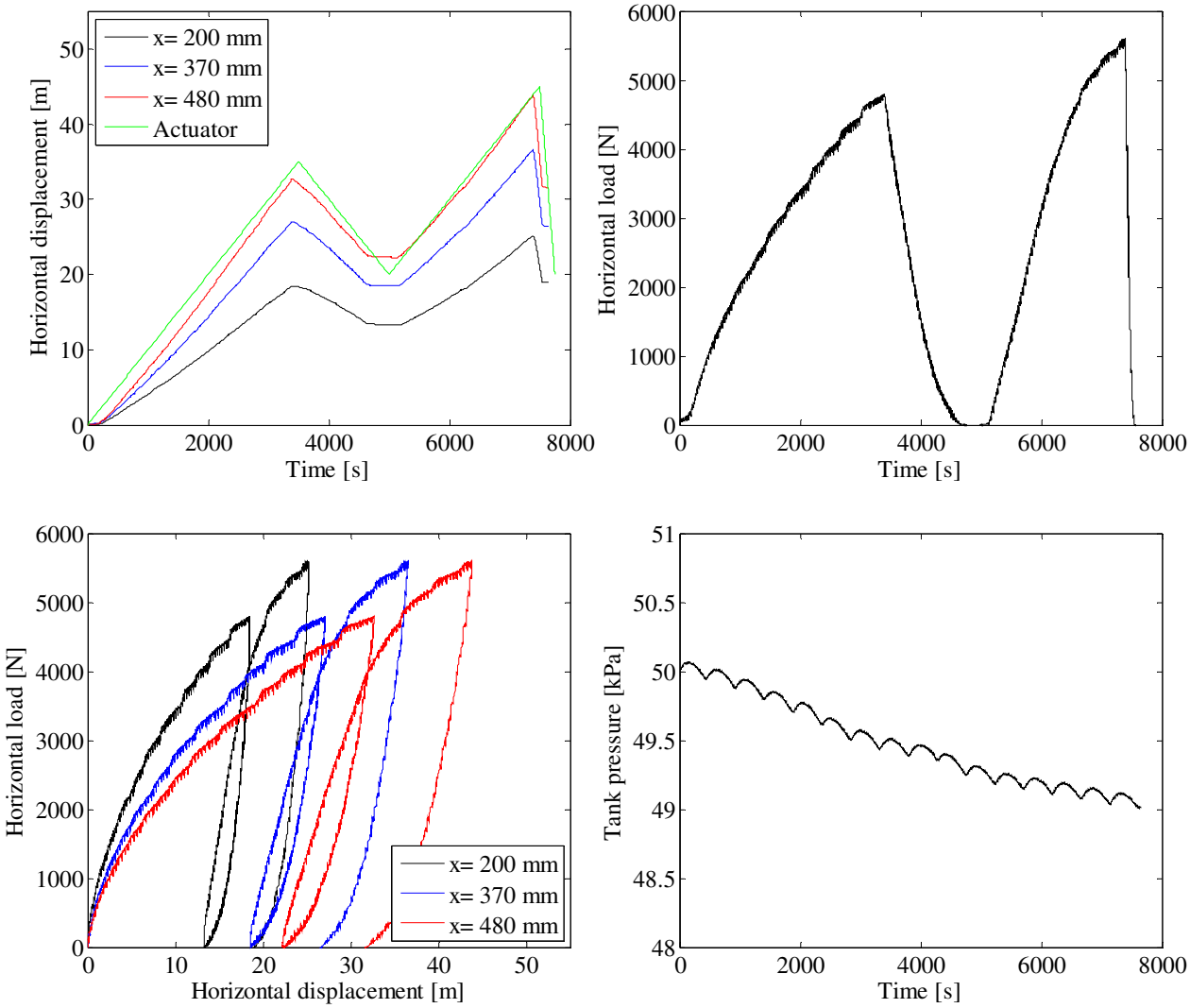

FIGURE 53. TOP LEFT: PILE DISPLACEMENT VERSUS TIME – TOP RIGHT: HORIZONTAL LOAD VERSUS TIME – BOTTOM LEFT: HORIZONTAL LOAD VERSUS PILE DISPLACEMENT – BOTTOM RIGHT: TANK PRESSURE VERSUS TIME.

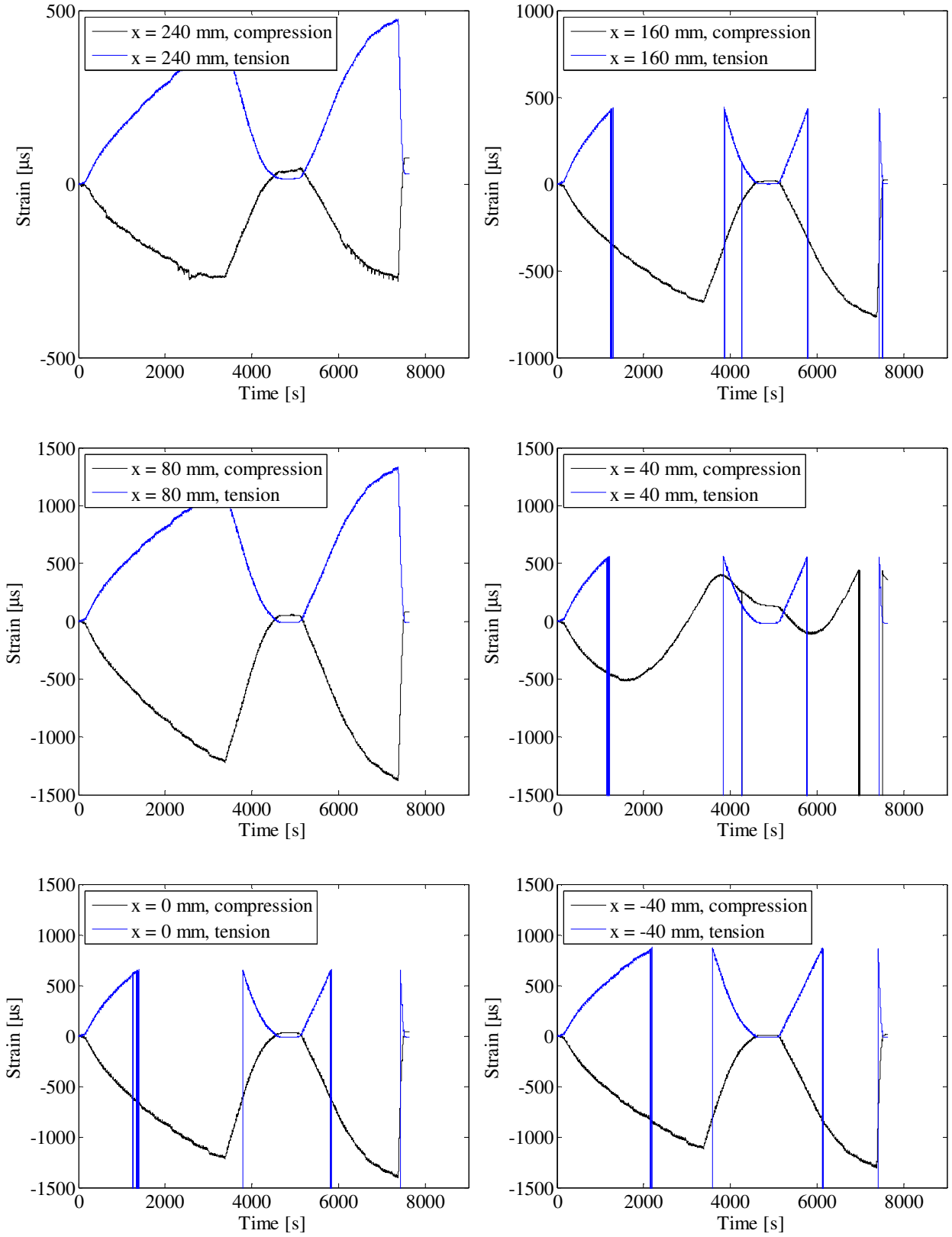

FIGURE 54. STRAIN GAUGE MEASUREMENTS.

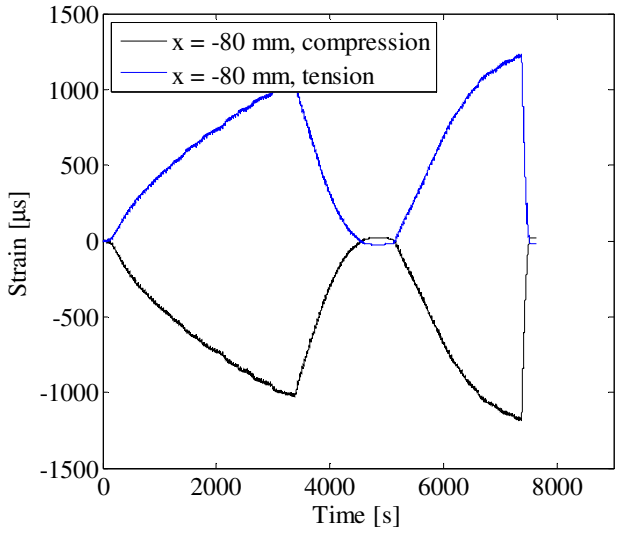

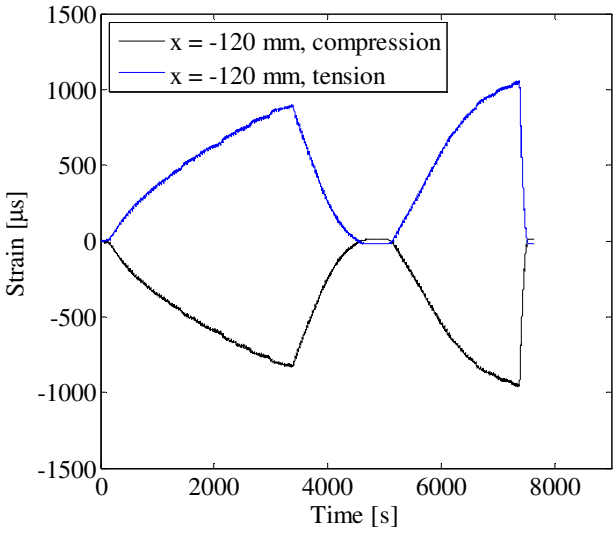

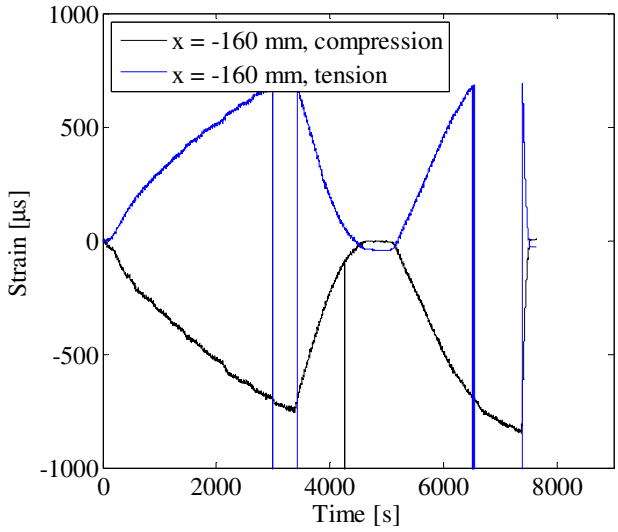

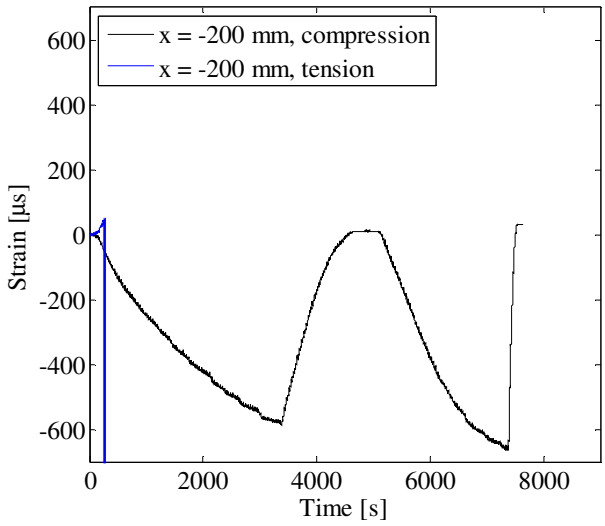

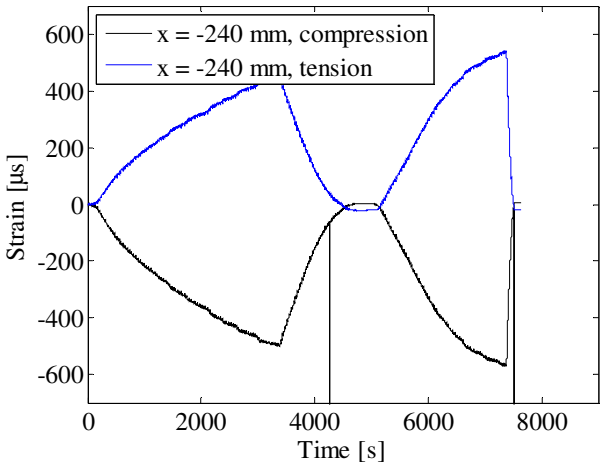

FIGURE 55. STRAIN GAUGE MEASUREMENTS.

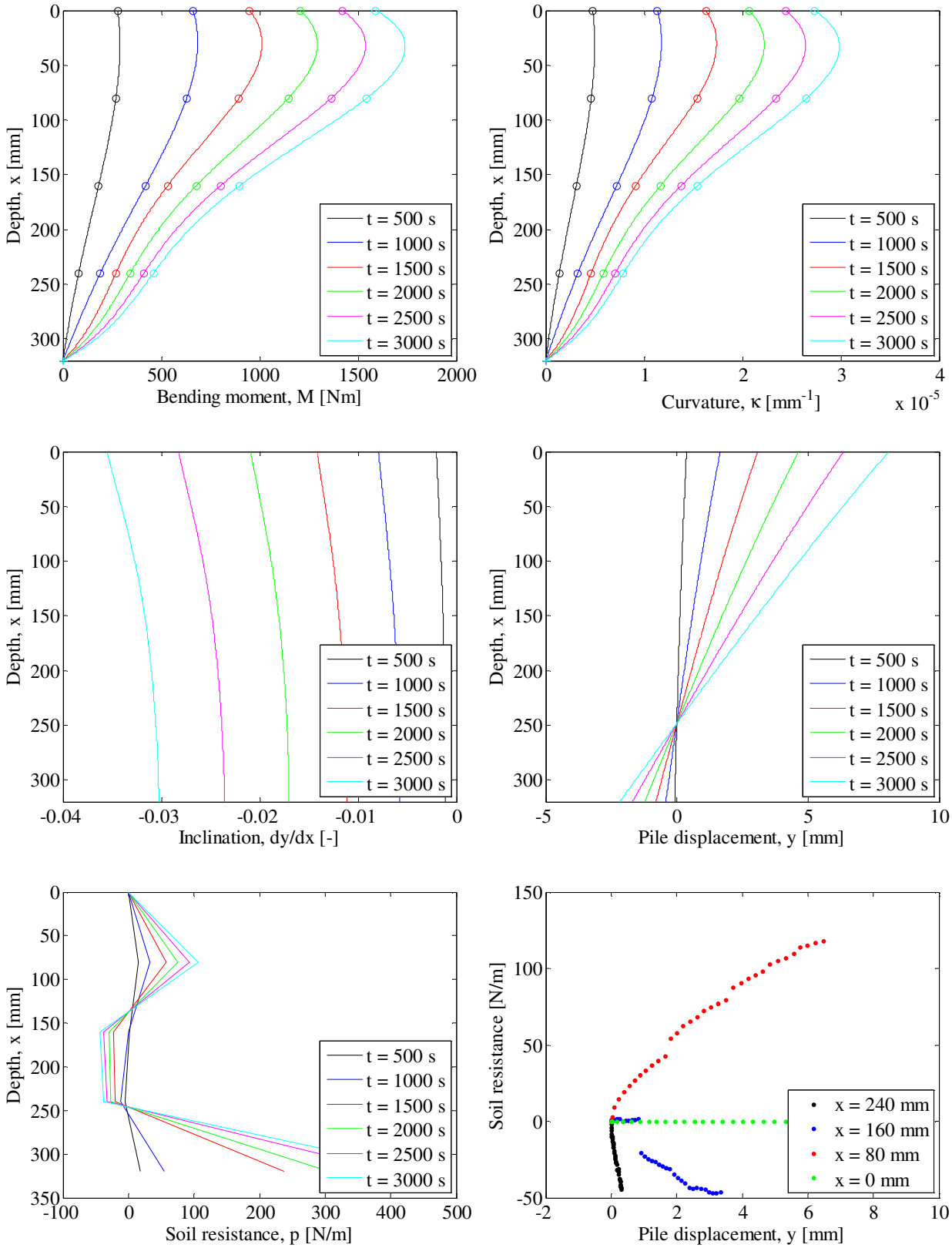

FIGURE 56. INTERPRETATION OF STRAIN GAUGE MEASUREMENTS. TOP LEFT: PILE BENDING MOMENT VERSUS DEPTH – TOP RIGHT: PILE CURVATURE VERSUS DEPTH – CENTER LEFT: PILE INCLINATION VERSUS DEPTH – CENTER RIGHT: PILE DISPLACEMENT VERSUS DEPTH – BOTTOM LEFT: SOIL RESISTANCE VERSUS DEPTH – BOTTOM RIGHT: P-Y CURVES.

Test 13: D = 80 mm, L_p = 320 mm and P_0 = 100 kPa (Closed-ended)

Pile type: Closed-ended	**Completed:** Fall 2010
Pile diameter (mm): 80	**No. of strain gauge levels:** 11 (5 below soil surface)
Embedded pile length (mm): 320	**Overburden pressure (kPa):** 100
Slenderness ratio, *L*/*D*: 4	**Load eccentricity (mm):** 370
Pile wall thickness (mm): 5	**By:** A. B. Moreno, L. Mikalauskas and J. L. T. Diaz
Comments: The water flow through the membrane were approximately 30 l/hour.	

Soil parameters:

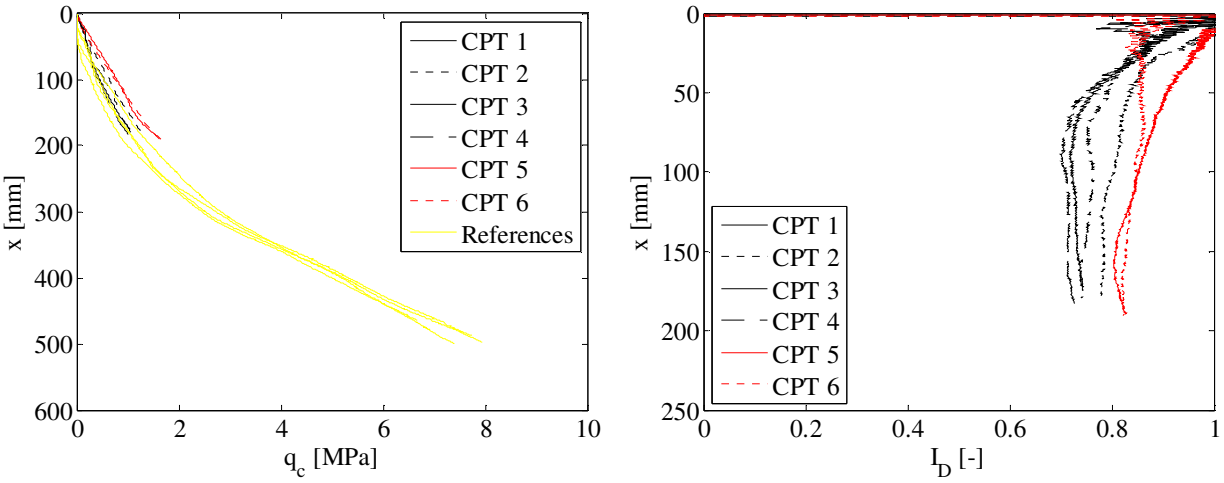

FIGURE 57. CPT-RESULTS FROM TEST 13. LEFT: TIP RESISTANCE VERSUS DEPTH – RIGHT: RELATIVE DENSITY VERSUS DEPTH.

TABLE 16. ESTIMATED SOIL PARAMETERS FOR TEST 13.

Relative density, I_D	Internal friction angle, φ_{tr}	Dilatancy angle, ψ_{tr}	Effective unit weight, γ'	Tangential Young's modulus of elasticity, E_0	Poisson's ratio, ν
[-]	[◦]	[◦]	[kN/m^3]	[MPa]	[-]
0.78	45.7	15.9	10.2	40.3	0.23

Test results:

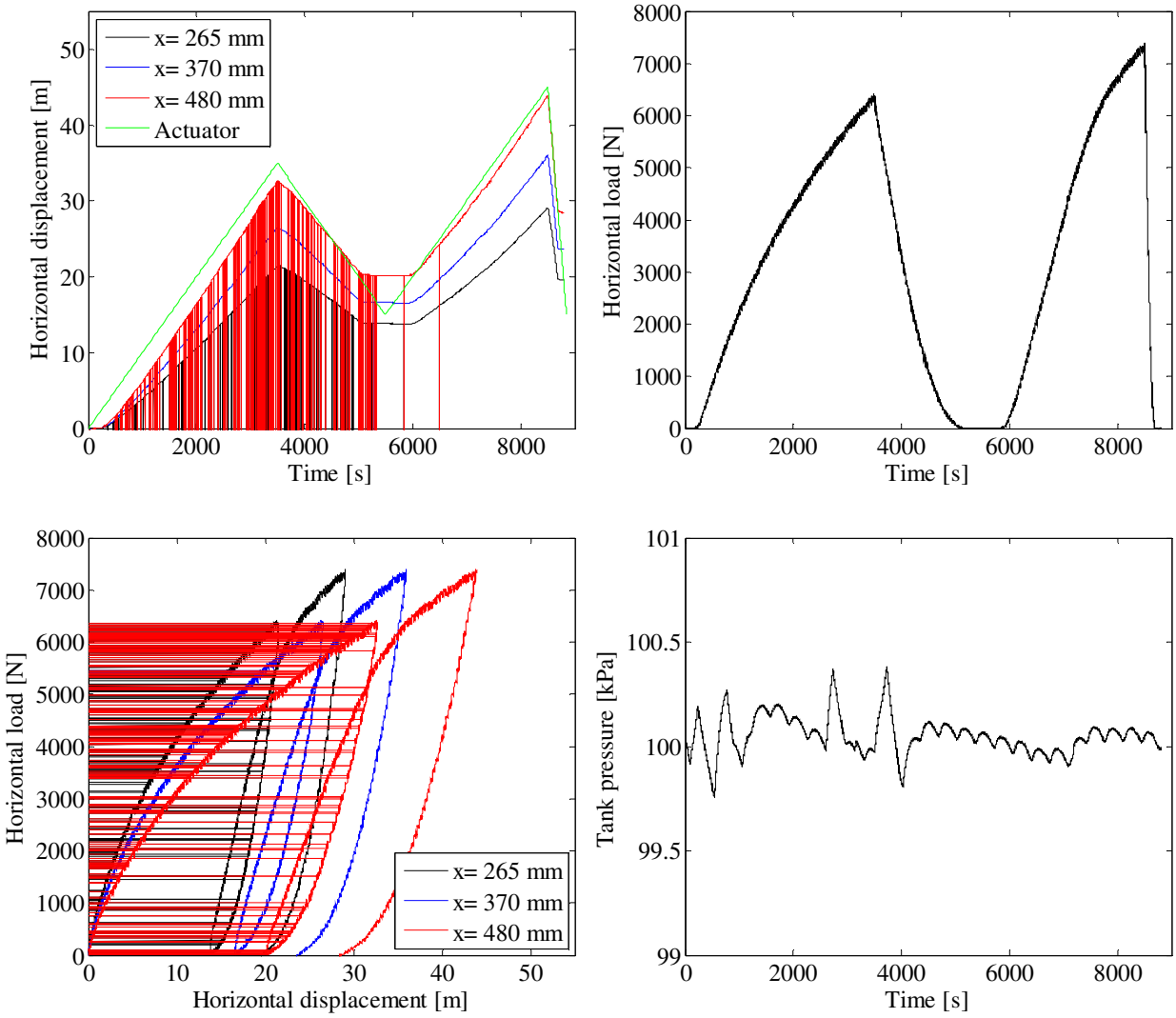

FIGURE 58. TOP LEFT: PILE DISPLACEMENT VERSUS TIME – TOP RIGHT: HORIZONTAL LOAD VERSUS TIME – BOTTOM LEFT: HORIZONTAL LOAD VERSUS PILE DISPLACEMENT – BOTTOM RIGHT: TANK PRESSURE VERSUS TIME.

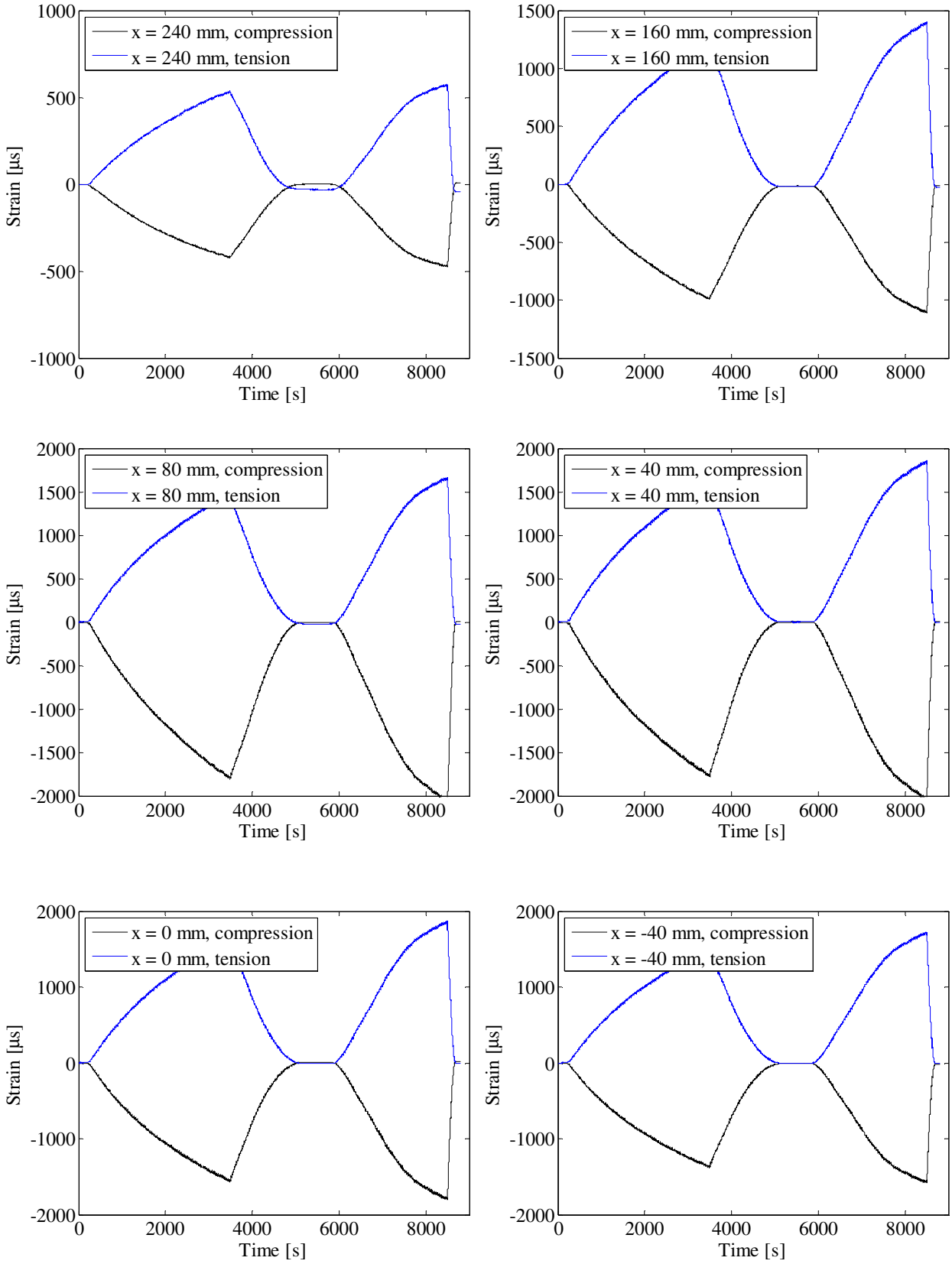

FIGURE 59. STRAIN GAUGE MEASUREMENTS.

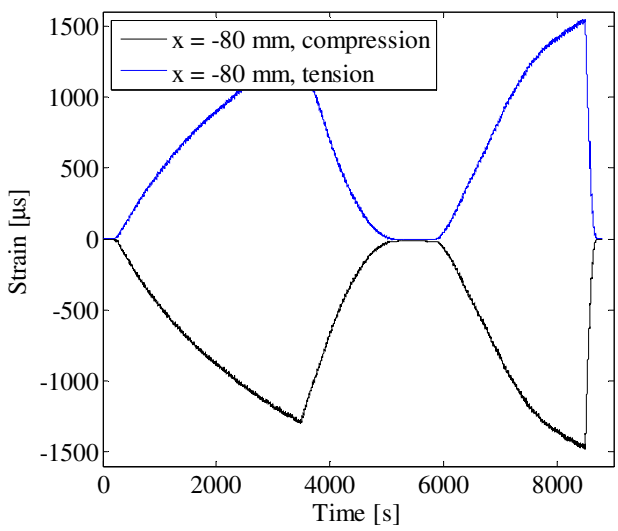

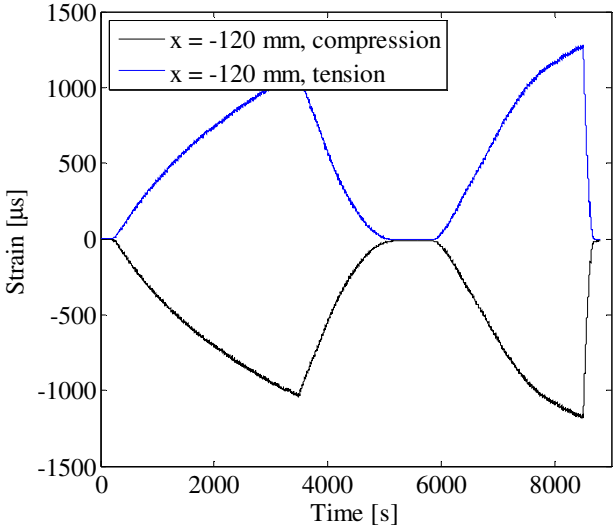

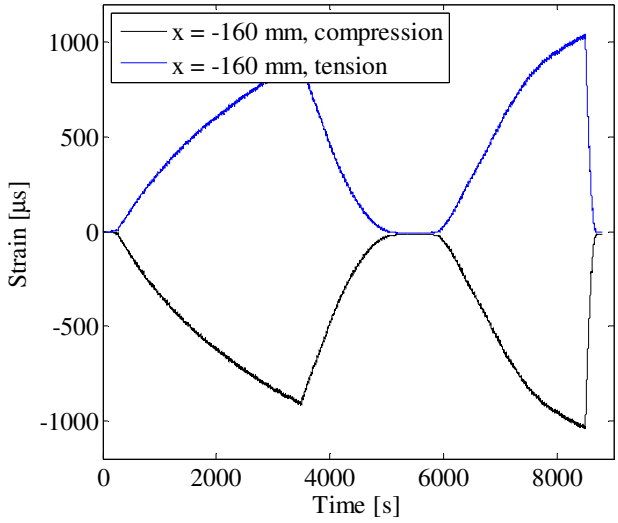

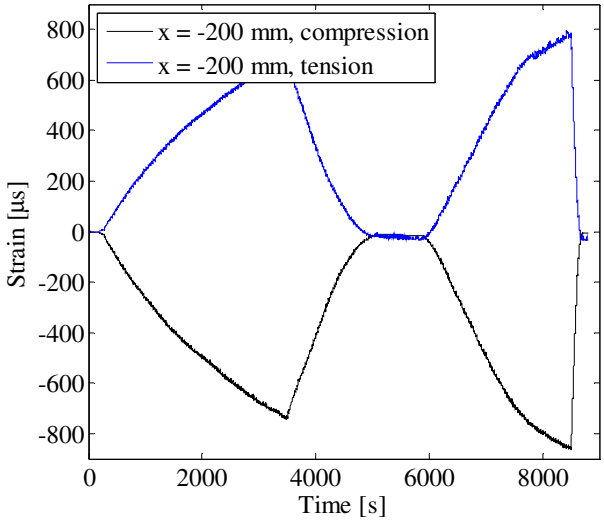

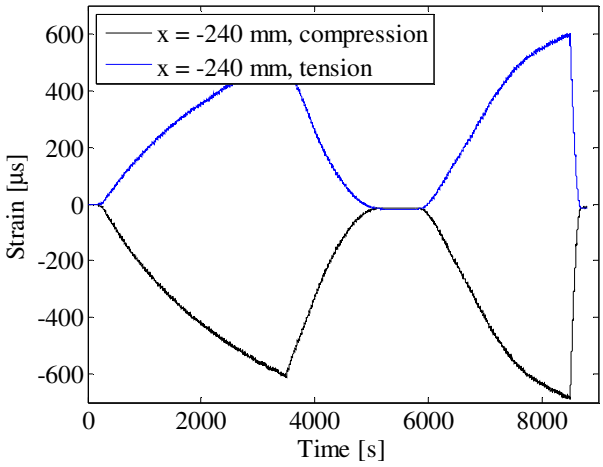

FIGURE 60. STRAIN GAUGE MEASUREMENTS.

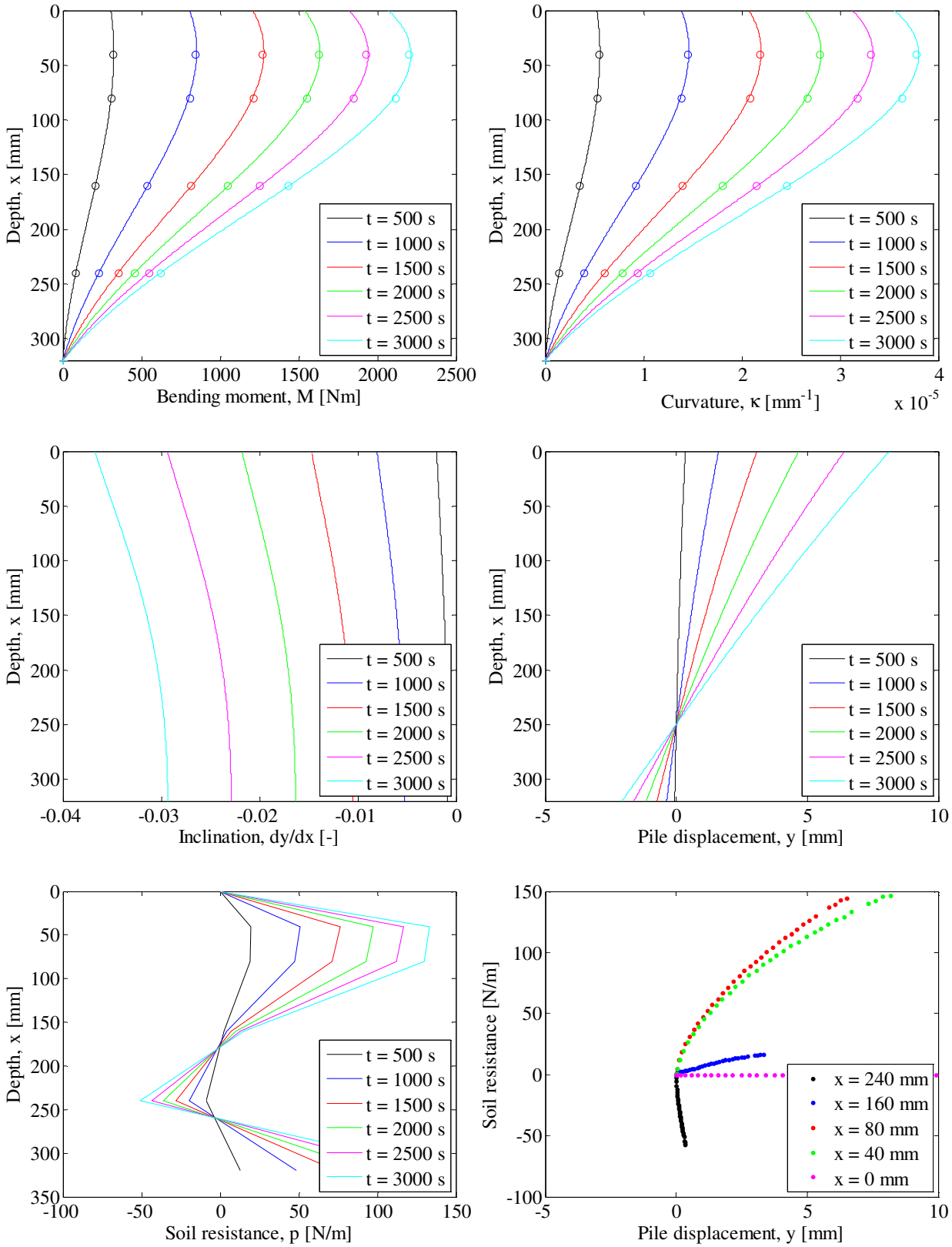

FIGURE 61 INTERPRETATION OF STRAIN GAUGE MEASUREMENTS. TOP LEFT: PILE BENDING MOMENT VERSUS DEPTH – TOP RIGHT: PILE CURVATURE VERSUS DEPTH – CENTER LEFT: PILE INCLINATION VERSUS DEPTH – CENTER RIGHT: PILE DISPLACEMENT VERSUS DEPTH – BOTTOM LEFT: SOIL RESISTANCE VERSUS DEPTH – BOTTOM RIGHT: P-Y CURVES.

Test 14: D = 80 mm, L_p = 400 mm and P_0 = 0 kPa (Closed-ended)

Pile type: Closed-ended	**Completed:** Spring 2009
Pile diameter (mm): 80	**No. of strain gauge levels:** 5 (All below soil surface)
Embedded pile length (mm): 400	**Overburden pressure (kPa):** 0
Slenderness ratio, L/D: 5	**Load eccentricity (mm):** 370
Pile wall thickness (mm): 5	**By:** S. P. H. Sørensen, K. T. Brødbæk and M. Møller
Comments:	

Soil parameters:

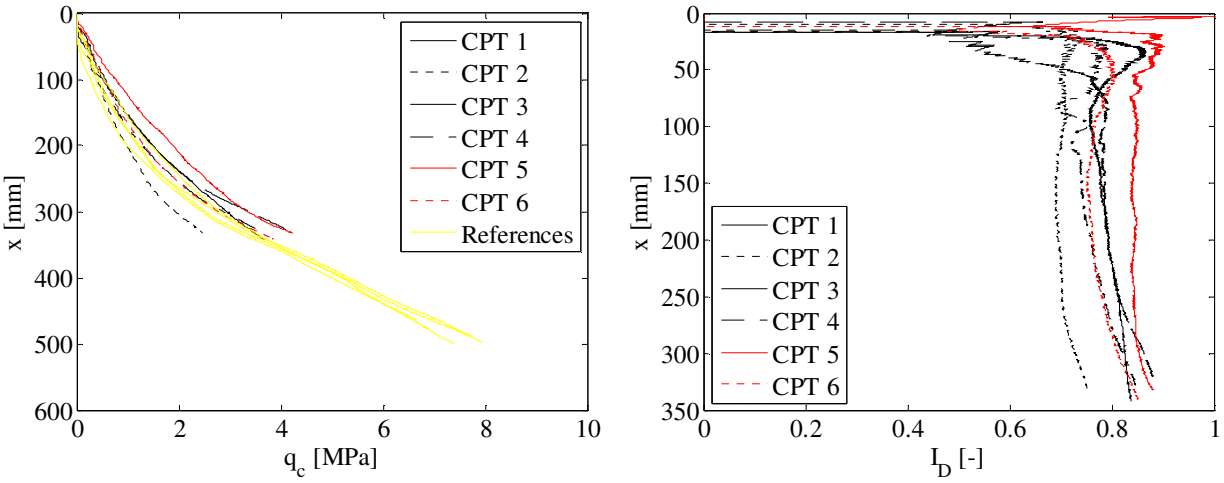

FIGURE 62. CPT-RESULTS FROM TEST 14. LEFT: TIP RESISTANCE VERSUS DEPTH – RIGHT: RELATIVE DENSITY VERSUS DEPTH.

TABLE 17. ESTIMATED SOIL PARAMETERS FOR TEST 14.

Relative density, I_D	Internal friction angle, φ_{tr}	Dilatancy angle, ψ_{tr}	Effective unit weight, γ'	Tangential Young's modulus of elasticity, E_0	Poisson's ratio, ν
[-]	[◦]	[◦]	[kN/m^3]	[MPa]	[-]
0.79	52.6	17.5	10.2	-	0.23

Test results:

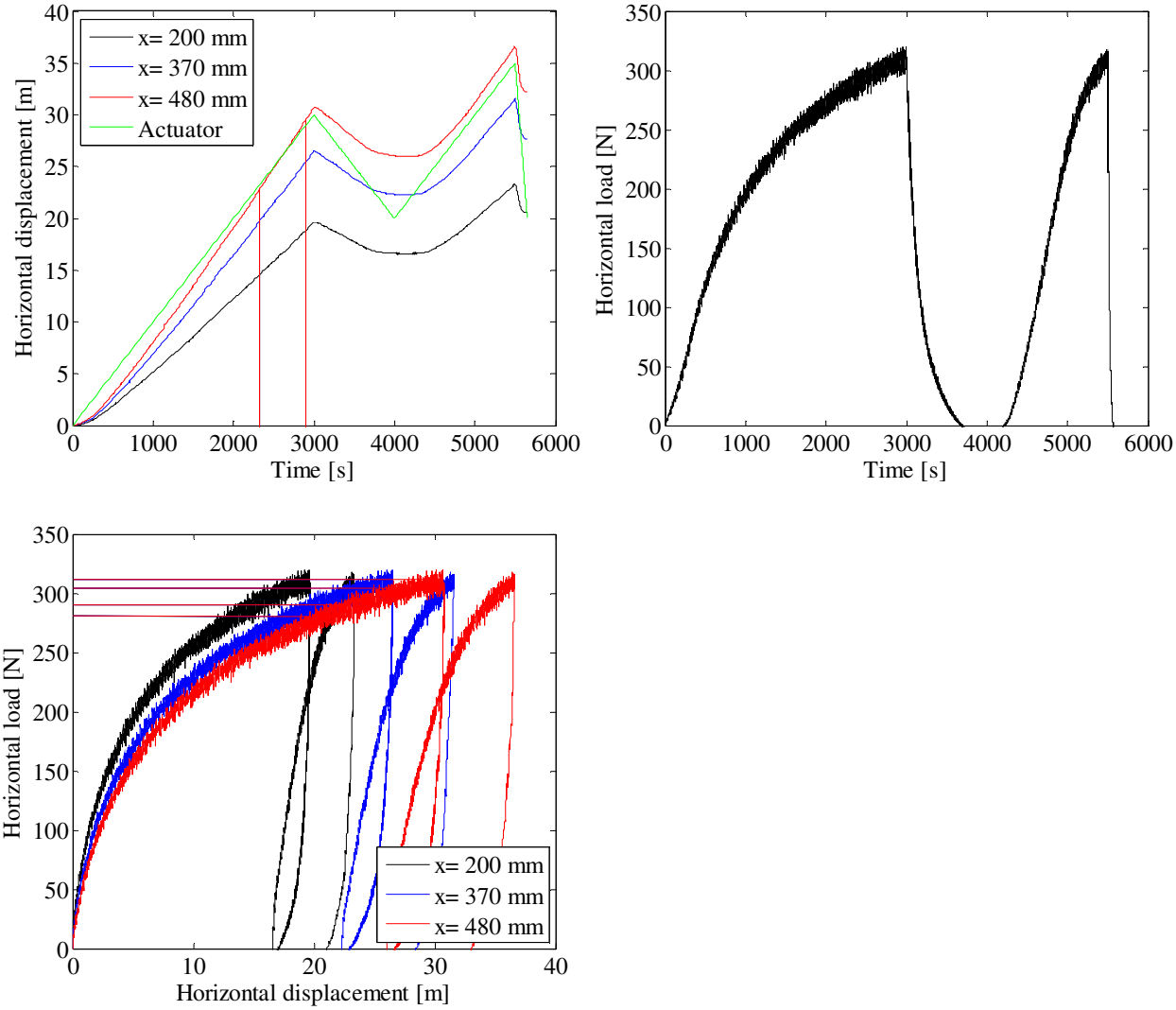

FIGURE 63. TOP LEFT: PILE DISPLACEMENT VERSUS TIME – TOP RIGHT: HORIZONTAL LOAD VERSUS TIME – BOTTOM LEFT: HORIZONTAL LOAD VERSUS PILE DISPLACEMENT.

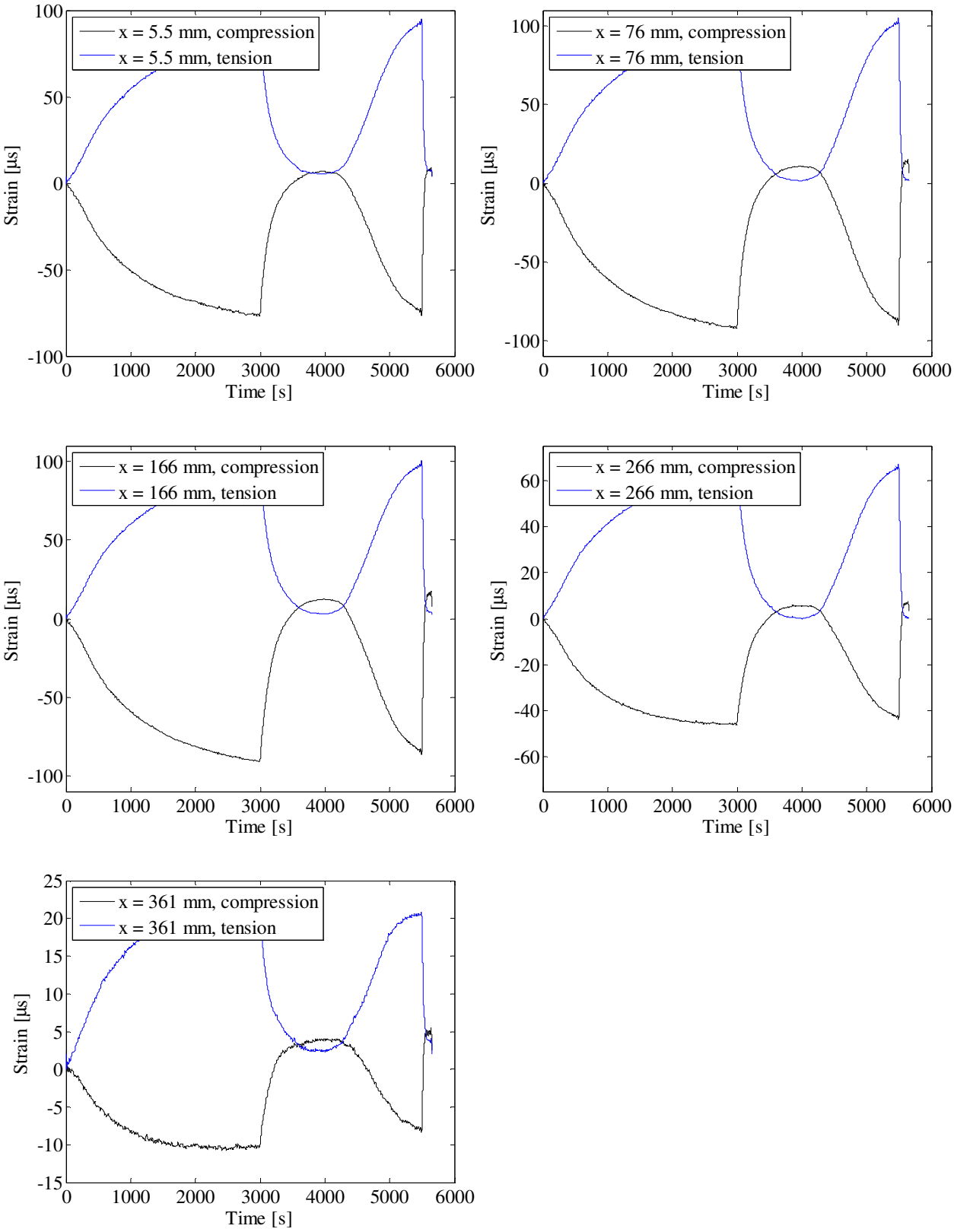

FIGURE 64. STRAIN GAUGE MEASUREMENTS.

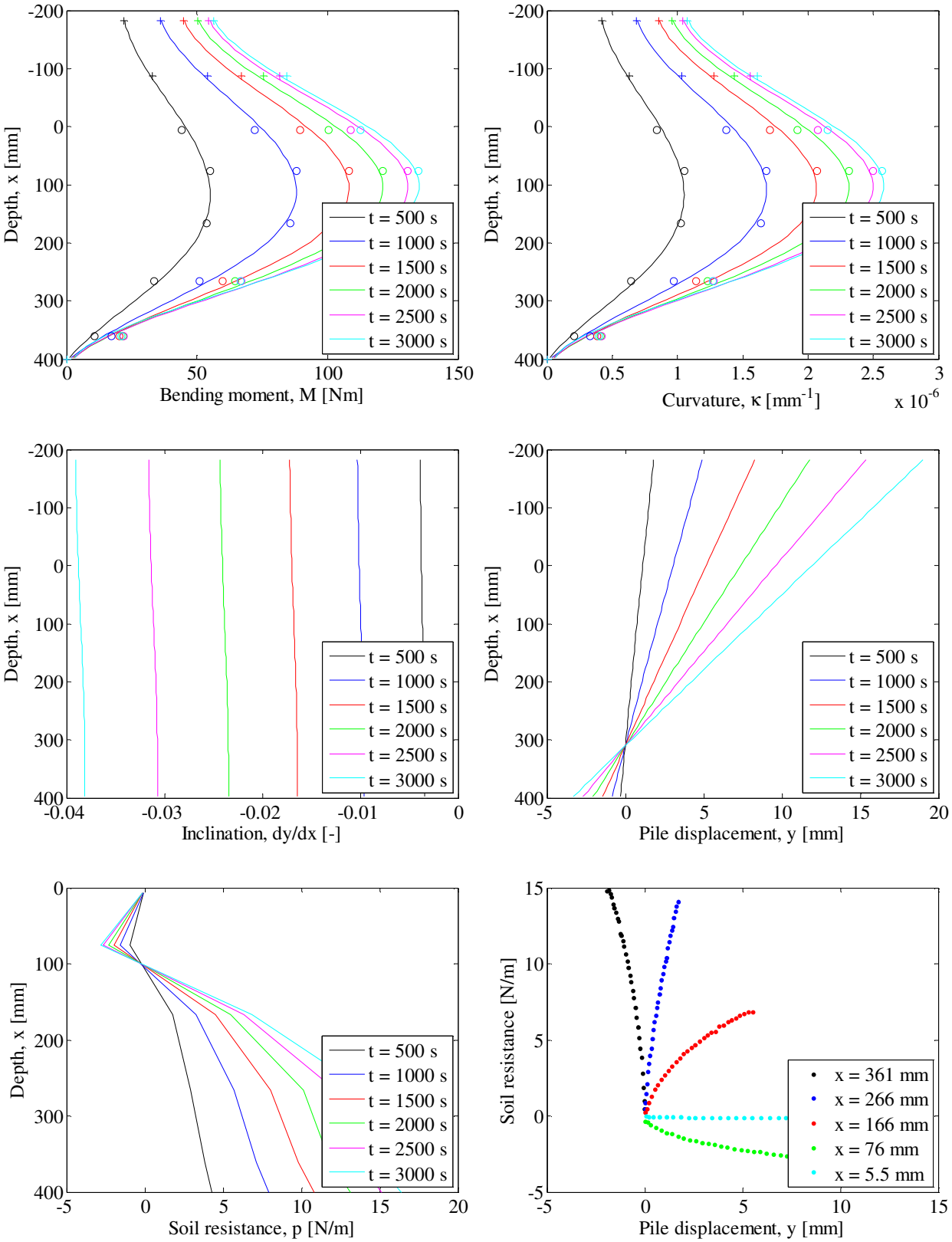

FIGURE 65. INTERPRETATION OF STRAIN GAUGE MEASUREMENTS. TOP LEFT: PILE BENDING MOMENT VERSUS DEPTH – TOP RIGHT: PILE CURVATURE VERSUS DEPTH – CENTER LEFT: PILE INCLINATION VERSUS DEPTH – CENTER RIGHT: PILE DISPLACEMENT VERSUS DEPTH – BOTTOM LEFT: SOIL RESISTANCE VERSUS DEPTH – BOTTOM RIGHT: P-Y CURVES.

Test 15: D = 80 mm, L_p = 400 mm and P_0 = 0 kPa (Closed-ended)

Pile type: Closed-ended	**Completed:** Spring 2010
Pile diameter (mm): 80	**No. of strain gauge levels:** 11 (7 below soil surface)
Embedded pile length (mm): 400	**Overburden pressure (kPa):** 0
Slenderness ratio, L/D: 5	**Load eccentricity (mm):** 370
Pile wall thickness (mm): 5	**By:** A. B. Moreno, L. Mikalauskas and J. L. T. Diaz
Comments: This test consists of two sub-tests. In the first sub-test the wire connecting the pile with the hydraulic piston was too tight and therefore the initial part of the load-displacement curve could not be observed. The first sub-test is therefore not used. The second sub-test is used in the interpretations. During this test strain gauge 16 stopped measuring at the beginning of the tests. Therefore the other strain gauge in that respective level is assumed to be representative.	

Soil parameters:

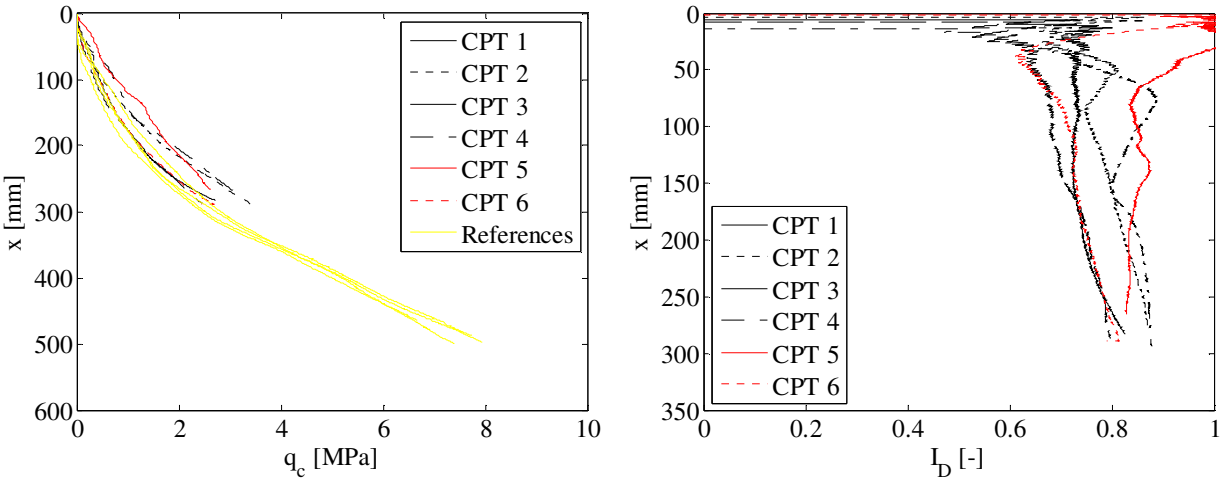

FIGURE 66. CPT-RESULTS FROM TEST 15. LEFT: TIP RESISTANCE VERSUS DEPTH – RIGHT: RELATIVE DENSITY VERSUS DEPTH.

TABLE 18. ESTIMATED SOIL PARAMETERS FOR TEST 15.

Relative density, I_D	Internal friction angle, φ_{tr}	Dilatancy angle, ψ_{tr}	Effective unit weight, γ'	Tangential Young's modulus of elasticity, E_0	Poisson's ratio, ν
[-]	[◦]	[◦]	[kN/m^3]	[MPa]	[-]
0.79	52.7	18.2	10.2	-	0.23

Test results:

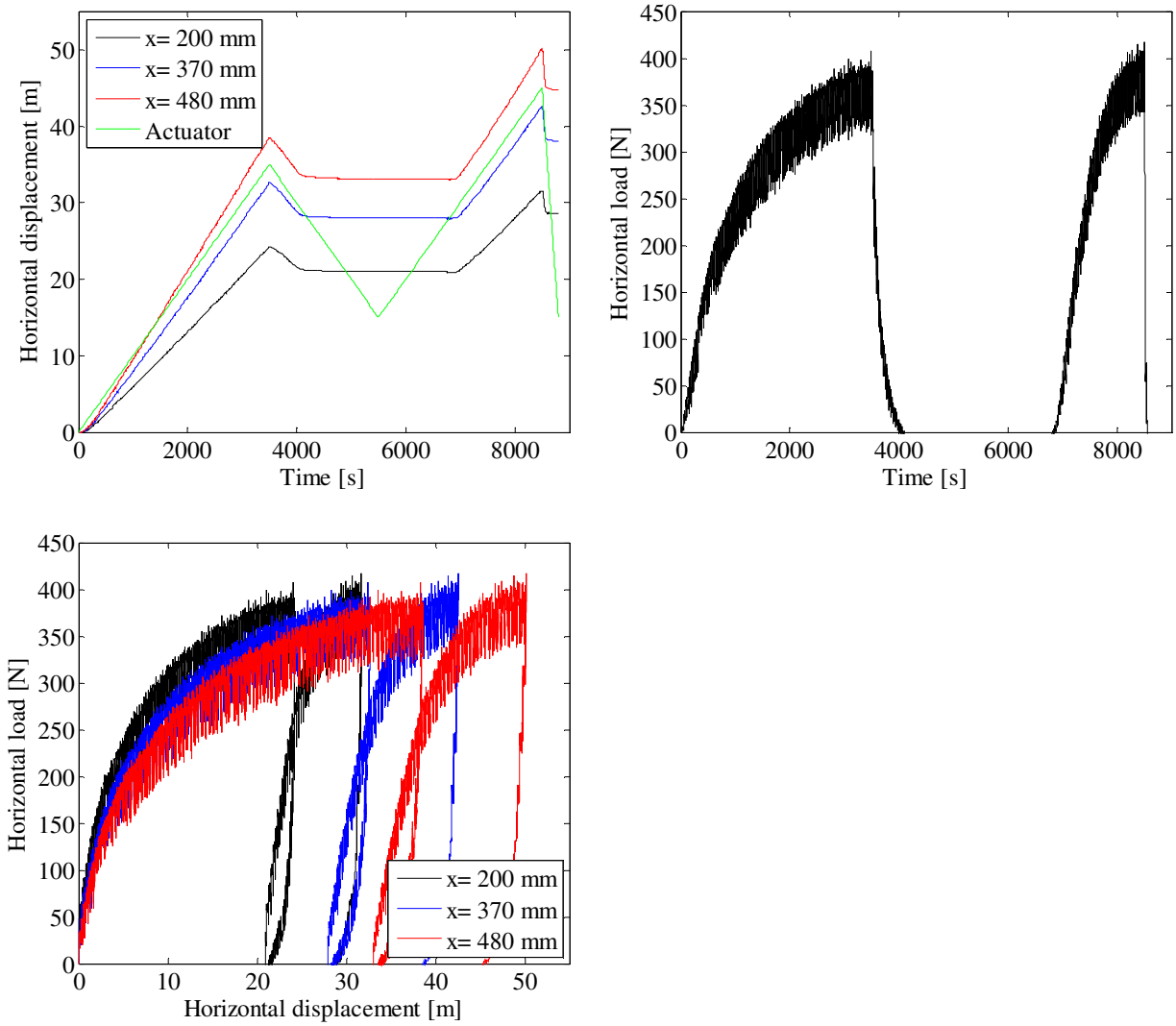

FIGURE 67. TOP LEFT: PILE DISPLACEMENT VERSUS TIME – TOP RIGHT: HORIZONTAL LOAD VERSUS TIME – BOTTOM LEFT: HORIZONTAL LOAD VERSUS PILE DISPLACEMENT.

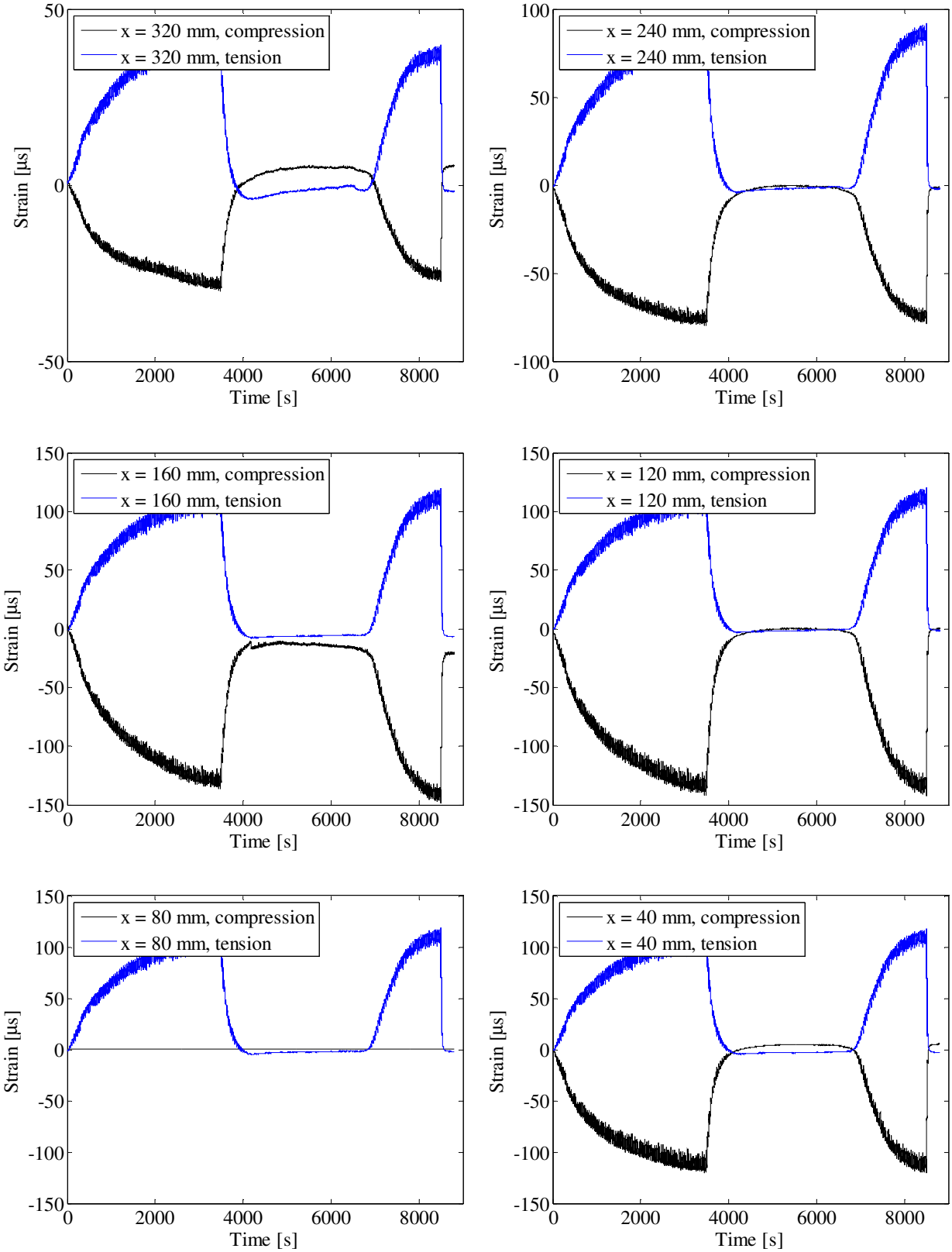

FIGURE 68. STRAIN GAUGE MEASUREMENTS.

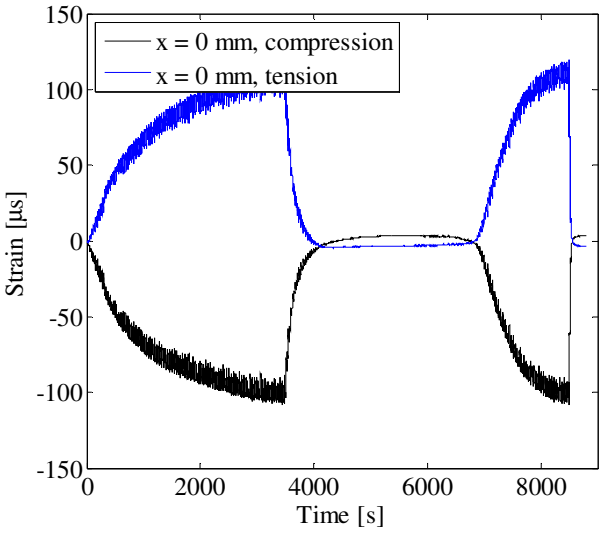

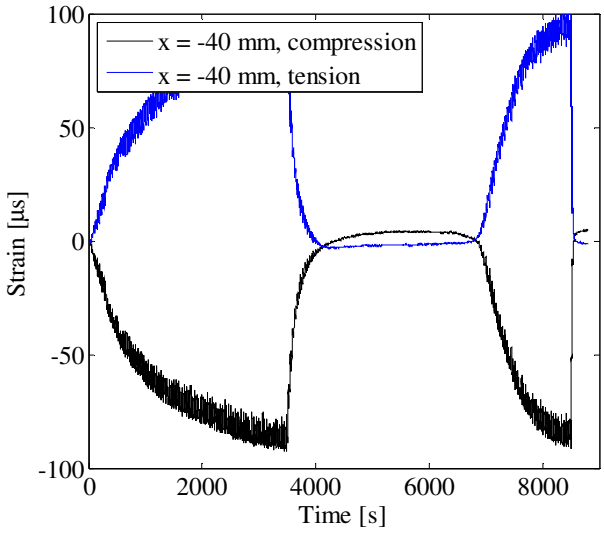

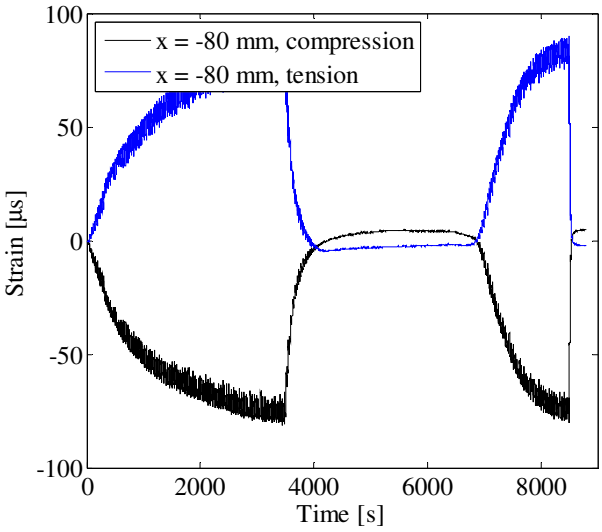

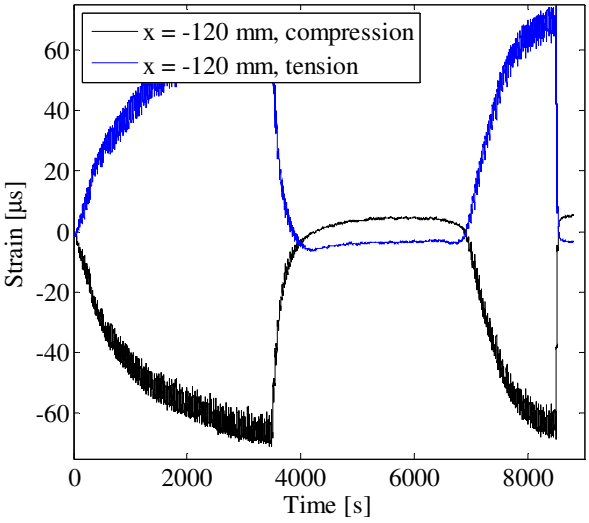

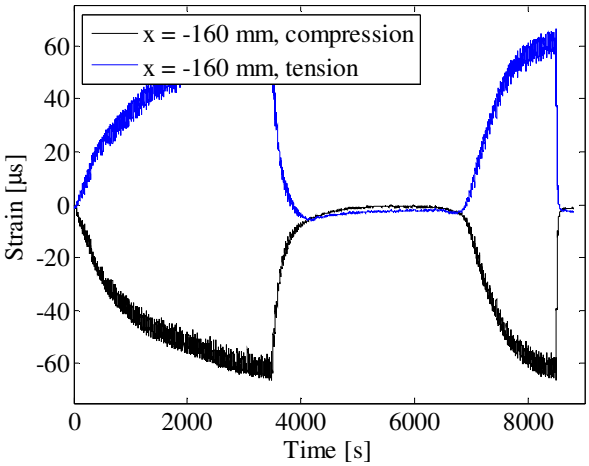

FIGURE 69. STRAIN GAUGE MEASUREMENTS.

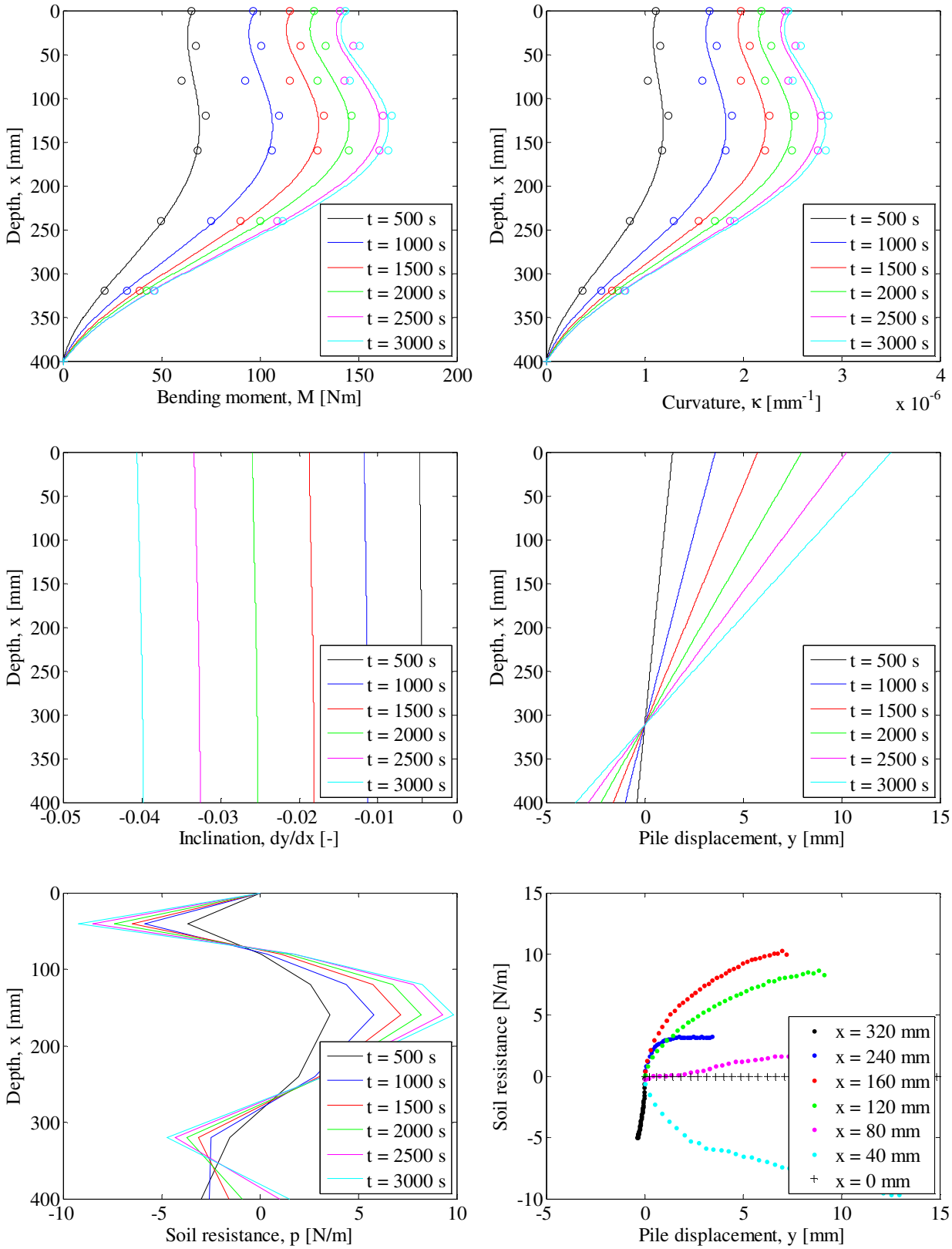

FIGURE 70. INTERPRETATION OF STRAIN GAUGE MEASUREMENTS. TOP LEFT: PILE BENDING MOMENT VERSUS DEPTH – TOP RIGHT: PILE CURVATURE VERSUS DEPTH – CENTER LEFT: PILE INCLINATION VERSUS DEPTH – CENTER RIGHT: PILE DISPLACEMENT VERSUS DEPTH – BOTTOM LEFT: SOIL RESISTANCE VERSUS DEPTH – BOTTOM RIGHT: P-Y CURVES.

Test 16: D = 80 mm, L_p = 400 mm and P_0 = 25 kPa (Closed-ended)

Pile type: Closed-ended	**Completed:** Summer 2011
Pile diameter (mm): 80	**No. of strain gauge levels:** 11(All below soil surface)
Embedded pile length (mm): 400	**Overburden pressure (kPa):** 25
Slenderness ratio, L/D: 5	**Load eccentricity (mm):** 370
Pile wall thickness (mm): 5	**By:** S. P. H. Sørensen and L. Mikalauskas
Comments: Strain gauge number 5 did not function. The hydraulic piston applying the horizontal loading was prior to the test placed in its middle position. Hence, it was only possible to apply a horizontal displacement of approximately 20 mm in the height of the actuator. The water flow through the membrane was approximately 20 L/hour.	

Soil parameters:

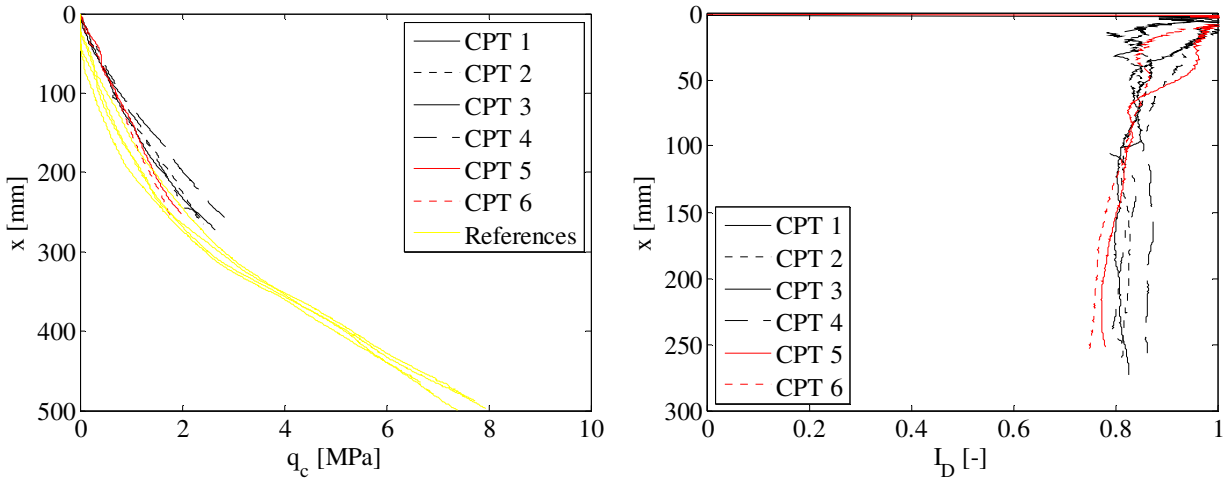

FIGURE 71. CPT-RESULTS FROM TEST 16. LEFT: TIP RESISTANCE VERSUS DEPTH – RIGHT: RELATIVE DENSITY VERSUS DEPTH.

TABLE 19. ESTIMATED SOIL PARAMETERS FOR TEST 16.

Relative density, I_D	Internal friction angle, φ_{tr}	Dilatancy angle, ψ_{tr}	Effective unit weight, γ'	Tangential Young's modulus of elasticity, E_0	Poisson's ratio, ν
[-]	[◦]	[◦]	[kN/m^3]	[MPa]	[-]
0.82	52.7	18.5	10.2	16.2	0.23

Test results:

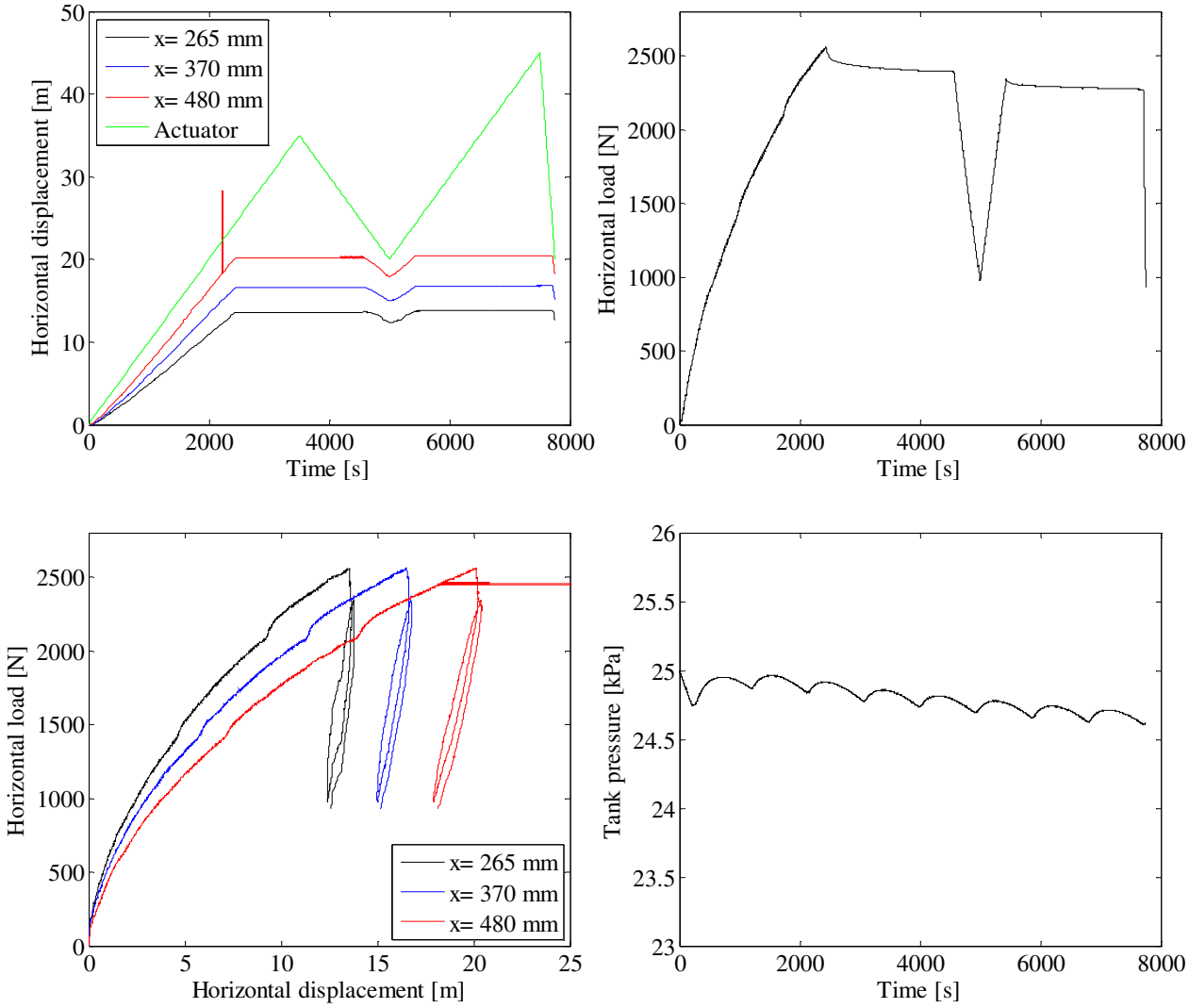

FIGURE 72. TOP LEFT: PILE DISPLACEMENT VERSUS TIME – TOP RIGHT: HORIZONTAL LOAD VERSUS TIME – BOTTOM LEFT: HORIZONTAL LOAD VERSUS PILE DISPLACEMENT – BOTTOM RIGHT: TANK PRESSURE VERSUS TIME.

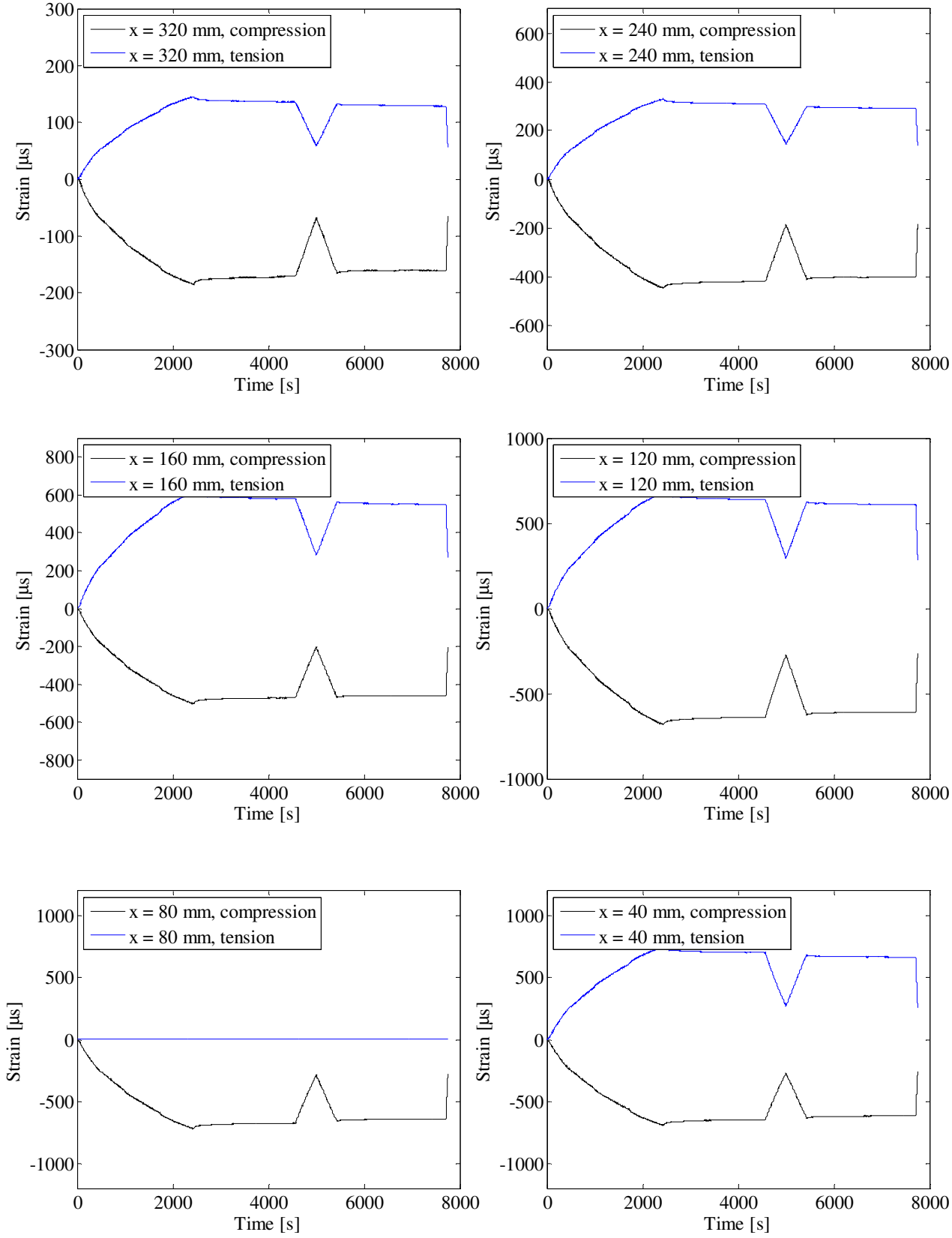

FIGURE 73. STRAIN GAUGE MEASUREMENTS.

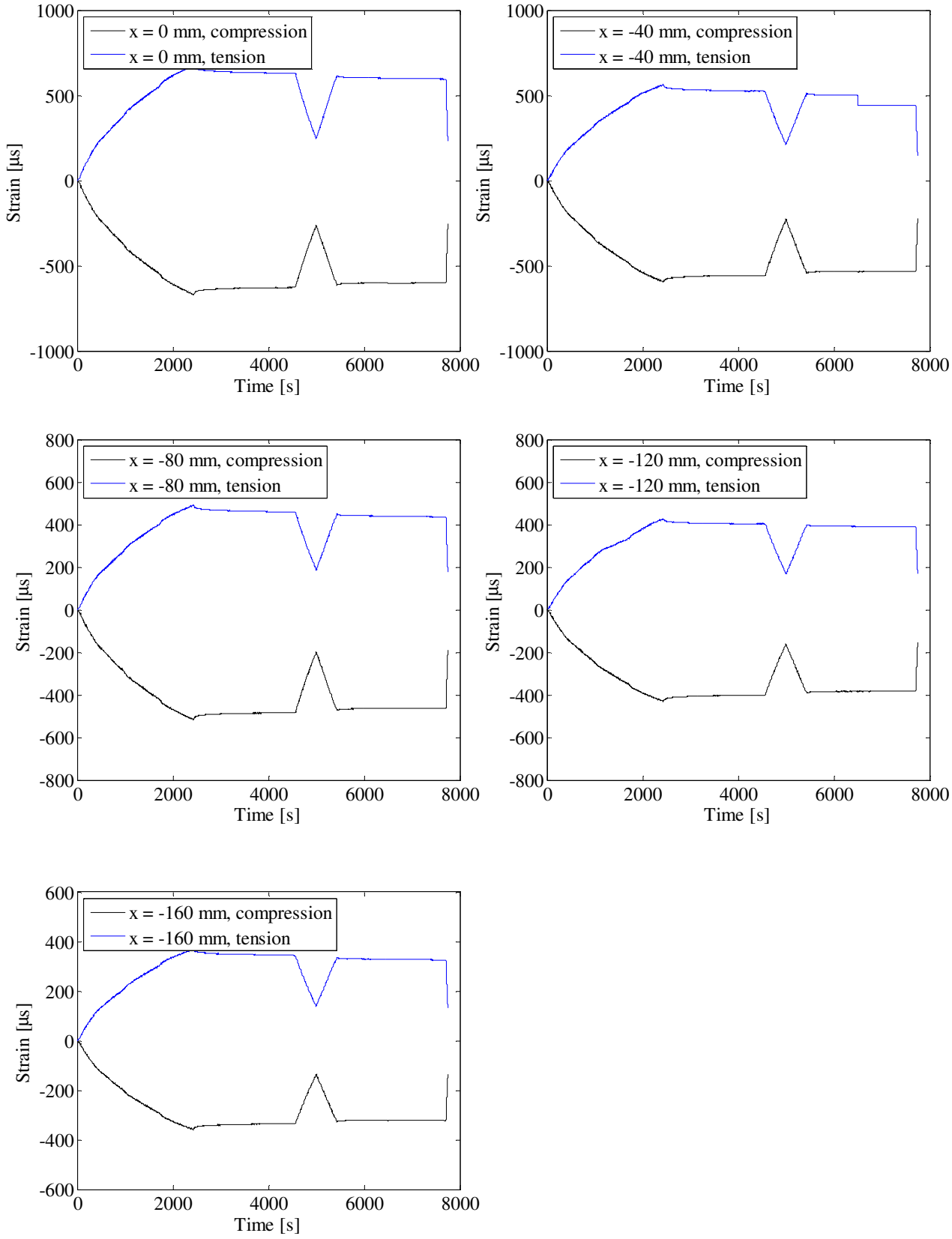

FIGURE 74. STRAIN GAUGE MEASUREMENTS.

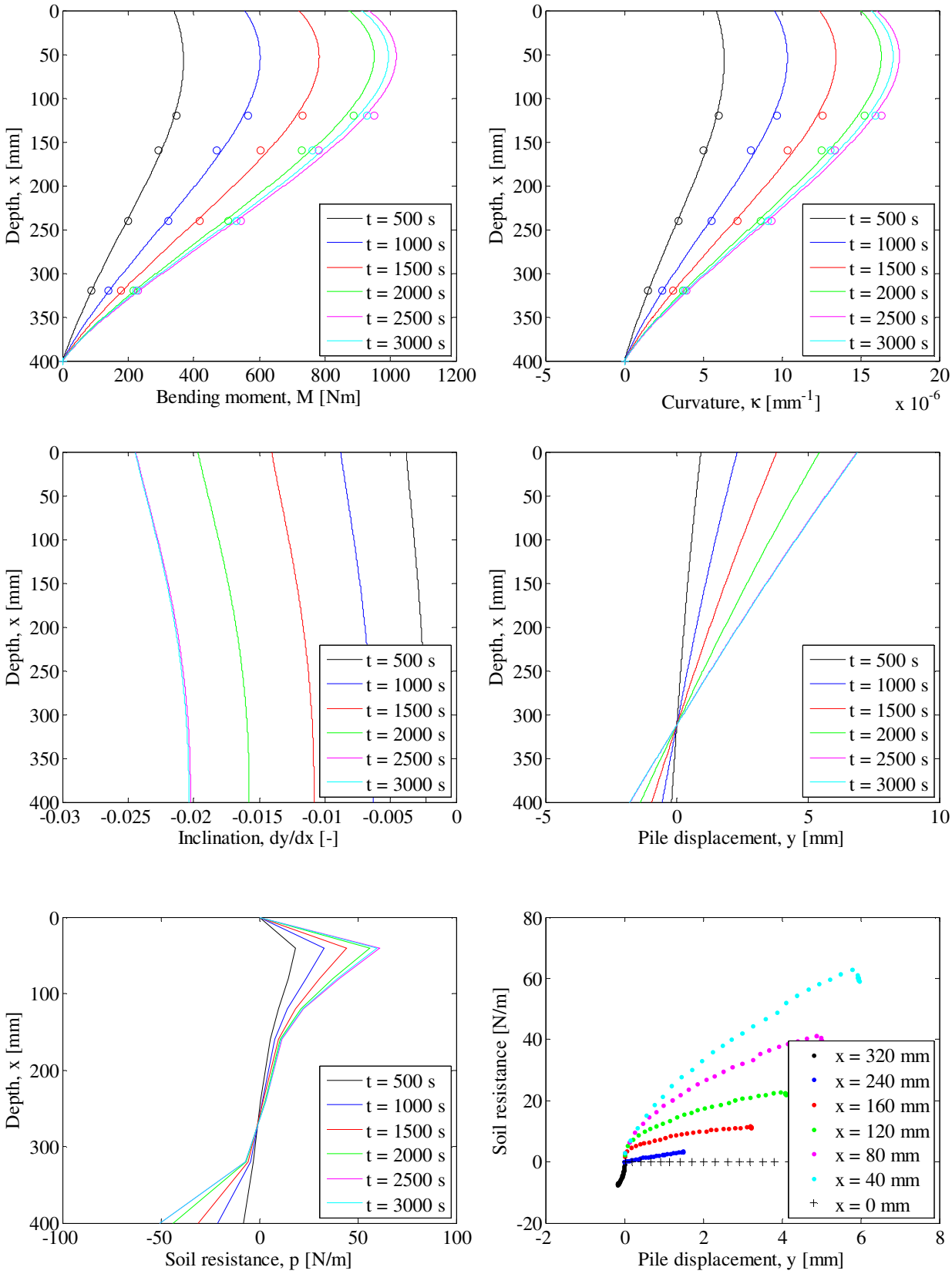

FIGURE 75. INTERPRETATION OF STRAIN GAUGE MEASUREMENTS. TOP LEFT: PILE BENDING MOMENT VERSUS DEPTH – TOP RIGHT: PILE CURVATURE VERSUS DEPTH – CENTER LEFT: PILE INCLINATION VERSUS DEPTH – CENTER RIGHT: PILE DISPLACEMENT VERSUS DEPTH – BOTTOM LEFT: SOIL RESISTANCE VERSUS DEPTH – BOTTOM RIGHT: P-Y CURVES.

Test 17: D = 80 mm, L_p = 400 mm and P_0 = 50 kPa (Closed-ended)

Pile type: Closed-ended	**Completed:** Spring 2009
Pile diameter (mm): 80	**No. of strain gauge levels:** 5 (All below soil surface)
Embedded pile length (mm): 400	**Overburden pressure (kPa):** 50
Slenderness ratio, L/D: 5	**Load eccentricity (mm):** 370
Pile wall thickness (mm): 5	**By:** S. P. H. Sørensen, K. T. Brødbæk and M. Møller
Comments: The strain gauges exposed to tension at depths of 5.5, 76, and 266 mm, respectively do not work properly at strains larger than 1260, 1740, and 110 µm, respectively. Hence, the strain gauges loaded in compression is considered to be representative at these depths for strains exceeding 1260, 1740, and 110 µm. Furthermore, large variations in tank pressure are observed after 2500 s. A sudden increase in the load is similarly observed after 2500 s and this might therefore be a result of the varying tank pressure. Test results after 2500 s are therefore not analysed.	

Soil parameters:

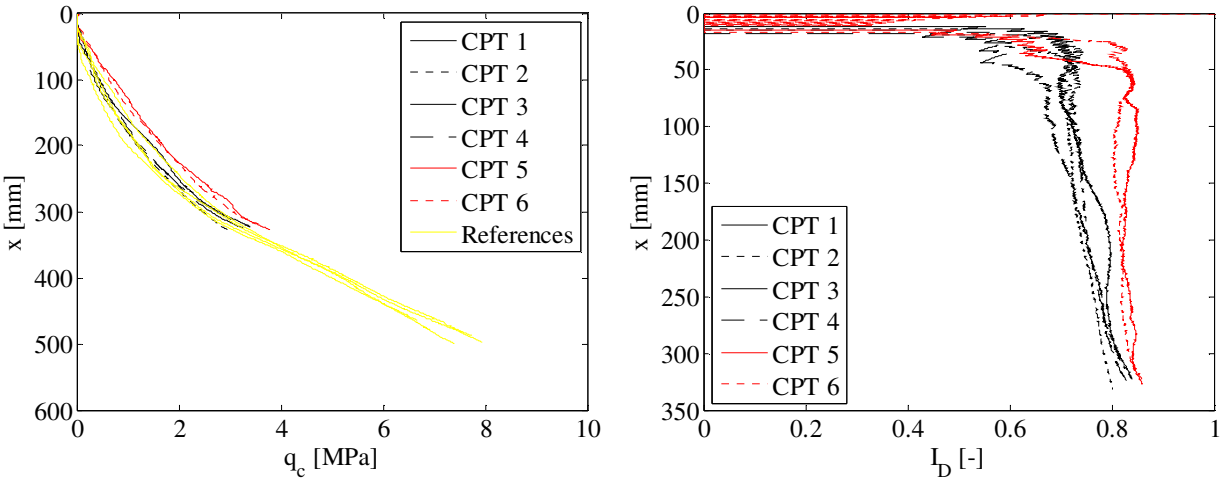

FIGURE 76. CPT-RESULTS FROM TEST 17. LEFT: TIP RESISTANCE VERSUS DEPTH – RIGHT: RELATIVE DENSITY VERSUS DEPTH.

TABLE 20. ESTIMATED SOIL PARAMETERS FOR TEST 17.

Relative density, I_D	Internal friction angle, φ_{tr}	Dilatancy angle, ψ_{tr}	Effective unit weight, γ'	Tangential Young's modulus of elasticity, E_0	Poisson's ratio, ν
[-]	[◦]	[◦]	[kN/m^3]	[MPa]	[-]
0.79	48.5	16.7	10.2	25.4	0.23

Test results:

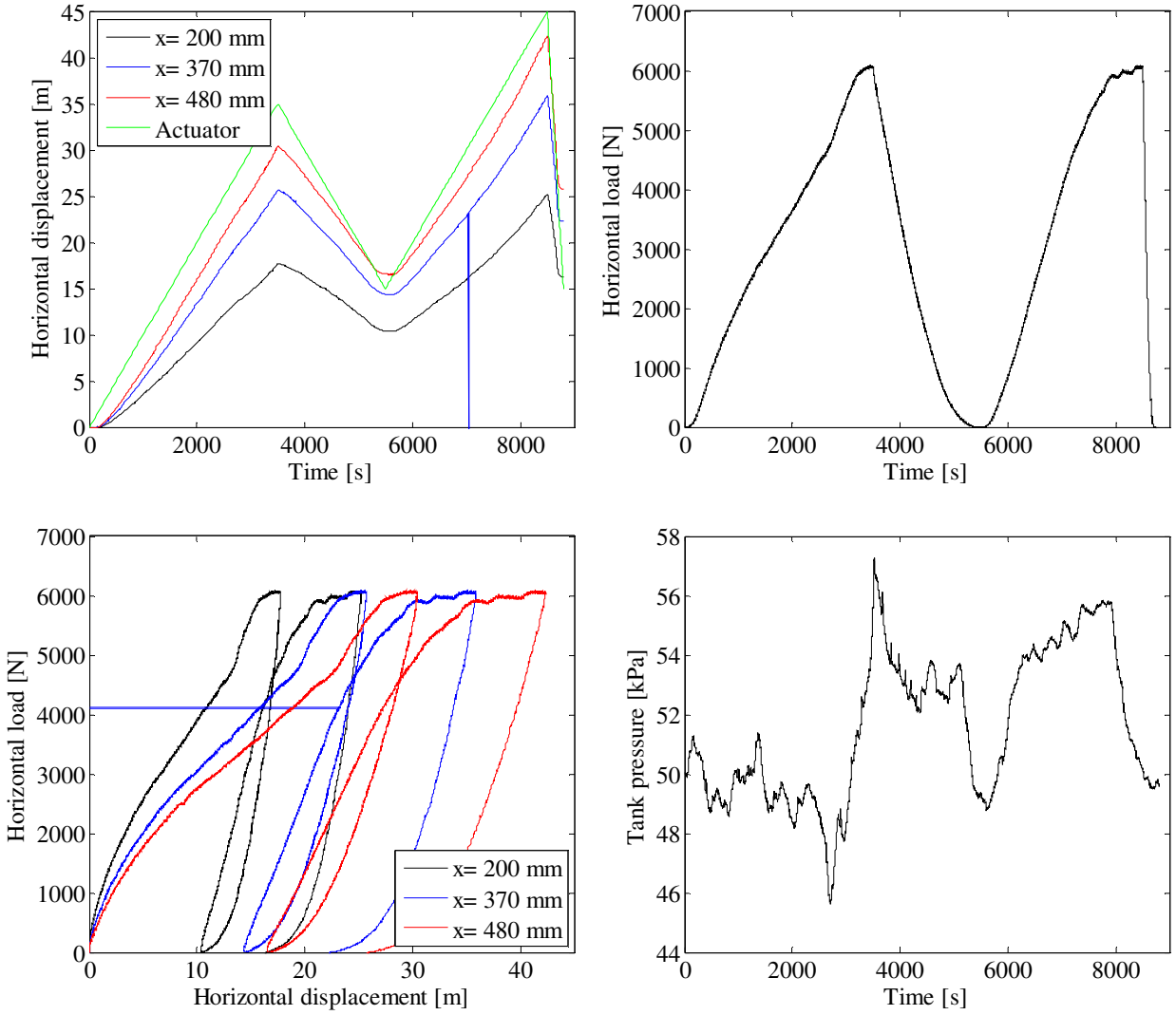

FIGURE 77. TOP LEFT: PILE DISPLACEMENT VERSUS TIME – TOP RIGHT: HORIZONTAL LOAD VERSUS TIME – BOTTOM LEFT: HORIZONTAL LOAD VERSUS PILE DISPLACEMENT – BOTTOM RIGHT: TANK PRESSURE VERSUS TIME.

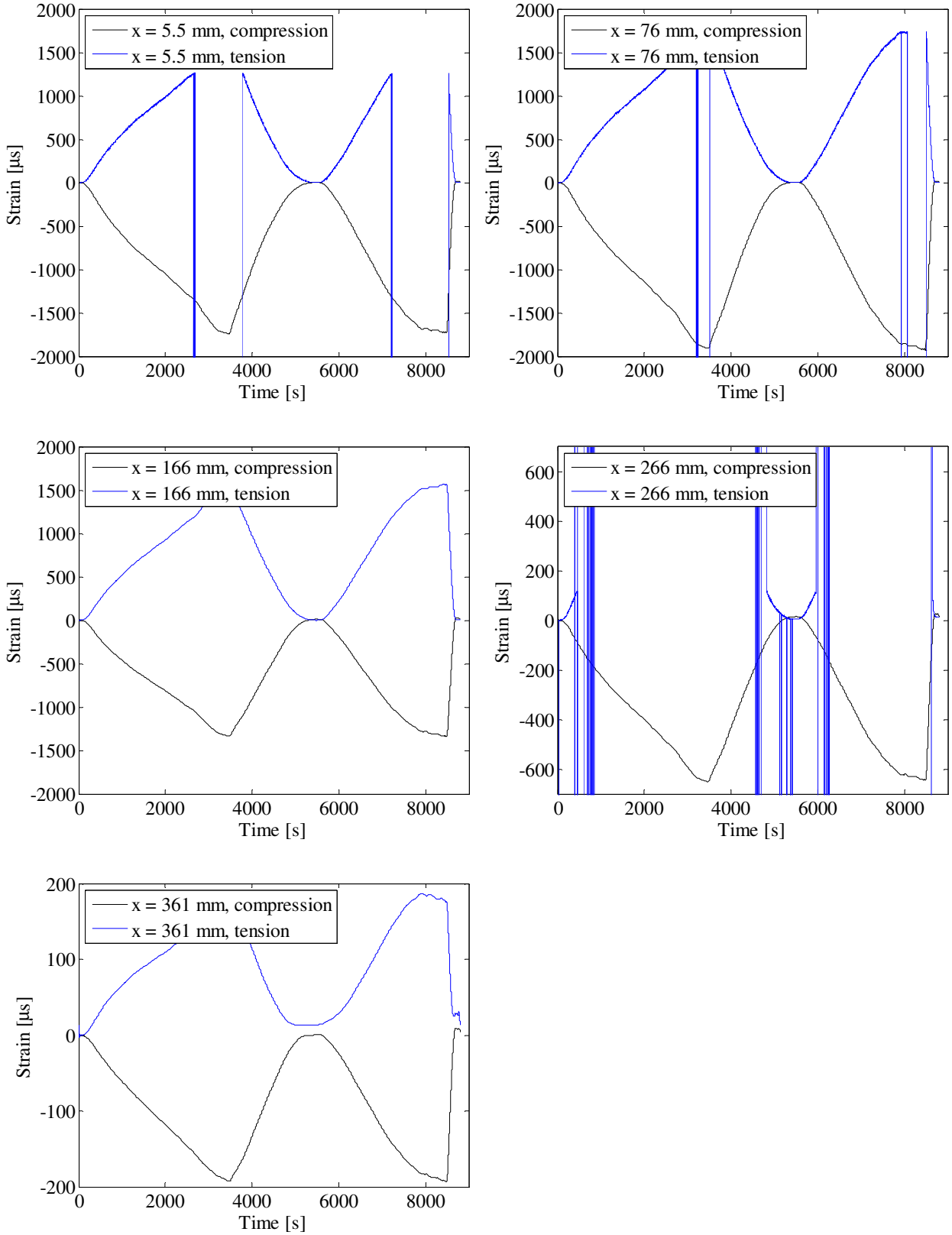

FIGURE 78. STRAIN GAUGE MEASUREMENTS.

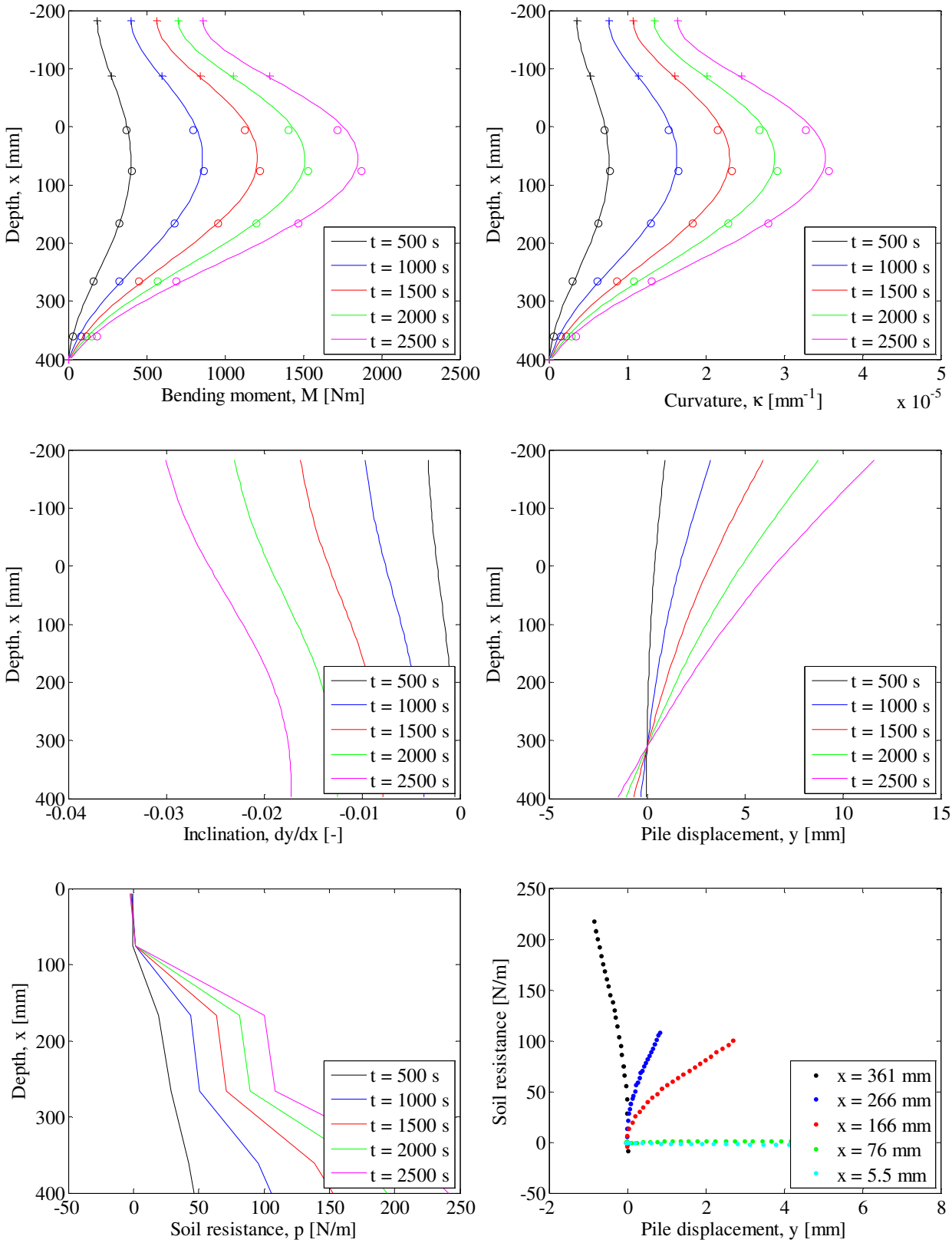

FIGURE 79. INTERPRETATION OF STRAIN GAUGE MEASUREMENTS. TOP LEFT: PILE BENDING MOMENT VERSUS DEPTH – TOP RIGHT: PILE CURVATURE VERSUS DEPTH – CENTER LEFT: PILE INCLINATION VERSUS DEPTH – CENTER RIGHT: PILE DISPLACEMENT VERSUS DEPTH – BOTTOM LEFT: SOIL RESISTANCE VERSUS DEPTH – BOTTOM RIGHT: P-Y CURVES.

Test 18: D = 80 mm, L_p = 400 mm and P_0 = 50 kPa (Closed-ended)

Pile type: Closed-ended	**Completed:** Spring 2010
Pile diameter (mm): 80	**No. of strain gauge levels:** 11 (7 below soil surface)
Embedded pile length (mm): 400	**Overburden pressure (kPa):** 50
Slenderness ratio, L/D: 5	**Load eccentricity (mm):** 370
Pile wall thickness (mm): 5	**By:** A. B. Moreno, L. Mikalauskas
Comments: This test was carried out four times. The first three times the water flow through the membrane were approximately 200 l/hour. A new membrane solved the problem with respect to the water flow. And only the fourth sub-test is therefore considered. For the fourth sub-test strain gauge 16 did not work. Further, the displacement transducer in the height of the hydraulic piston failed.	

Soil parameters:

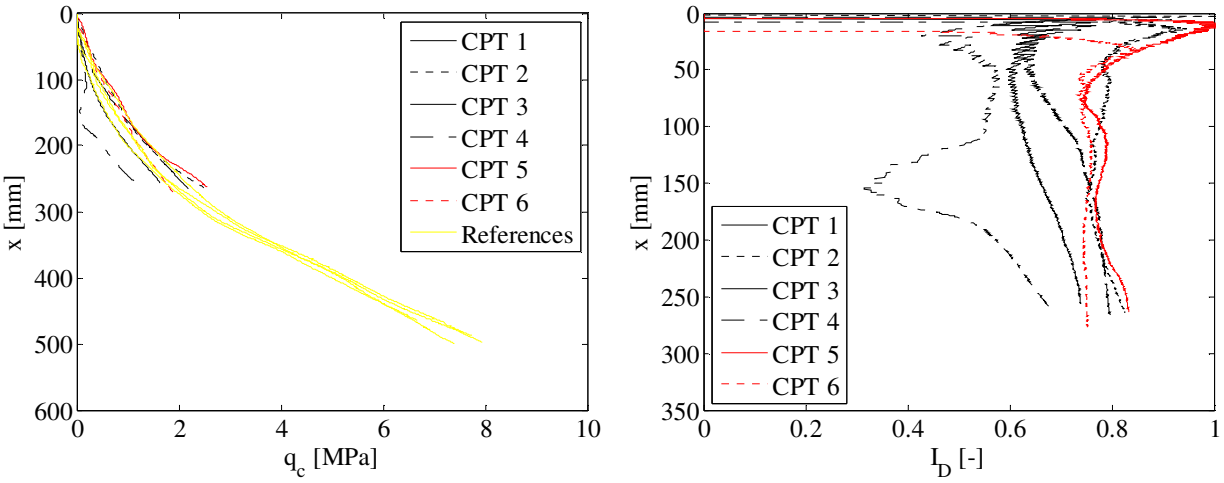

FIGURE 80. CPT-RESULTS FROM TEST 18. LEFT: TIP RESISTANCE VERSUS DEPTH – RIGHT: RELATIVE DENSITY VERSUS DEPTH.

TABLE 21. ESTIMATED SOIL PARAMETERS FOR TEST 18.

Relative density, I_D	Internal friction angle, φ_{tr}	Dilatancy angle, ψ_{tr}	Effective unit weight, γ'	Tangential Young's modulus of elasticity, E_0	Poisson's ratio, ν
[-]	[◦]	[◦]	[kN/m^3]	[MPa]	[-]
0.76	48.0	16.3	10.1	24.2	0.23

Test results:

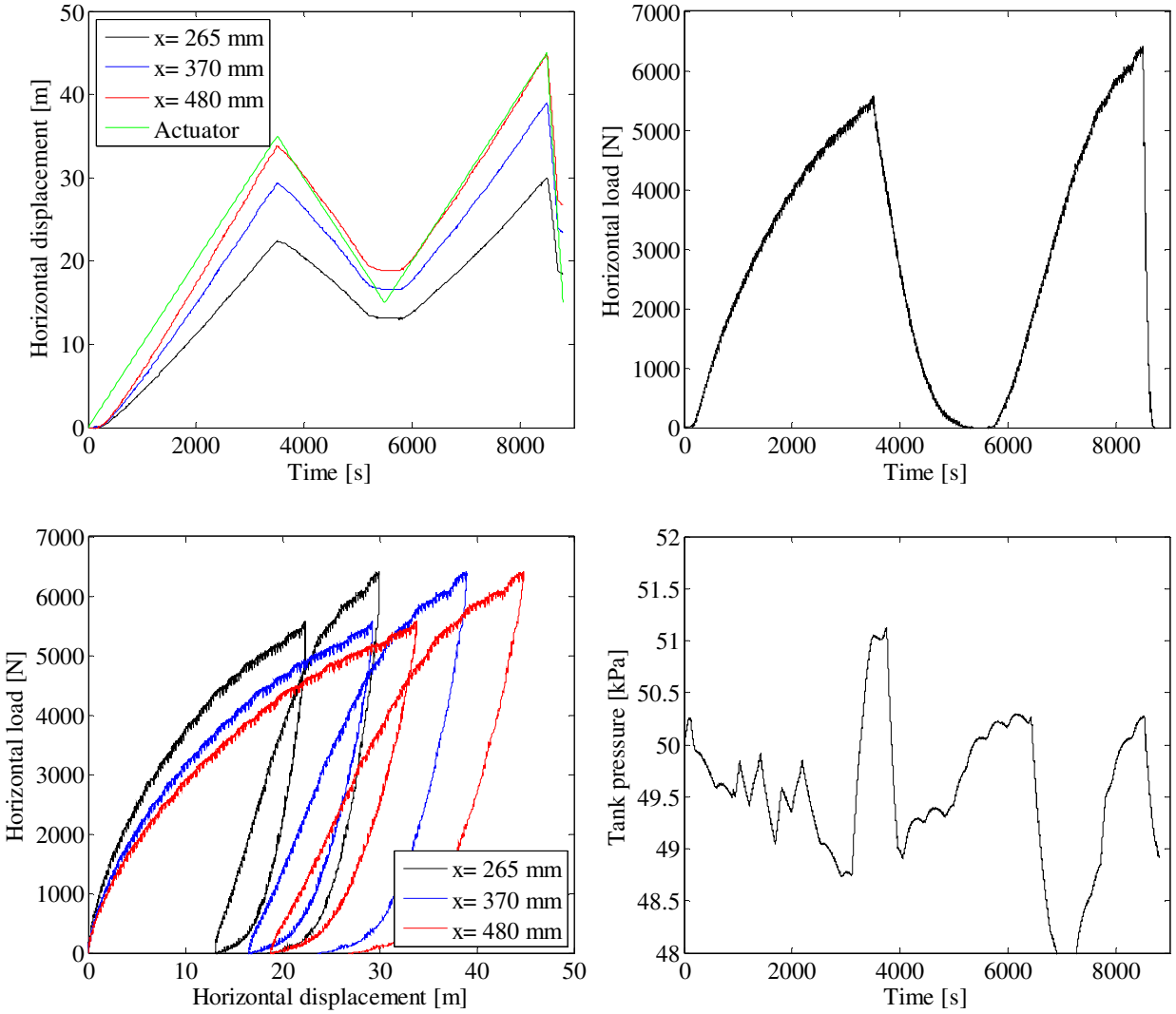

FIGURE 81. TOP LEFT: PILE DISPLACEMENT VERSUS TIME – TOP RIGHT: HORIZONTAL LOAD VERSUS TIME – BOTTOM LEFT: HORIZONTAL LOAD VERSUS PILE DISPLACEMENT – BOTTOM RIGHT: TANK PRESSURE VERSUS TIME.

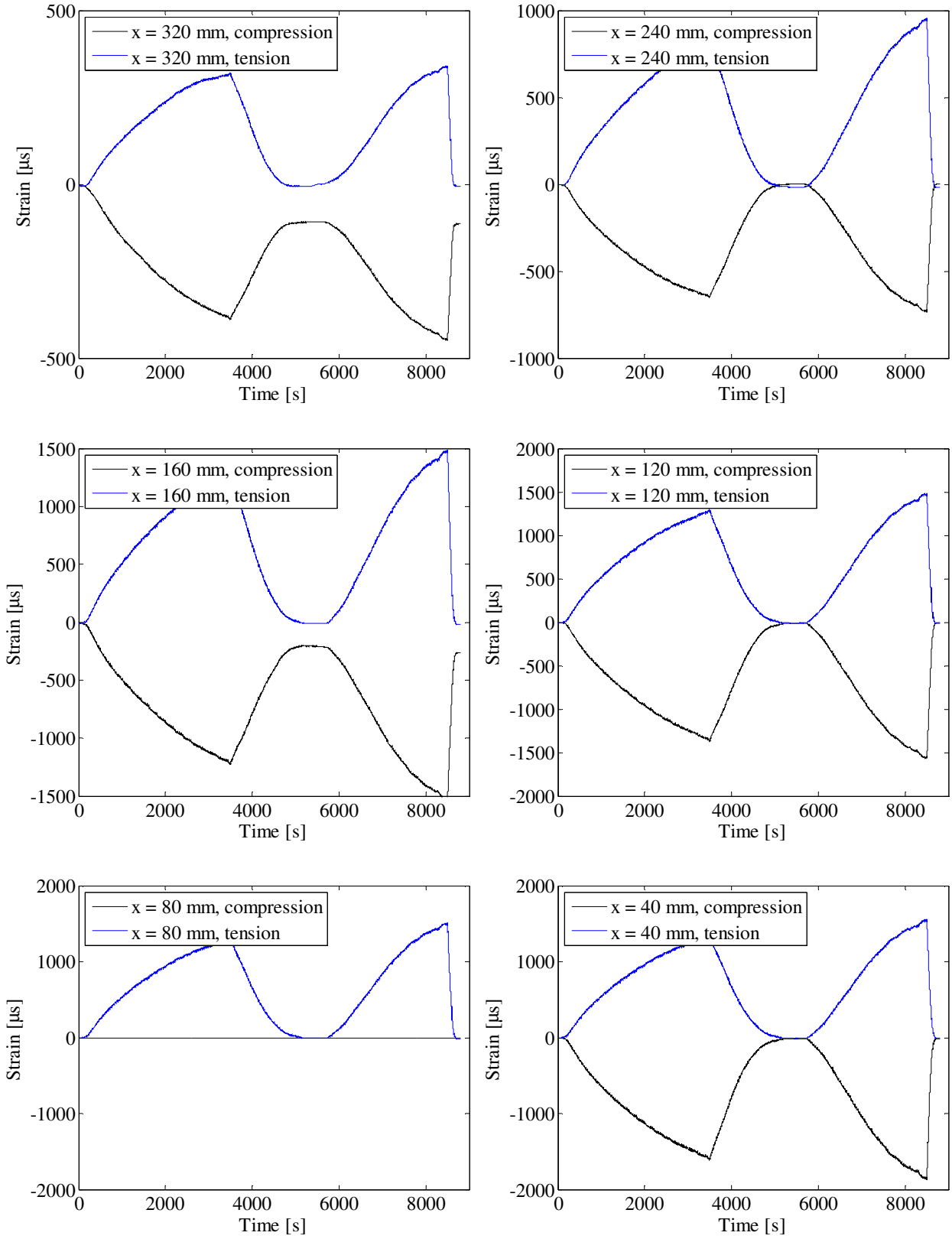

FIGURE 82. STRAIN GAUGE MEASUREMENTS.

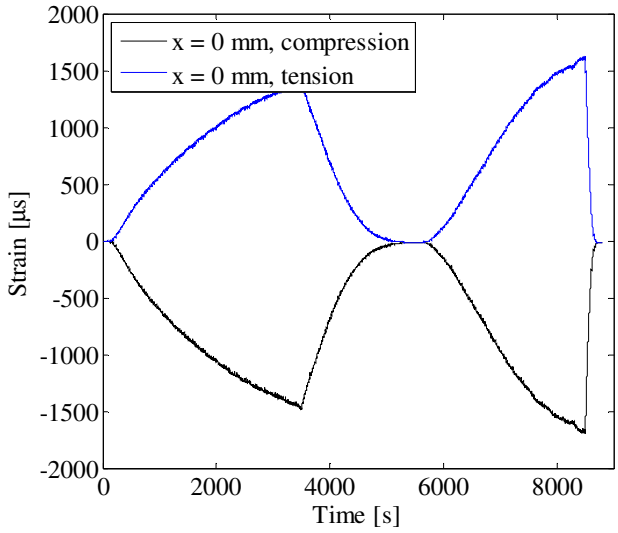

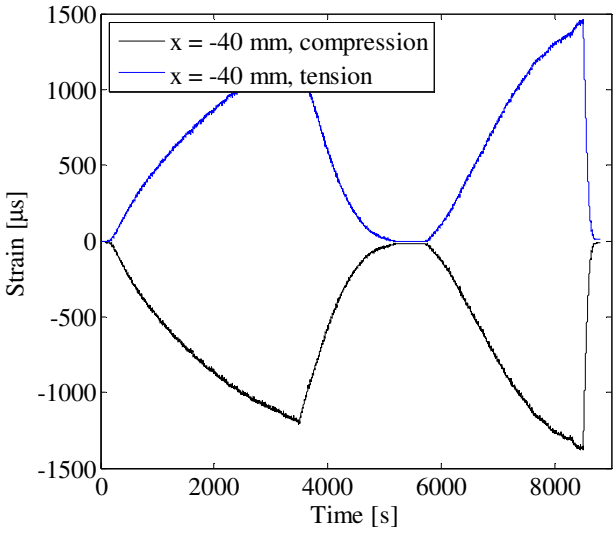

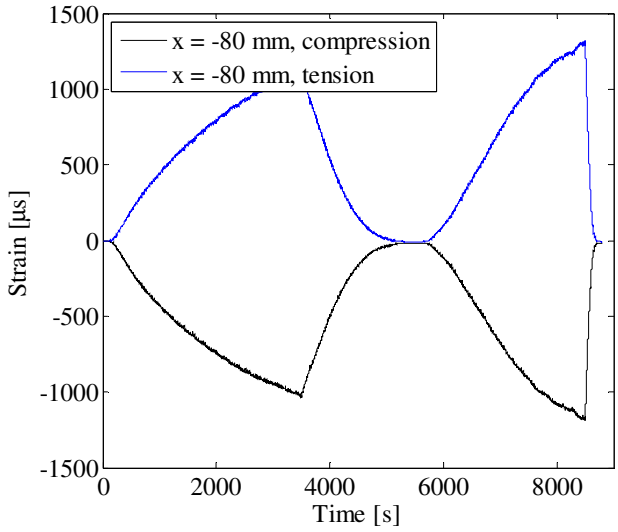

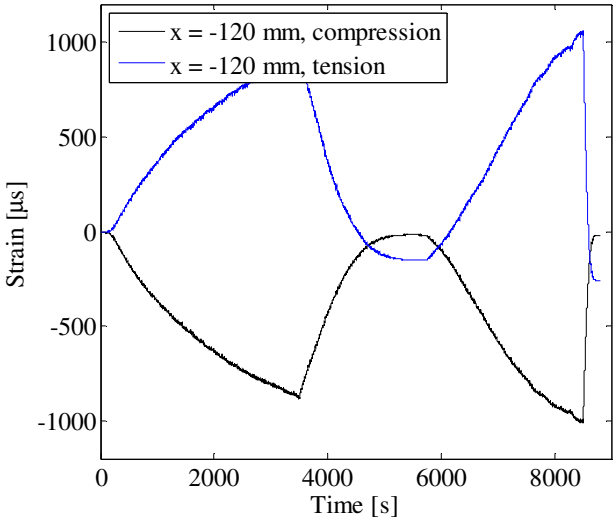

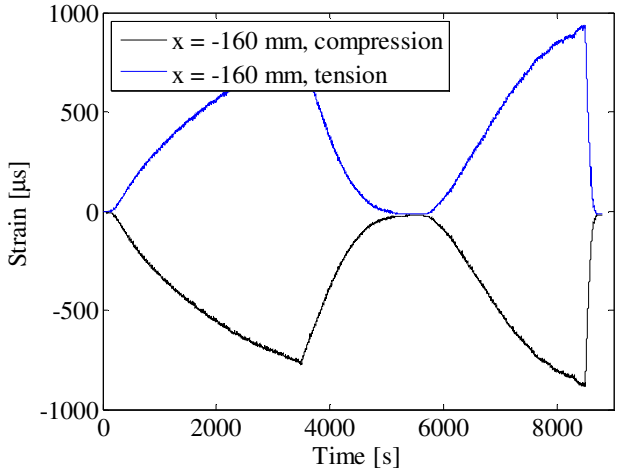

FIGURE 83. STRAIN GAUGE MEASUREMENTS.

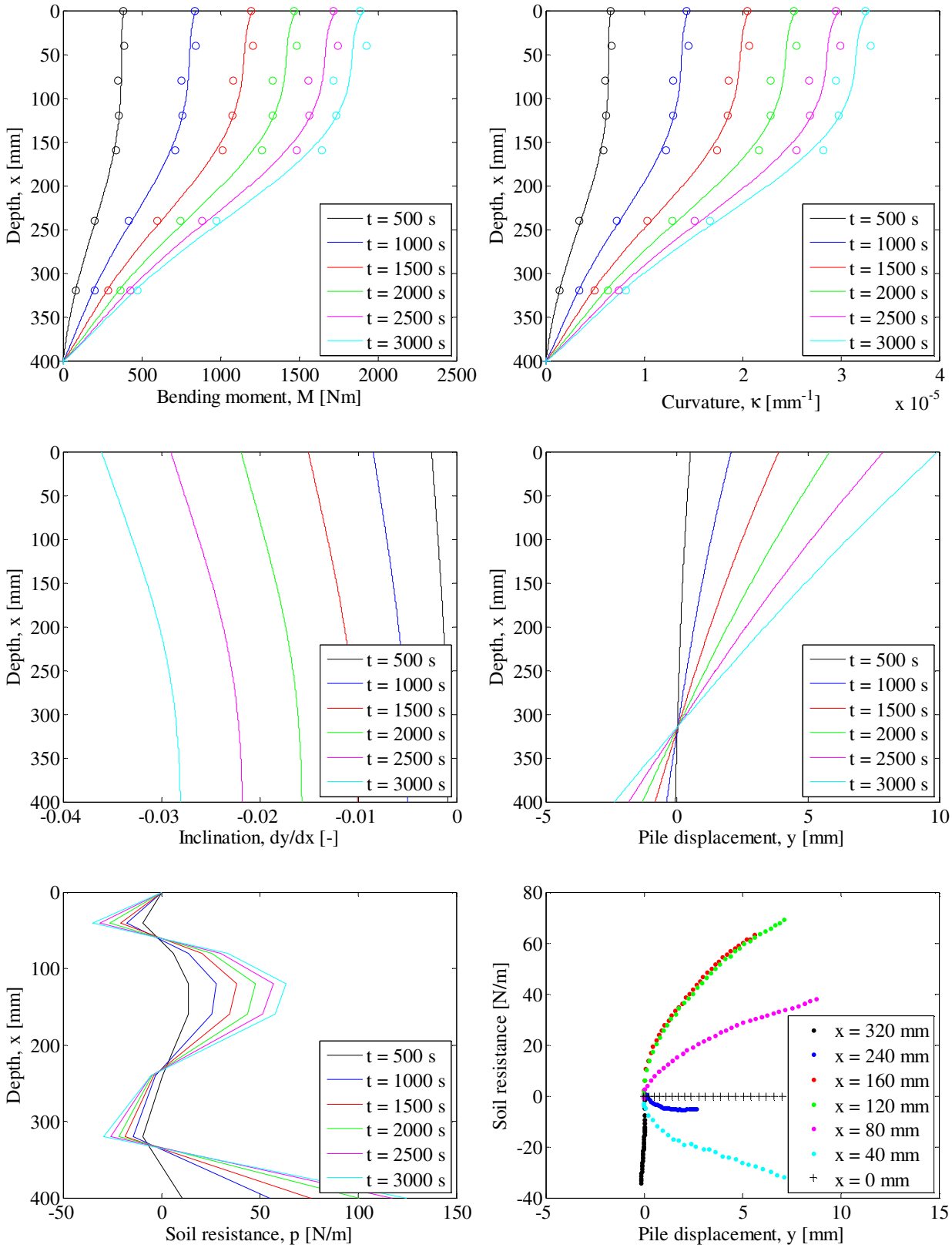

FIGURE 84. INTERPRETATION OF STRAIN GAUGE MEASUREMENTS. TOP LEFT: PILE BENDING MOMENT VERSUS DEPTH – TOP RIGHT: PILE CURVATURE VERSUS DEPTH – CENTER LEFT: PILE INCLINATION VERSUS DEPTH – CENTER RIGHT: PILE DISPLACEMENT VERSUS DEPTH – BOTTOM LEFT: SOIL RESISTANCE VERSUS DEPTH – BOTTOM RIGHT: P-Y CURVES.

Test 19: D = 80 mm, L_p = 400 mm and P_0 = 75 kPa (Closed-ended)

Pile type: Closed-ended	**Completed:** Summer 2011
Pile diameter (mm): 80	**No. of strain gauge levels:** 5 (All below soil surface)
Embedded pile length (mm): 400	**Overburden pressure (kPa):** 75
Slenderness ratio, *L*/*D*: 5	**Load eccentricity (mm):** 370
Pile wall thickness (mm): 5	**By:** S. P. H. Sørensen and L. Mikalauskas
Comments: Strain gauge number 5 did not function. The water flow through the membrane was approximately 70 L/hour.	

Soil parameters:

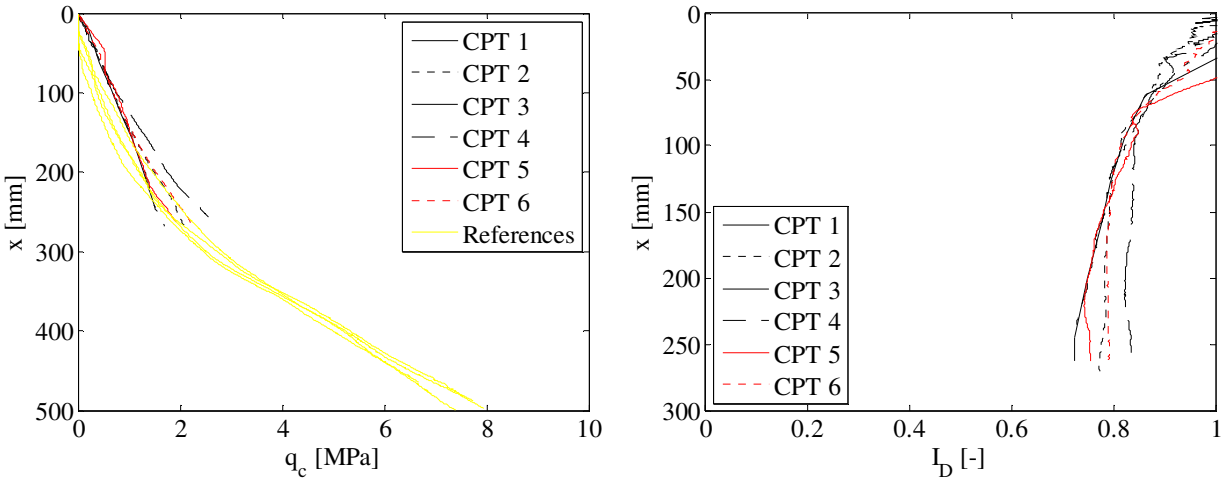

FIGURE 85. CPT-RESULTS FROM TEST 19. LEFT: TIP RESISTANCE VERSUS DEPTH – RIGHT: RELATIVE DENSITY VERSUS DEPTH.

TABLE 22. ESTIMATED SOIL PARAMETERS FOR TEST 19.

Relative density, I_D	Internal friction angle, φ_{tr}	Dilatancy angle, ψ_{tr}	Effective unit weight, γ'	Tangential Young's modulus of elasticity, E_0	Poisson's ratio, ν
[-]	[◦]	[◦]	[kN/m^3]	[MPa]	[-]
0.79	47.1	16.5	10.2	33.9	0.23

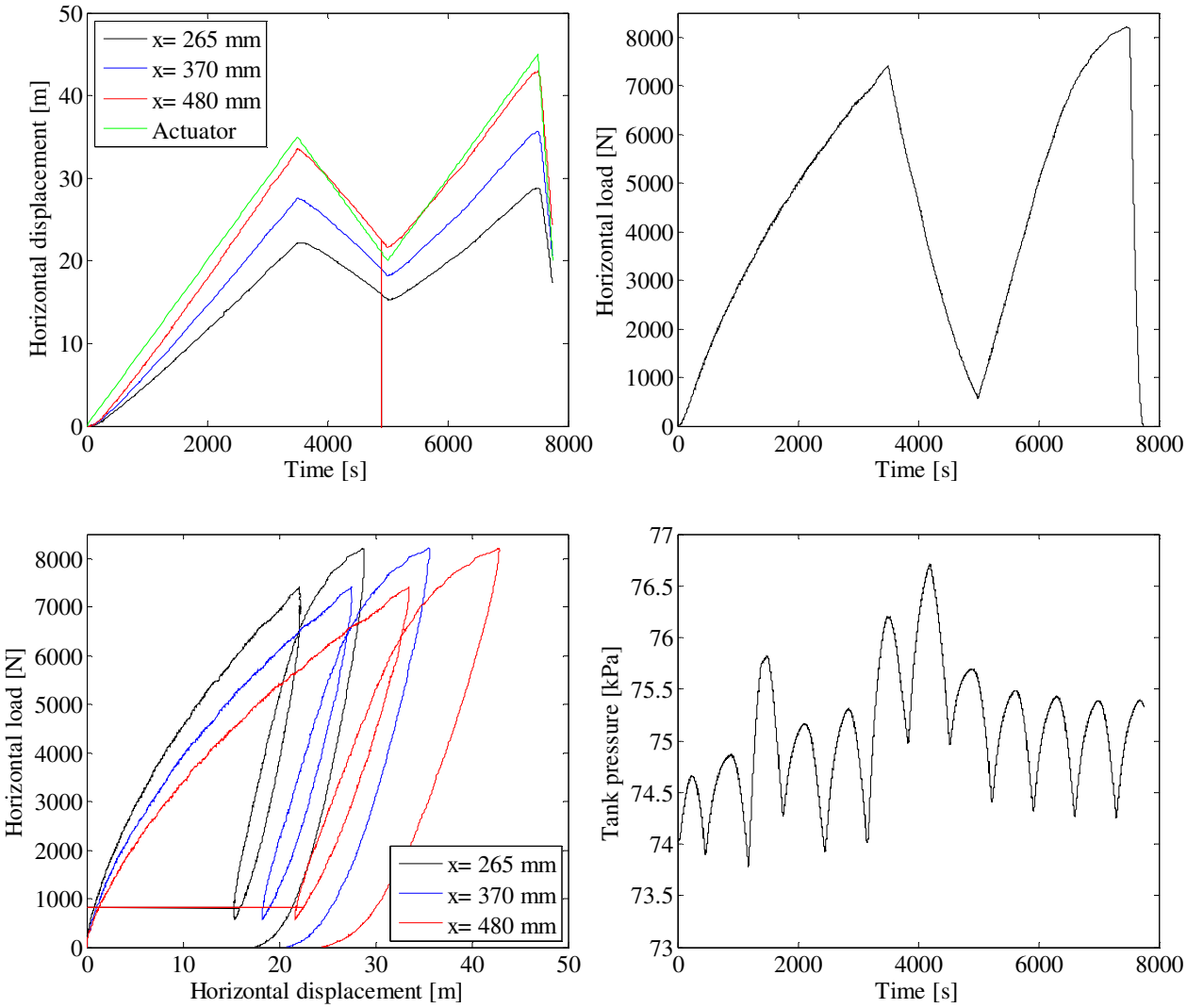

FIGURE 86. TOP LEFT: PILE DISPLACEMENT VERSUS TIME – TOP RIGHT: HORIZONTAL LOAD VERSUS TIME – BOTTOM LEFT: HORIZONTAL LOAD VERSUS PILE DISPLACEMENT – BOTTOM RIGHT: TANK PRESSURE VERSUS TIME.

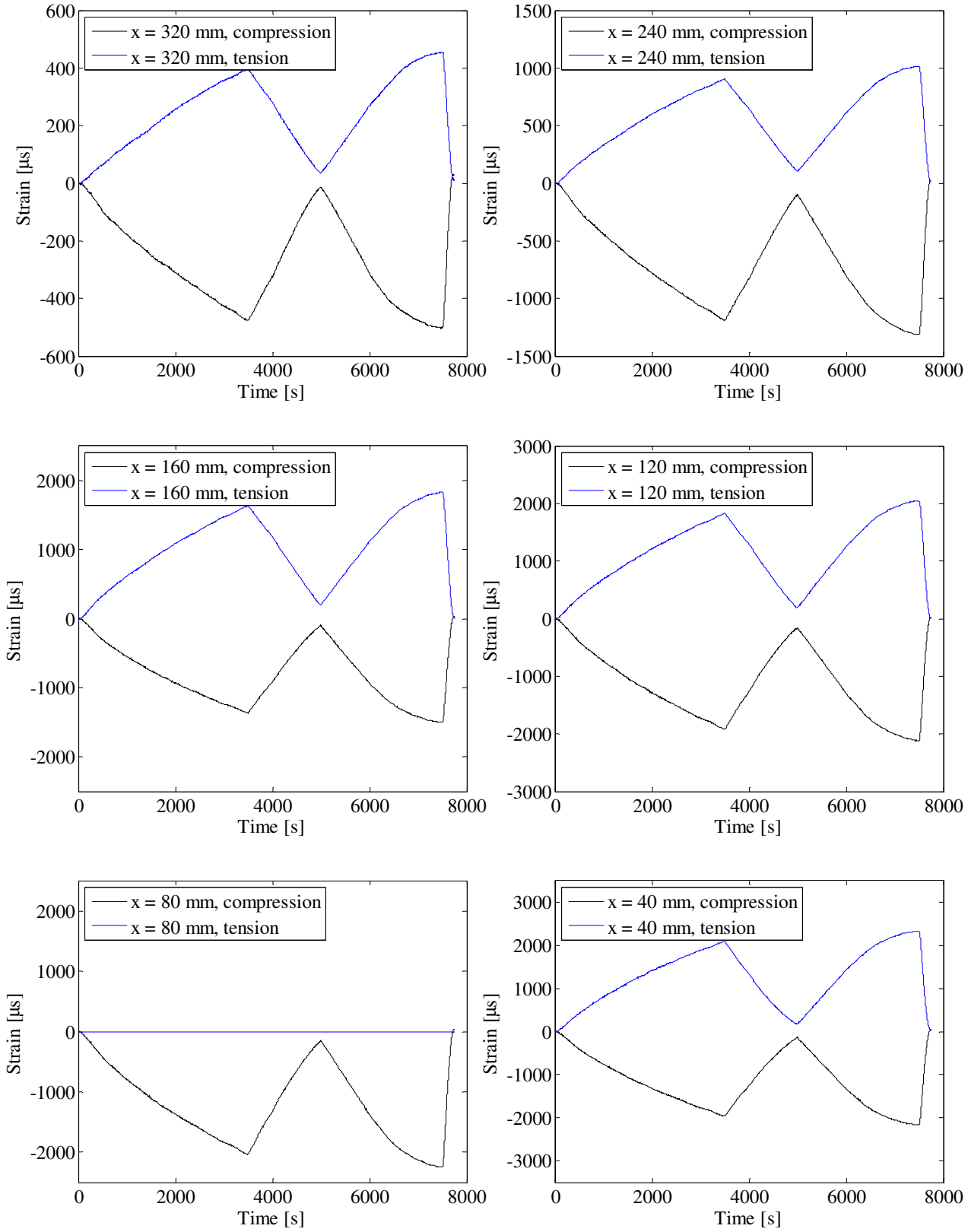

FIGURE 87. STRAIN GAUGE MEASUREMENTS.

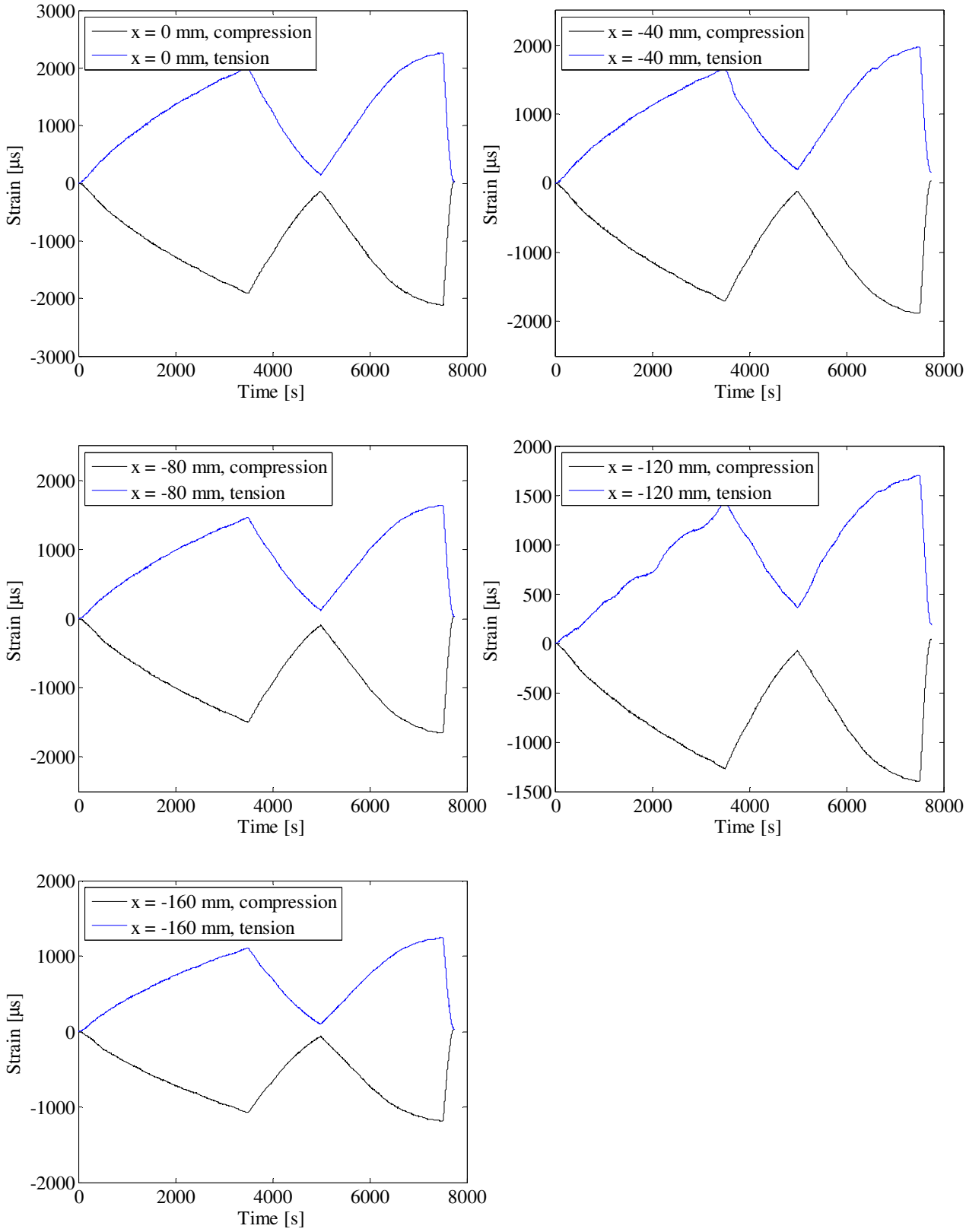

FIGURE 88. STRAIN GAUGE MEASUREMENTS.

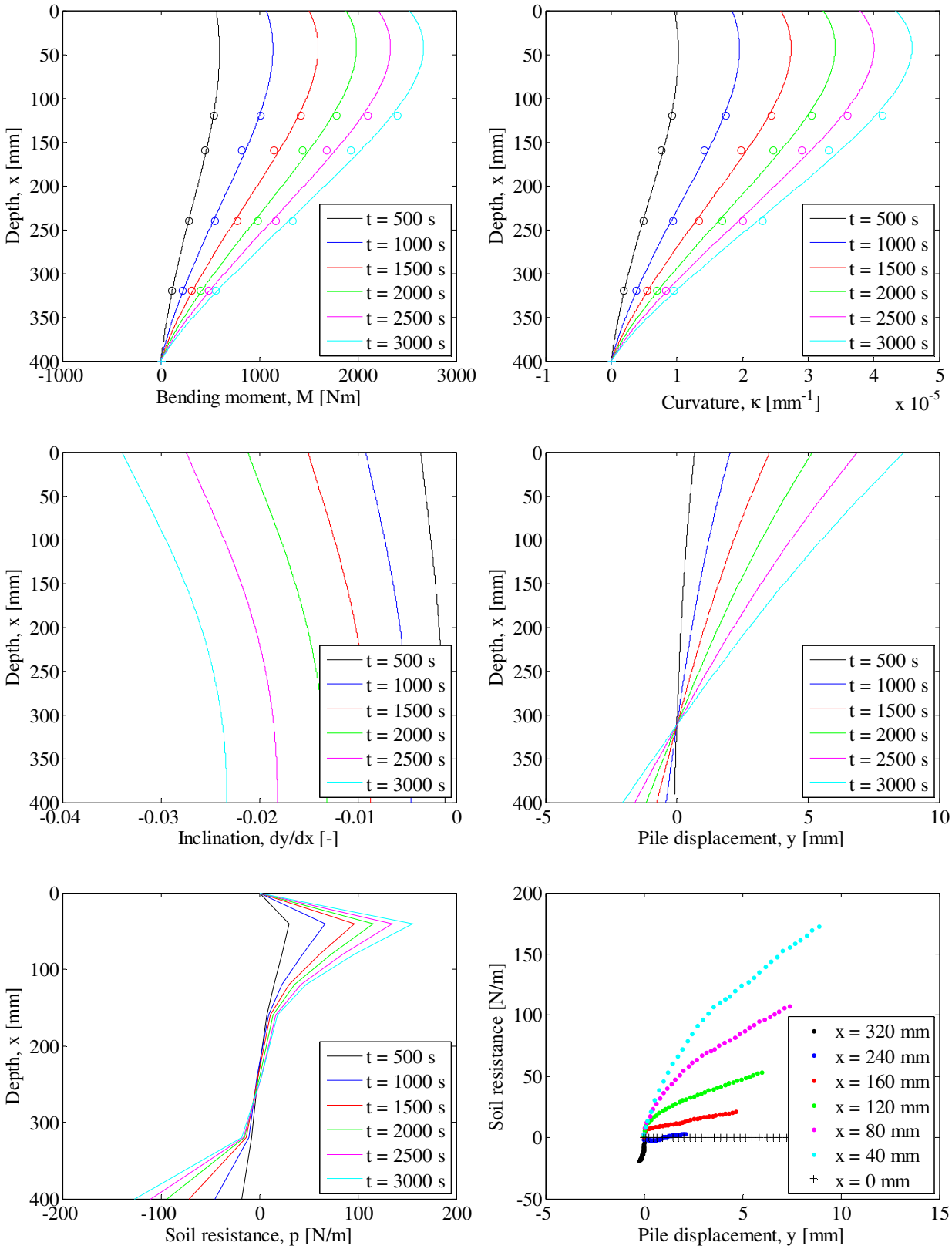

FIGURE 89. INTERPRETATION OF STRAIN GAUGE MEASUREMENTS. TOP LEFT: PILE BENDING MOMENT VERSUS DEPTH – TOP RIGHT: PILE CURVATURE VERSUS DEPTH – CENTER LEFT: PILE INCLINATION VERSUS DEPTH – CENTER RIGHT: PILE DISPLACEMENT VERSUS DEPTH – BOTTOM LEFT: SOIL RESISTANCE VERSUS DEPTH – BOTTOM RIGHT: P-Y CURVES.

Test 20: D = 80 mm, L_p = 400 mm and P_0 = 100 kPa (Closed-ended)

Pile type: Closed-ended	**Completed:** Spring 2009
Pile diameter (mm): 80	**No. of strain gauge levels:** 5 (All below soil surface)
Embedded pile length (mm): 400	**Overburden pressure (kPa):** 100
Slenderness ratio, L/D: 5	**Load eccentricity (mm):** 370
Pile wall thickness (mm): 5	**By:** S. P. H. Sørensen, K. T. Brødbæk and M. Møller
Comments: The strain gauges exposed to tension at depths of 5.5, 76, and 266 mm, respectively do not work properly at strains larger than 1230, 1720, and 220 µm, respectively. Hence, the strain gauges loaded in compression are assumed to be representative at these depths for strains exceeding 1230, 1720, and 220 µm, respectively	

Soil parameters:

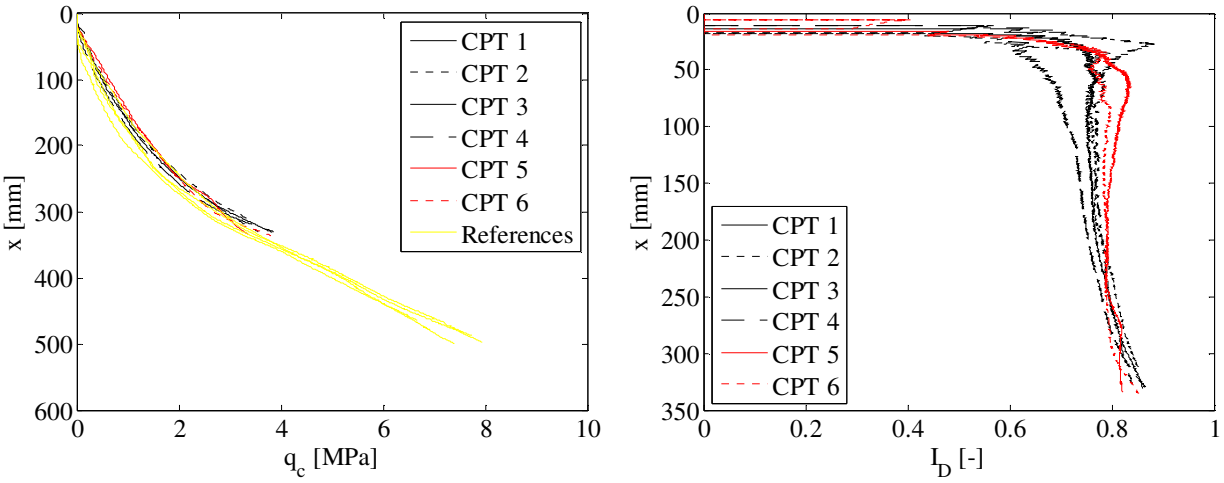

FIGURE 90. CPT-RESULTS FROM TEST 20. LEFT: TIP RESISTANCE VERSUS DEPTH – RIGHT: RELATIVE DENSITY VERSUS DEPTH.

TABLE 23. ESTIMATED SOIL PARAMETERS FOR TEST 20.

Relative density, I_D	Internal friction angle, φ_{tr}	Dilatancy angle, ψ_{tr}	Effective unit weight, γ'	Tangential Young's modulus of elasticity, E_0	Poisson's ratio, ν
[-]	[◦]	[◦]	[kN/m^3]	[MPa]	[-]
0.79	45.9	15.3	10.2	41.1	0.23

Test results:

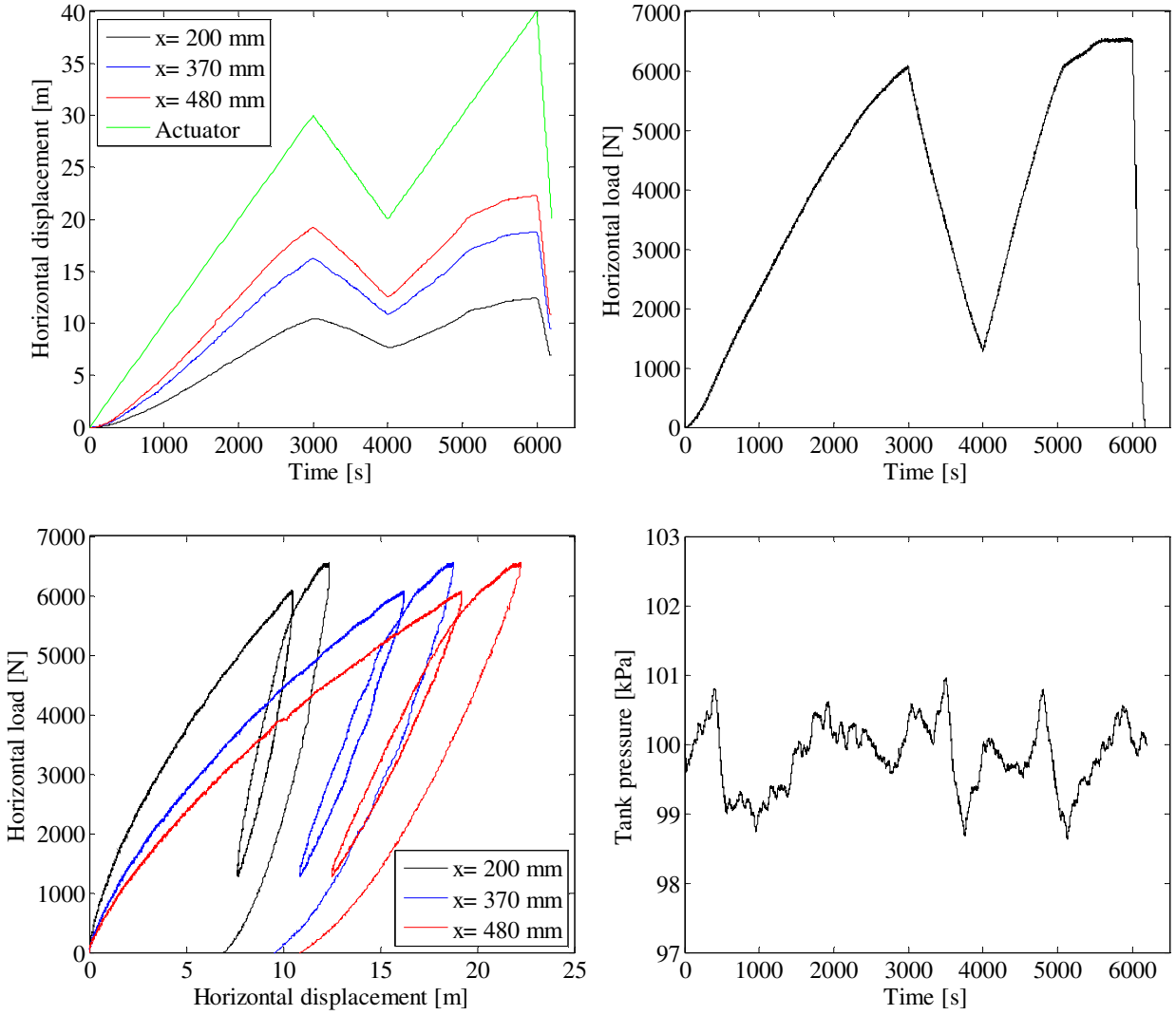

FIGURE 91. TOP LEFT: PILE DISPLACEMENT VERSUS TIME – TOP RIGHT: HORIZONTAL LOAD VERSUS TIME – BOTTOM LEFT: HORIZONTAL LOAD VERSUS PILE DISPLACEMENT – BOTTOM RIGHT: TANK PRESSURE VERSUS TIME.

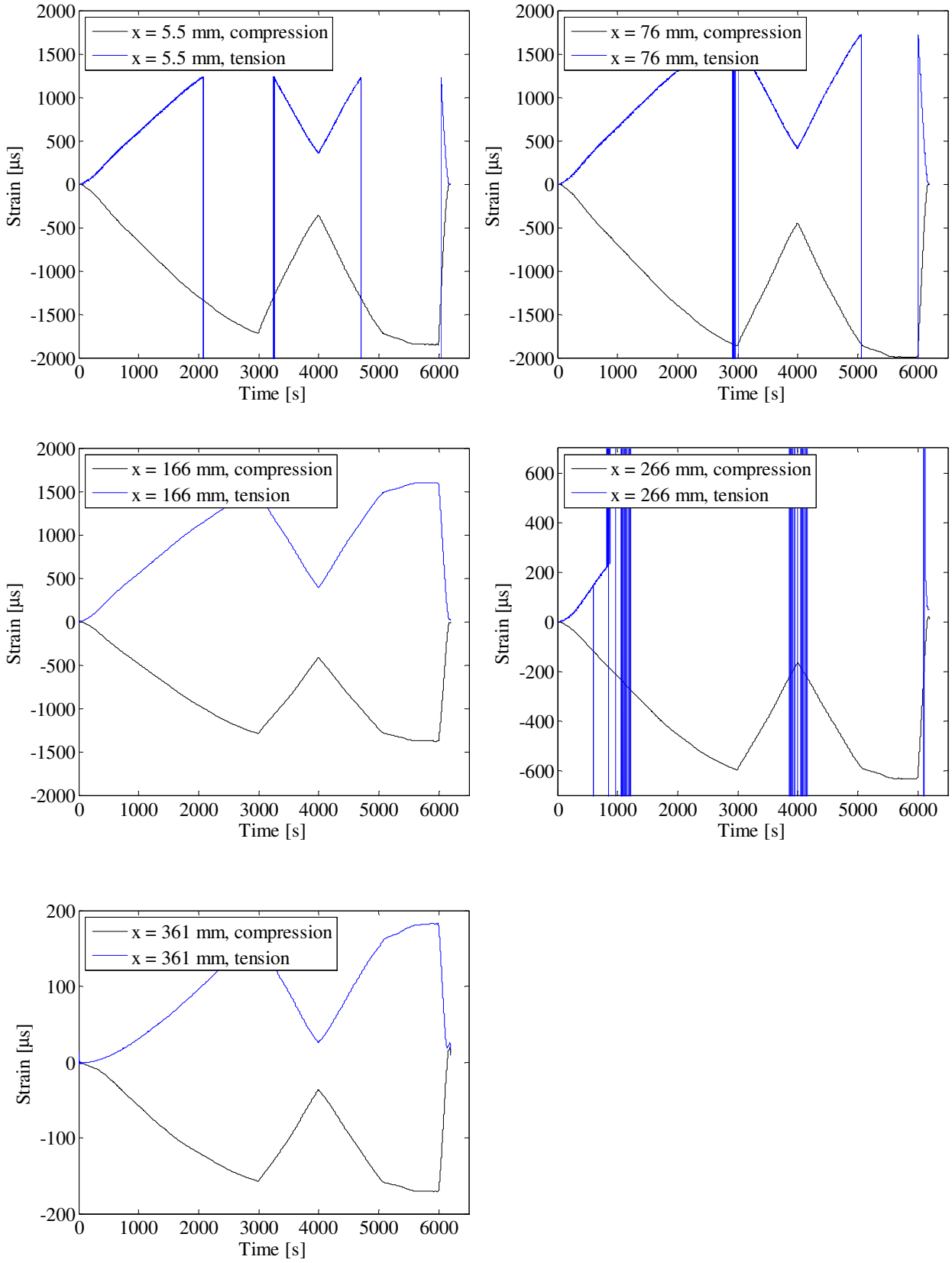

FIGURE 92. STRAIN GAUGE MEASUREMENTS.

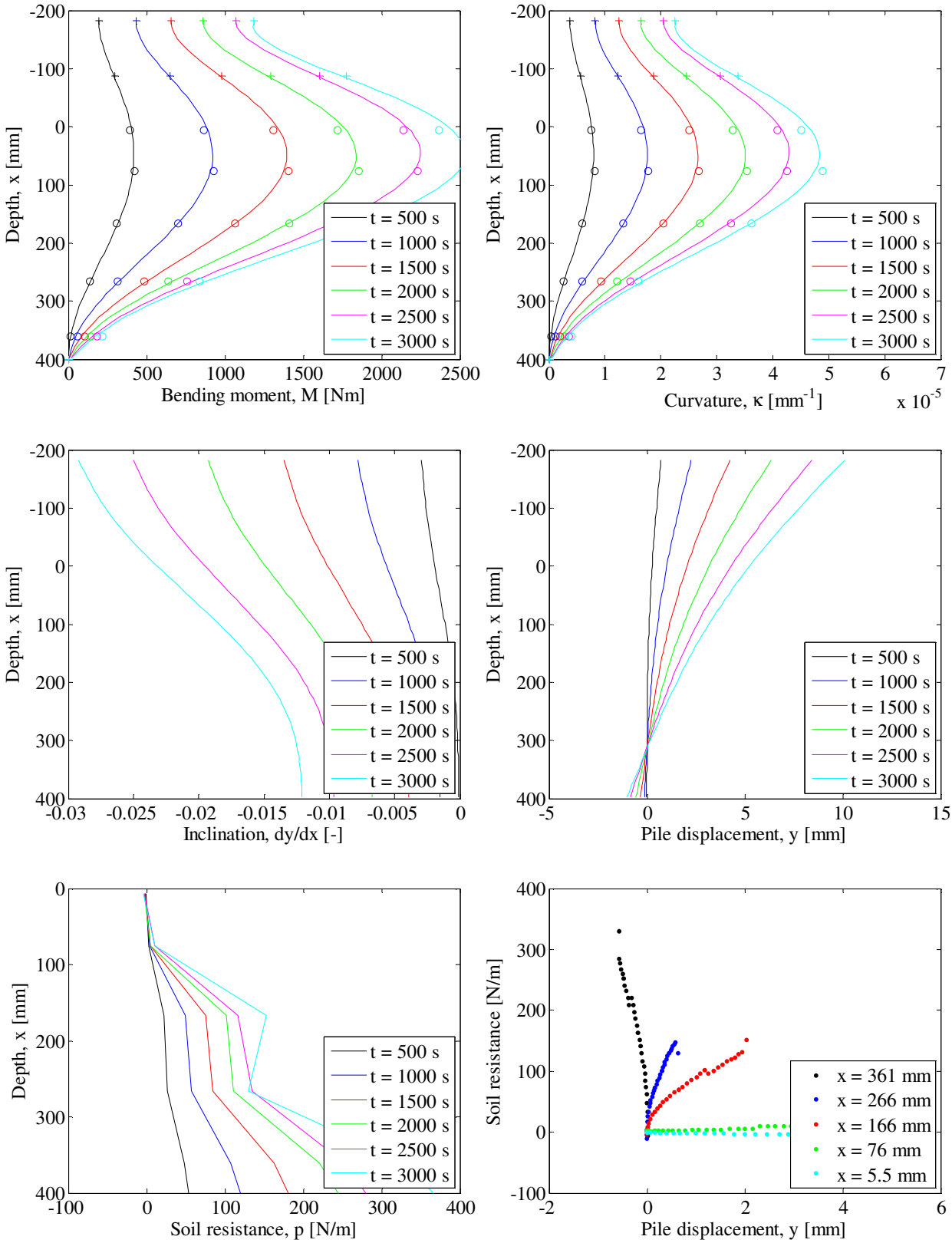

FIGURE 93. INTERPRETATION OF STRAIN GAUGE MEASUREMENTS. TOP LEFT: PILE BENDING MOMENT VERSUS DEPTH – TOP RIGHT: PILE CURVATURE VERSUS DEPTH – CENTER LEFT: PILE INCLINATION VERSUS DEPTH – CENTER RIGHT: PILE DISPLACEMENT VERSUS DEPTH – BOTTOM LEFT: SOIL RESISTANCE VERSUS DEPTH – BOTTOM RIGHT: P-Y CURVES.

Test 21: D = 80 mm, L_p = 400 mm and P_0 = 100 kPa (Closed-ended)

Pile type: Closed-ended	**Completed:** Fall 2010
Pile diameter (mm): 80	**No. of strain gauge levels:** 11 (7 below soil surface)
Embedded pile length (mm): 400	**Overburden pressure (kPa):** 100
Slenderness ratio, L/D: 5	**Load eccentricity (mm):** 370
Pile wall thickness (mm): 5	**By:** A. B. Moreno, L. Mikalauskas and J. L. T. Diaz
Comments: The water flow through the membrane was approximately 40 l/hour.	

Soil parameters:

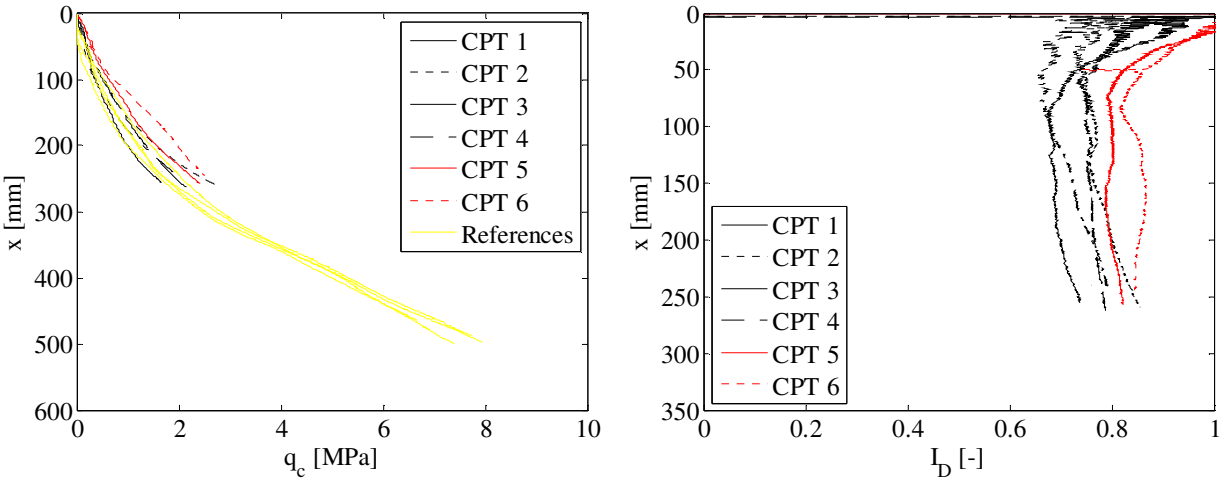

FIGURE 94. CPT-RESULTS FROM TEST 21. LEFT: TIP RESISTANCE VERSUS DEPTH – RIGHT: RELATIVE DENSITY VERSUS DEPTH.

TABLE 24. ESTIMATED SOIL PARAMETERS FOR TEST 21.

Relative density, I_D	Internal friction angle, φ_{tr}	Dilatancy angle, ψ_{tr}	Effective unit weight, γ'	Tangential Young's modulus of elasticity, E_0	Poisson's ratio, ν
[-]	[◦]	[◦]	[kN/m^3]	[MPa]	[-]
0.78	45.7	15.9	10.1	40.3	0.23

Test results:

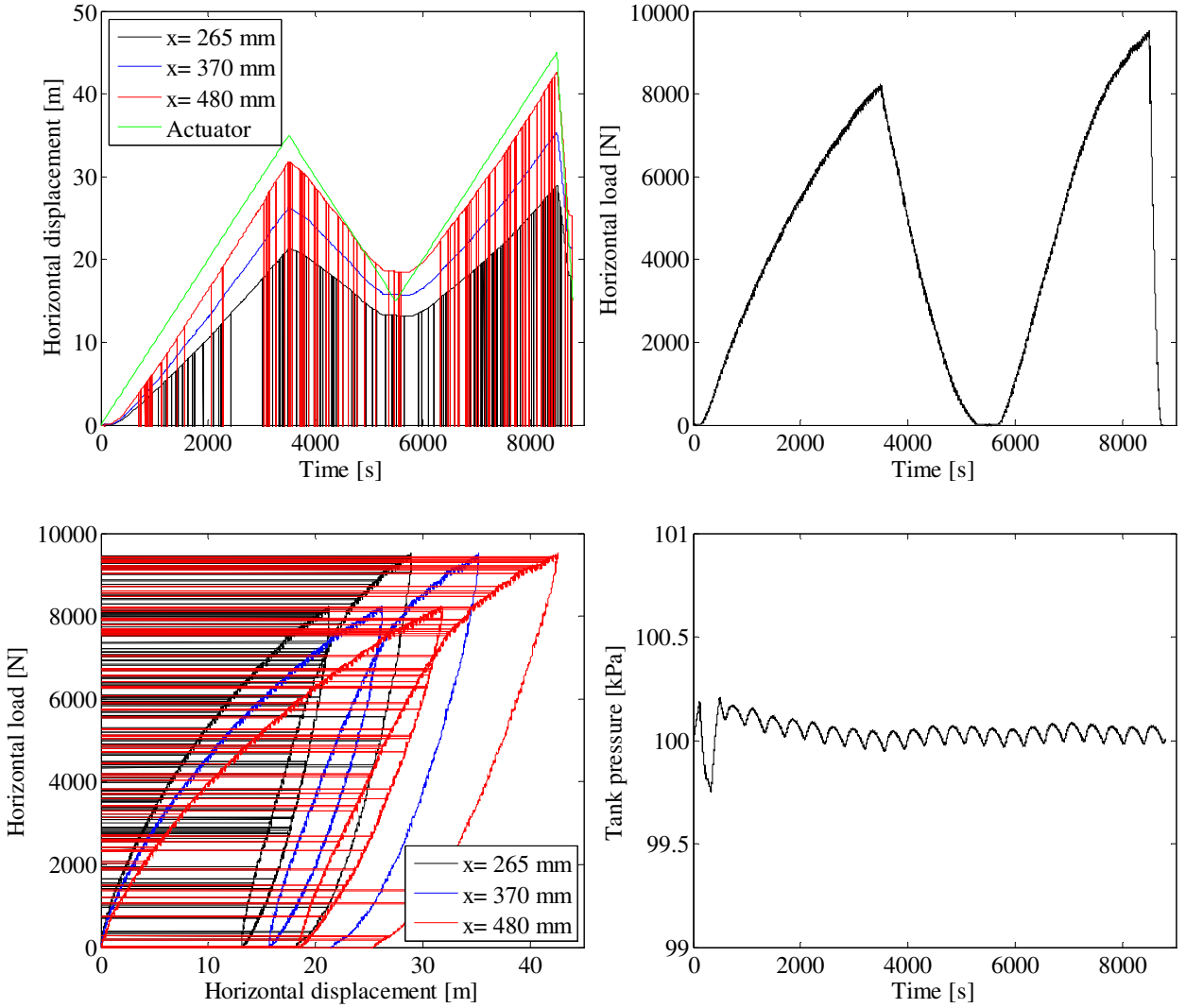

FIGURE 95. TOP LEFT: PILE DISPLACEMENT VERSUS TIME – TOP RIGHT: HORIZONTAL LOAD VERSUS TIME – BOTTOM LEFT: HORIZONTAL LOAD VERSUS PILE DISPLACEMENT – BOTTOM RIGHT: TANK PRESSURE VERSUS TIME.

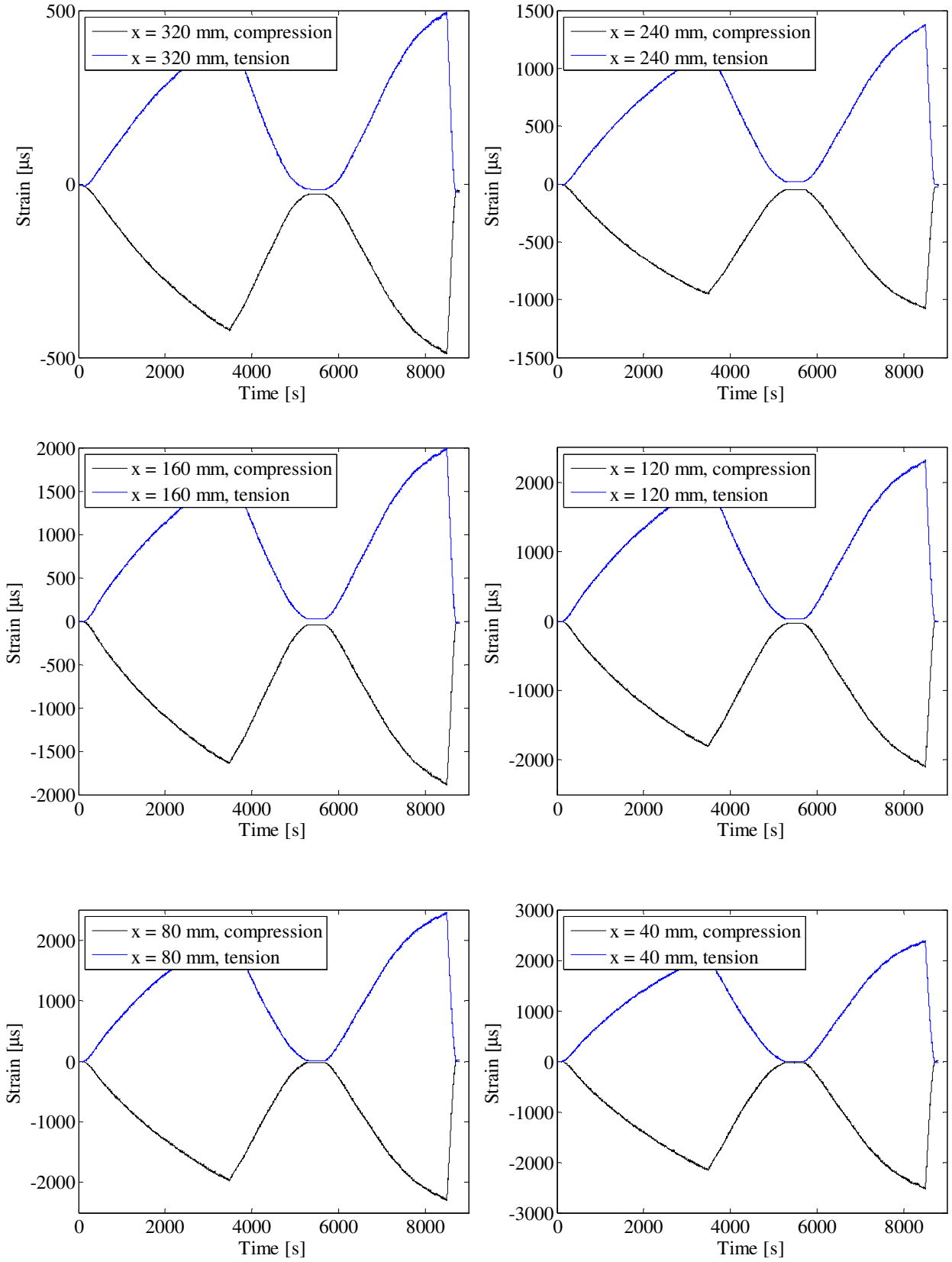

FIGURE 96. STRAIN GAUGE MEASUREMENTS.

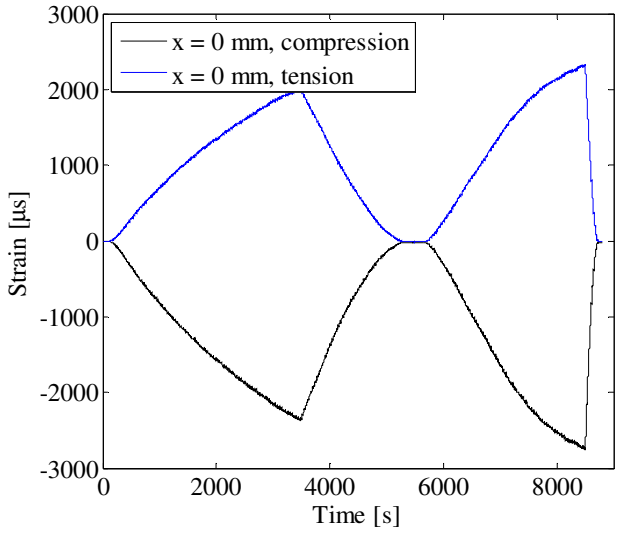

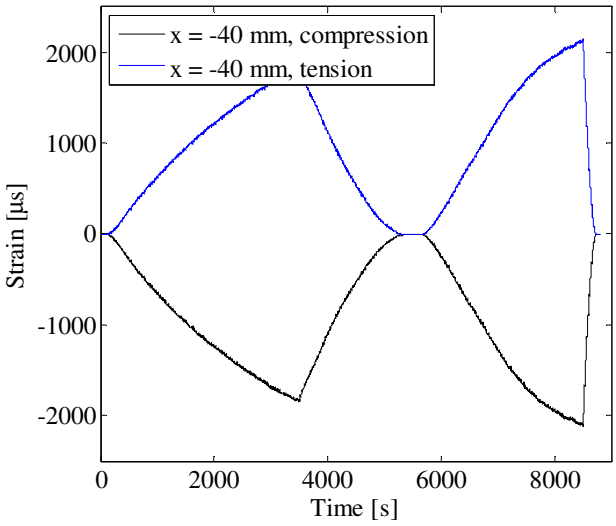

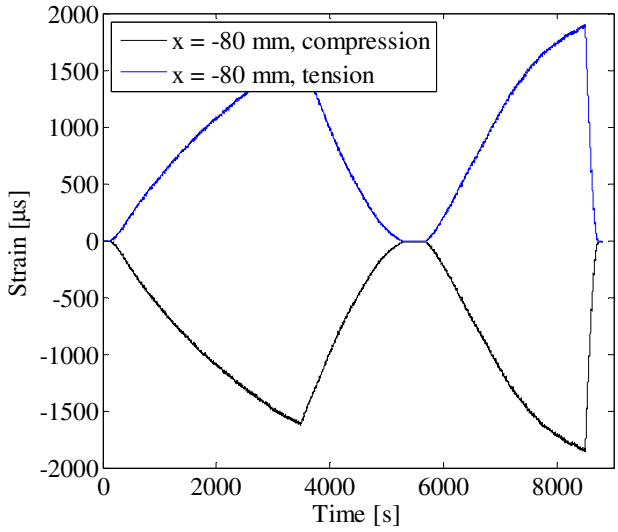

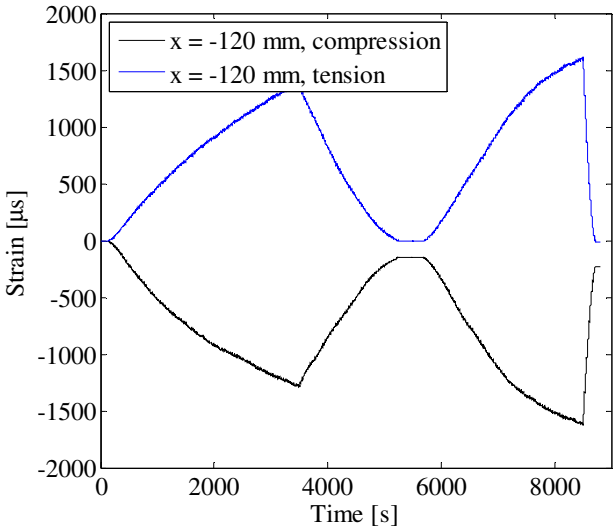

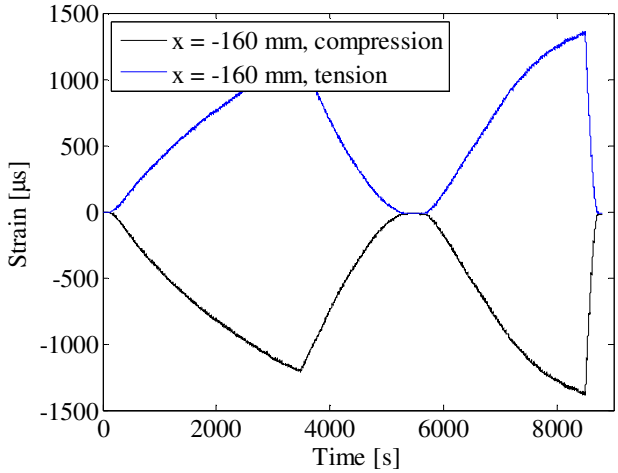

FIGURE 97. STRAIN GAUGE MEASUREMENTS.

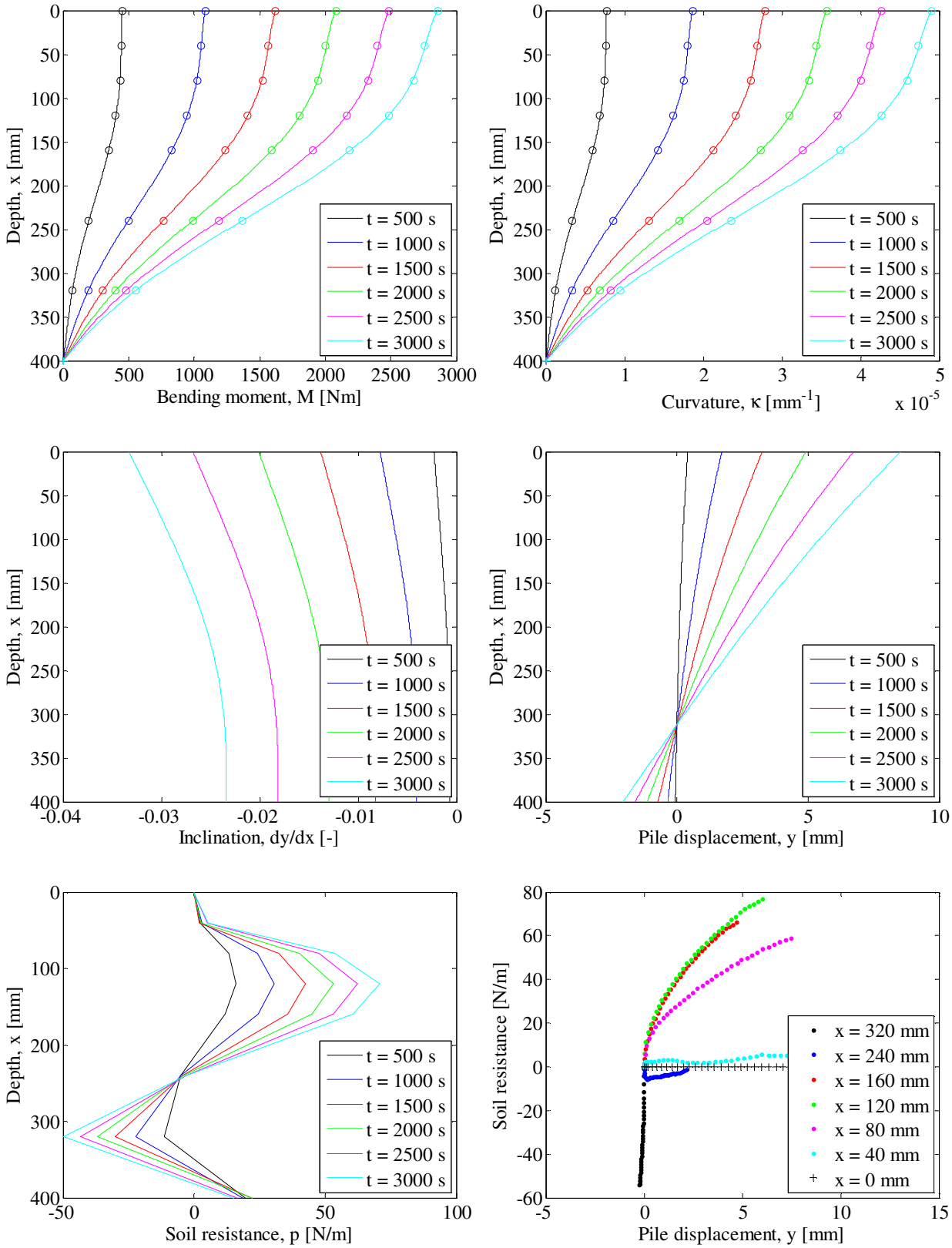

FIGURE 98. INTERPRETATION OF STRAIN GAUGE MEASUREMENTS. TOP LEFT: PILE BENDING MOMENT VERSUS DEPTH – TOP RIGHT: PILE CURVATURE VERSUS DEPTH – CENTER LEFT: PILE INCLINATION VERSUS DEPTH – CENTER RIGHT: PILE DISPLACEMENT VERSUS DEPTH – BOTTOM LEFT: SOIL RESISTANCE VERSUS DEPTH – BOTTOM RIGHT: P-Y CURVES.

Test 22: D = 80 mm, L_p = 480 mm and P_0 = 0 kPa (Open-ended)

Pile type: Open-ended	**Completed:** Summer 2010
Pile diameter (mm): 80	**No. of strain gauge levels:** 0
Embedded pile length (mm): 480	**Overburden pressure (kPa):** 0
Slenderness ratio, *L*/*D*: 6	**Load eccentricity (mm):** 370
Pile wall thickness (mm): 5	**By:** S. P. H. Sørensen
Comments:	

Soil parameters:

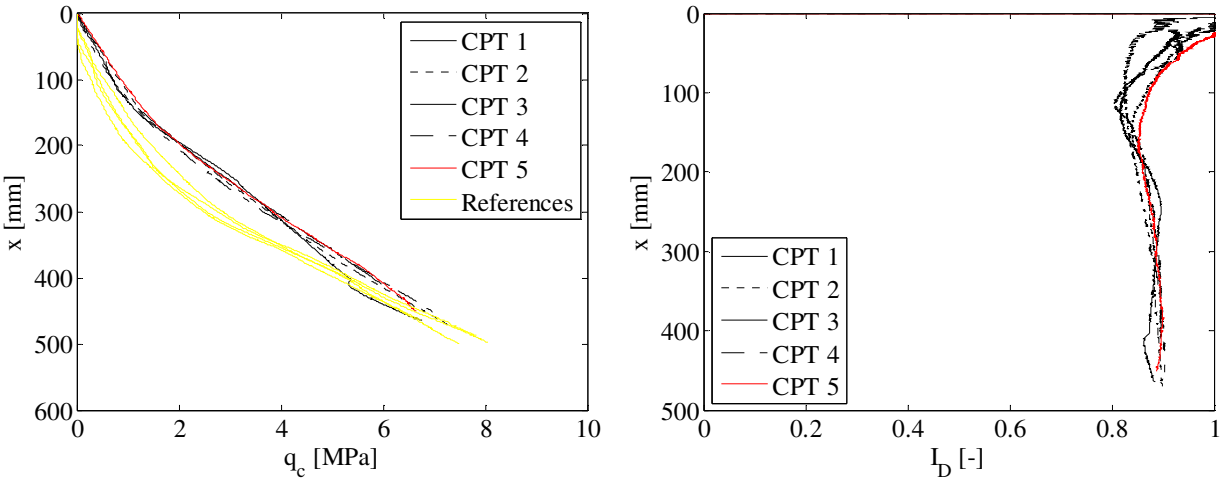

FIGURE 99. CPT-RESULTS FROM TEST 22. LEFT: TIP RESISTANCE VERSUS DEPTH – RIGHT: RELATIVE DENSITY VERSUS DEPTH.

TABLE 25. ESTIMATED SOIL PARAMETERS FOR TEST 22.

Relative density, I_D	Internal friction angle, φ_{tr}	Dilatancy angle, ψ_{tr}	Effective unit weight, γ'	Tangential Young's modulus of elasticity, E_0	Poisson's ratio, ν
[-]	[◦]	[◦]	[kN/m^3]	[MPa]	[-]
0.87	53.9	19.8	10.3	-	0.23

Test results:

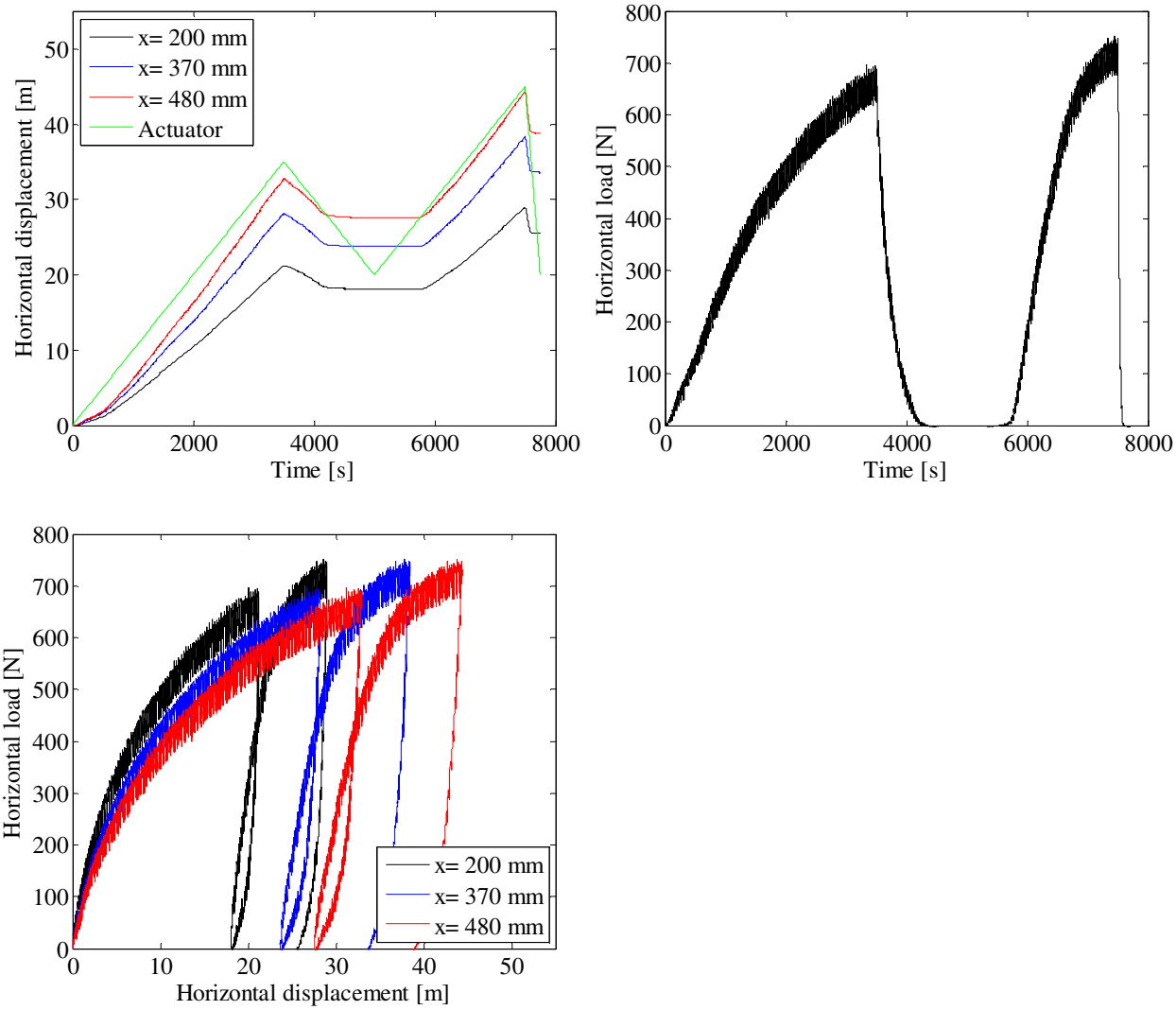

FIGURE 100. TOP LEFT: PILE DISPLACEMENT VERSUS TIME – TOP RIGHT: HORIZONTAL LOAD VERSUS TIME – BOTTOM LEFT: HORIZONTAL LOAD VERSUS PILE DISPLACEMENT.

Test 23: D = 80 mm, L_p = 480 mm and P_0 = 0 kPa (Closed-ended)

Pile type: Closed-ended	**Completed:** Summer 2010
Pile diameter (mm): 80	**No. of strain gauge levels:** 11 (9 below soil surface)
Embedded pile length (mm): 480	**Overburden pressure (kPa):** 0
Slenderness ratio, *L*/*D*: 6	**Load eccentricity (mm):** 370
Pile wall thickness (mm): 5	**By:** S. P. H. Sørensen
Comments: No signal was received from strain gauge 3, 7, 12, 16 and 17. In the interpretation of the strain gauge measurements strain gauge 1, 4, 5, 14 and 18 are therefore assumed to be representative for the curvature at these depths.	

Soil parameters:

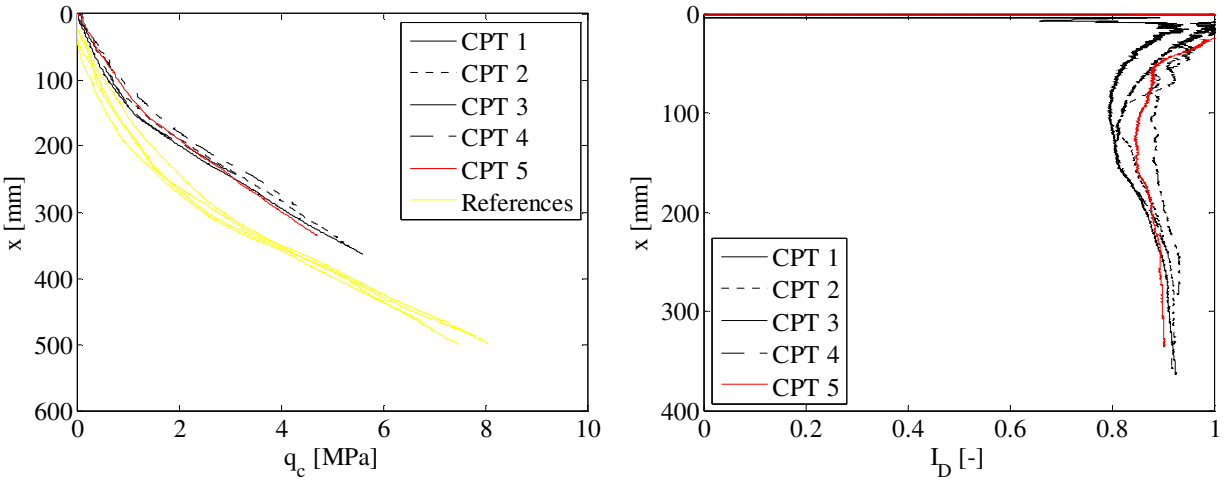

FIGURE 101. CPT-RESULTS FROM TEST 23. LEFT: TIP RESISTANCE VERSUS DEPTH – RIGHT: RELATIVE DENSITY VERSUS DEPTH.

TABLE 26. ESTIMATED SOIL PARAMETERS FOR TEST 23.

Relative density, I_D	Internal friction angle, φ_{tr}	Dilatancy angle, ψ_{tr}	Effective unit weight, γ'	Tangential Young's modulus of elasticity, E_0	Poisson's ratio, ν
[-]	[◦]	[◦]	[kN/m^3]	[MPa]	[-]
0.88	54.0	19.9	10.4	-	0.23

Test results:

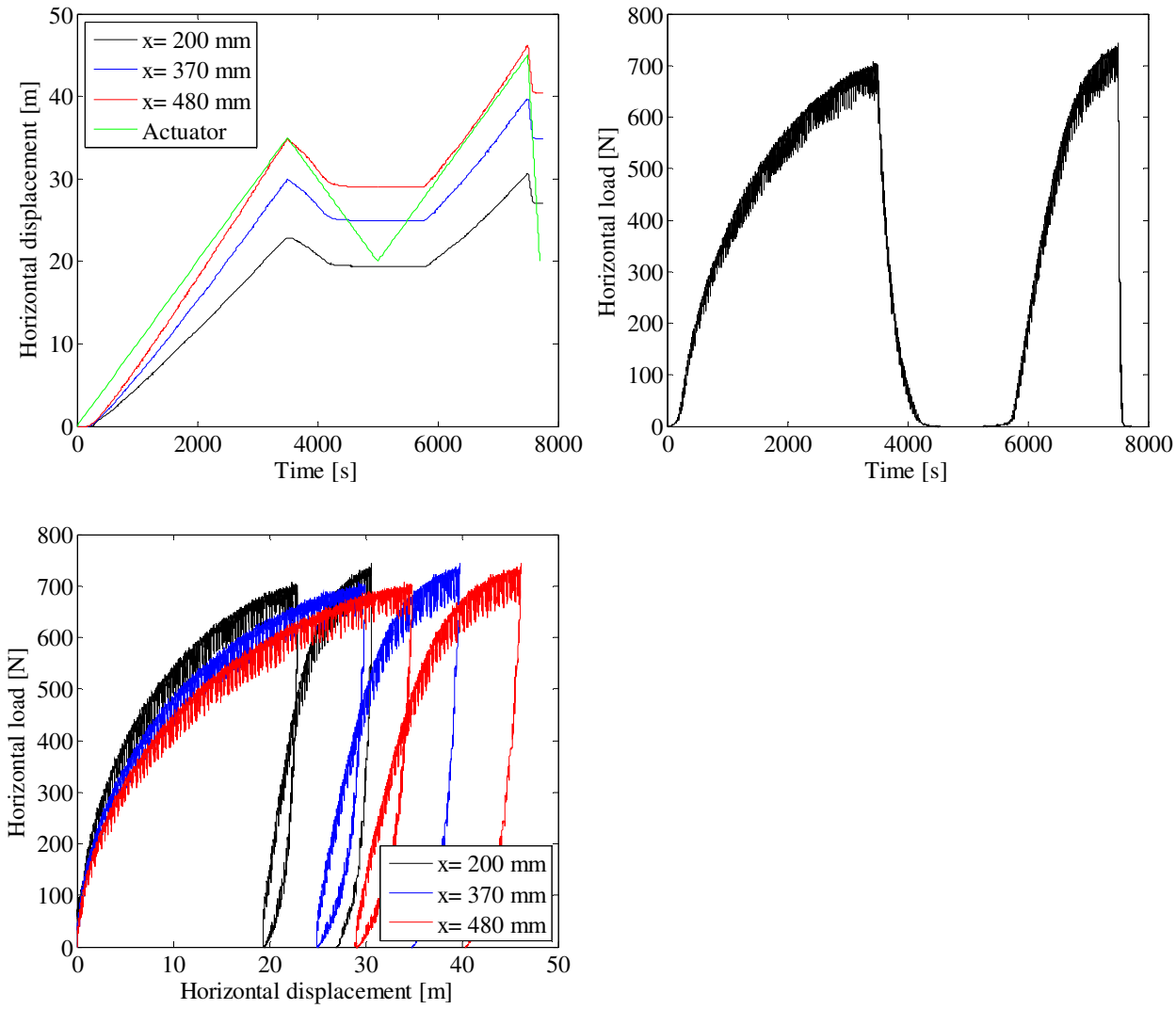

FIGURE 102. TOP LEFT: PILE DISPLACEMENT VERSUS TIME – TOP RIGHT: HORIZONTAL LOAD VERSUS TIME – BOTTOM LEFT: HORIZONTAL LOAD VERSUS PILE DISPLACEMENT.

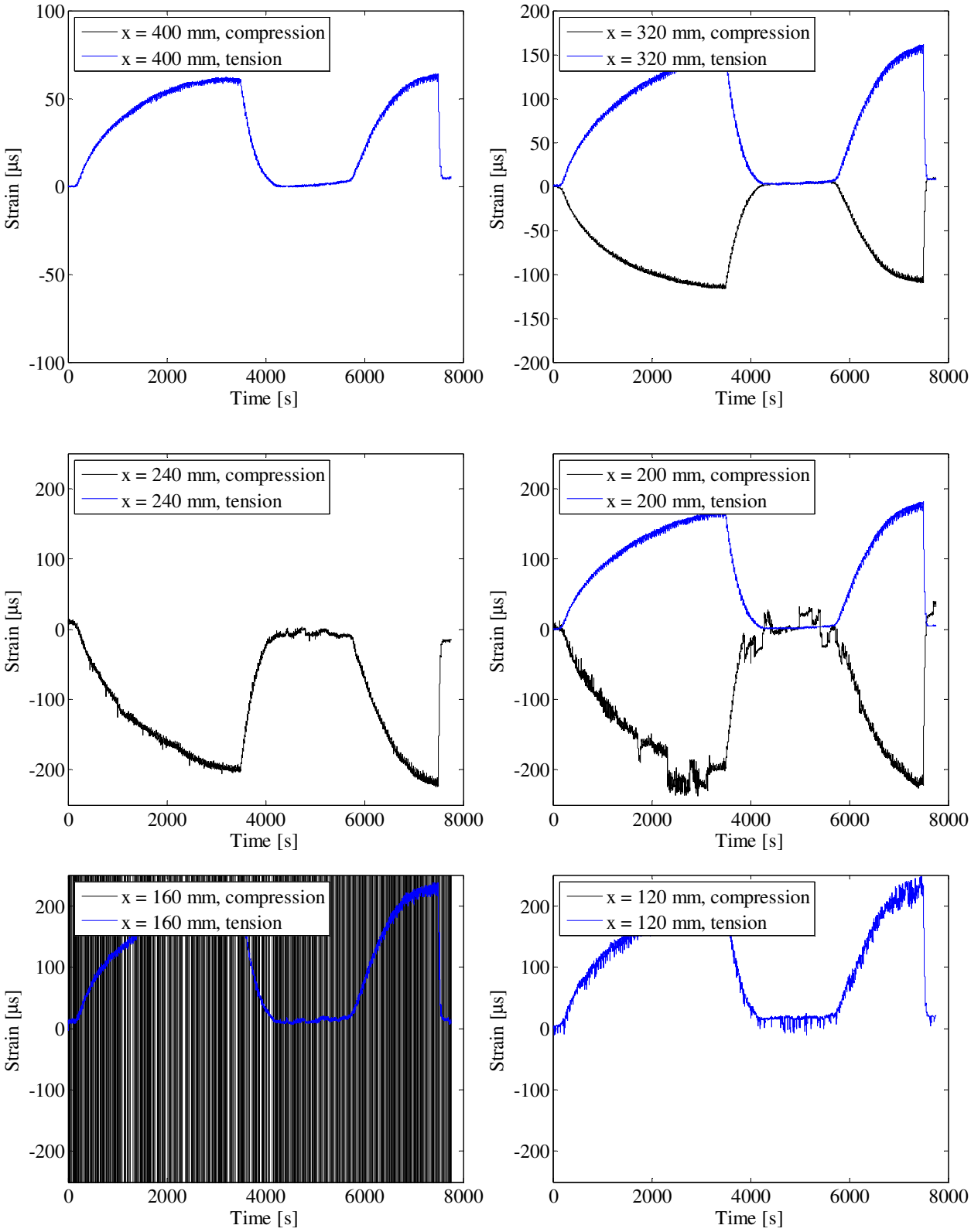

FIGURE 103. STRAIN GAUGE MEASUREMENTS.

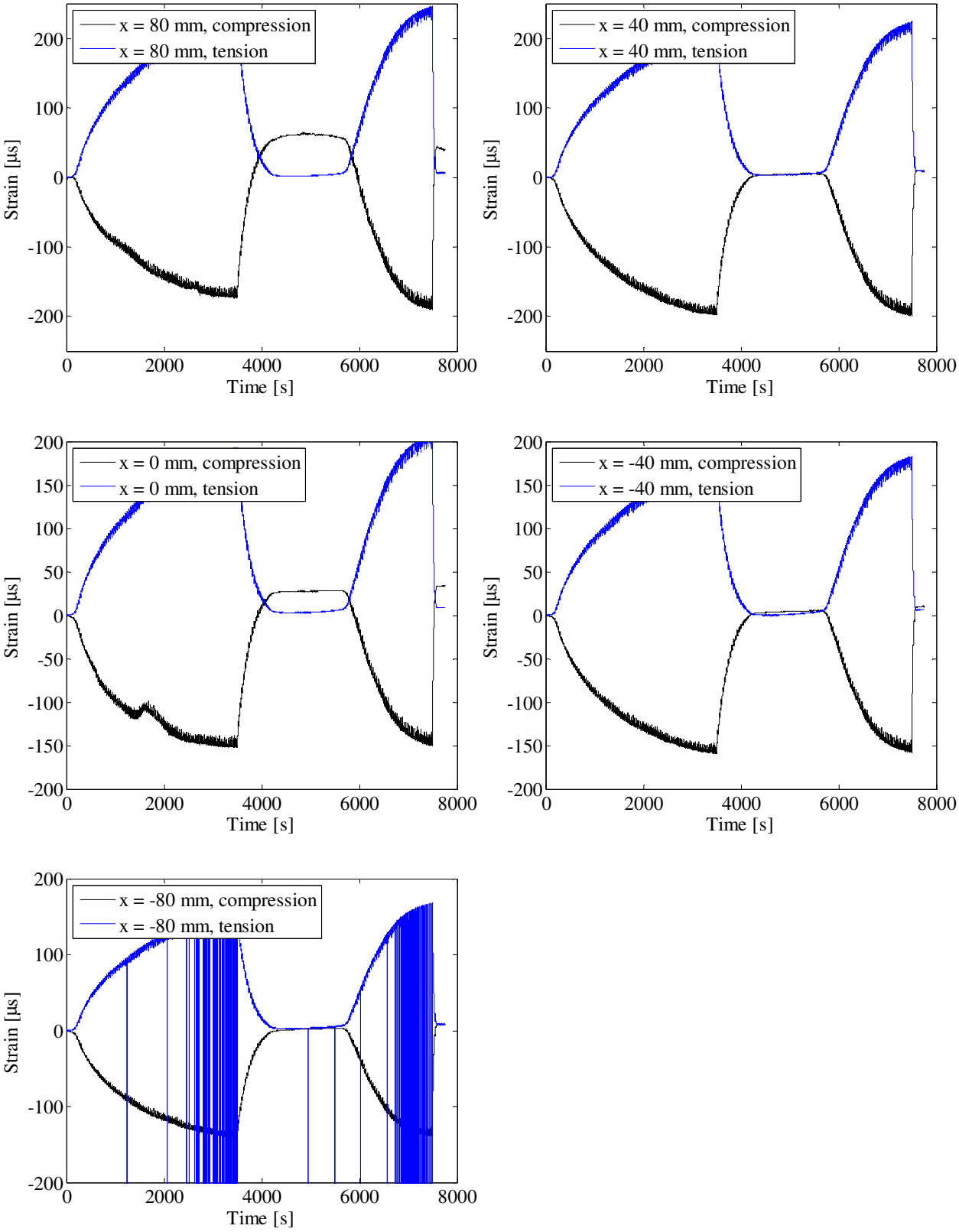

FIGURE 104. STRAIN GAUGE MEASUREMENTS.

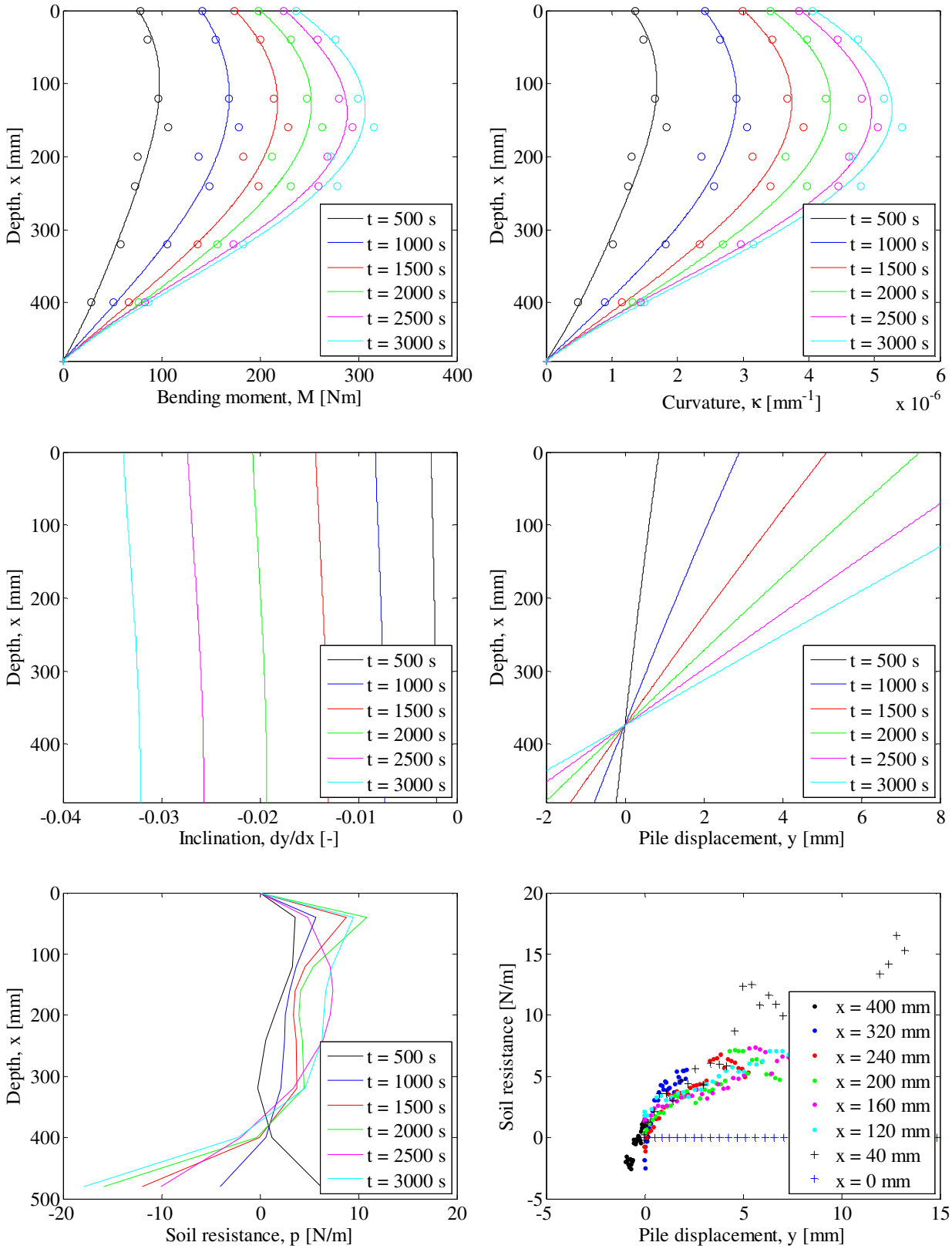

FIGURE 105. INTERPRETATION OF STRAIN GAUGE MEASUREMENTS. TOP LEFT: PILE BENDING MOMENT VERSUS DEPTH – TOP RIGHT: PILE CURVATURE VERSUS DEPTH – CENTER LEFT: PILE INCLINATION VERSUS DEPTH – CENTER RIGHT: PILE DISPLACEMENT VERSUS DEPTH – BOTTOM LEFT: SOIL RESISTANCE VERSUS DEPTH – BOTTOM RIGHT: P-Y CURVES.

Test 24: D = 80 mm, L_p = 480 mm and P_0 = 50 kPa (Closed-ended)

Pile type: Closed-ended	**Completed:** Fall 2010
Pile diameter (mm): 80	**No. of strain gauge levels:** 11 (9 below soil surface)
Embedded pile length (mm): 480	**Overburden pressure (kPa):** 50
Slenderness ratio, *L*/*D*: 6	**Load eccentricity (mm):** 370
Pile wall thickness (mm): 5	**By:** A. B. Moreno, L. Mikalauskas and J. L. T. Diaz
Comments: Three sub-tests were conducted. In the first one the fire hose were leaking air causing a larger water flow through the gaps between the membrane and the wall of the pressure tank. This sub-test is therefore not considered. In sub-test number two the loading arrangement failed. A third sub-test was therefore conducted. Only the third tests have been employed in the interpretation.	

Soil parameters:

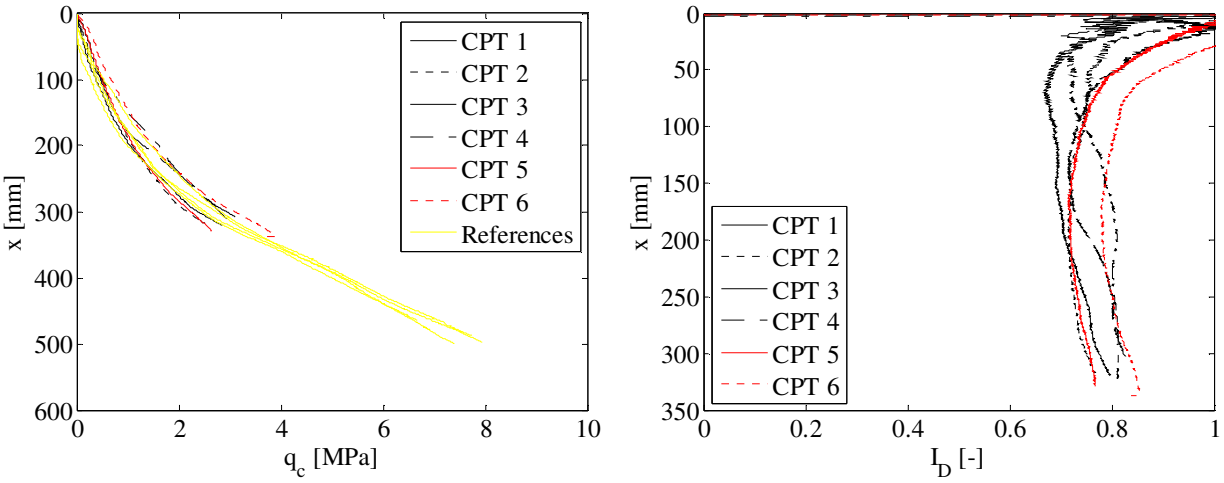

FIGURE 106. CPT-RESULTS FROM TEST 24. LEFT: TIP RESISTANCE VERSUS DEPTH – RIGHT: RELATIVE DENSITY VERSUS DEPTH.

TABLE 27. ESTIMATED SOIL PARAMETERS FOR TEST 24.

Relative density, I_D	Internal friction angle, φ_{tr}	Dilatancy angle, ψ_{tr}	Effective unit weight, γ'	Tangential Young's modulus of elasticity, E_0	Poisson's ratio, ν
[-]	[◦]	[◦]	[kN/m^3]	[MPa]	[-]
0.76	48.0	16.4	10.1	24.2	0.23

Test results:

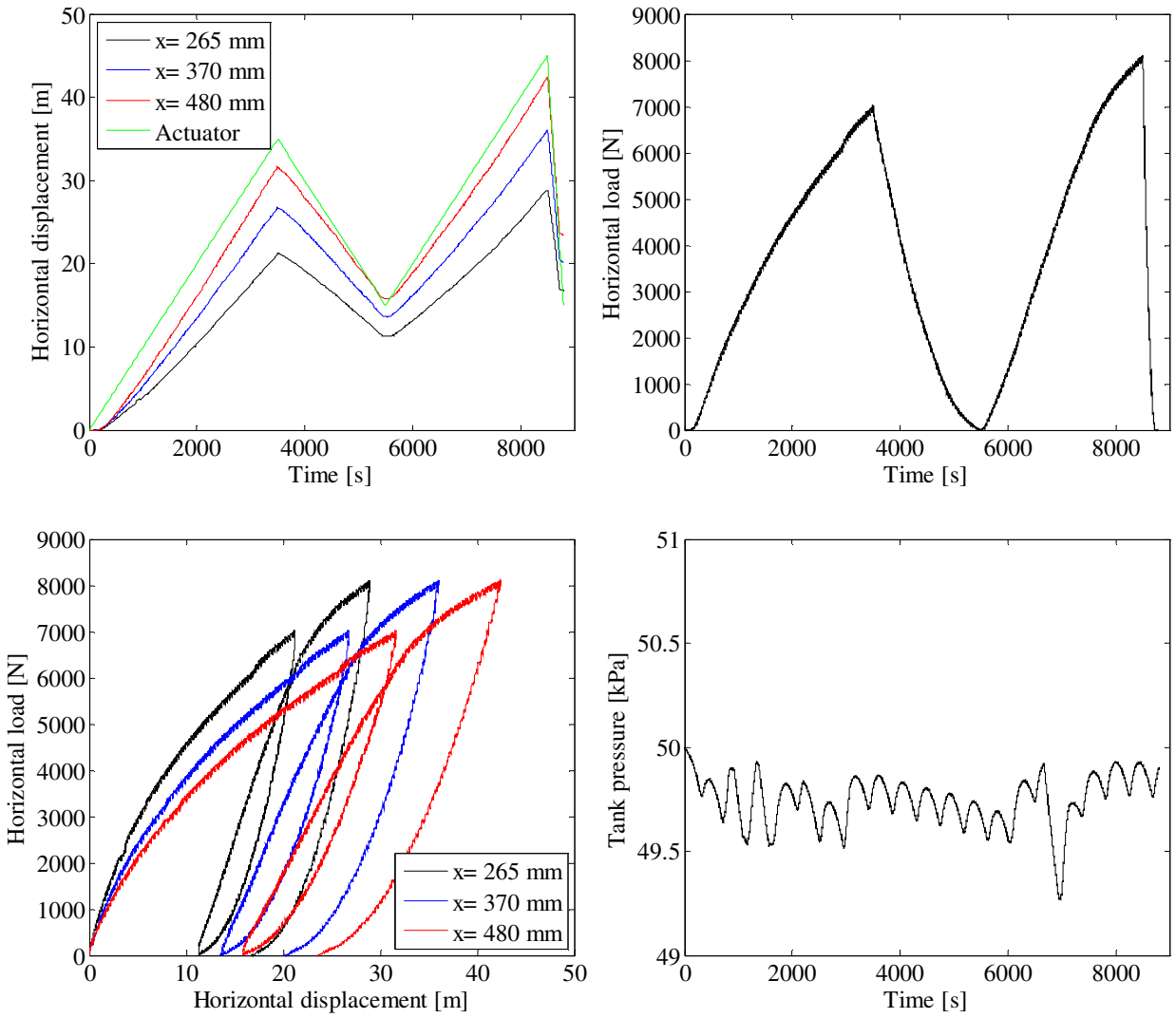

FIGURE 107. TOP LEFT: PILE DISPLACEMENT VERSUS TIME – TOP RIGHT: HORIZONTAL LOAD VERSUS TIME – BOTTOM LEFT: HORIZONTAL LOAD VERSUS PILE DISPLACEMENT – BOTTOM RIGHT: TANK PRESSURE VERSUS TIME.

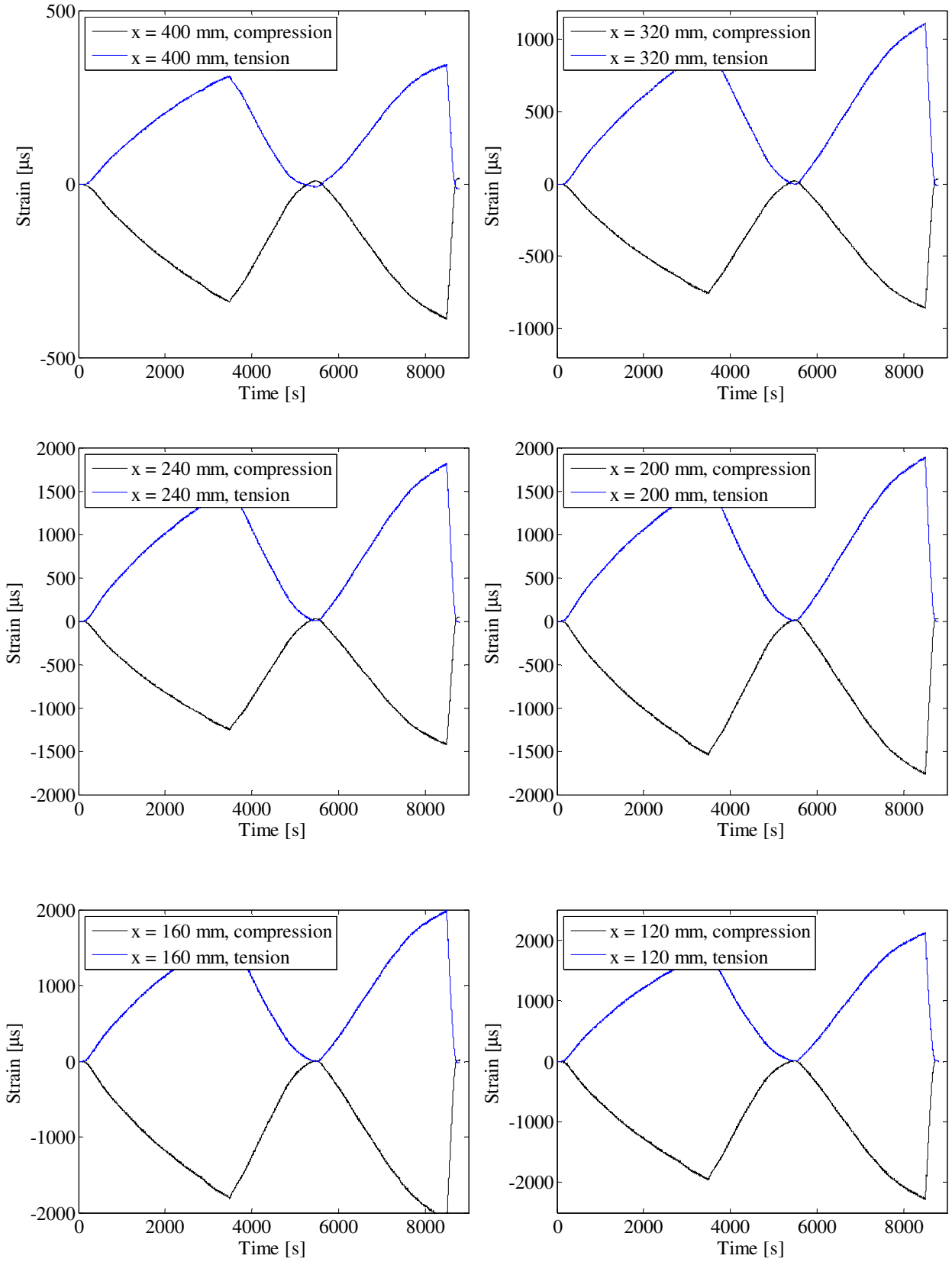

FIGURE 108. STRAIN GAUGE MEASUREMENTS.

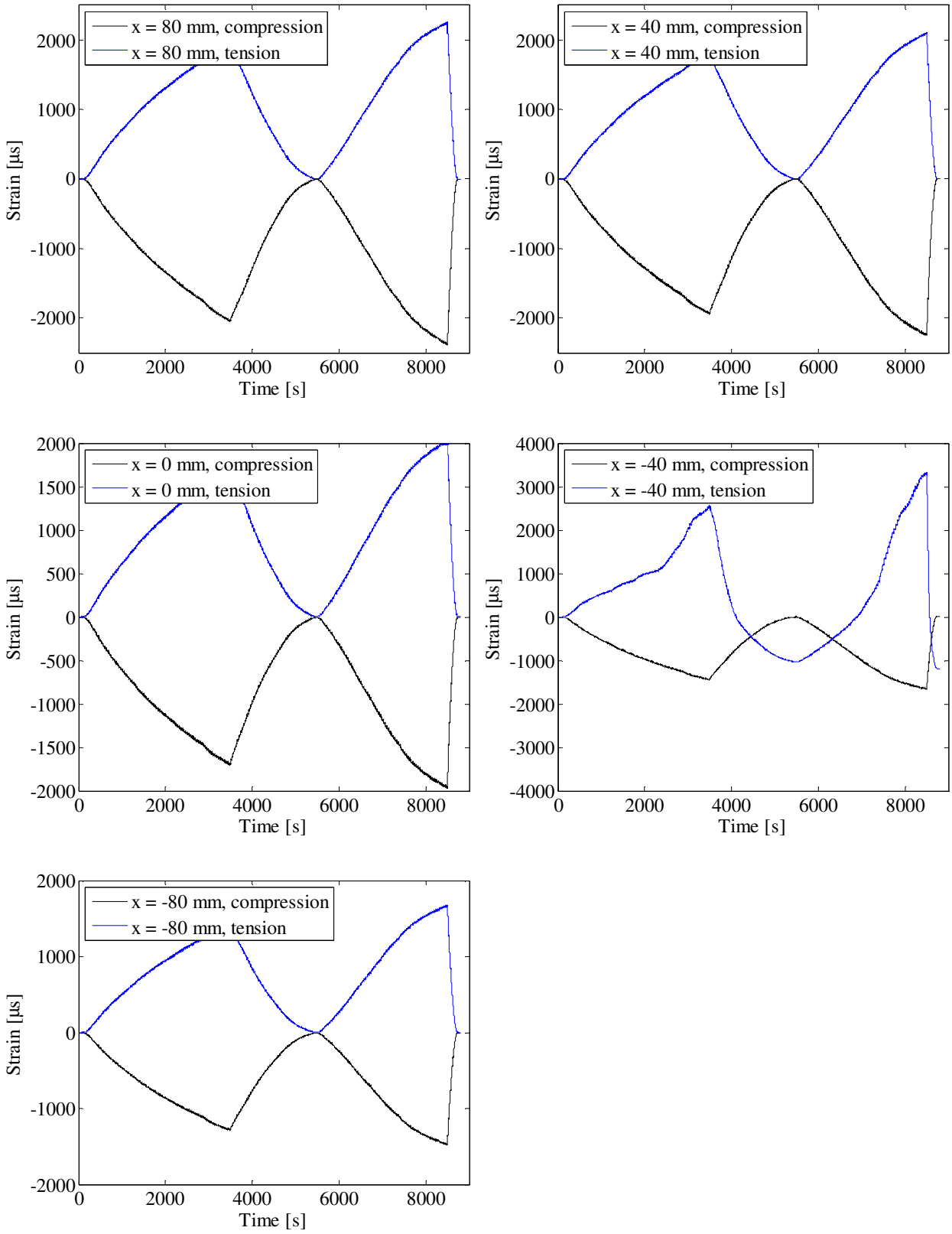

FIGURE 109. STRAIN GAUGE MEASUREMENTS.

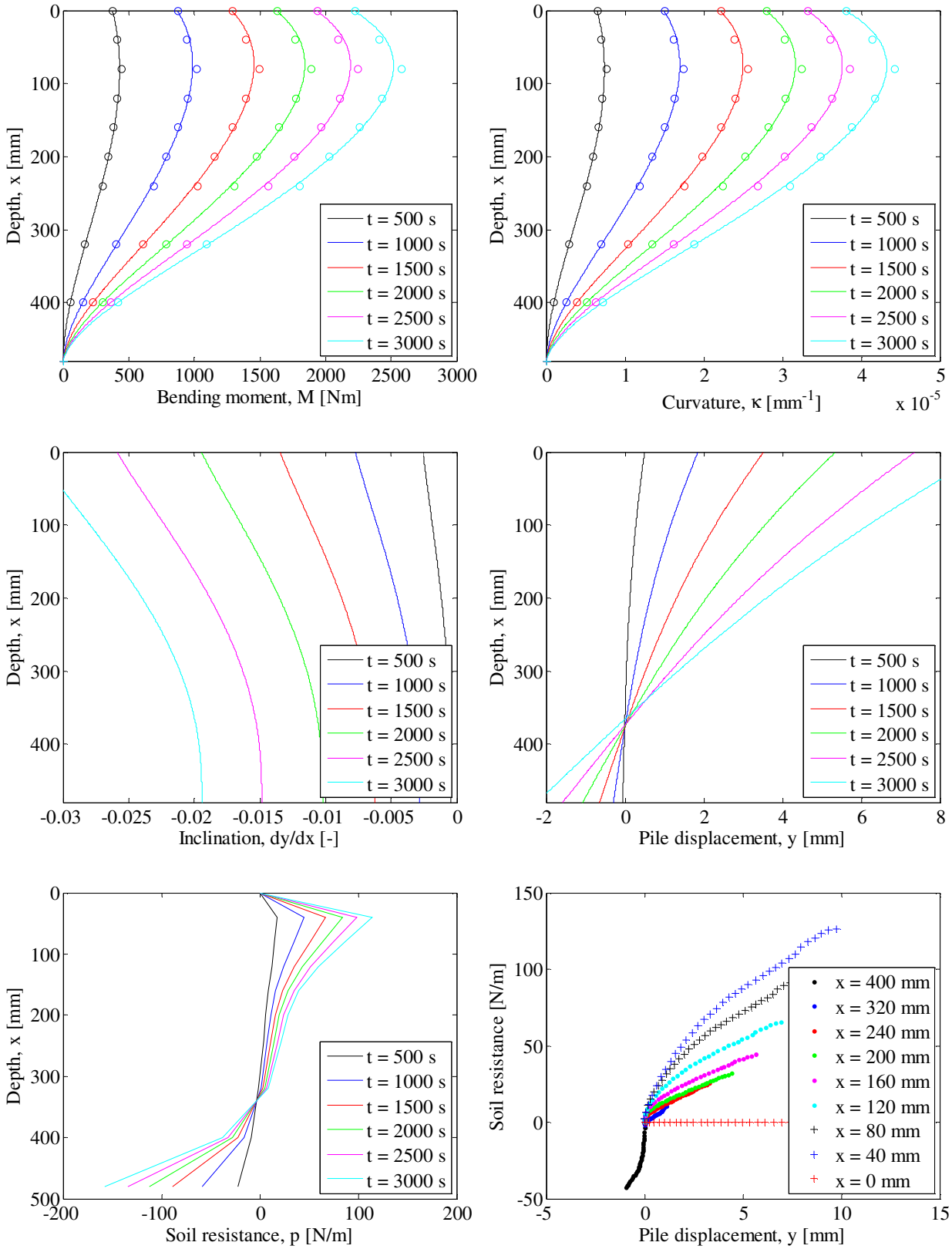

FIGURE 110. INTERPRETATION OF STRAIN GAUGE MEASUREMENTS. TOP LEFT: PILE BENDING MOMENT VERSUS DEPTH – TOP RIGHT: PILE CURVATURE VERSUS DEPTH – CENTER LEFT: PILE INCLINATION VERSUS DEPTH – CENTER RIGHT: PILE DISPLACEMENT VERSUS DEPTH – BOTTOM LEFT: SOIL RESISTANCE VERSUS DEPTH – BOTTOM RIGHT: P-Y CURVES.

Test 25: D = 80 mm, L_p = 480 mm and P_0 = 100 kPa (Closed-ended)

Pile type: Closed-ended	**Completed:** fall 2010
Pile diameter (mm): 80	**No. of strain gauge levels:** 11 (9 below soil surface)
Embedded pile length (mm): 480	**Overburden pressure (kPa):** 100
Slenderness ratio, L/D: 6	**Load eccentricity (mm):** 370
Pile wall thickness (mm): 5	**By:** A. B. Moreno, L. Mikalauskas and J. L. T. Diaz
Comments: The water flow through the membrane was approximately 50 l/hour.	

Soil parameters:

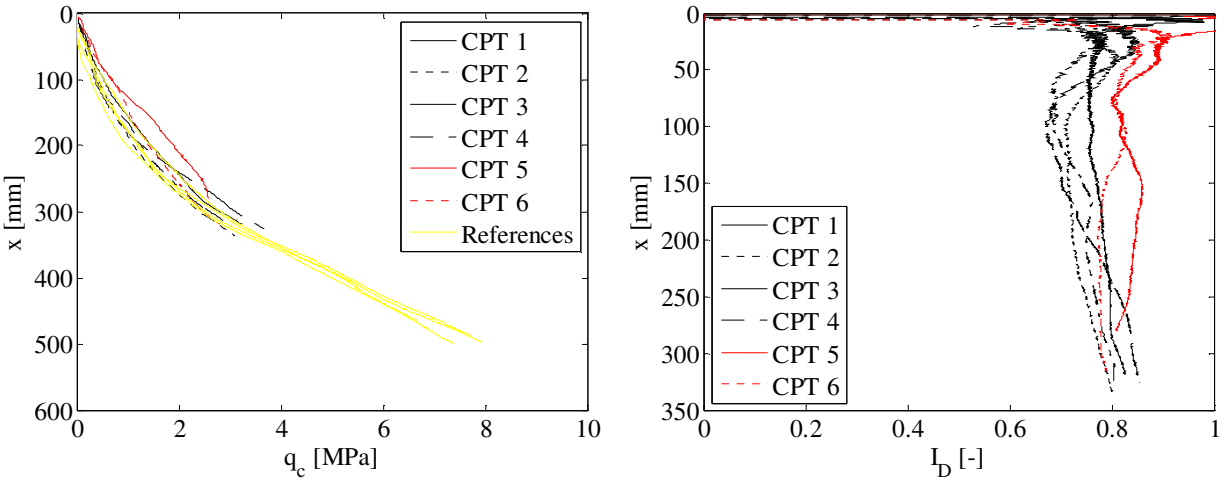

FIGURE 111. CPT-RESULTS FROM TEST 25. LEFT: TIP RESISTANCE VERSUS DEPTH – RIGHT: RELATIVE DENSITY VERSUS DEPTH.

TABLE 28. ESTIMATED SOIL PARAMETERS FOR TEST 25.

Relative density, I_D	Internal friction angle, φ_{tr}	Dilatancy angle, ψ_{tr}	Effective unit weight, γ'	Tangential Young's modulus of elasticity, E_0	Poisson's ratio, ν
[-]	[◦]	[◦]	[kN/m^3]	[MPa]	[-]
0.78	45.7	15.9	10.1	40.3	0.23

Test results:

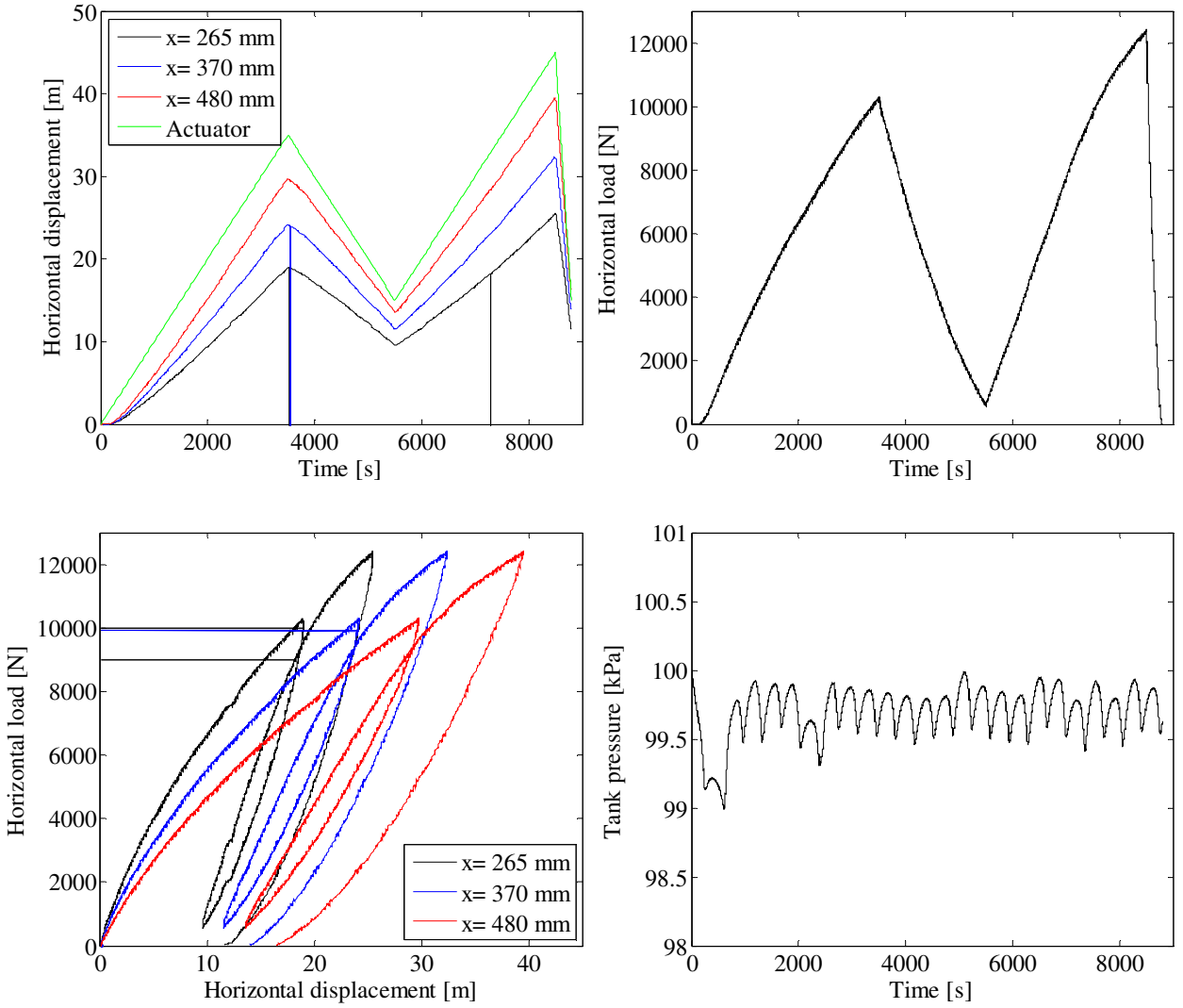

FIGURE 112. TOP LEFT: PILE DISPLACEMENT VERSUS TIME – TOP RIGHT: HORIZONTAL LOAD VERSUS TIME – BOTTOM LEFT: HORIZONTAL LOAD VERSUS PILE DISPLACEMENT – BOTTOM RIGHT: TANK PRESSURE VERSUS TIME.

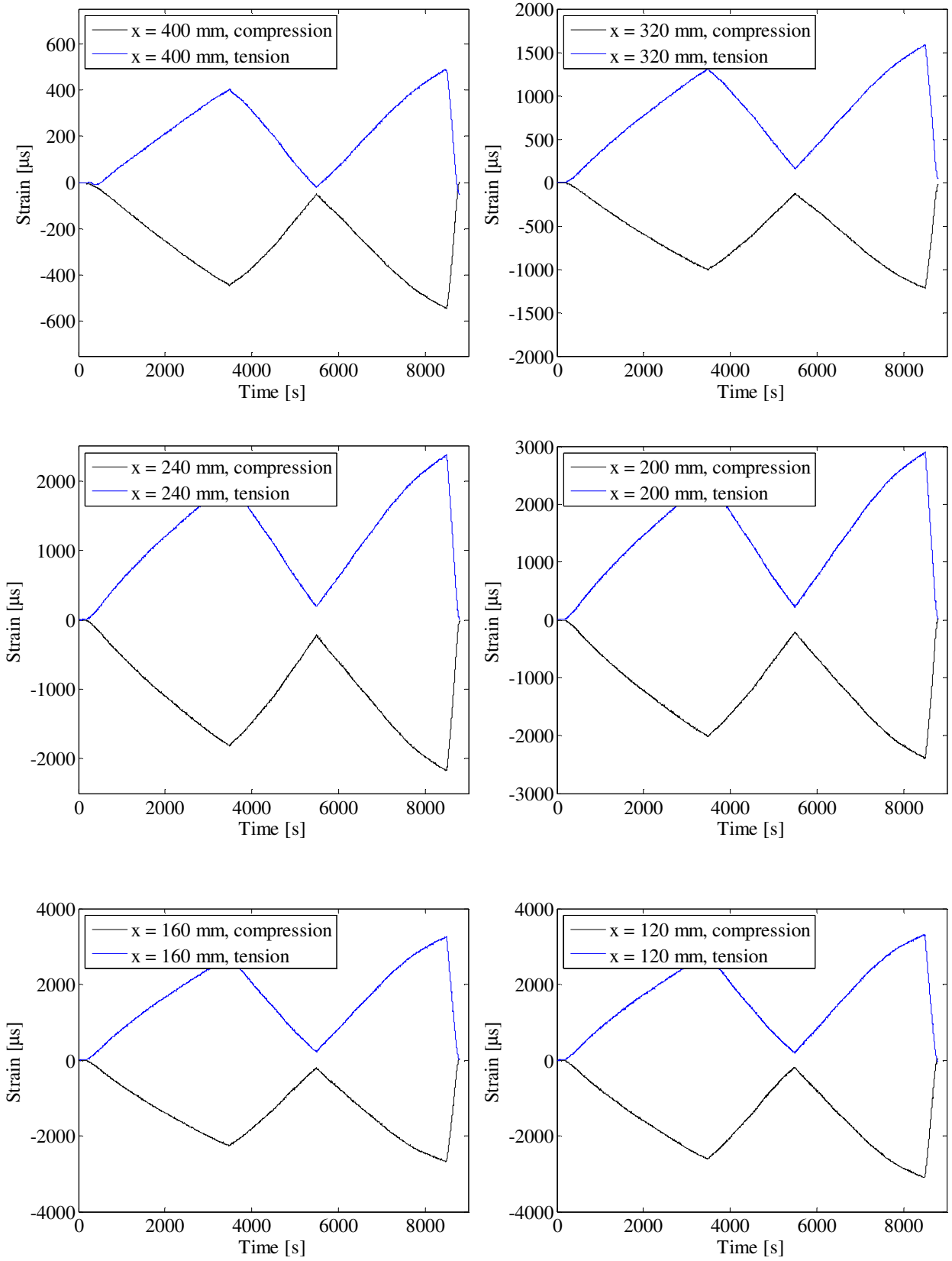

FIGURE 113. STRAIN GAUGE MEASUREMENTS.

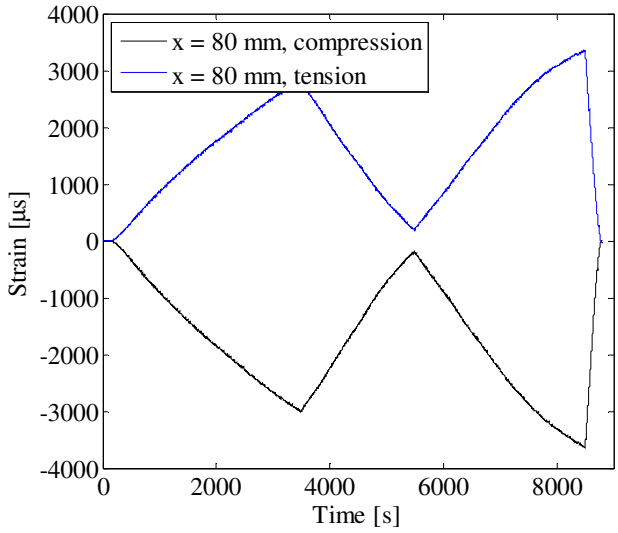

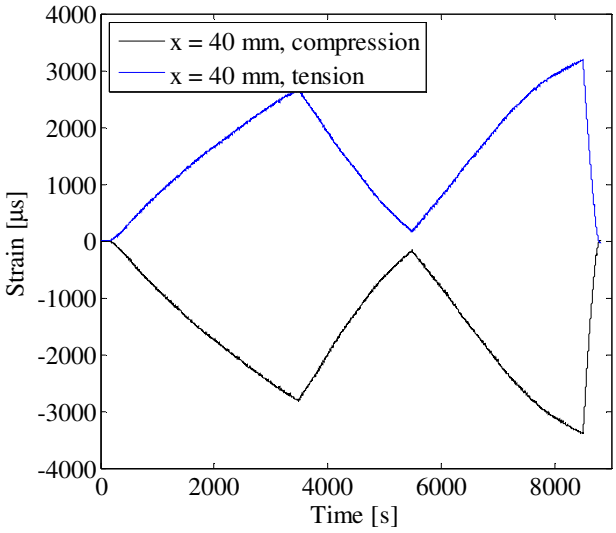

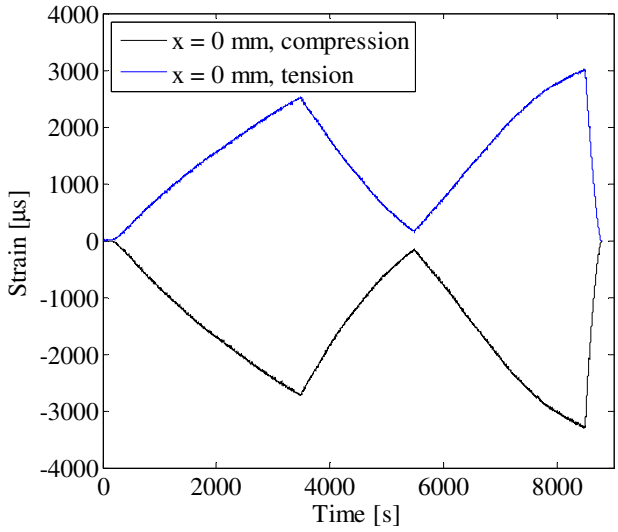

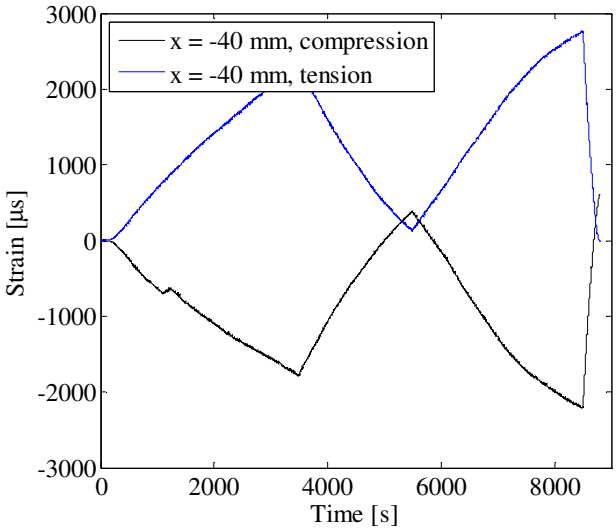

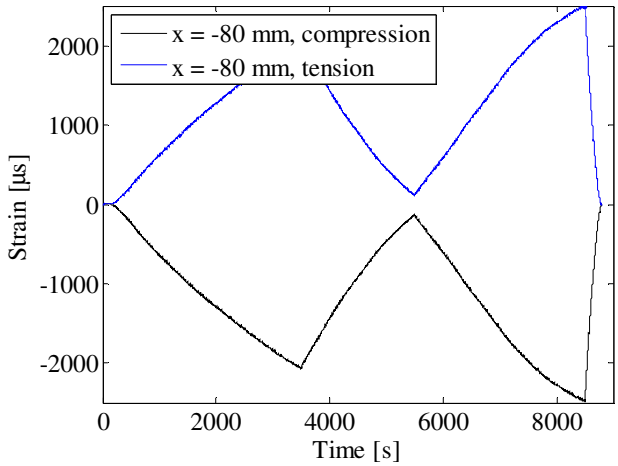

FIGURE 114. STRAIN GAUGE MEASUREMENTS.

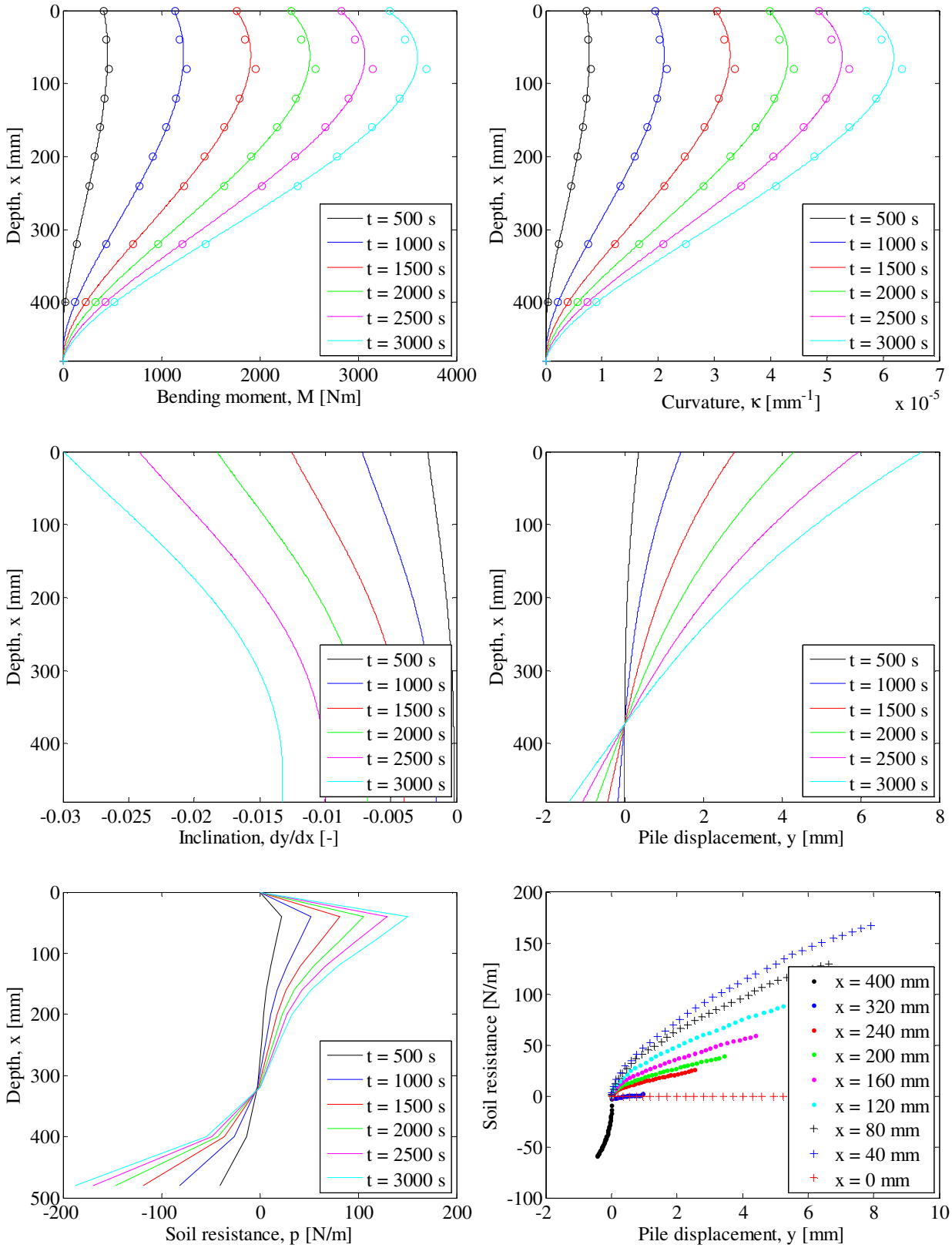

FIGURE 115. INTERPRETATION OF STRAIN GAUGE MEASUREMENTS. TOP LEFT: PILE BENDING MOMENT VERSUS DEPTH – TOP RIGHT: PILE CURVATURE VERSUS DEPTH – CENTER LEFT: PILE INCLINATION VERSUS DEPTH – CENTER RIGHT: PILE DISPLACEMENT VERSUS DEPTH – BOTTOM LEFT: SOIL RESISTANCE VERSUS DEPTH – BOTTOM RIGHT: P-Y CURVES.

Test 26: D = 100 mm, L_p = 500 mm and P_0 = 0 kPa (Closed-ended)

Pile type: Closed-ended	**Completed:** Spring 2010
Pile diameter (mm): 100	**No. of strain gauge levels:** 0
Embedded pile length (mm): 500	**Overburden pressure (kPa):** 0
Slenderness ratio, *L*/*D*: 5	**Load eccentricity (mm):** 370
Pile wall thickness (mm): 5	**By:** H. R. Roesen and K. Thomassen
Comments:	

Soil parameters:

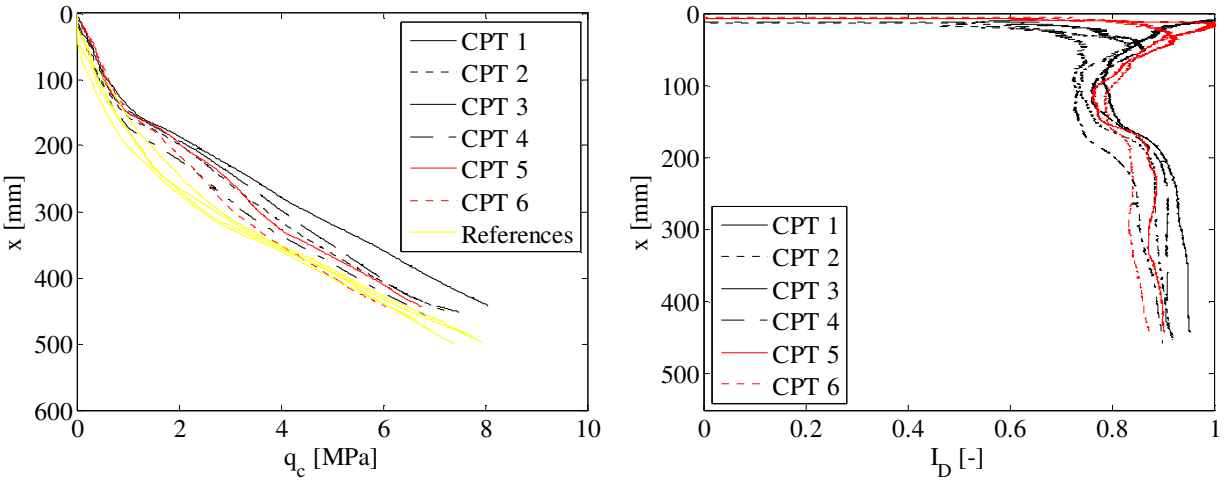

FIGURE 116. LEFT: CPT-RESULTS FROM TEST 26. TIP RESISTANCE VERSUS DEPTH – RIGHT: RELATIVE DENSITY VERSUS DEPTH.

TABLE 29. ESTIMATED SOIL PARAMETERS FOR TEST 26.

Relative density, I_D	Internal friction angle, φ_{tr}	Dilatancy angle, ψ_{tr}	Effective unit weight, γ'	Tangential Young's modulus of elasticity, E_0	Poisson's ratio, ν
[-]	[◦]	[◦]	[kN/m^3]	[MPa]	[-]
0.86	53.8	19.6	10.3	-	0.23

Test results:

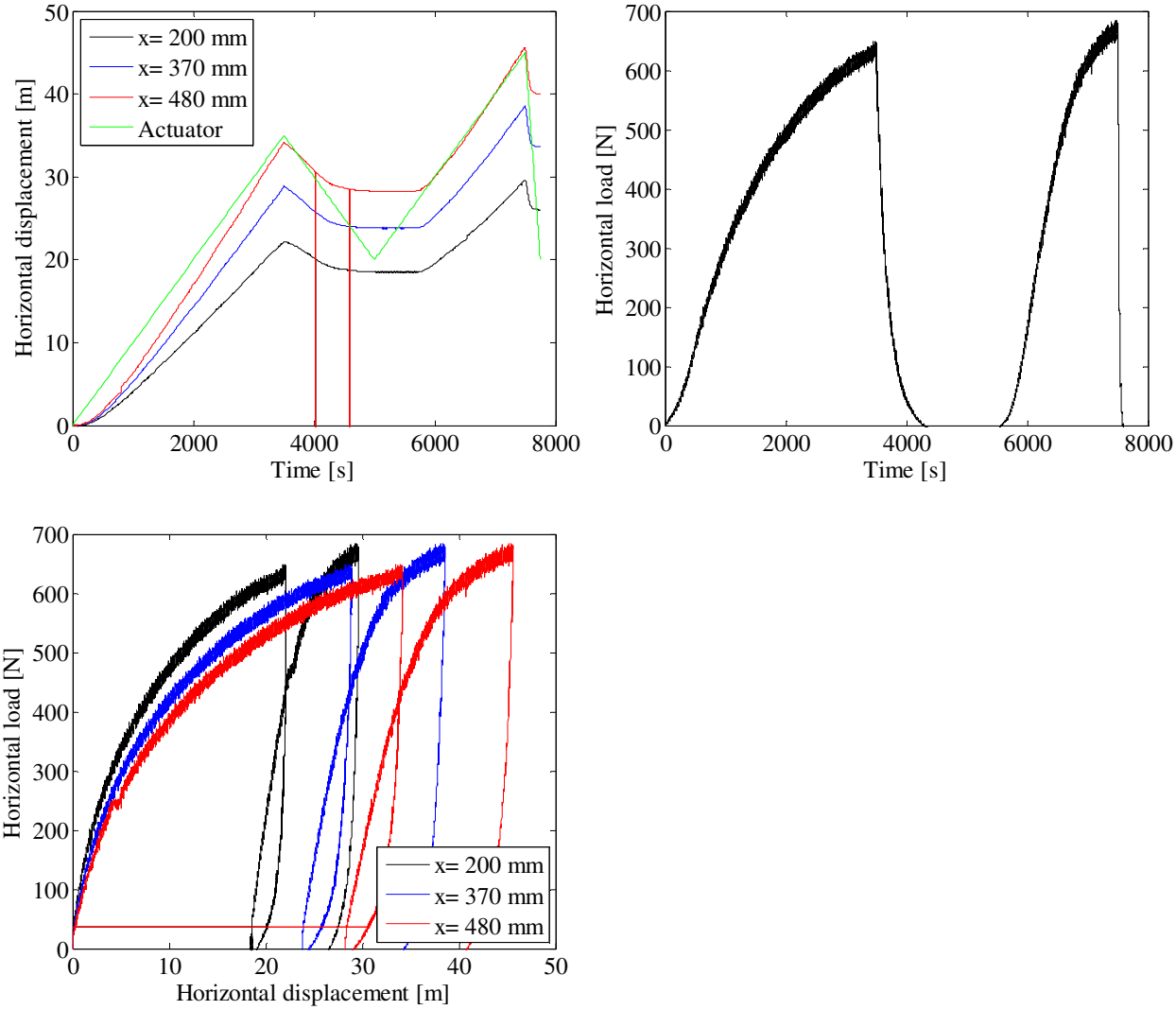

FIGURE 117. TOP LEFT: PILE DISPLACEMENT VERSUS TIME – TOP RIGHT: HORIZONTAL LOAD VERSUS TIME – BOTTOM LEFT: HORIZONTAL LOAD VERSUS PILE DISPLACEMENT.

Test 27: D = 100 mm, L_p = 500 mm and P_0 = 50 kPa (Closed-ended)

Pile type: Closed-ended	**Completed:** Spring 2010
Pile diameter (mm): 100	**No. of strain gauge levels:** 0
Embedded pile length (mm): 500	**Overburden pressure (kPa):** 50
Slenderness ratio, *L*/*D*: 5	**Load eccentricity (mm):** 370
Pile wall thickness (mm): 5	**By:** H. R. Roesen and K. Thomassen

Comments:

This test consists of four tests due to technical problems. In the first test the wire connecting the pile and the horizontal hydraulic piston snapped at a load of 5 kN. Afterwards the pile was brought back to upright position and the soil was prepared again. The results from this sub-test are not used.

For the second sub-test a new wire was constructed. During the test the bracket in which the wire was connected to the pile showed large plastic deformations. Therefore the pile itself was not exposed to the expected displacement.

Sub-test 3 was conducted without preparing the soil and pile rotation after sub-test 2. A new wire was constructed and used for this test. The wire snapped at a load of approximately 8 kN. After sub-test 3 the rotation of the pile was not changed and similarly the soil was not vibrated.

Before sub-test 4 a new wire was ordered. However, the welding between the wire and the force transducer snapped at a load of 11 kN.

During the first 3 sub-tests the pressure transducer showed large fluctuations larger than what can be considered physically possible. The transducer reported an error before sub-test 4 and was therefore replaced. The new pressure transducer showed more realistic results.

Soil parameters:

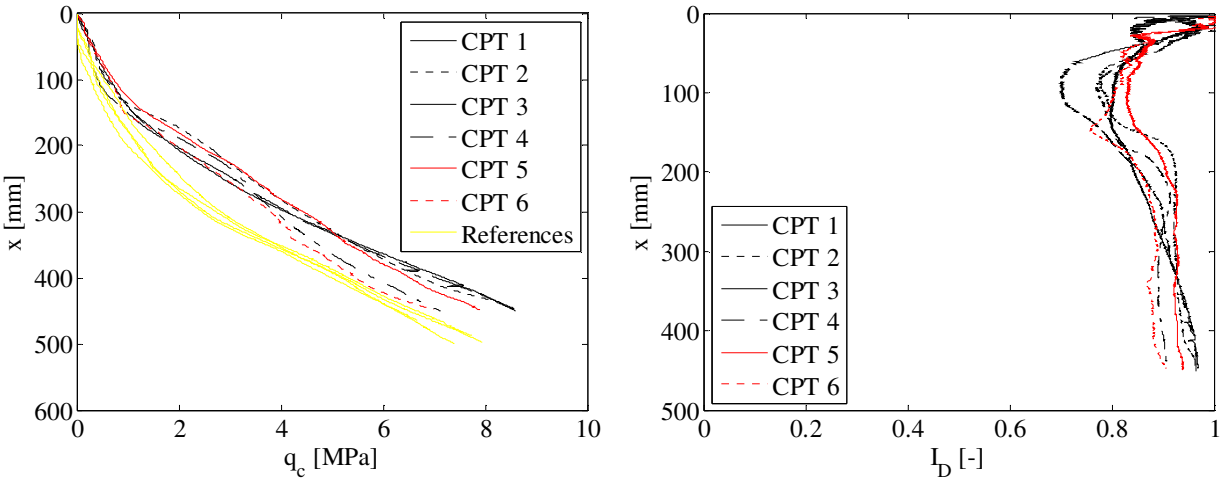

FIGURE 118. CPT-RESULTS FROM TEST 27. LEFT: TIP RESISTANCE VERSUS DEPTH – RIGHT: RELATIVE DENSITY VERSUS DEPTH.

TABLE 30. ESTIMATED SOIL PARAMETERS FOR TEST 27.

Relative density, I_D	Internal friction angle, φ_{tr}	Dilatancy angle, ψ_{tr}	Effective unit weight, γ'	Tangential Young's modulus of elasticity, E_0	Poisson's ratio, ν
[-]	[◦]	[◦]	[kN/m^3]	[MPa]	[-]
0.89	50.3	19.0	10.4	31.0	0.23

Test results:

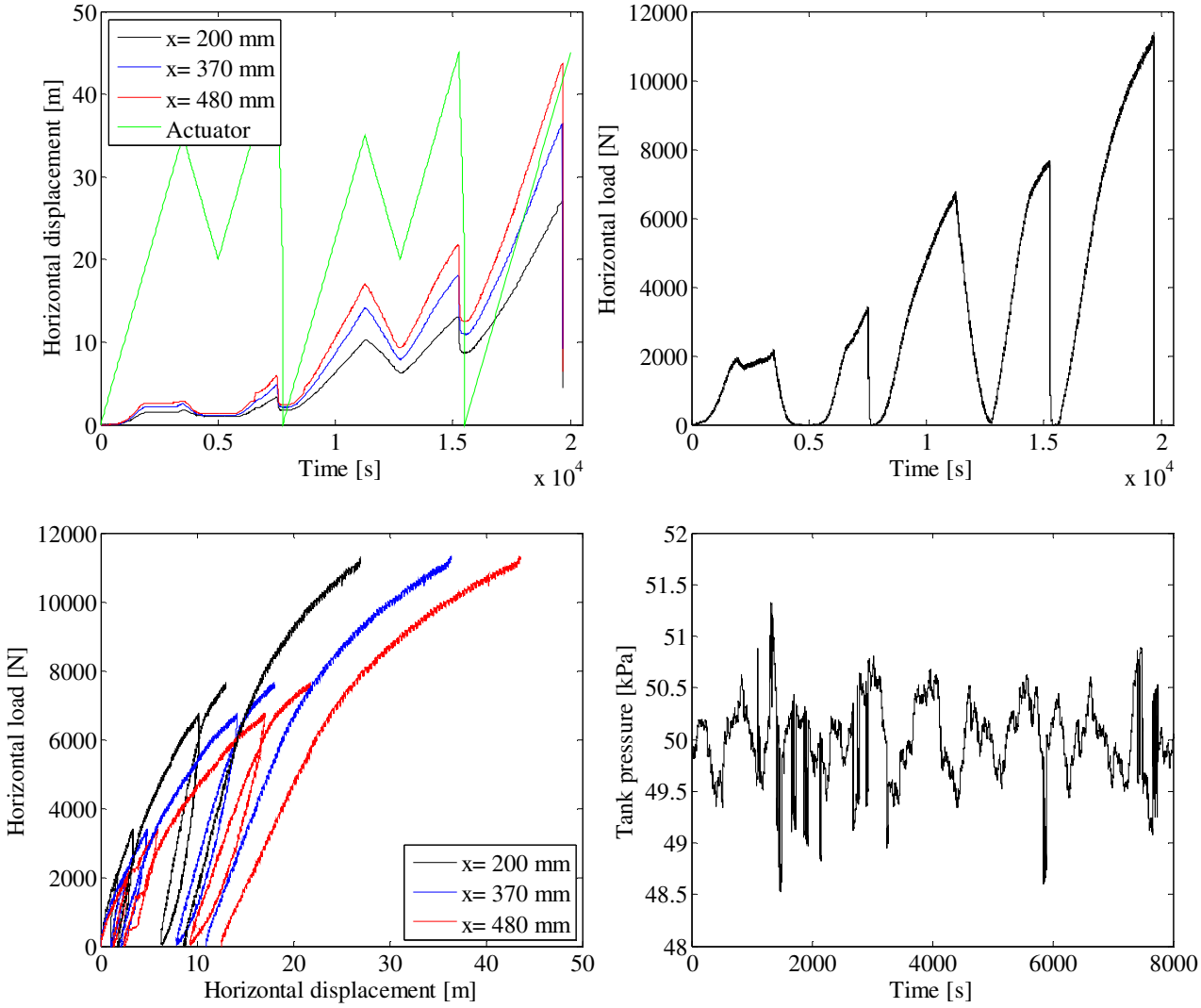

FIGURE 119. TOP LEFT: PILE DISPLACEMENT VERSUS TIME – TOP RIGHT: HORIZONTAL LOAD VERSUS TIME – BOTTOM LEFT: HORIZONTAL LOAD VERSUS PILE DISPLACEMENT – BOTTOM RIGHT: TANK PRESSURE VERSUS TIME.

Test 28: D = 100 mm, L_p = 500 mm and P_0 = 50 kPa (Closed-ended)

Pile type: Closed-ended	**Completed:** Fall 2010
Pile diameter (mm): 100	**No. of strain gauge levels:** 0
Embedded pile length (mm): 500	**Overburden pressure (kPa):** 50
Slenderness ratio, *L*/*D*: 5	**Load eccentricity (mm):** 370
Pile wall thickness (mm): 5	**By:** A. B. Moreno, L. Mikalauskas and J. L. T. Diaz
Comments: The water flow through gaps in the membrane where at approximately 80 l/hour.	

Soil parameters:

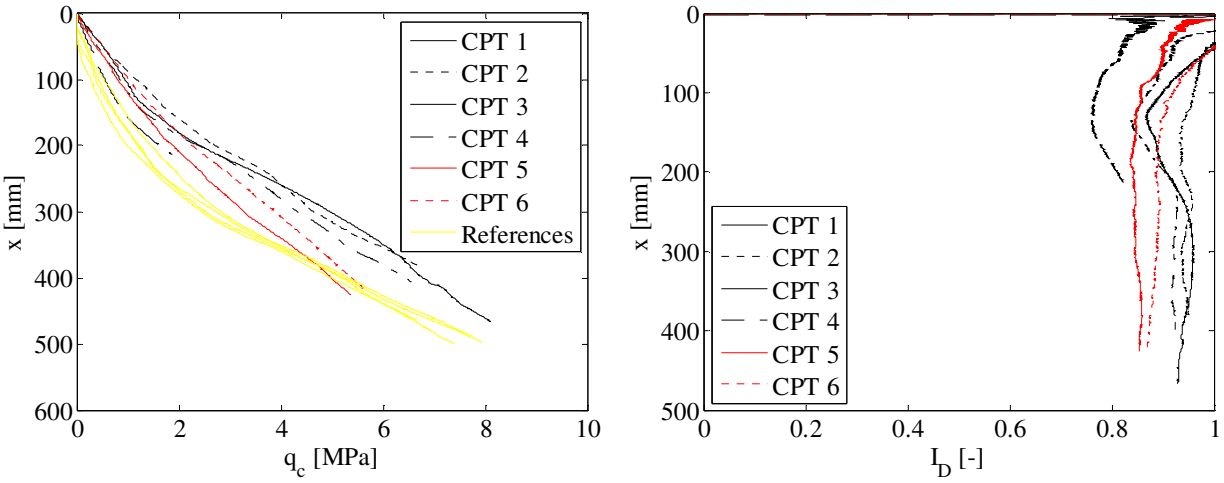

FIGURE 120. CPT-RESULTS FROM TEST 28. LEFT: TIP RESISTANCE VERSUS DEPTH – RIGHT: RELATIVE DENSITY VERSUS DEPTH.

TABLE 31. ESTIMATED SOIL PARAMETERS FOR TEST 28.

Relative density, I_D	Internal friction angle, φ_{tr}	Dilatancy angle, ψ_{tr}	Effective unit weight, γ'	Tangential Young's modulus of elasticity, E_0	Poisson's ratio, ν
[-]	[◦]	[◦]	[kN/m^3]	[MPa]	[-]
0.89	50.4	19.1	10.4	30.9	0.23

Test results:

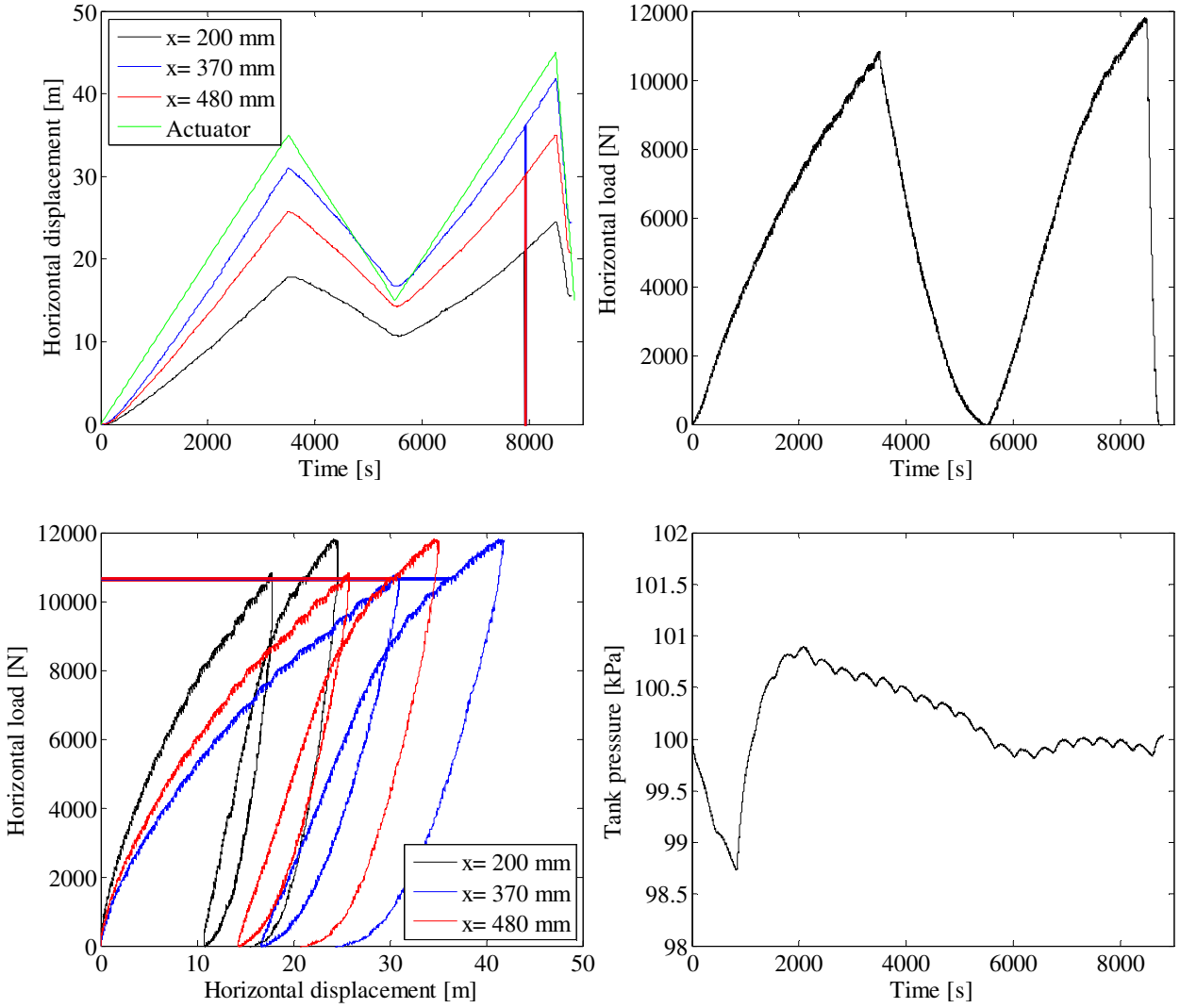

FIGURE 121. TOP LEFT: PILE DISPLACEMENT VERSUS TIME – TOP RIGHT: HORIZONTAL LOAD VERSUS TIME – BOTTOM LEFT: HORIZONTAL LOAD VERSUS PILE DISPLACEMENT – BOTTOM RIGHT: TANK PRESSURE VERSUS TIME.

Test 29: D = 100 mm, L_p = 500 mm and P_0 = 100 kPa (Closed-ended)

Pile type: Closed-ended	**Completed:** Spring 2010
Pile diameter (mm): 100	**No. of strain gauge levels:** 0
Embedded pile length (mm): 500	**Overburden pressure (kPa):** 100
Slenderness ratio, *L*/*D*: 5	**Load eccentricity (mm):** 370
Pile wall thickness (mm): 5	**By:** H. R. Roesen and K. Thomassen
Comments:	

Soil parameters:

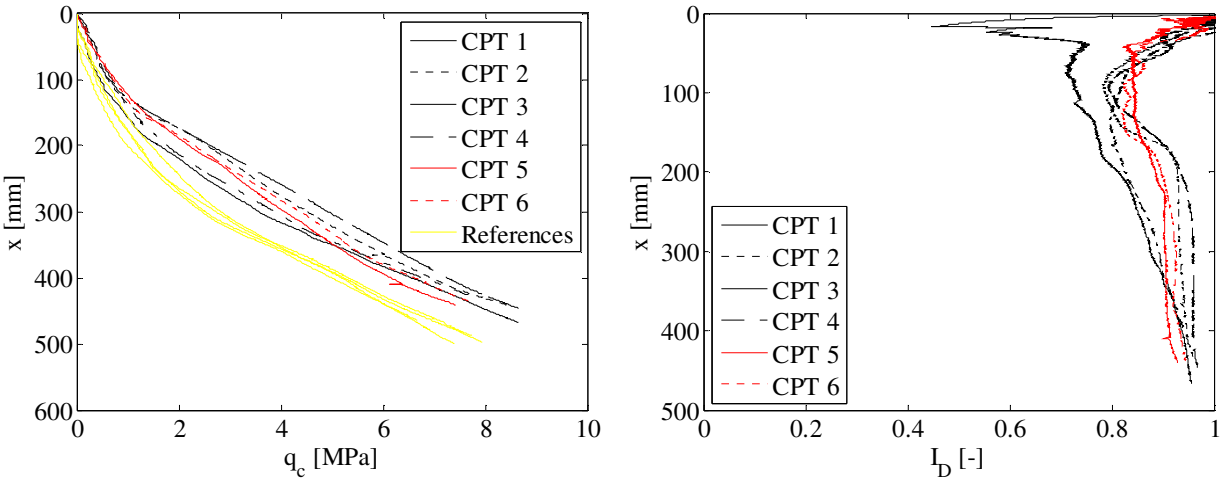

FIGURE 122. CPT-RESULTS FROM TEST 29. LEFT: TIP RESISTANCE VERSUS DEPTH – RIGHT: RELATIVE DENSITY VERSUS DEPTH.

TABLE 32. ESTIMATED SOIL PARAMETERS FOR TEST 29.

Relative density, I_D	Internal friction angle, φ_{tr}	Dilatancy angle, ψ_{tr}	Effective unit weight, γ'	Tangential Young's modulus of elasticity, E_0	Poisson's ratio, ν
[-]	[◦]	[◦]	[kN/m^3]	[MPa]	[-]
0.90	47.7	18.3	10.4	50.9	0.23

Test results:

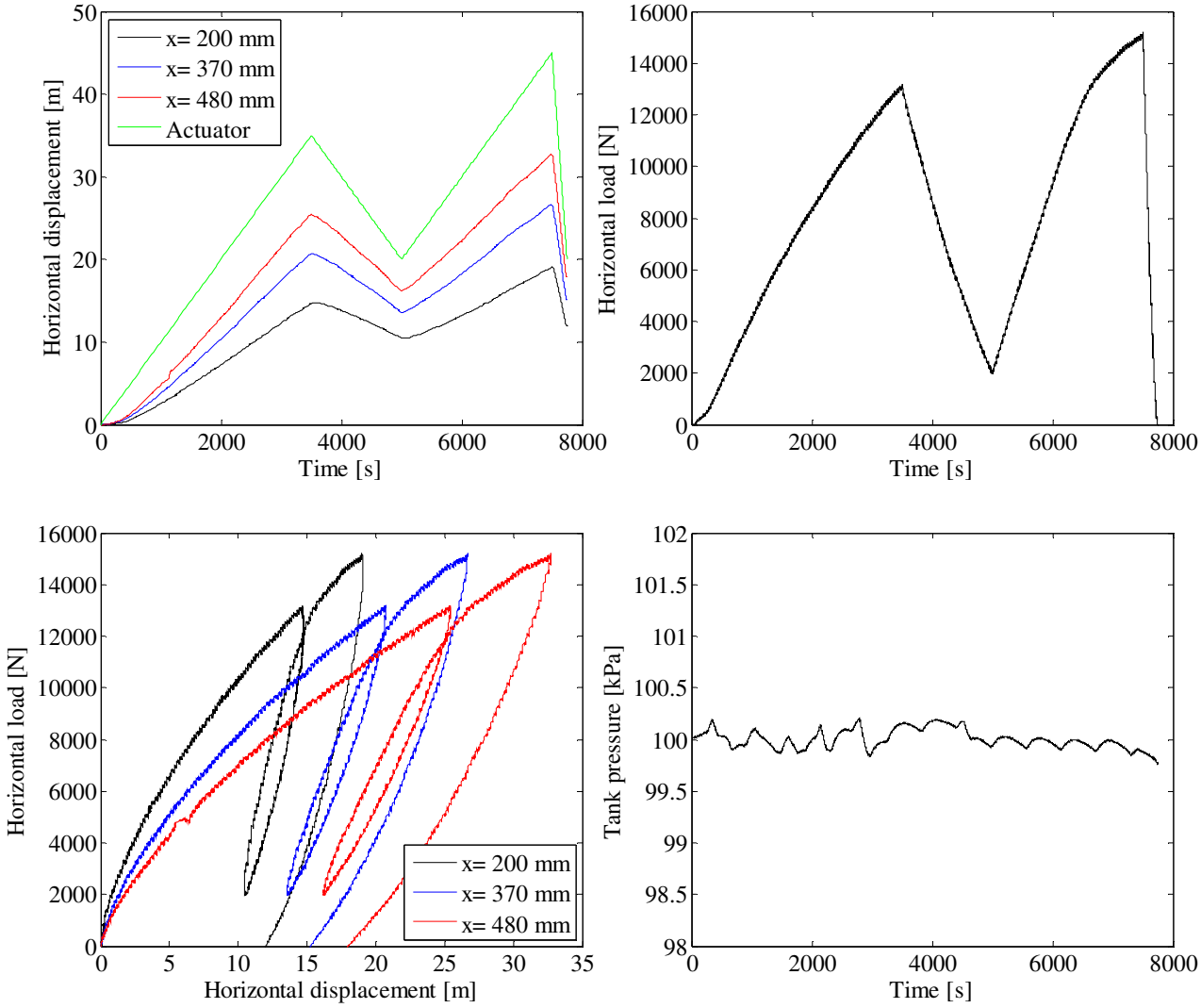

FIGURE 123. TOP LEFT: PILE DISPLACEMENT VERSUS TIME – TOP RIGHT: HORIZONTAL LOAD VERSUS TIME – BOTTOM LEFT: HORIZONTAL LOAD VERSUS PILE DISPLACEMENT – BOTTOM RIGHT: TANK PRESSURE VERSUS TIME.

Comparison of numerical simulations and laboratory tests

In the following the load-displacement relationships from the numerical modelling of the small-scale tests are compared with the experimental work. Further, the pile behaviour determined by the numerical modelling is shown. In the numerical modelling the soil parameters determined directly by means of the CPT's conducted prior to each test are employed. However, it should be noted that Young's modulus of elasticity for the soil has been set to 1 MPa for all the tests without overburden pressure.

Test 1: D = 40 mm, L_p = 200 mm and P_0 = 0 kPa (Closed-ended)

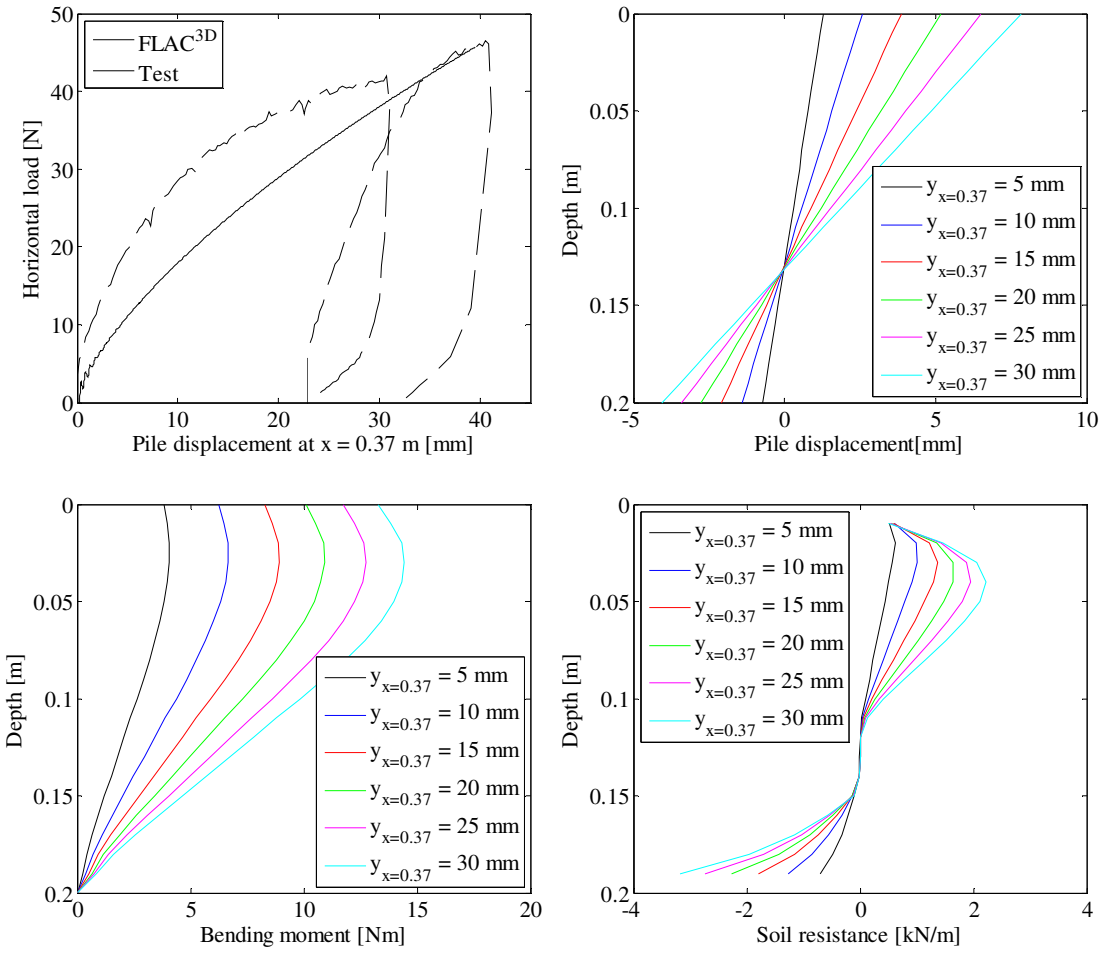

FIGURE 124. TOP LEFT: LOAD-DISPLACEMENT RELATIONSHIPS – TOP RIGHT: PILE DISPLACEMENT VERSUS DEPTH – BOTTOM LEFT: BENDING MOMENT VERSUS DEPTH – BOTTOM RIGHT: SOIL RESISTANCE VERSUS DEPTH.

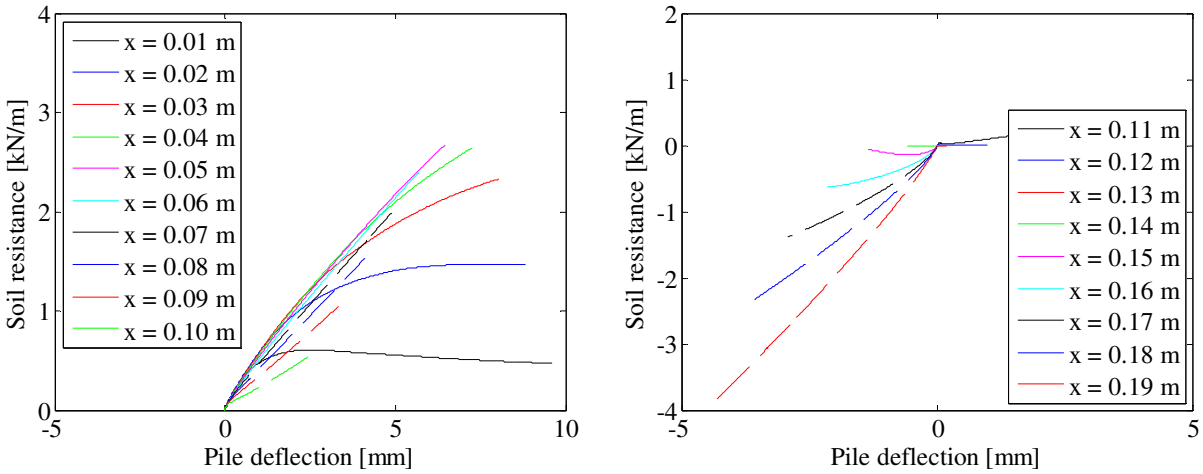

FIGURE 125. P-Y CURVES.

Test 2: D = 40 mm, L_p = 200 mm and P_0 = 50 kPa (Closed-ended)

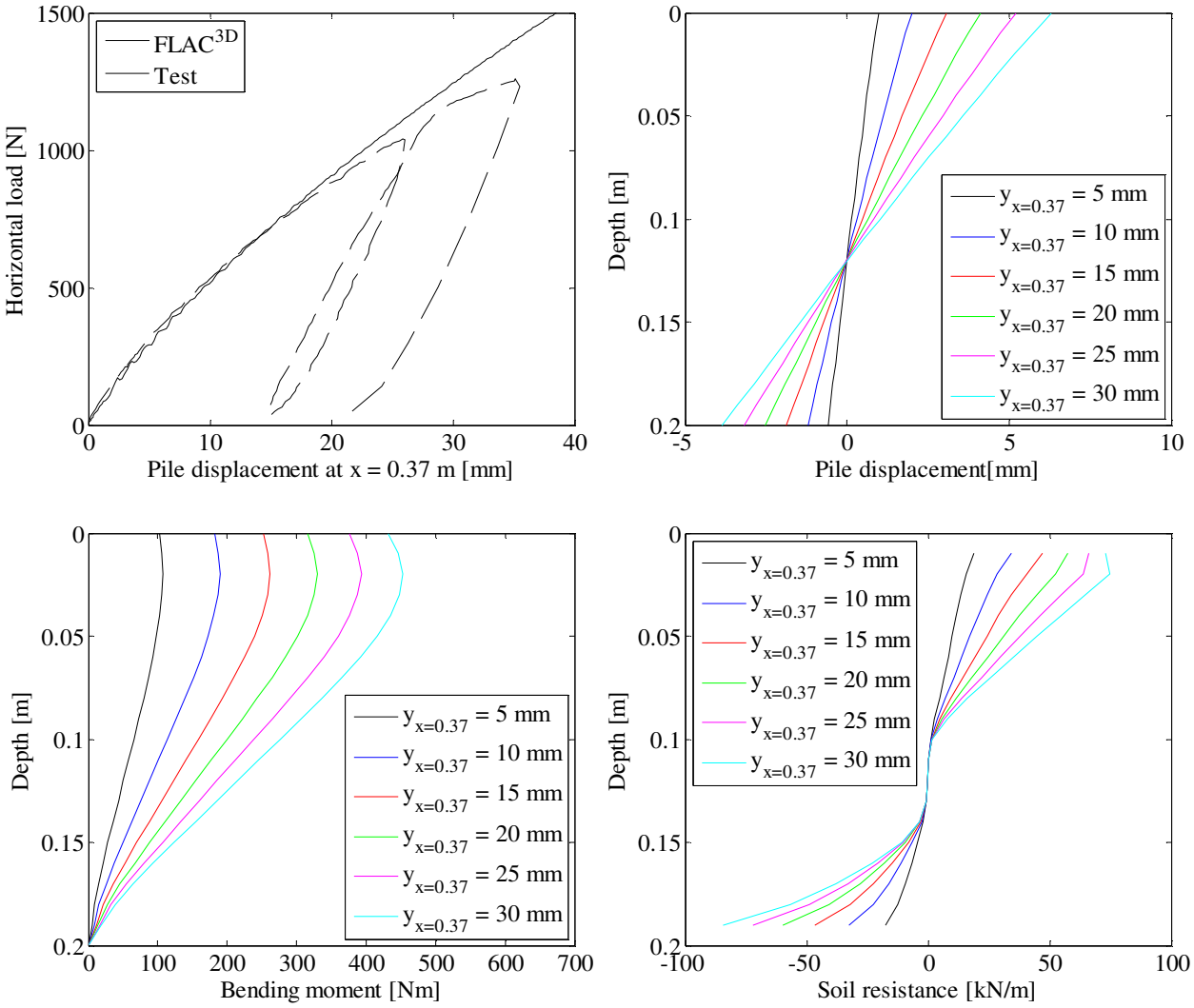

FIGURE 126. TOP LEFT: LOAD-DISPLACEMENT RELATIONSHIPS – TOP RIGHT: PILE DISPLACEMENT VERSUS DEPTH – BOTTOM LEFT: BENDING MOMENT VERSUS DEPTH – BOTTOM RIGHT: SOIL RESISTANCE VERSUS DEPTH.

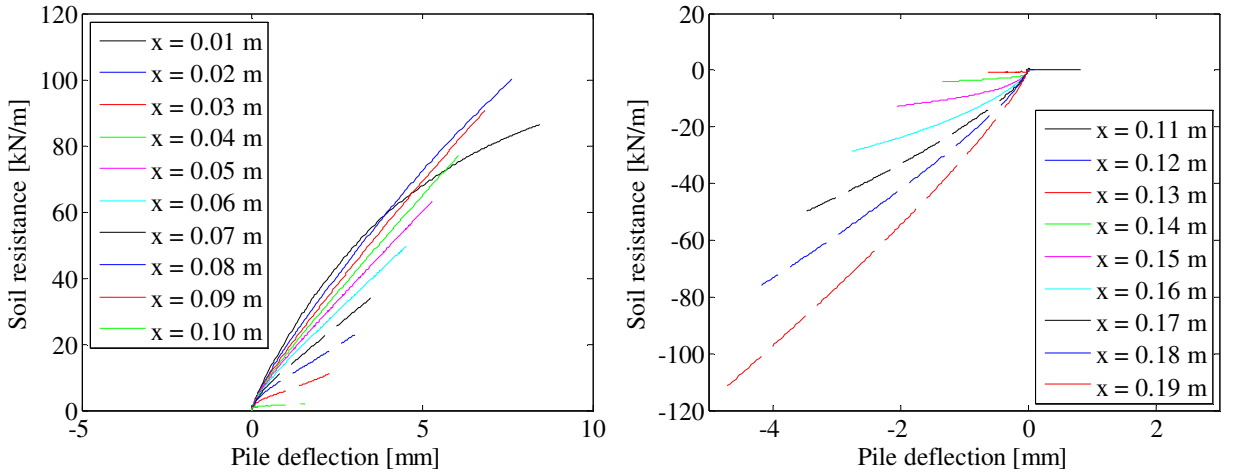

FIGURE 127. P-Y CURVES.

Test 3: D = 40 mm, L_p = 200 mm and P_0 = 100 kPa (Closed-ended)

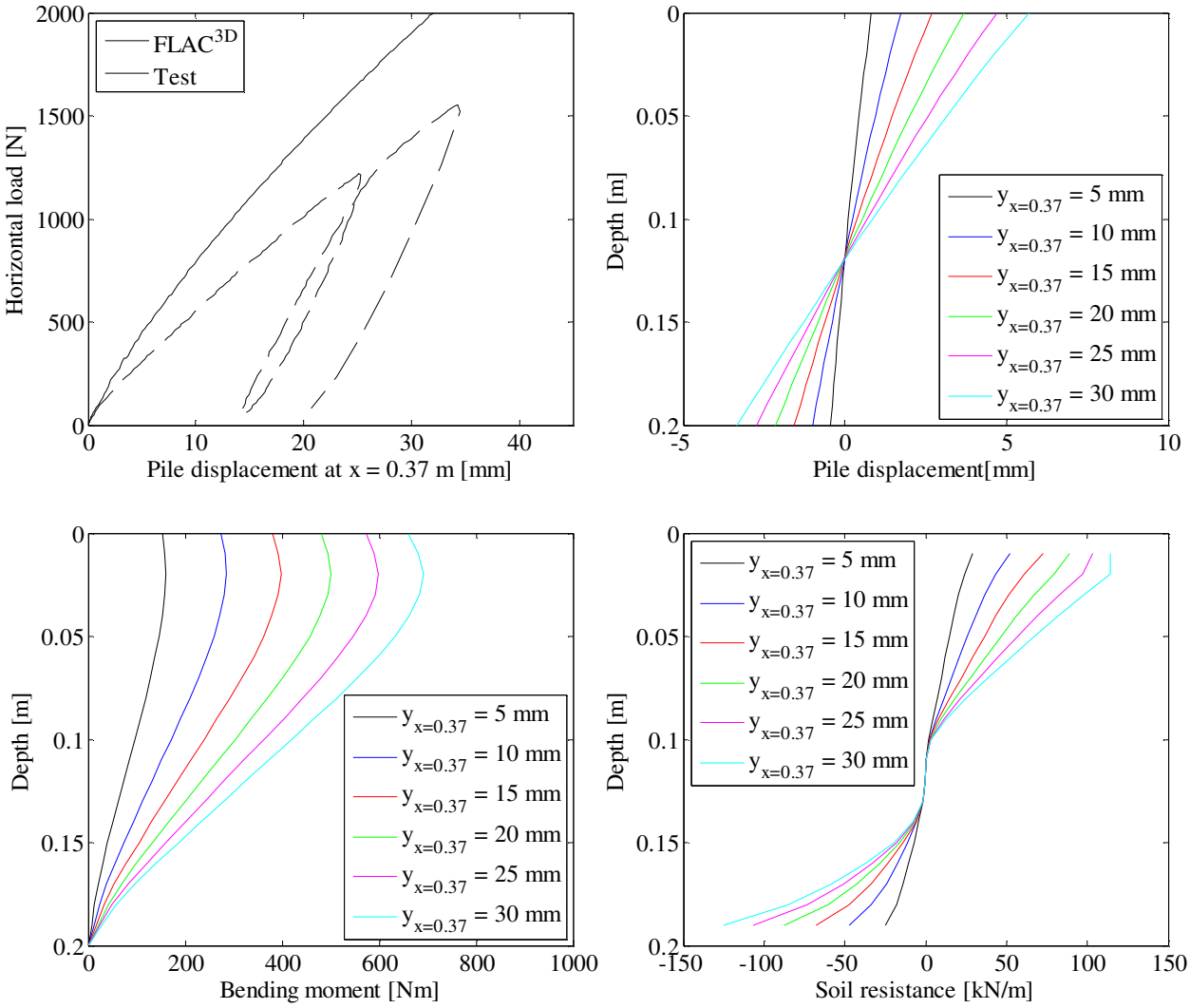

FIGURE 128. TOP LEFT: LOAD-DISPLACEMENT RELATIONSHIPS – TOP RIGHT: PILE DISPLACEMENT VERSUS DEPTH – BOTTOM LEFT: BENDING MOMENT VERSUS DEPTH – BOTTOM RIGHT: SOIL RESISTANCE VERSUS DEPTH.

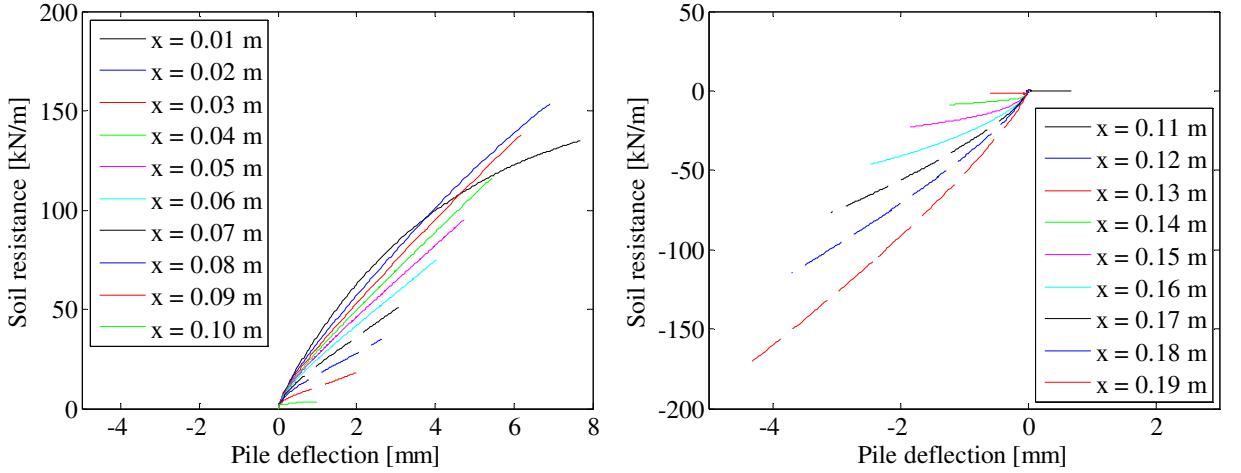

FIGURE 129. P-Y CURVES.

Test 4: D = 60 mm, L_p = 300 mm and P_0 = 0 kPa (Closed-ended)

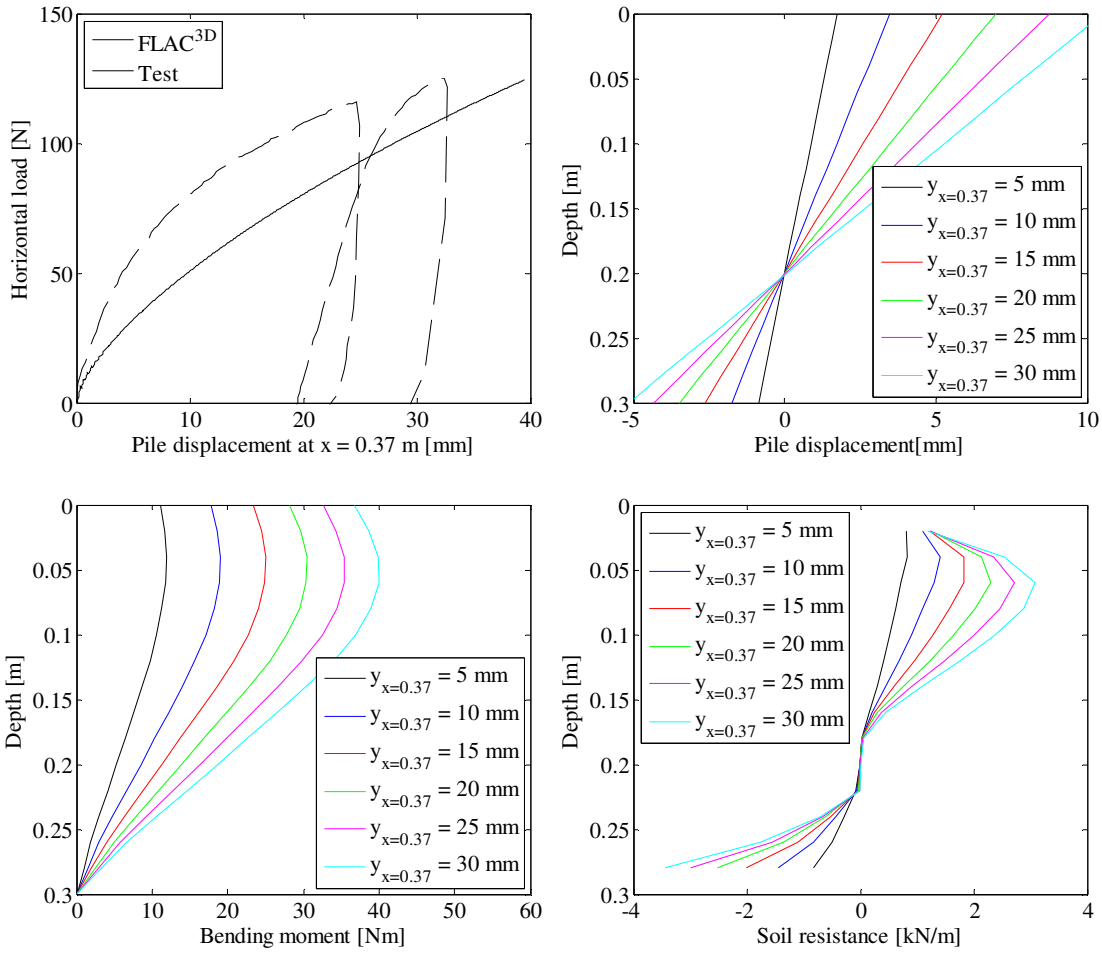

FIGURE 130. TOP LEFT: LOAD-DISPLACEMENT RELATIONSHIPS – TOP RIGHT: PILE DISPLACEMENT VERSUS DEPTH – BOTTOM LEFT: BENDING MOMENT VERSUS DEPTH – BOTTOM RIGHT: SOIL RESISTANCE VERSUS DEPTH.

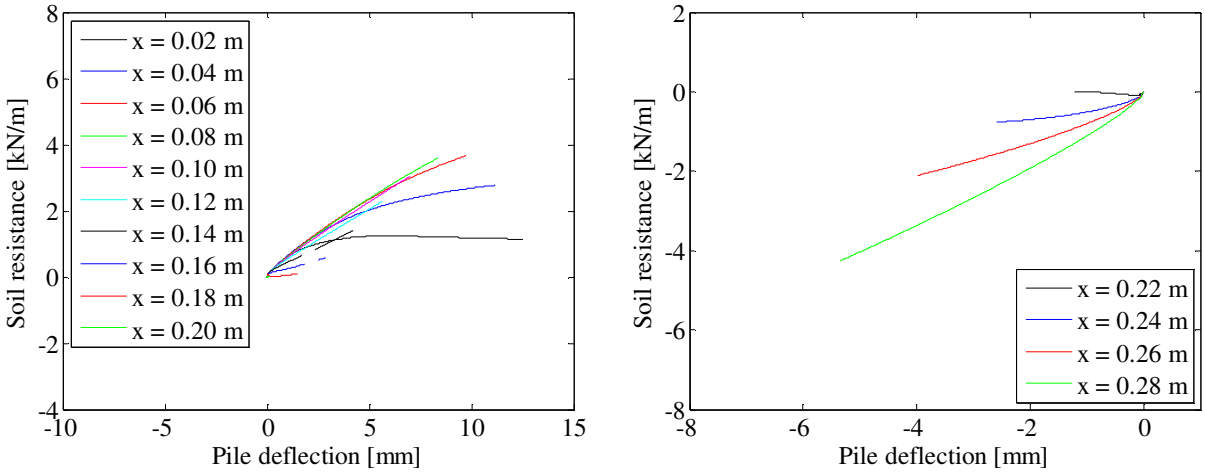

FIGURE 131. P-Y CURVES.

Test 5: D = 60 mm, L_p = 300 mm and P_0 = 50 kPa (Closed-ended)

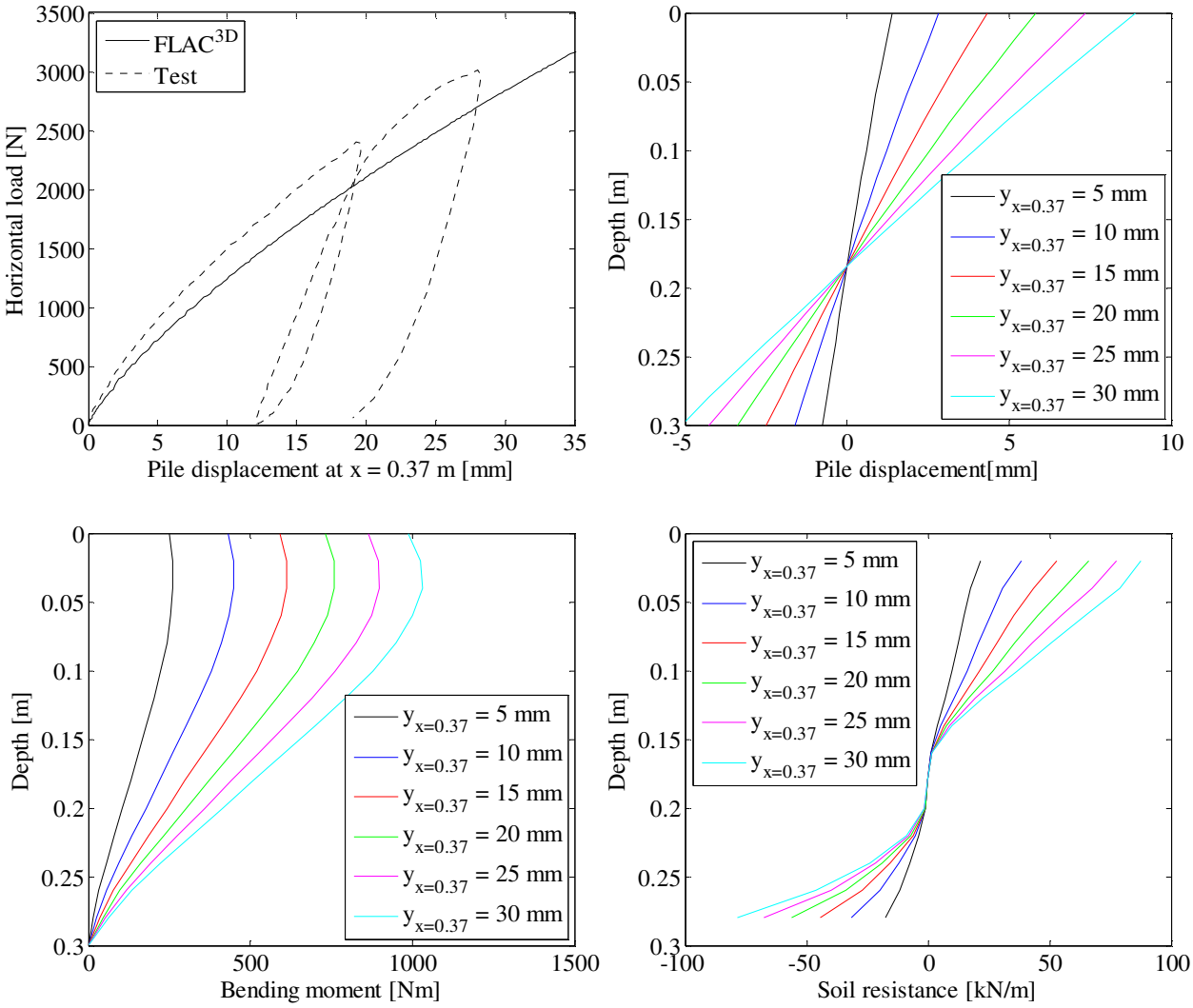

FIGURE 132. TOP LEFT: LOAD-DISPLACEMENT RELATIONSHIPS – TOP RIGHT: PILE DISPLACEMENT VERSUS DEPTH – BOTTOM LEFT: BENDING MOMENT VERSUS DEPTH – BOTTOM RIGHT: SOIL RESISTANCE VERSUS DEPTH.

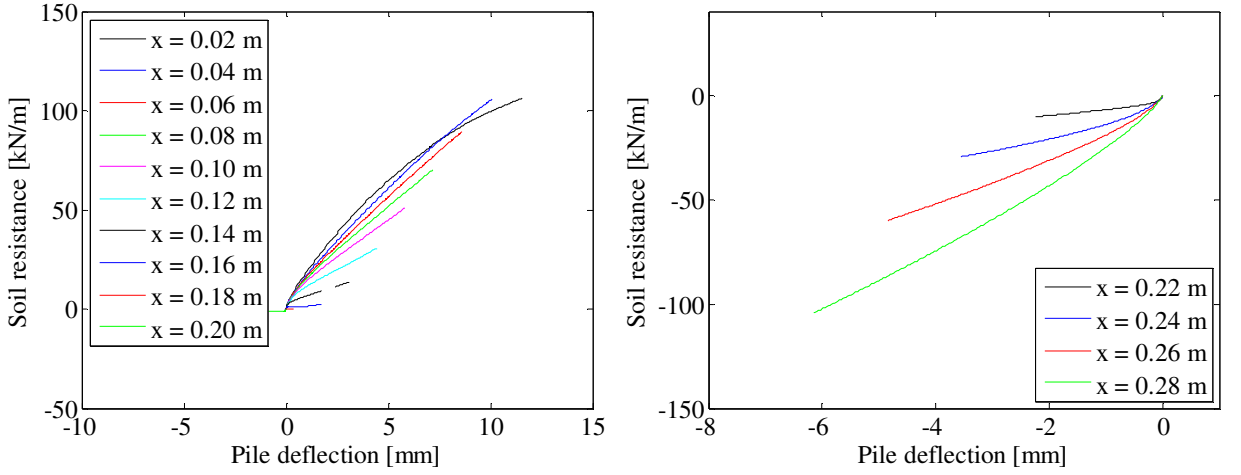

FIGURE 133. P-Y CURVES.

Test 6: D = 60 mm, L_p = 300 mm and P_0 = 100 kPa (Closed-ended)

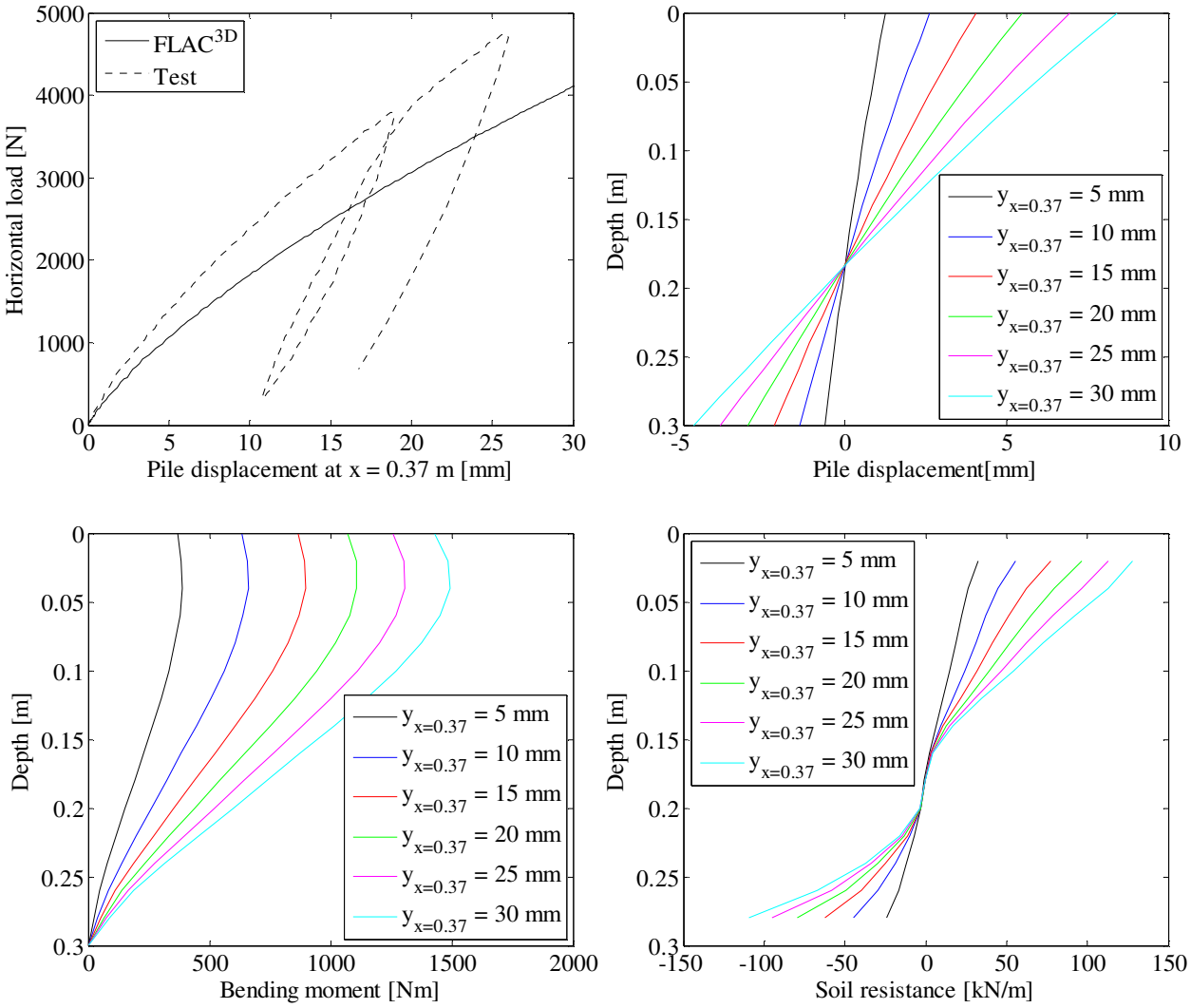

FIGURE 134. TOP LEFT: LOAD-DISPLACEMENT RELATIONSHIPS – TOP RIGHT: PILE DISPLACEMENT VERSUS DEPTH – BOTTOM LEFT: BENDING MOMENT VERSUS DEPTH – BOTTOM RIGHT: SOIL RESISTANCE VERSUS DEPTH.

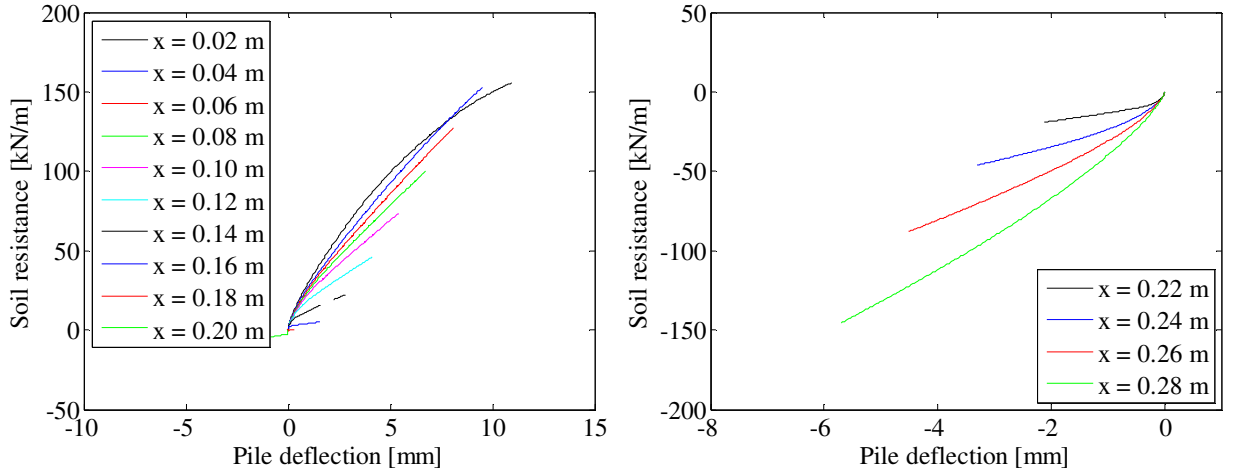

FIGURE 135. P-Y CURVES.

Test 7: D = 80 mm, L_p = 240 mm and P_0 = 0 kPa (Closed-ended)

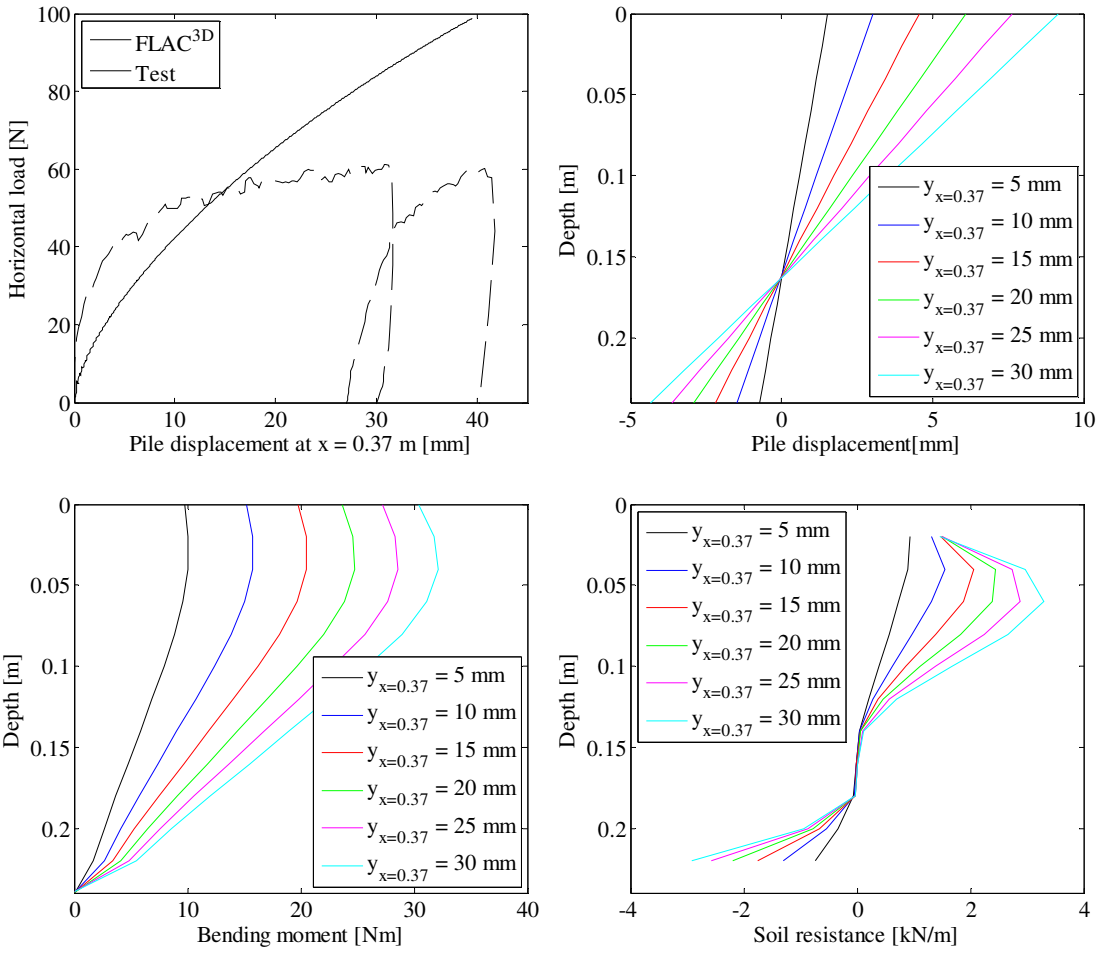

FIGURE 136. TOP LEFT: LOAD-DISPLACEMENT RELATIONSHIPS – TOP RIGHT: PILE DISPLACEMENT VERSUS DEPTH – BOTTOM LEFT: BENDING MOMENT VERSUS DEPTH – BOTTOM RIGHT: SOIL RESISTANCE VERSUS DEPTH. I_D = 0.75.

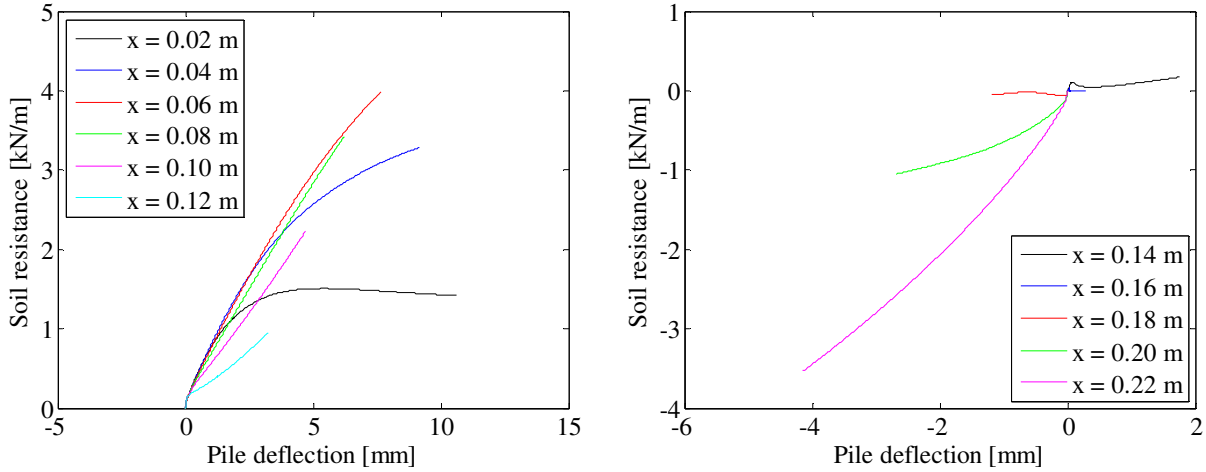

FIGURE 137. P-Y CURVES ASSUMING I_D = 0.75.

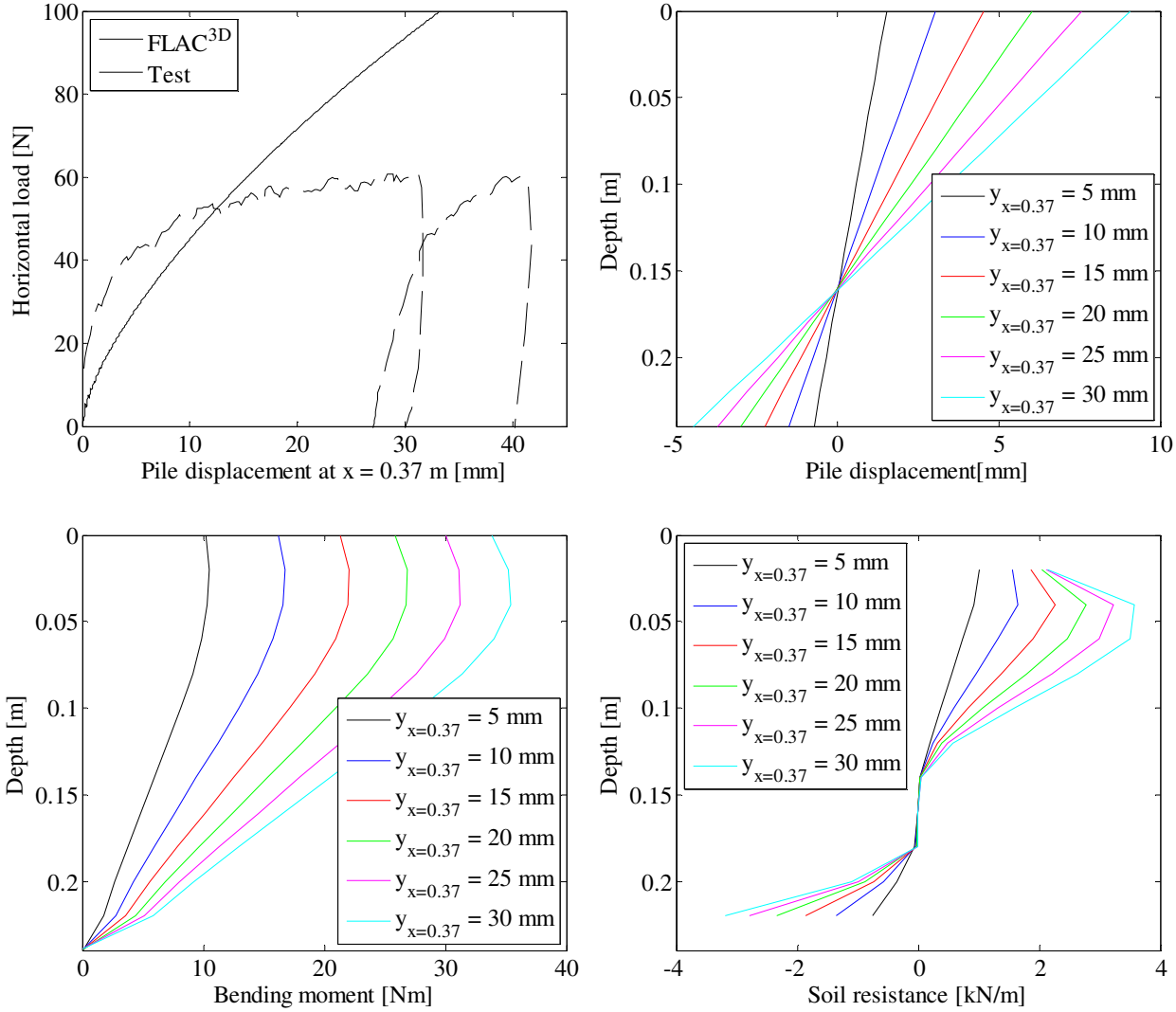

FIGURE 138. TOP LEFT: LOAD-DISPLACEMENT RELATIONSHIPS – TOP RIGHT: PILE DISPLACEMENT VERSUS DEPTH – BOTTOM LEFT: BENDING MOMENT VERSUS DEPTH – BOTTOM RIGHT: SOIL RESISTANCE VERSUS DEPTH. I_D = 0.91.

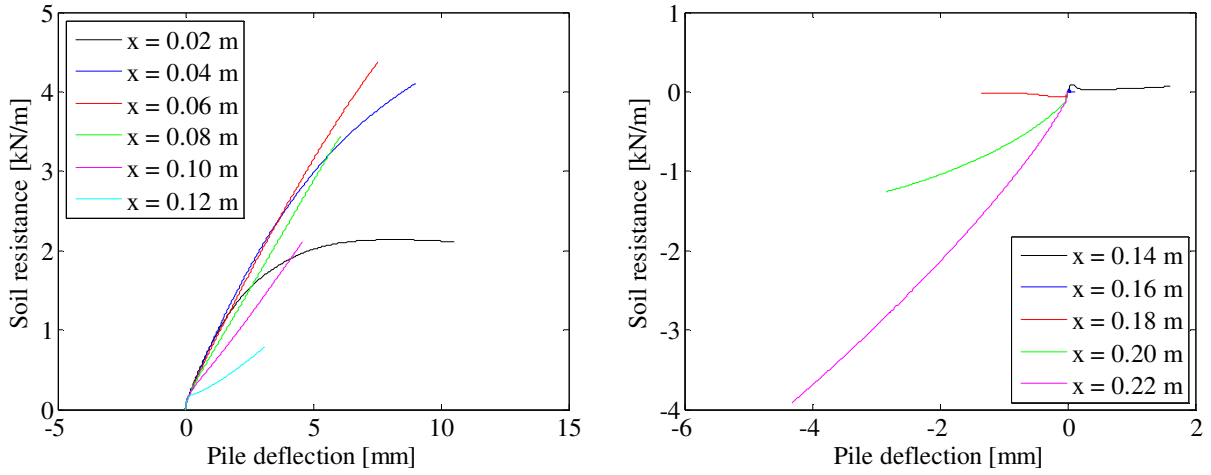

FIGURE 139. P-Y CURVES ASSUMING I_D = 0.91.

Test 8: D = 80 mm, L_p = 240 mm and P_0 = 50 kPa (Closed-ended)

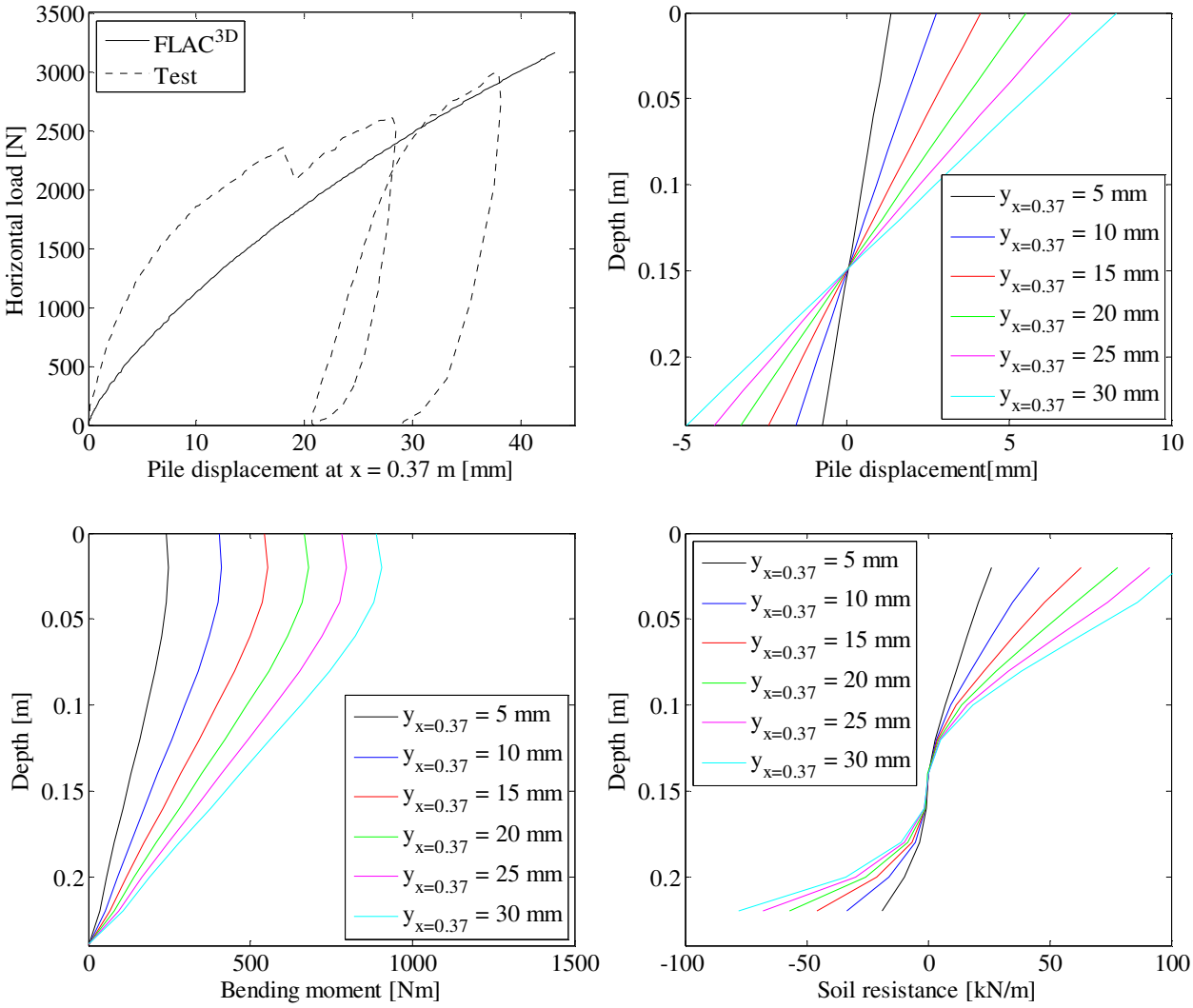

FIGURE 140. TOP LEFT: LOAD-DISPLACEMENT RELATIONSHIPS – TOP RIGHT: PILE DISPLACEMENT VERSUS DEPTH – BOTTOM LEFT: BENDING MOMENT VERSUS DEPTH – BOTTOM RIGHT: SOIL RESISTANCE VERSUS DEPTH. I_D = 0.75.

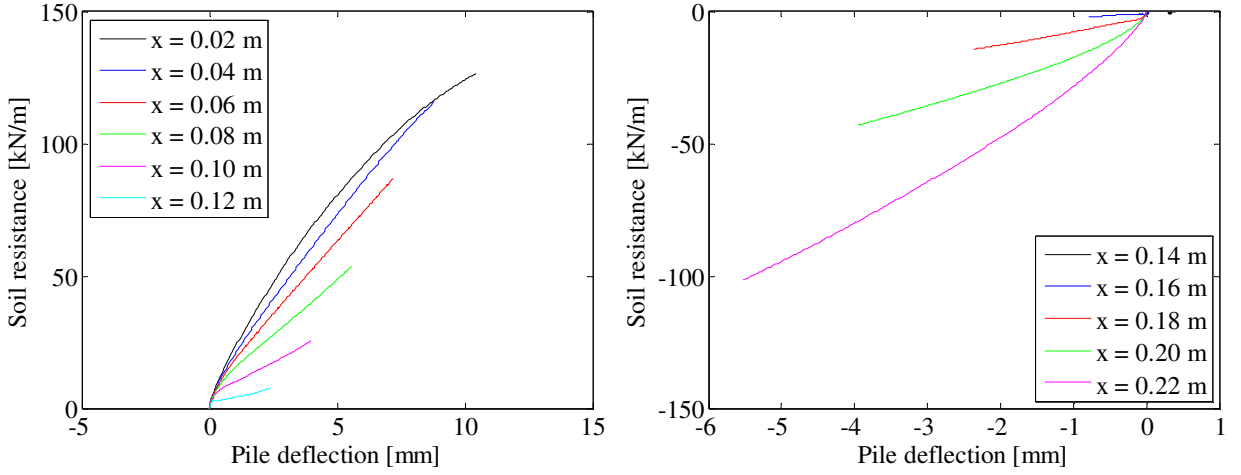

FIGURE 141. P-Y CURVES ASSUMING I_D = 0.75.

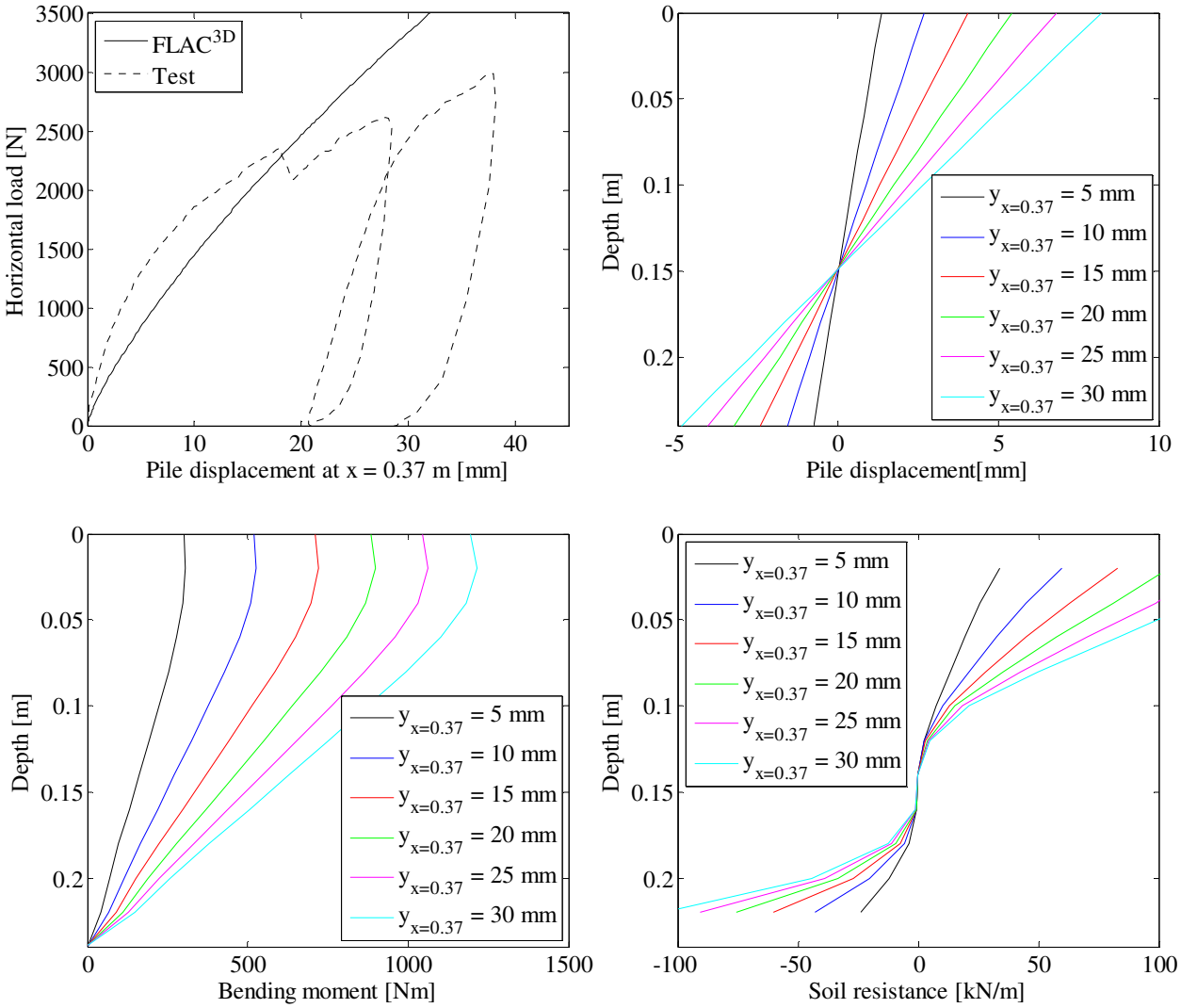

FIGURE 142. TOP LEFT: LOAD-DISPLACEMENT RELATIONSHIPS – TOP RIGHT: PILE DISPLACEMENT VERSUS DEPTH – BOTTOM LEFT: BENDING MOMENT VERSUS DEPTH – BOTTOM RIGHT: SOIL RESISTANCE VERSUS DEPTH. I_D = 0.91.

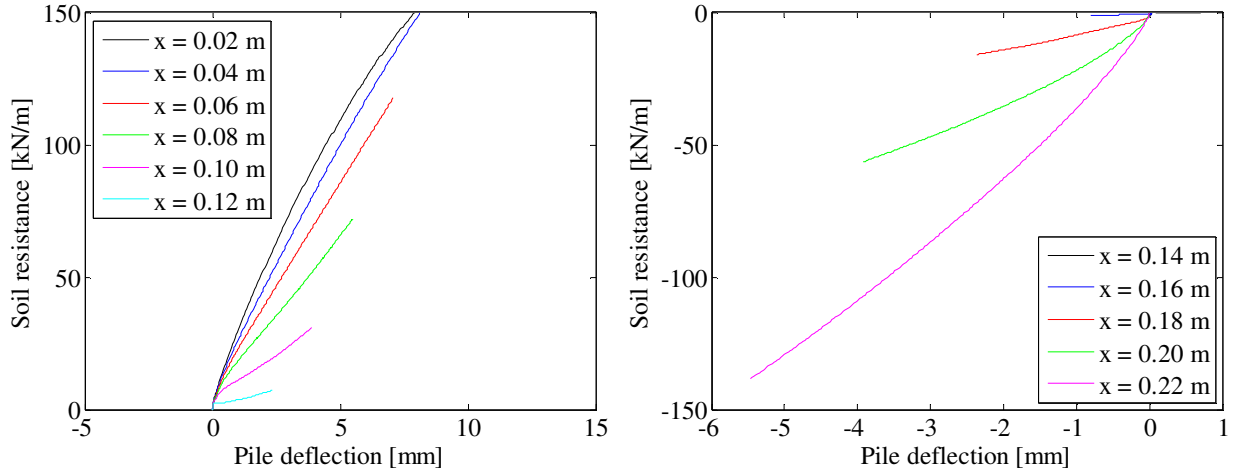

FIGURE 143. P-Y CURVES ASSUMING I_D = 0.91.

Test 9: D = 80 mm, L_p = 240 mm and P_0 = 100 kPa (Closed-ended)

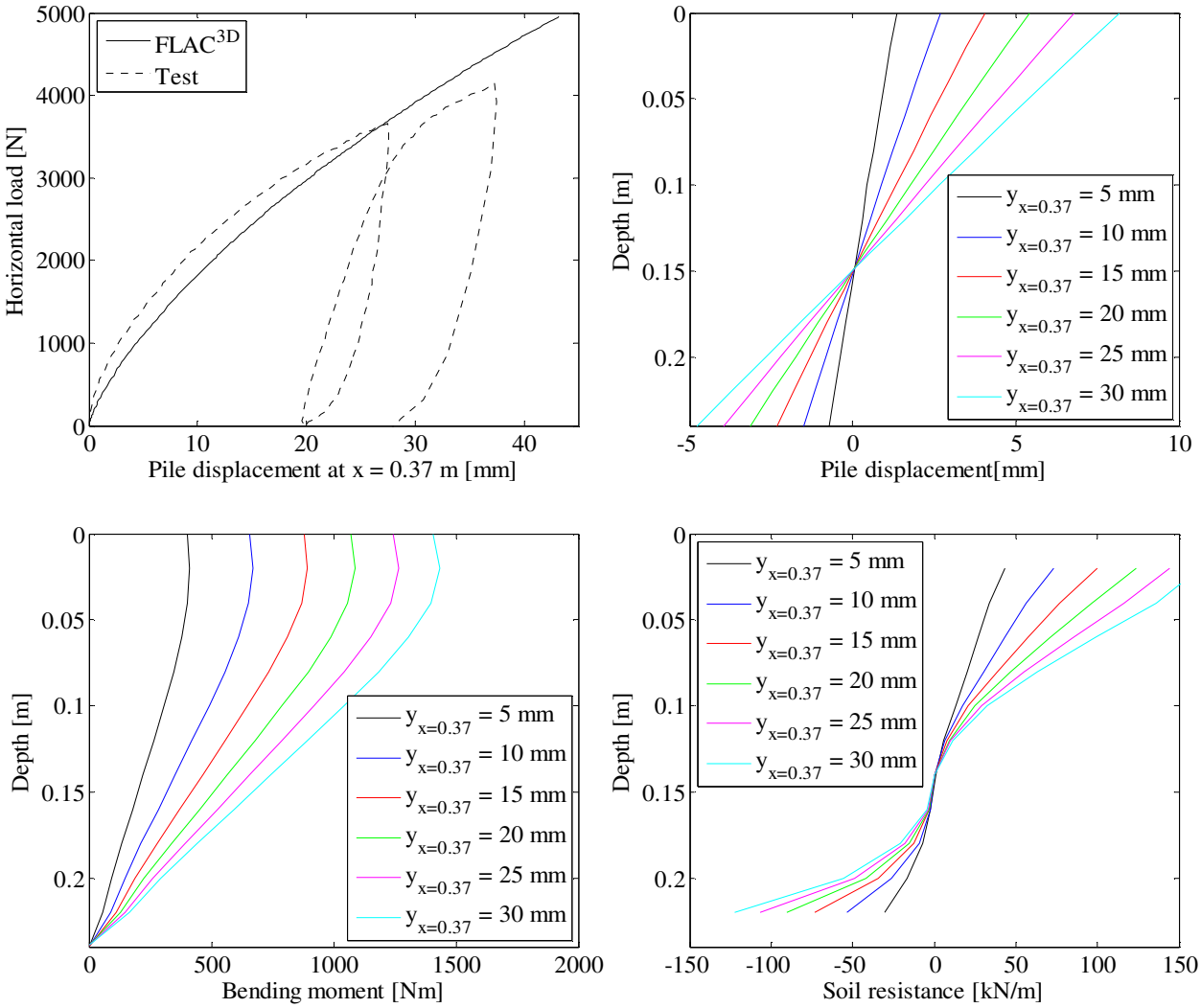

FIGURE 144. TOP LEFT: LOAD-DISPLACEMENT RELATIONSHIPS – TOP RIGHT: PILE DISPLACEMENT VERSUS DEPTH – BOTTOM LEFT: BENDING MOMENT VERSUS DEPTH – BOTTOM RIGHT: SOIL RESISTANCE VERSUS DEPTH. I_D = 0.75.

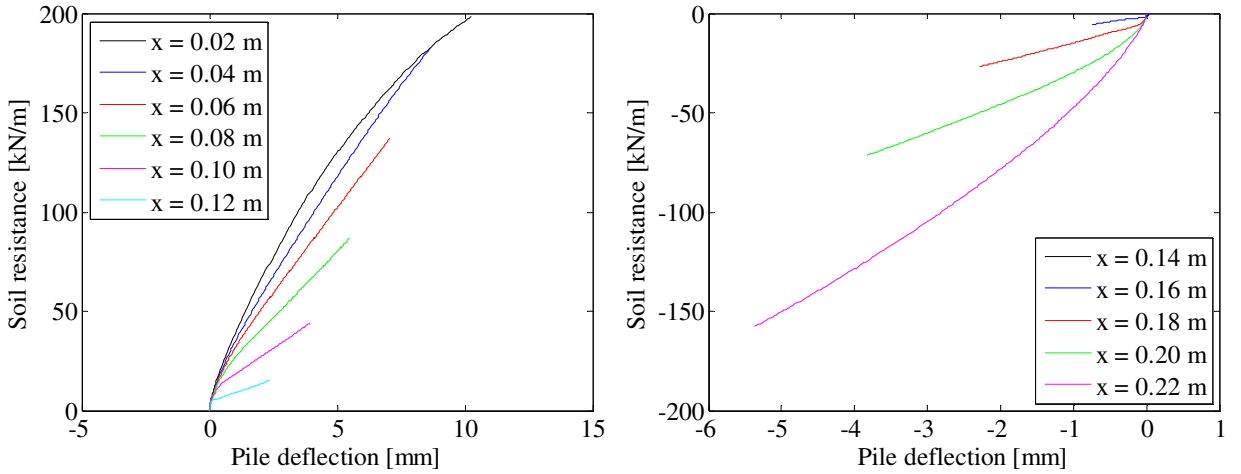

FIGURE 145. P-Y CURVES ASSUMING I_D = 0.75.

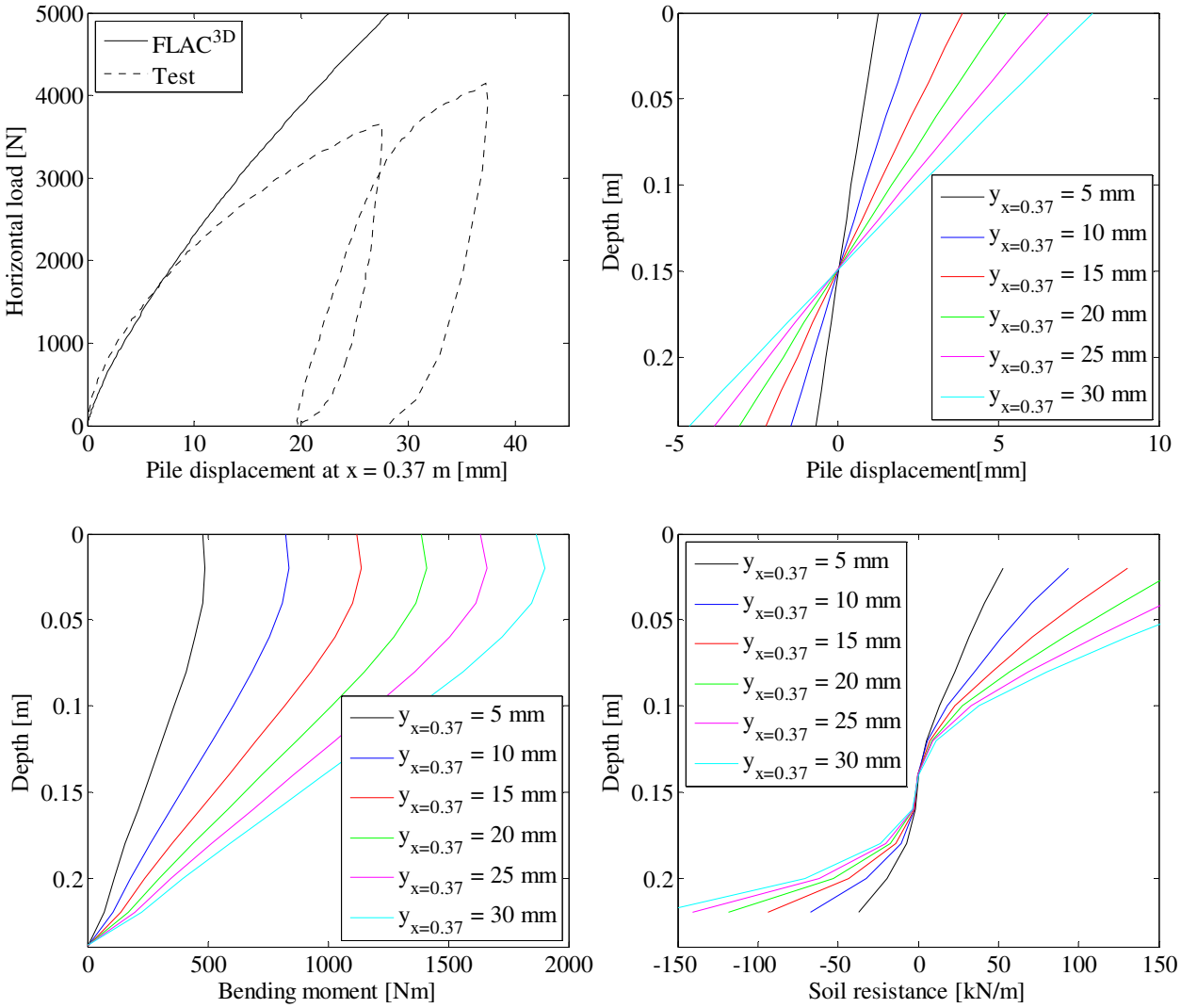

FIGURE 146. TOP LEFT: LOAD-DISPLACEMENT RELATIONSHIPS – TOP RIGHT: PILE DISPLACEMENT VERSUS DEPTH – BOTTOM LEFT: BENDING MOMENT VERSUS DEPTH – BOTTOM RIGHT: SOIL RESISTANCE VERSUS DEPTH. I_D = 0.91.

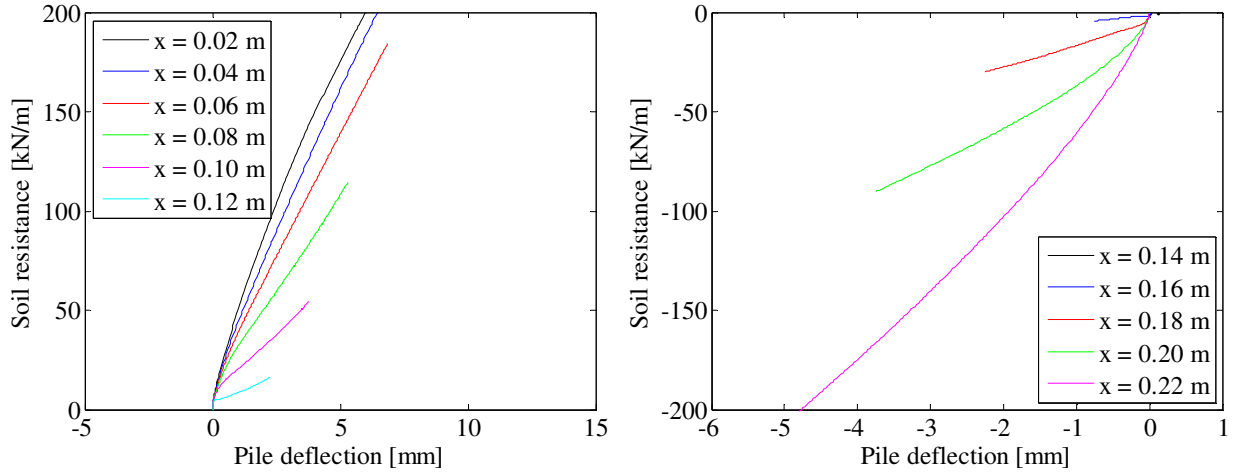

FIGURE 147. P-Y CURVES ASSUMING I_D = 0.91.

Test 10: D = 80 mm, L_p = 320 mm and P_0 = 0 kPa (Open-ended)

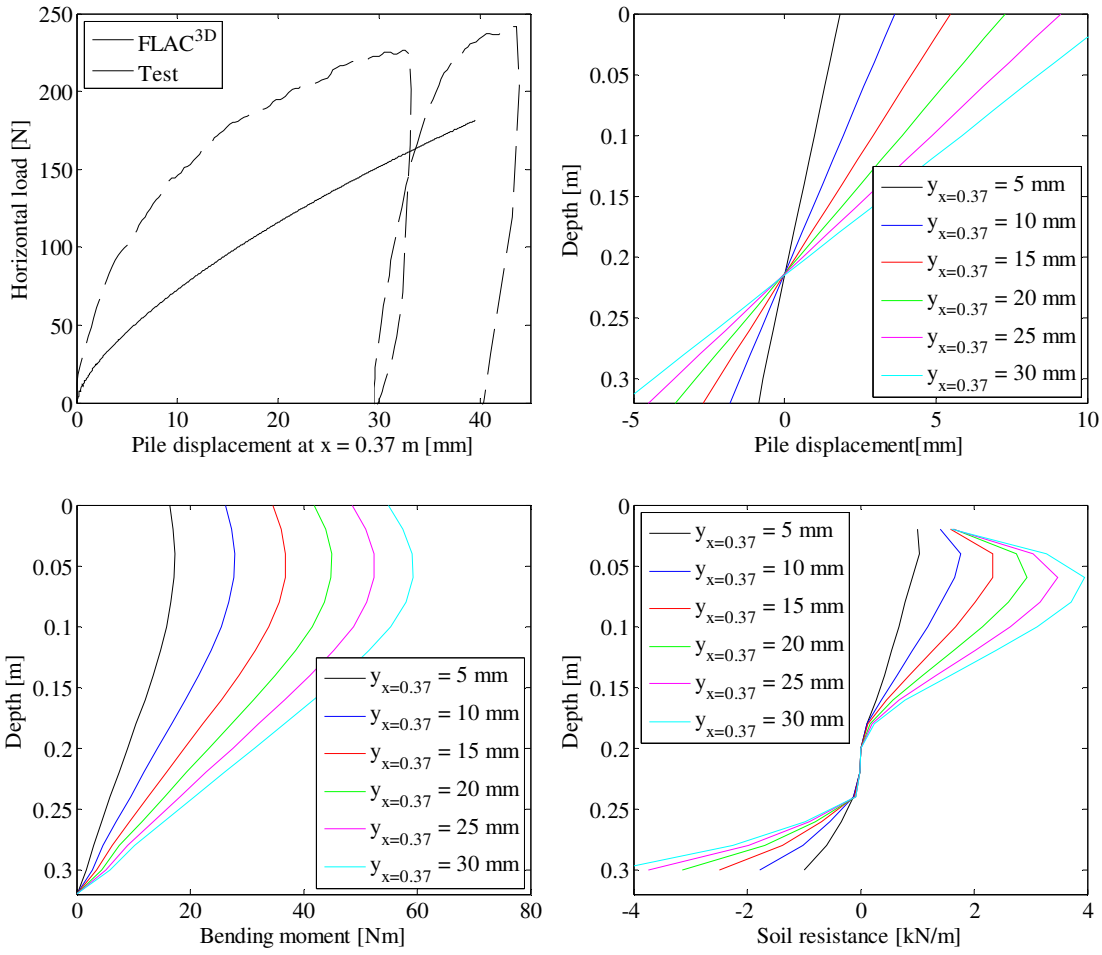

FIGURE 148. TOP LEFT: LOAD-DISPLACEMENT RELATIONSHIPS – TOP RIGHT: PILE DISPLACEMENT VERSUS DEPTH – BOTTOM LEFT: BENDING MOMENT VERSUS DEPTH – BOTTOM RIGHT: SOIL RESISTANCE VERSUS DEPTH.

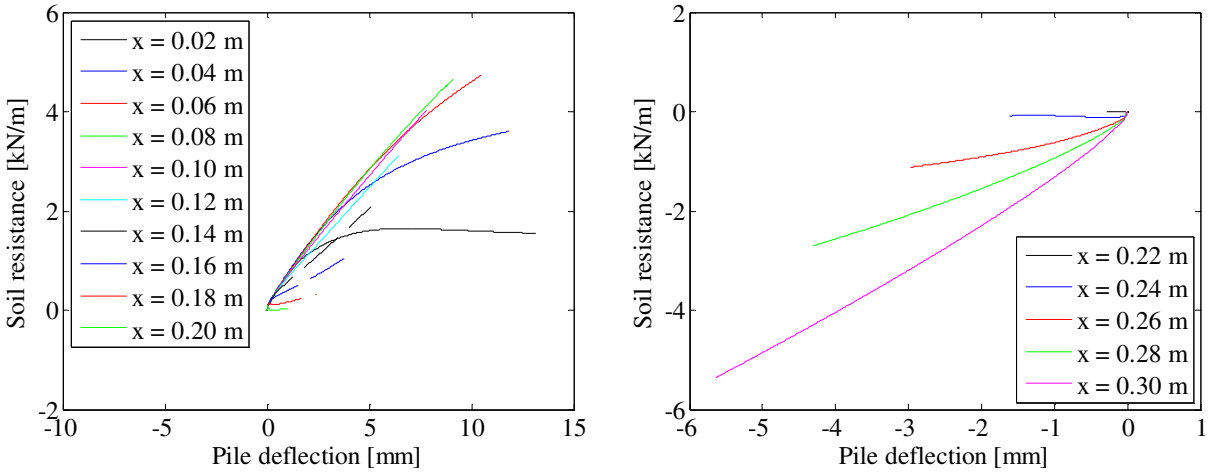

FIGURE 149. P-Y CURVES.

Test 11: D = 80 mm, L_p = 320 mm and P_0 = 0 kPa (Closed-ended)

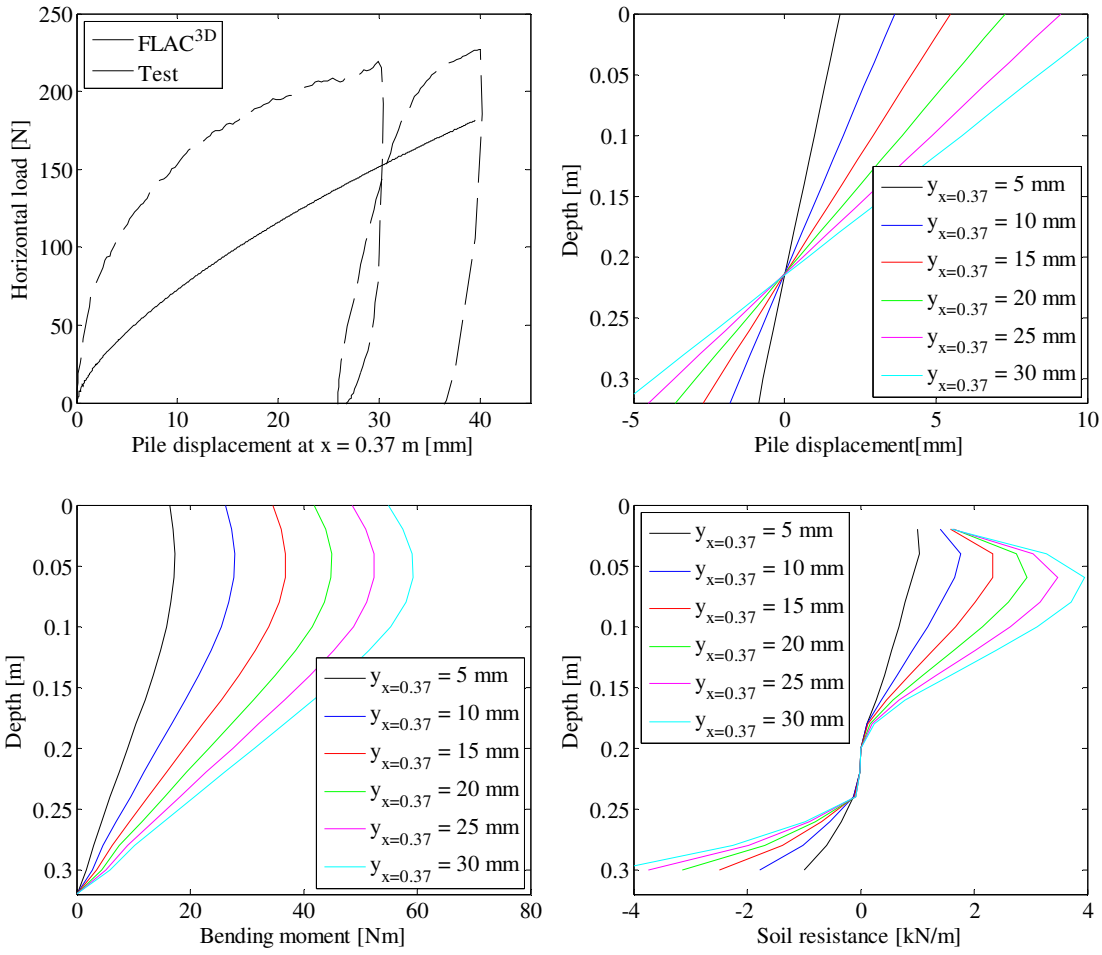

FIGURE 150. TOP LEFT: LOAD-DISPLACEMENT RELATIONSHIPS – TOP RIGHT: PILE DISPLACEMENT VERSUS DEPTH – BOTTOM LEFT: BENDING MOMENT VERSUS DEPTH – BOTTOM RIGHT: SOIL RESISTANCE VERSUS DEPTH.

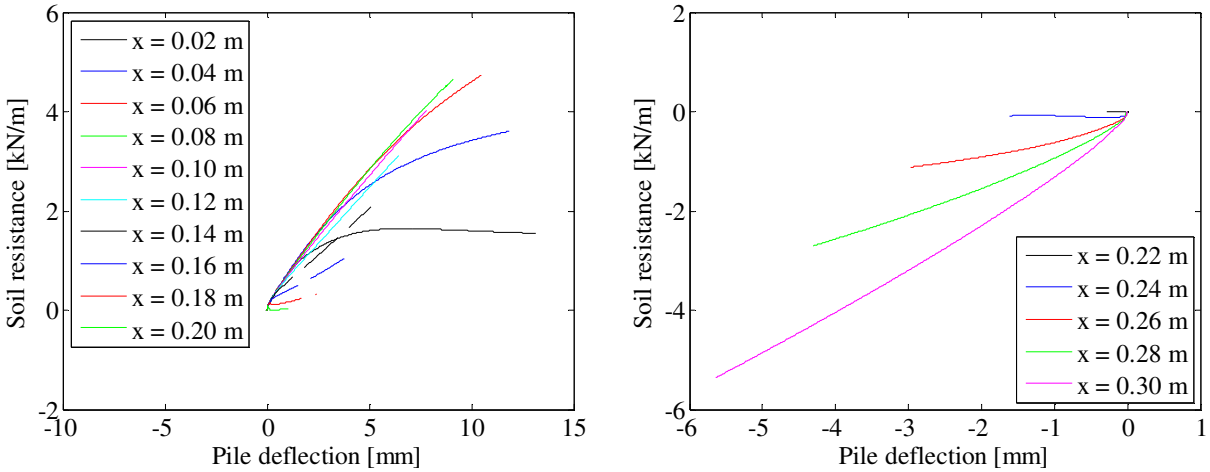

FIGURE 151. P-Y CURVES.

Test 12: D = 80 mm, L_p = 320 mm and P_0 = 50 kPa (Closed-ended)

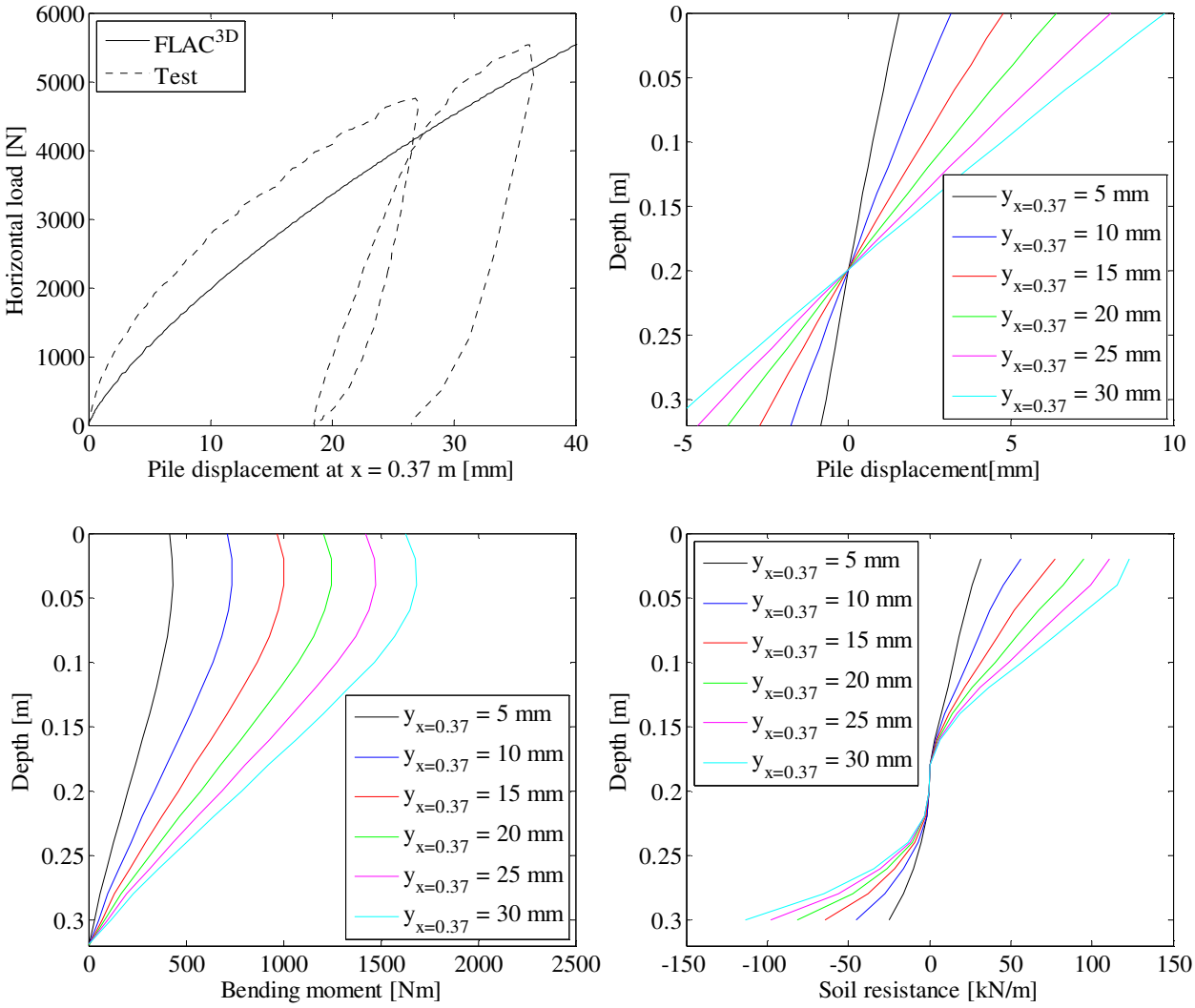

FIGURE 152. TOP LEFT: LOAD-DISPLACEMENT RELATIONSHIPS – TOP RIGHT: PILE DISPLACEMENT VERSUS DEPTH – BOTTOM LEFT: BENDING MOMENT VERSUS DEPTH – BOTTOM RIGHT: SOIL RESISTANCE VERSUS DEPTH.

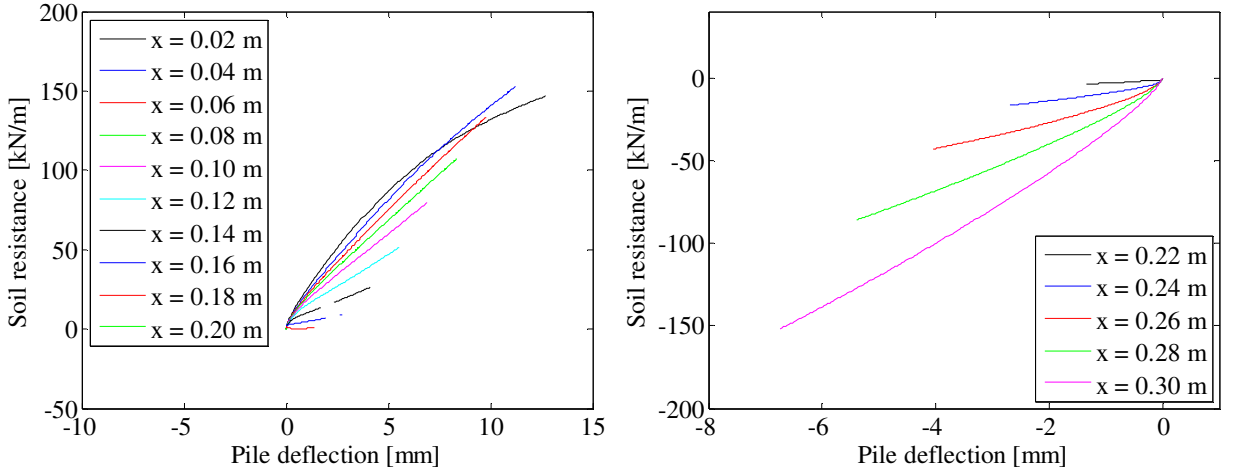

FIGURE 153. P-Y CURVES.

Test 13: D = 80 mm, L_p = 320 mm and P_0 = 100 kPa (Closed-ended)

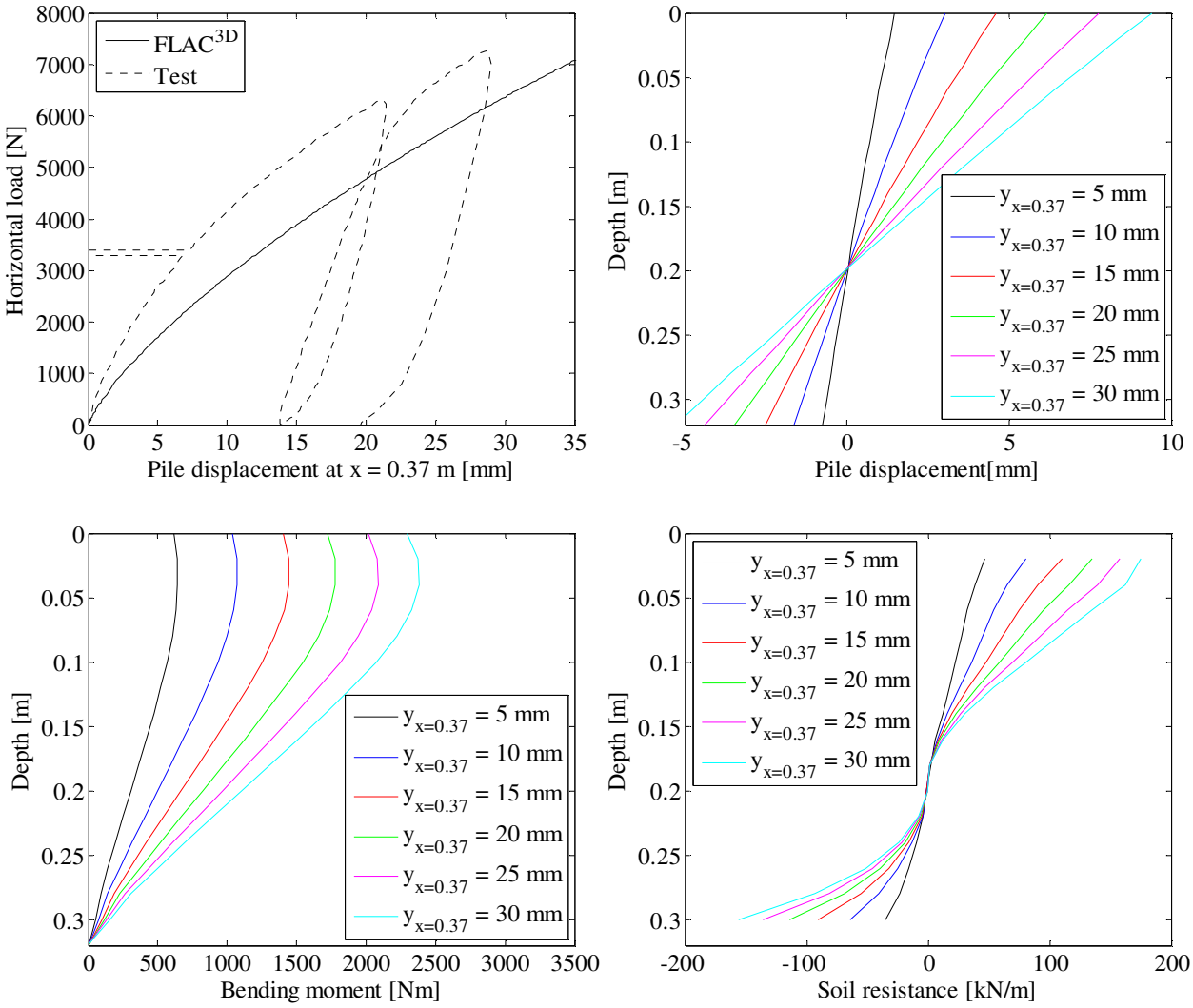

FIGURE 154. TOP LEFT: LOAD-DISPLACEMENT RELATIONSHIPS – TOP RIGHT: PILE DISPLACEMENT VERSUS DEPTH – BOTTOM LEFT: BENDING MOMENT VERSUS DEPTH – BOTTOM RIGHT: SOIL RESISTANCE VERSUS DEPTH.

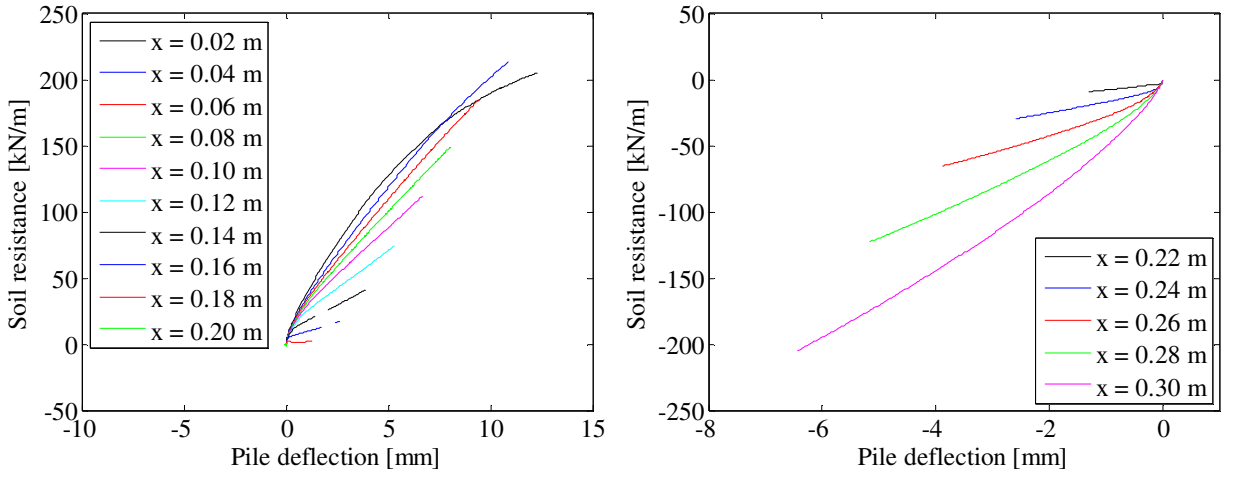

FIGURE 155. P-Y CURVES.

Test 14: D = 80 mm, L_p = 400 mm and P_0 = 0 kPa (Closed-ended)

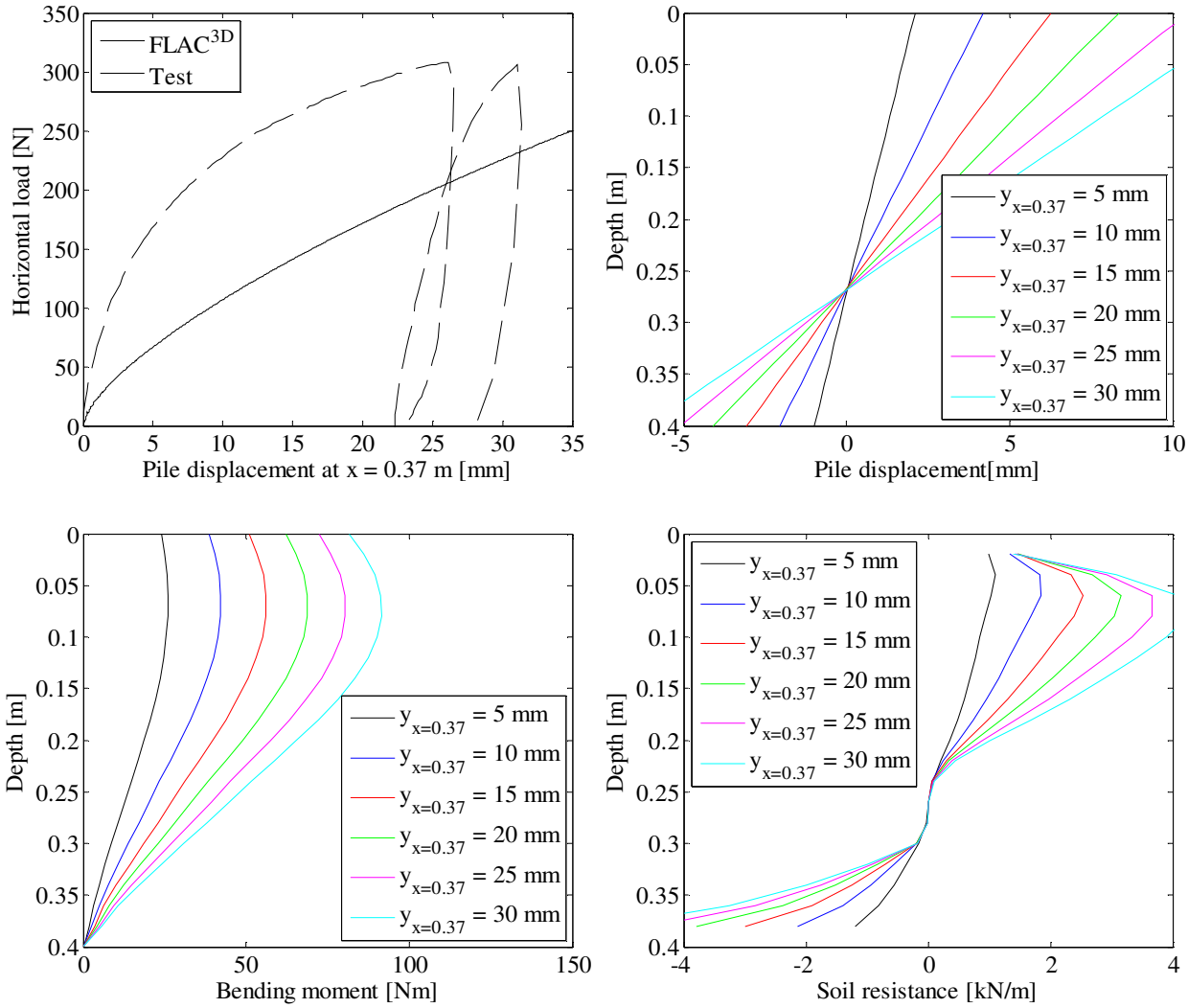

FIGURE 156. TOP LEFT: LOAD-DISPLACEMENT RELATIONSHIPS – TOP RIGHT: PILE DISPLACEMENT VERSUS DEPTH – BOTTOM LEFT: BENDING MOMENT VERSUS DEPTH – BOTTOM RIGHT: SOIL RESISTANCE VERSUS DEPTH.

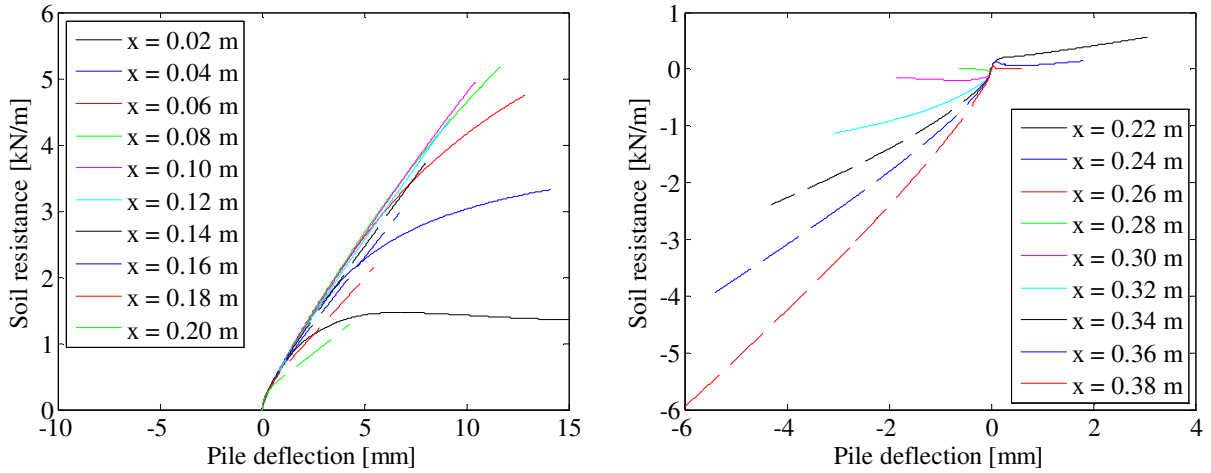

FIGURE 157. P-Y CURVES.

Test 15: D = 80 mm, L_p = 400 mm and P_0 = 0 kPa (Closed-ended)

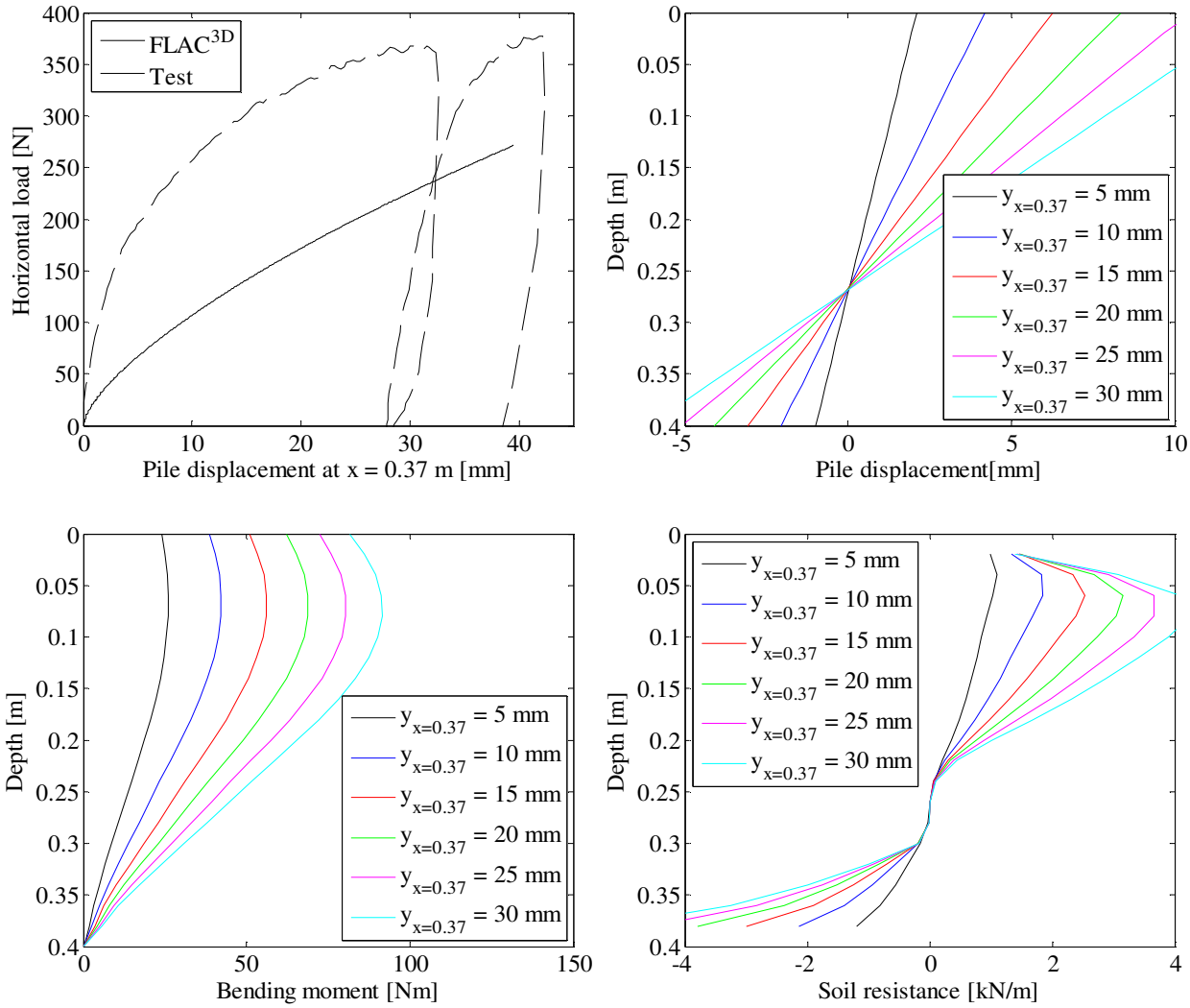

FIGURE 158. TOP LEFT: LOAD-DISPLACEMENT RELATIONSHIPS – TOP RIGHT: PILE DISPLACEMENT VERSUS DEPTH – BOTTOM LEFT: BENDING MOMENT VERSUS DEPTH – BOTTOM RIGHT: SOIL RESISTANCE VERSUS DEPTH.

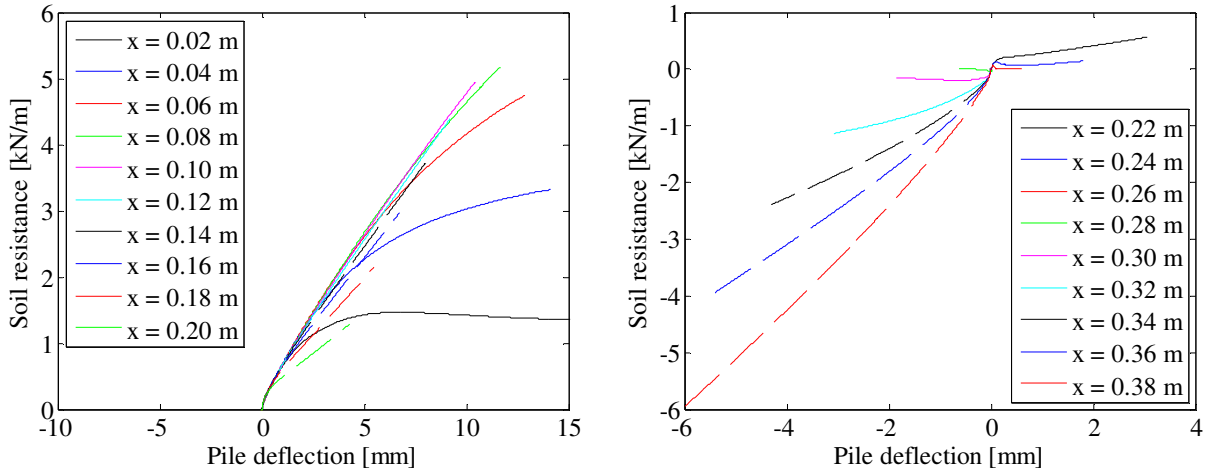

FIGURE 159. P-Y CURVES.

Test 16: D = 80 mm, L_p = 400 mm and P_0 = 25 kPa (Closed-ended)

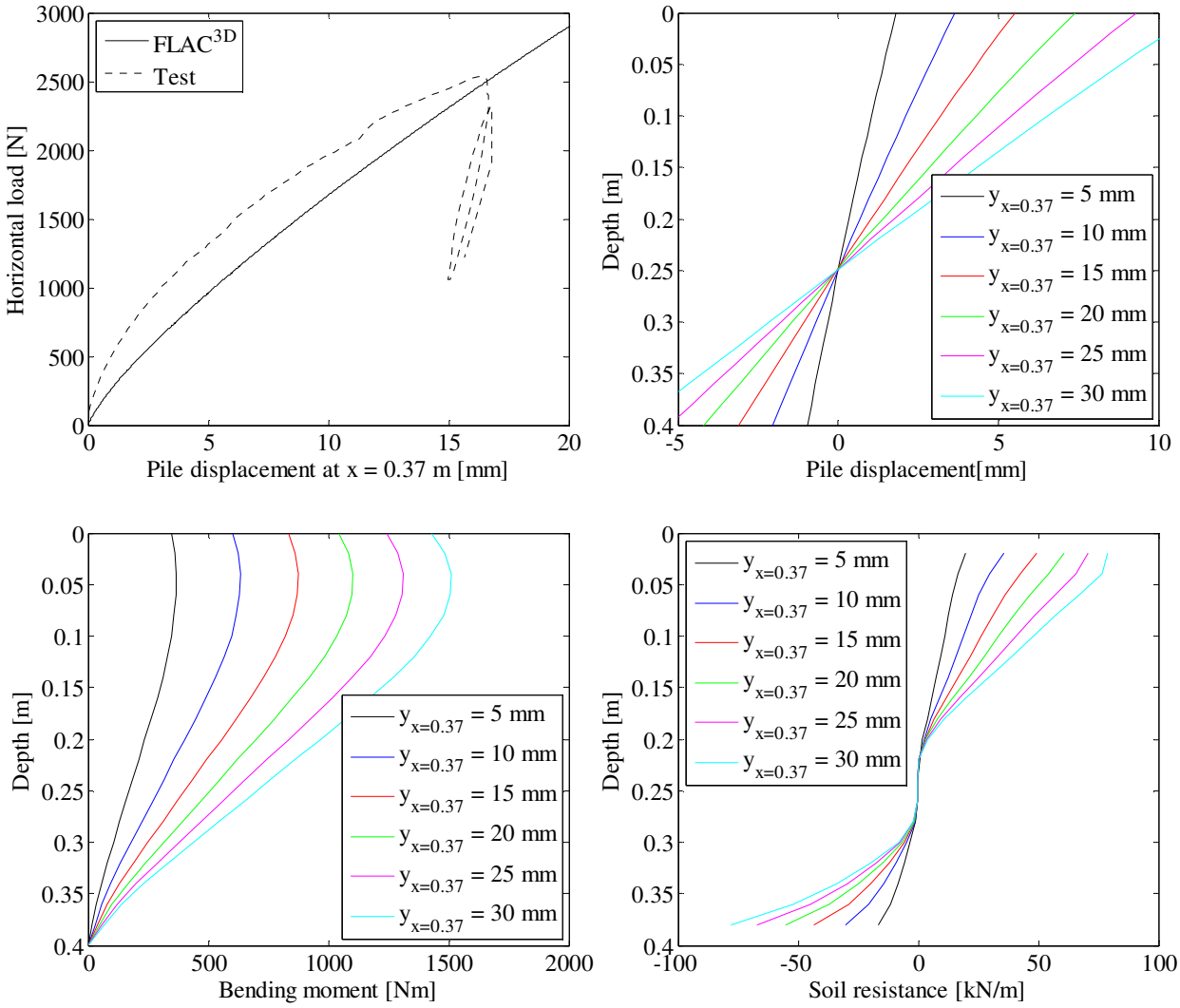

FIGURE 160. TOP LEFT: LOAD-DISPLACEMENT RELATIONSHIPS – TOP RIGHT: PILE DISPLACEMENT VERSUS DEPTH – BOTTOM LEFT: BENDING MOMENT VERSUS DEPTH – BOTTOM RIGHT: SOIL RESISTANCE VERSUS DEPTH.

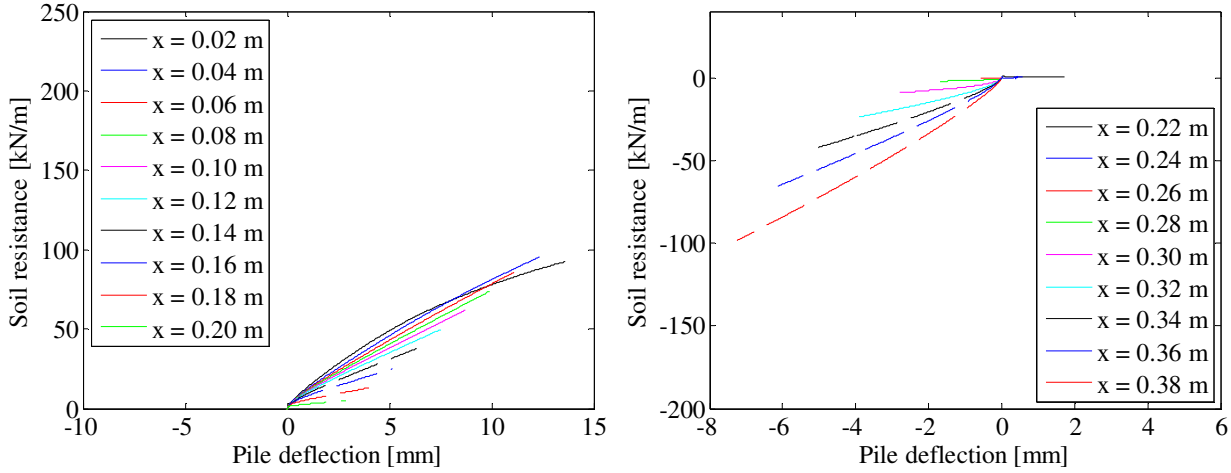

FIGURE 161. P-Y CURVES.

Test 17: D = 80 mm, L_p = 400 mm and P_0 = 50 kPa (Closed-ended)

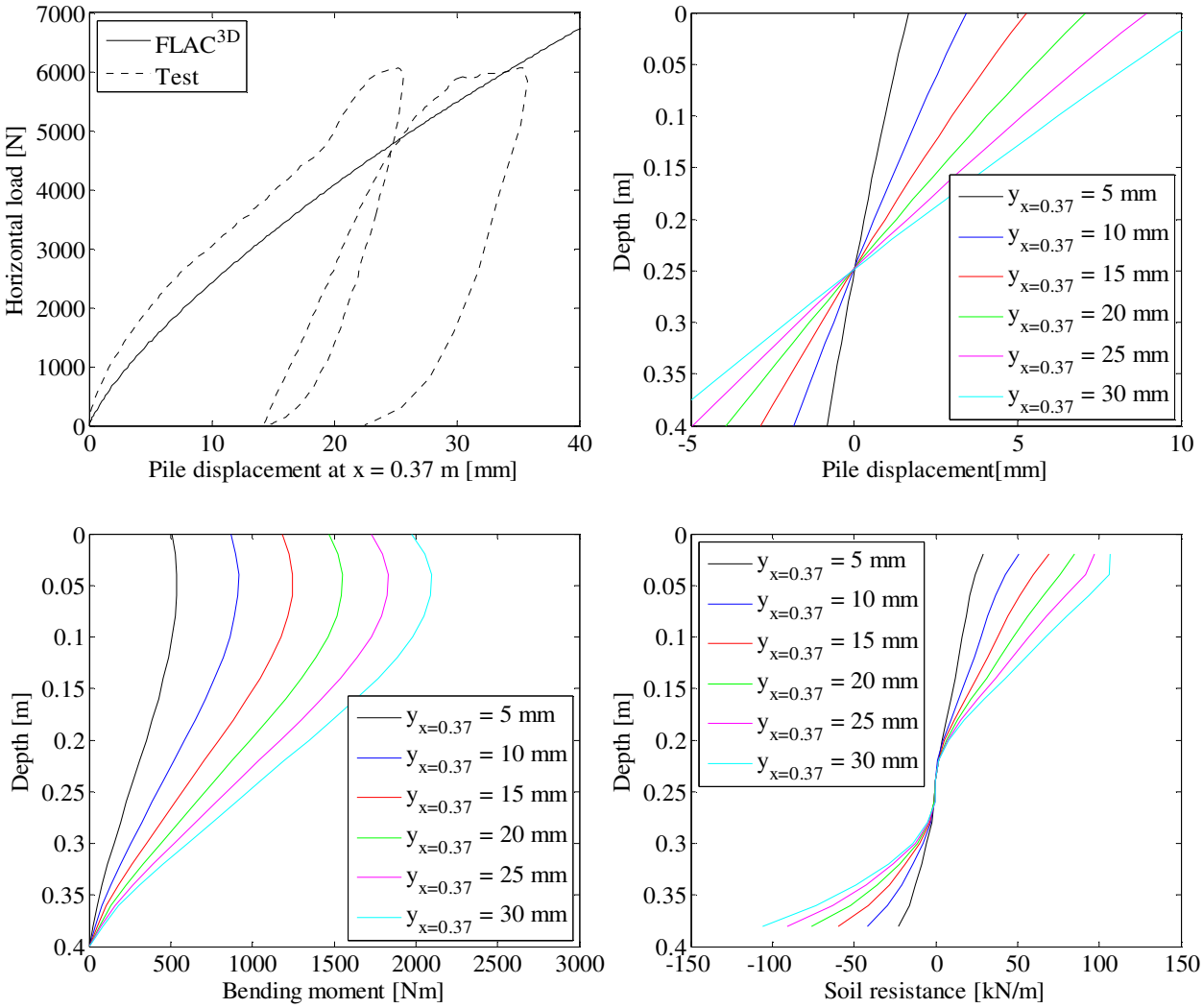

FIGURE 162. TOP LEFT: LOAD-DISPLACEMENT RELATIONSHIPS – TOP RIGHT: PILE DISPLACEMENT VERSUS DEPTH – BOTTOM LEFT: BENDING MOMENT VERSUS DEPTH – BOTTOM RIGHT: SOIL RESISTANCE VERSUS DEPTH.

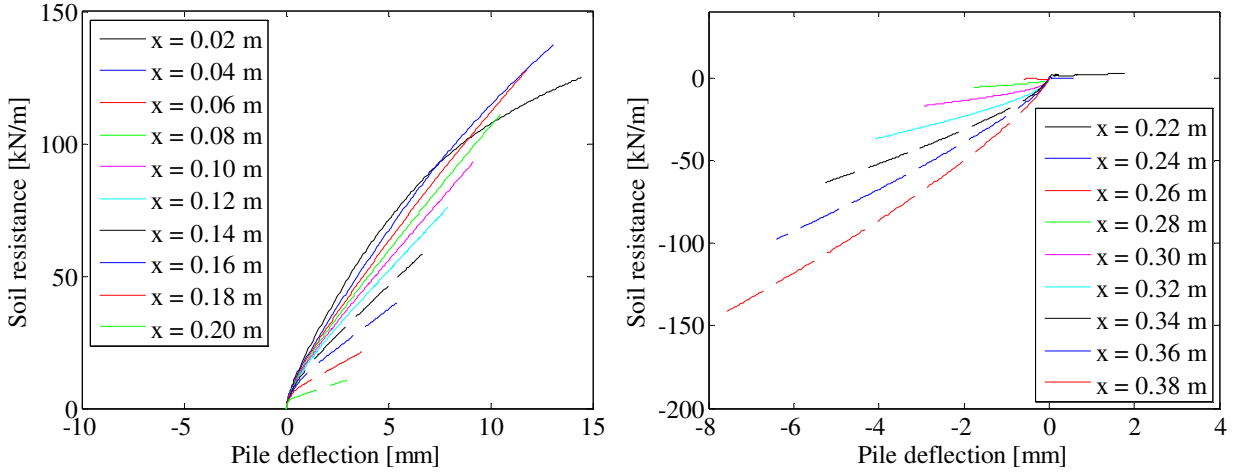

FIGURE 163. P-Y CURVES.

Test 18: D = 80 mm, L_p = 400 mm and P_0 = 50 kPa (Closed-ended)

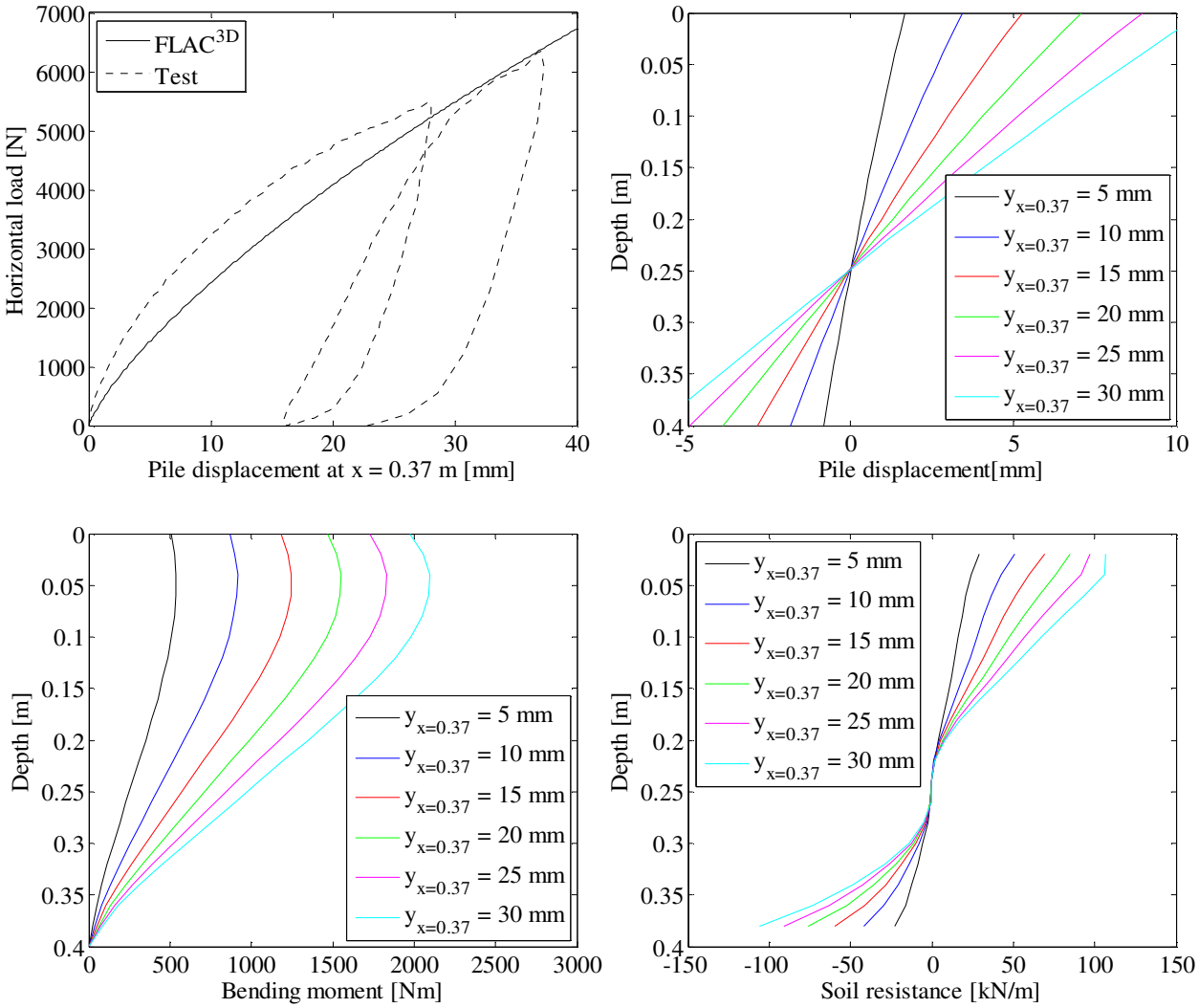

FIGURE 164. TOP LEFT: LOAD-DISPLACEMENT RELATIONSHIPS – TOP RIGHT: PILE DISPLACEMENT VERSUS DEPTH – BOTTOM LEFT: BENDING MOMENT VERSUS DEPTH – BOTTOM RIGHT: SOIL RESISTANCE VERSUS DEPTH.

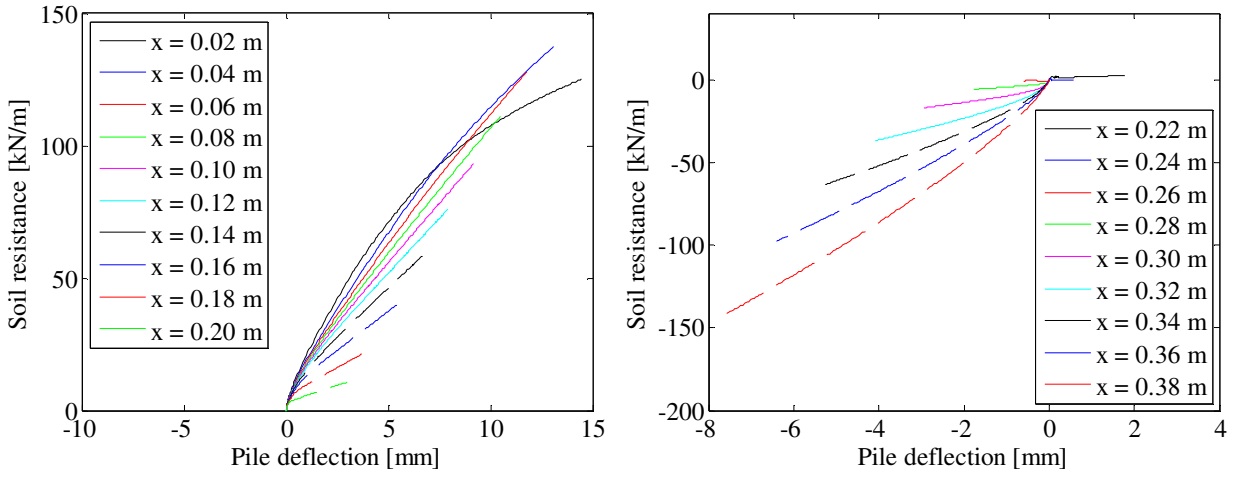

FIGURE 165. P-Y CURVES.

Test 19: D = 80 mm, L_p = 400 mm and P_0 = 75 kPa (Closed-ended)

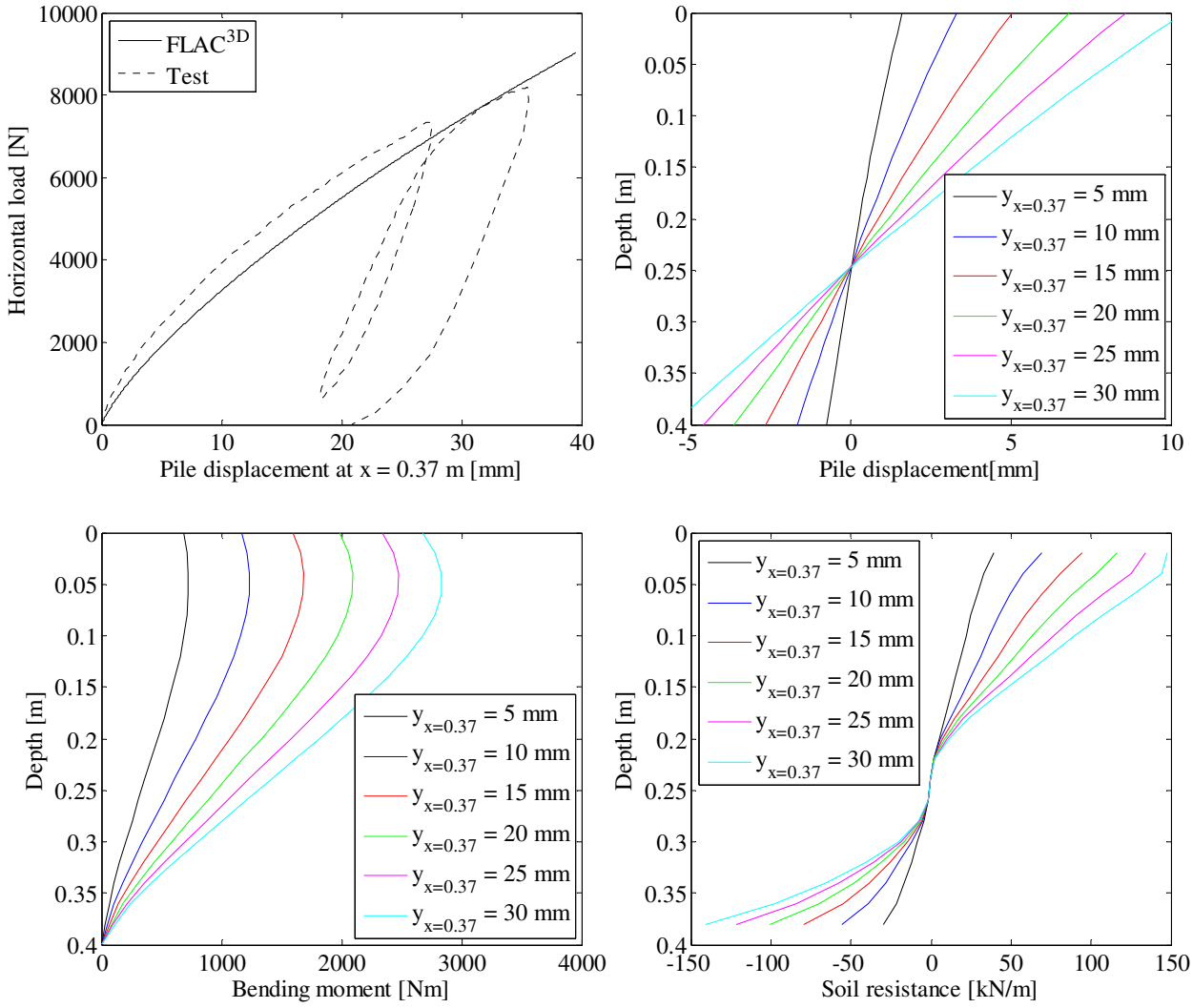

FIGURE 166. TOP LEFT: LOAD-DISPLACEMENT RELATIONSHIPS – TOP RIGHT: PILE DISPLACEMENT VERSUS DEPTH – BOTTOM LEFT: BENDING MOMENT VERSUS DEPTH – BOTTOM RIGHT: SOIL RESISTANCE VERSUS DEPTH.

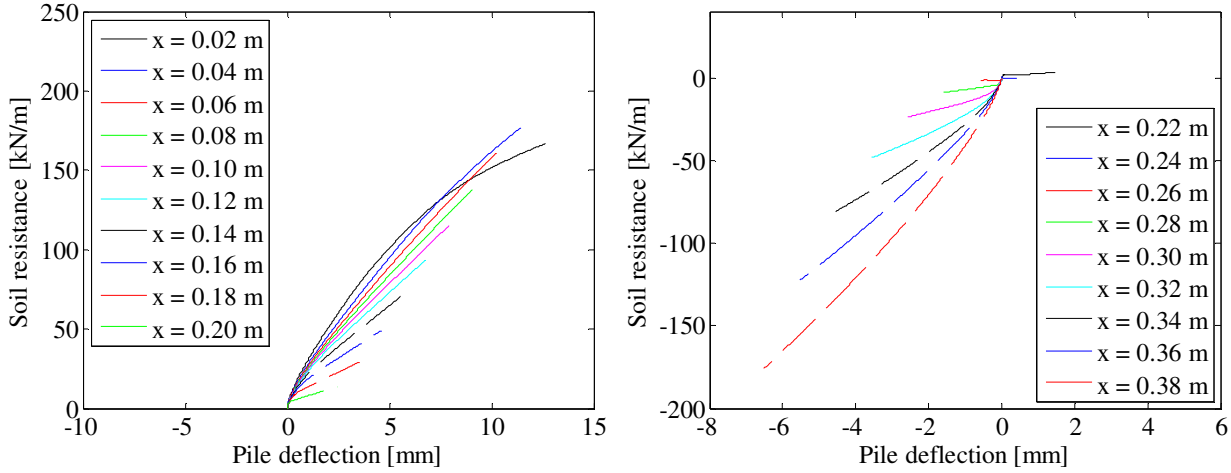

FIGURE 167. P-Y CURVES.

Test 20: D = 80 mm, L_p = 400 mm and P_0 = 100 kPa (Closed-ended)

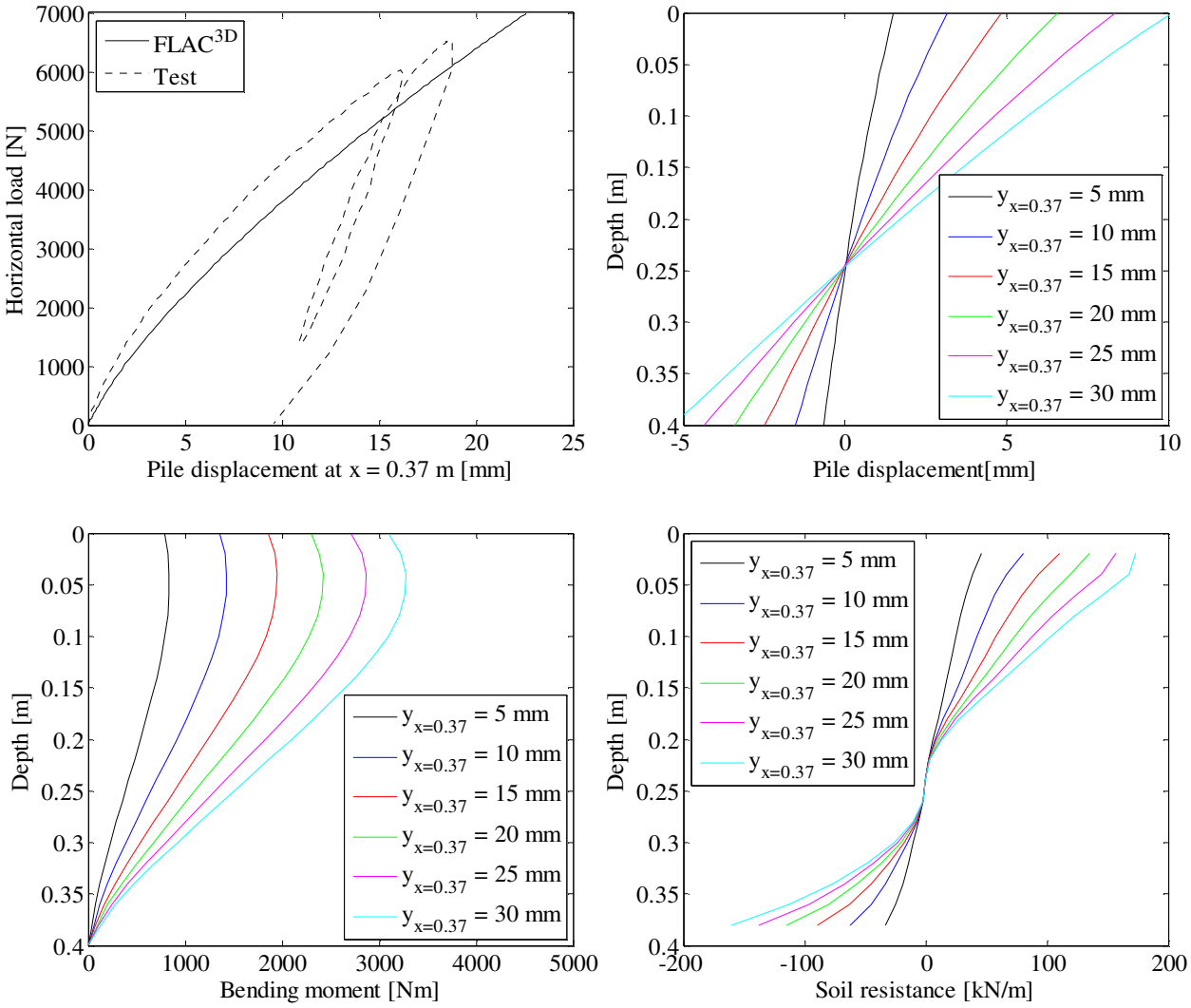

FIGURE 168. TOP LEFT: LOAD-DISPLACEMENT RELATIONSHIPS – TOP RIGHT: PILE DISPLACEMENT VERSUS DEPTH – BOTTOM LEFT: BENDING MOMENT VERSUS DEPTH – BOTTOM RIGHT: SOIL RESISTANCE VERSUS DEPTH.

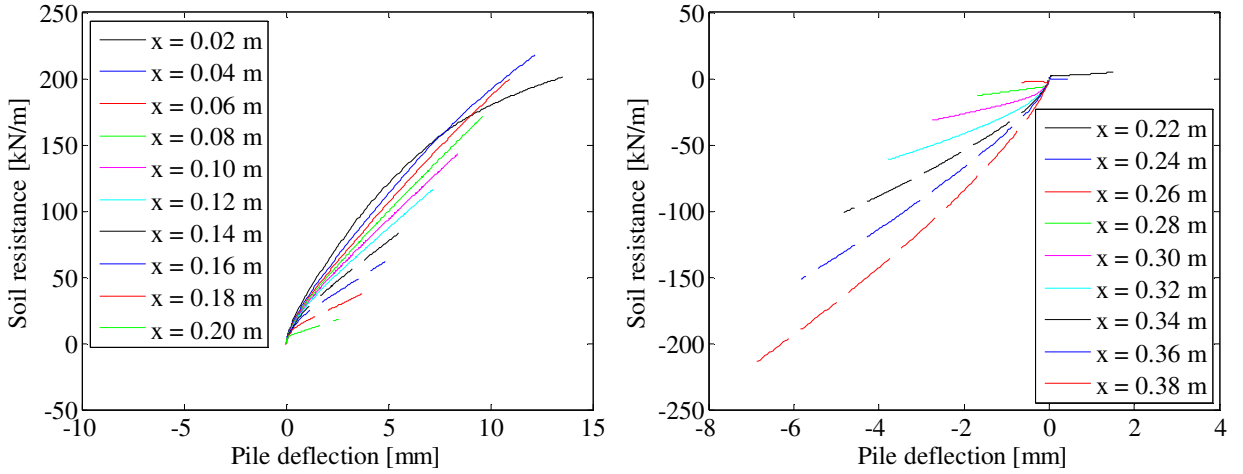

FIGURE 169. P-Y CURVES.

Test 21: D = 80 mm, L_p = 400 mm and P_0 = 100 kPa (Closed-ended)

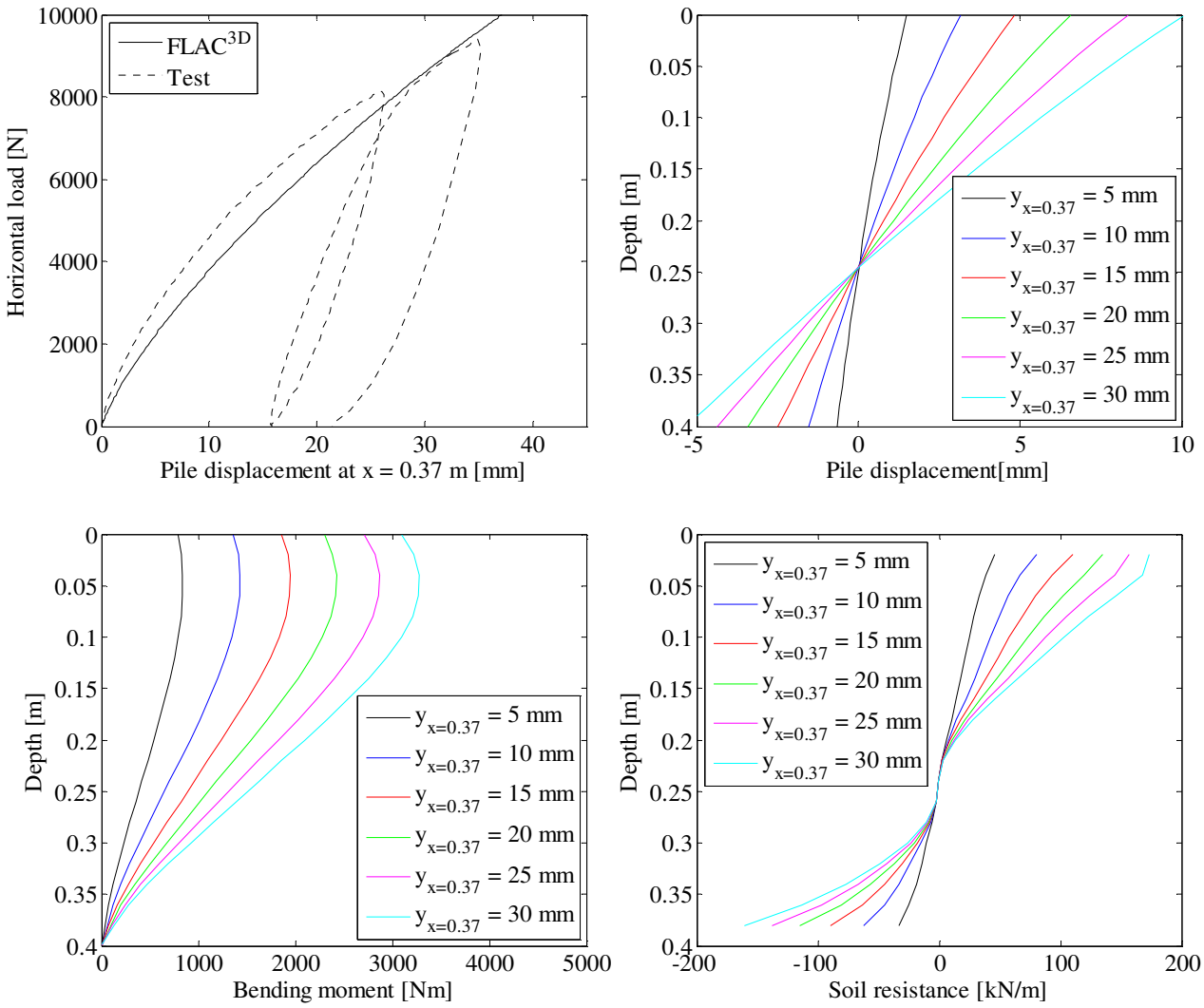

FIGURE 170. TOP LEFT: LOAD-DISPLACEMENT RELATIONSHIPS – TOP RIGHT: PILE DISPLACEMENT VERSUS DEPTH – BOTTOM LEFT: BENDING MOMENT VERSUS DEPTH – BOTTOM RIGHT: SOIL RESISTANCE VERSUS DEPTH.

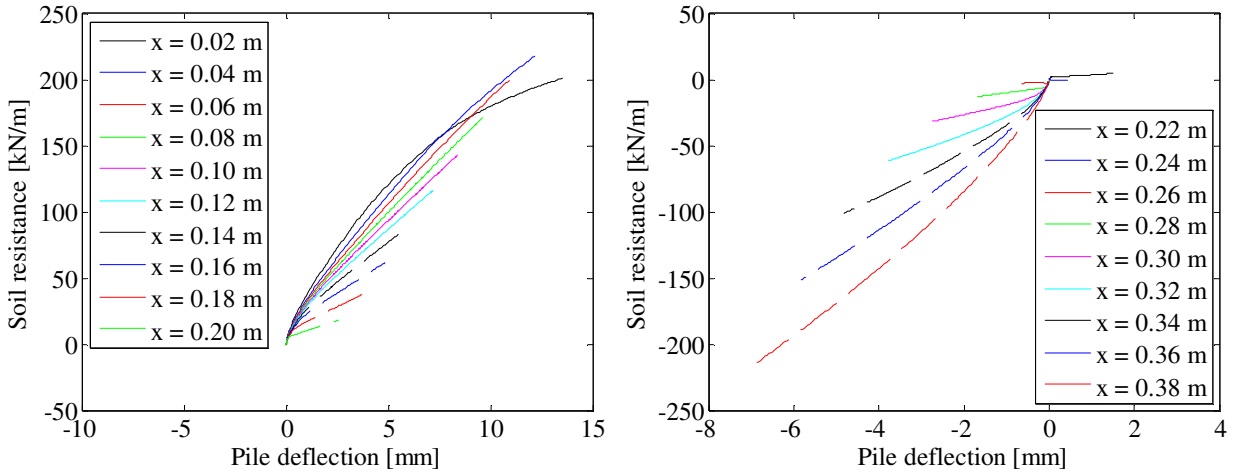

FIGURE 171. P-Y CURVES.

Test 22: D = 80 mm, L_p = 480 mm and P_0 = 0 kPa (Open-ended)

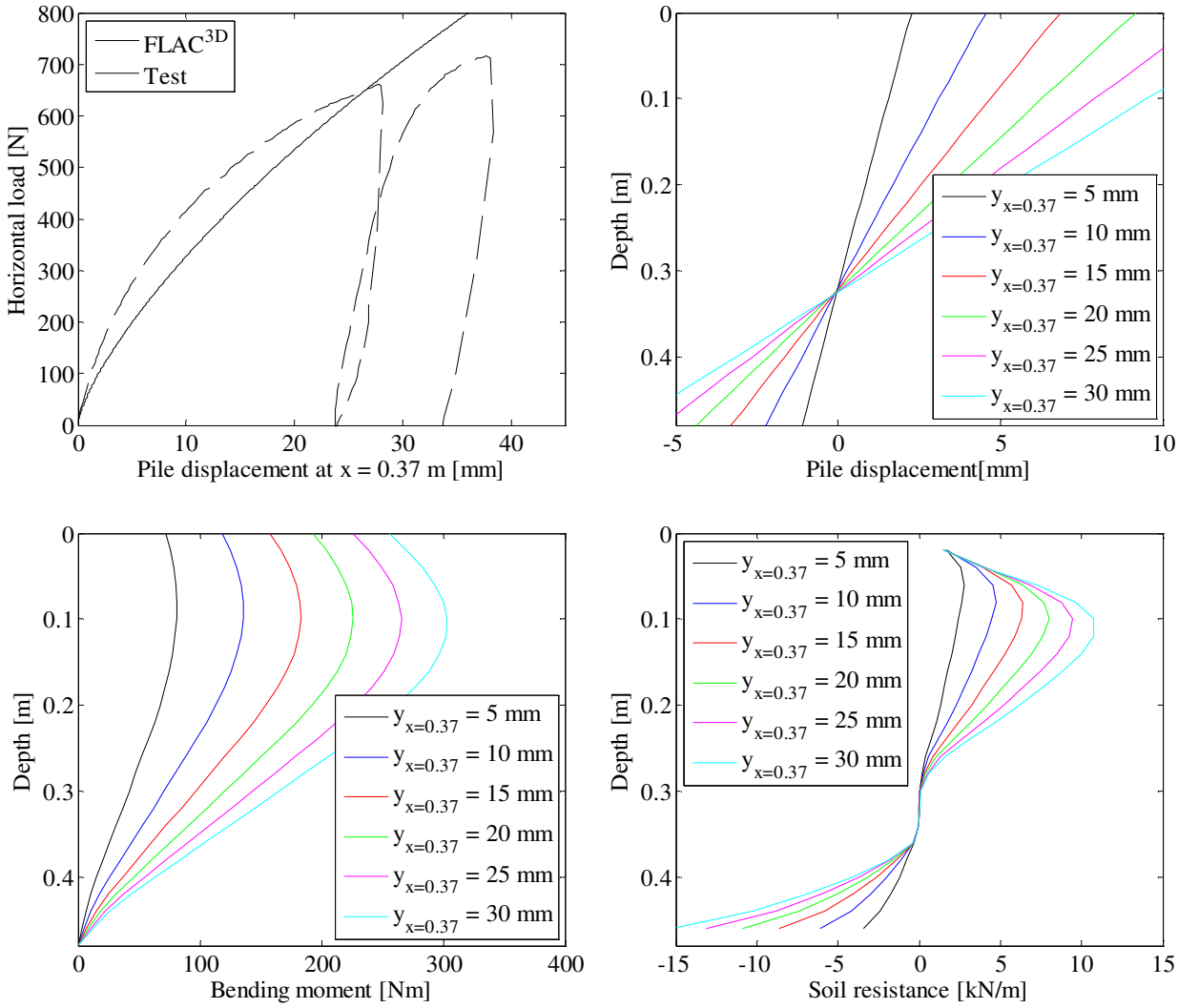

FIGURE 172. TOP LEFT: LOAD-DISPLACEMENT RELATIONSHIPS – TOP RIGHT: PILE DISPLACEMENT VERSUS DEPTH – BOTTOM LEFT: BENDING MOMENT VERSUS DEPTH – BOTTOM RIGHT: SOIL RESISTANCE VERSUS DEPTH.

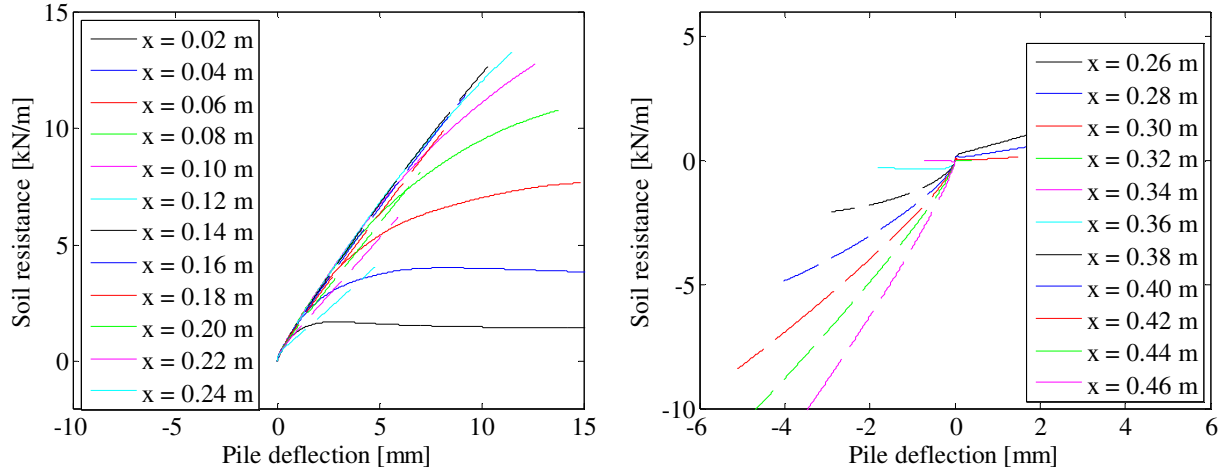

FIGURE 173. P-Y CURVES.

Test 23: D = 80 mm, L_p = 480 mm and P_0 = 0 kPa (Closed-ended)

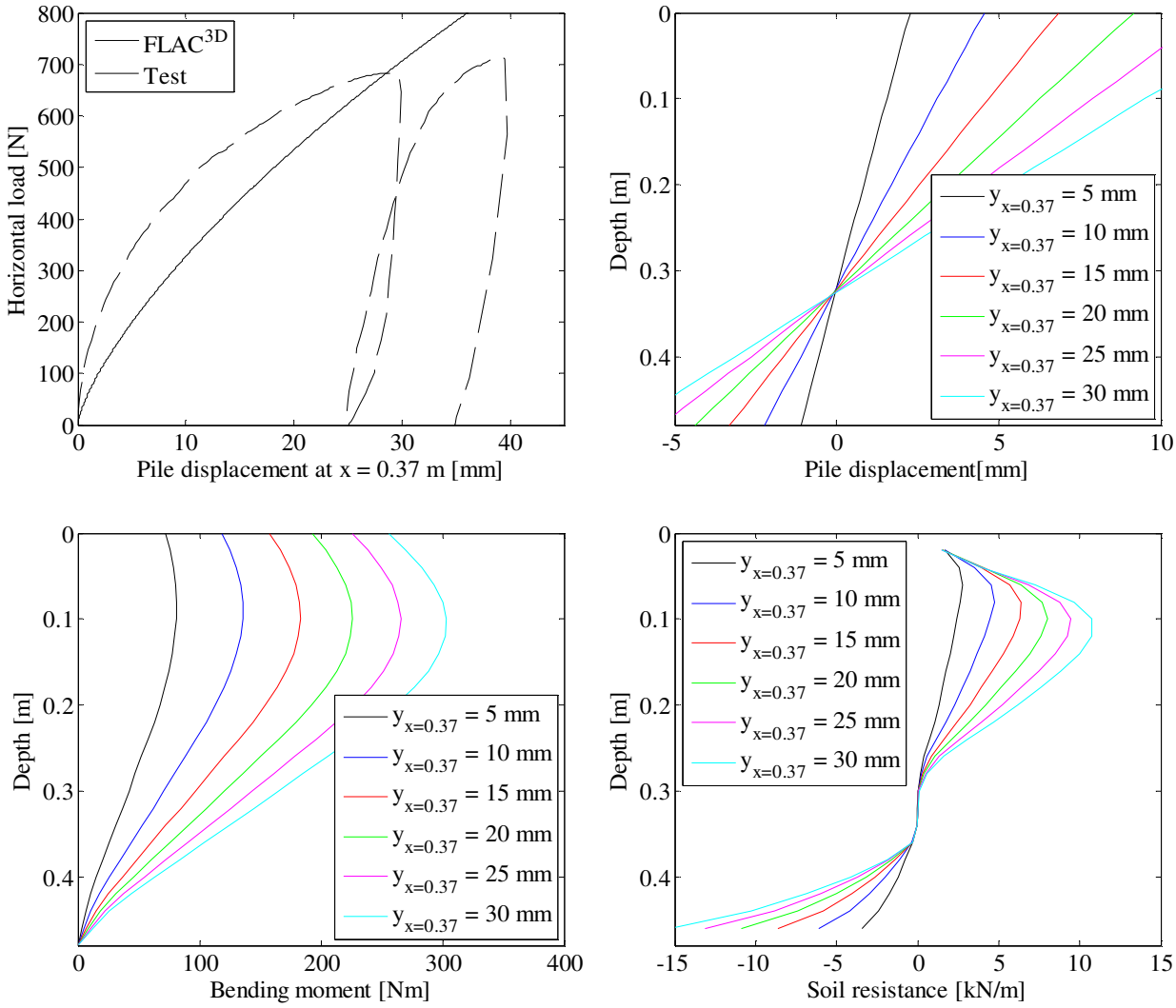

FIGURE 174. TOP LEFT: LOAD-DISPLACEMENT RELATIONSHIPS – TOP RIGHT: PILE DISPLACEMENT VERSUS DEPTH – BOTTOM LEFT: BENDING MOMENT VERSUS DEPTH – BOTTOM RIGHT: SOIL RESISTANCE VERSUS DEPTH.

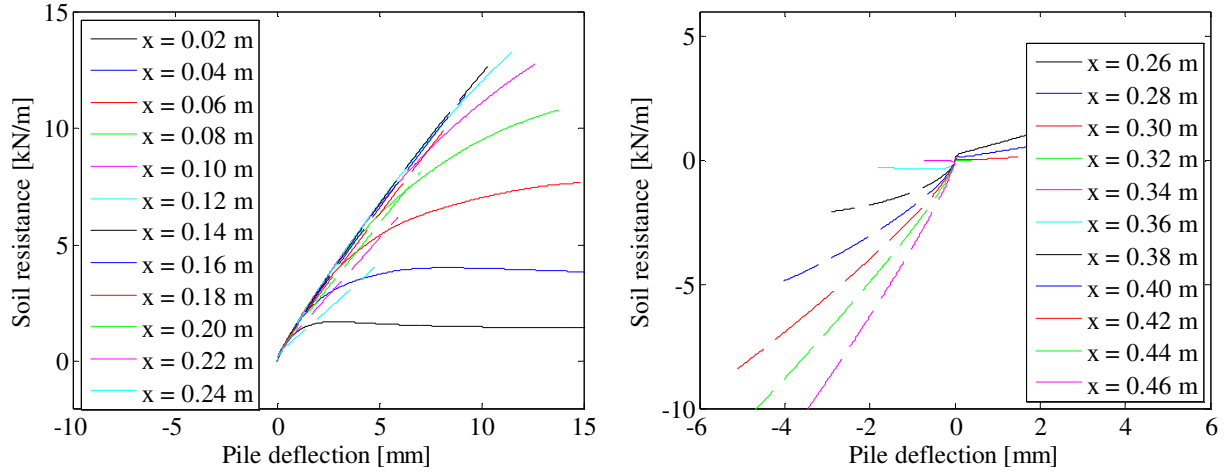

FIGURE 175. P-Y CURVES.

Test 24: D = 80 mm, L_p = 480 mm and P_0 = 50 kPa (Closed-ended)

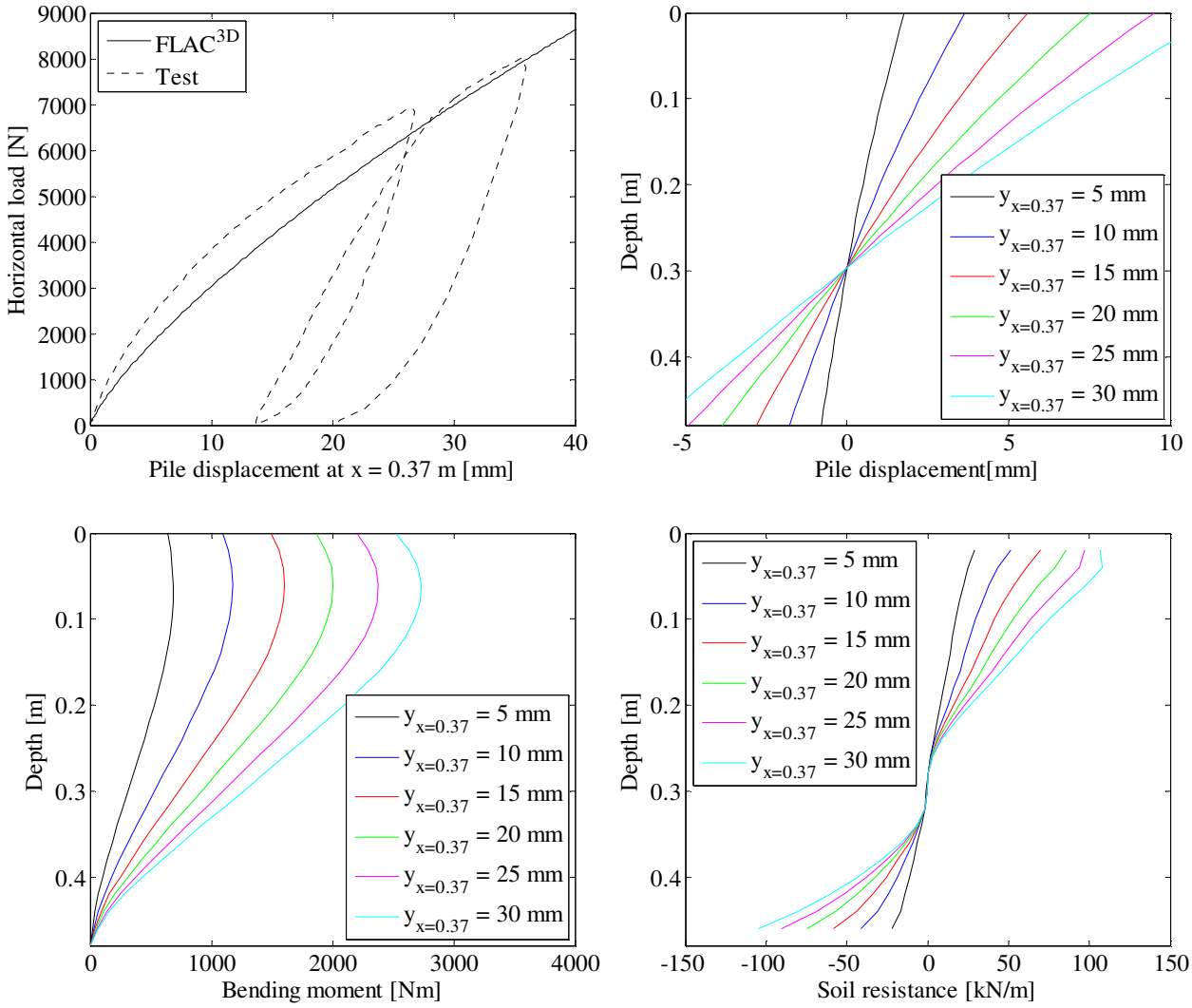

FIGURE 176. TOP LEFT: LOAD-DISPLACEMENT RELATIONSHIPS – TOP RIGHT: PILE DISPLACEMENT VERSUS DEPTH – BOTTOM LEFT: BENDING MOMENT VERSUS DEPTH – BOTTOM RIGHT: SOIL RESISTANCE VERSUS DEPTH.

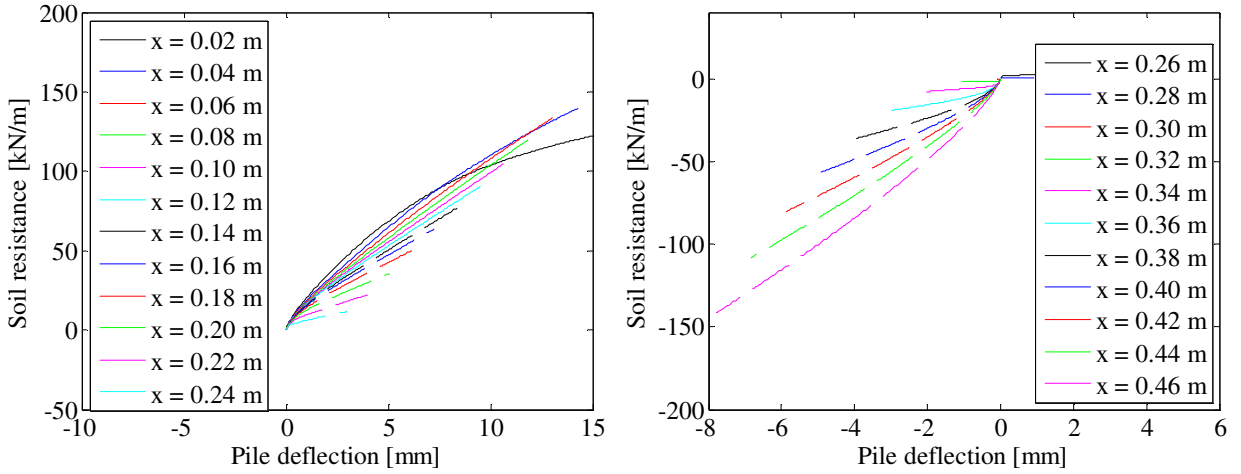

FIGURE 177. P-Y CURVES.

Test 25: D = 80 mm, L_p = 480 mm and P_0 = 100 kPa (Closed-ended)

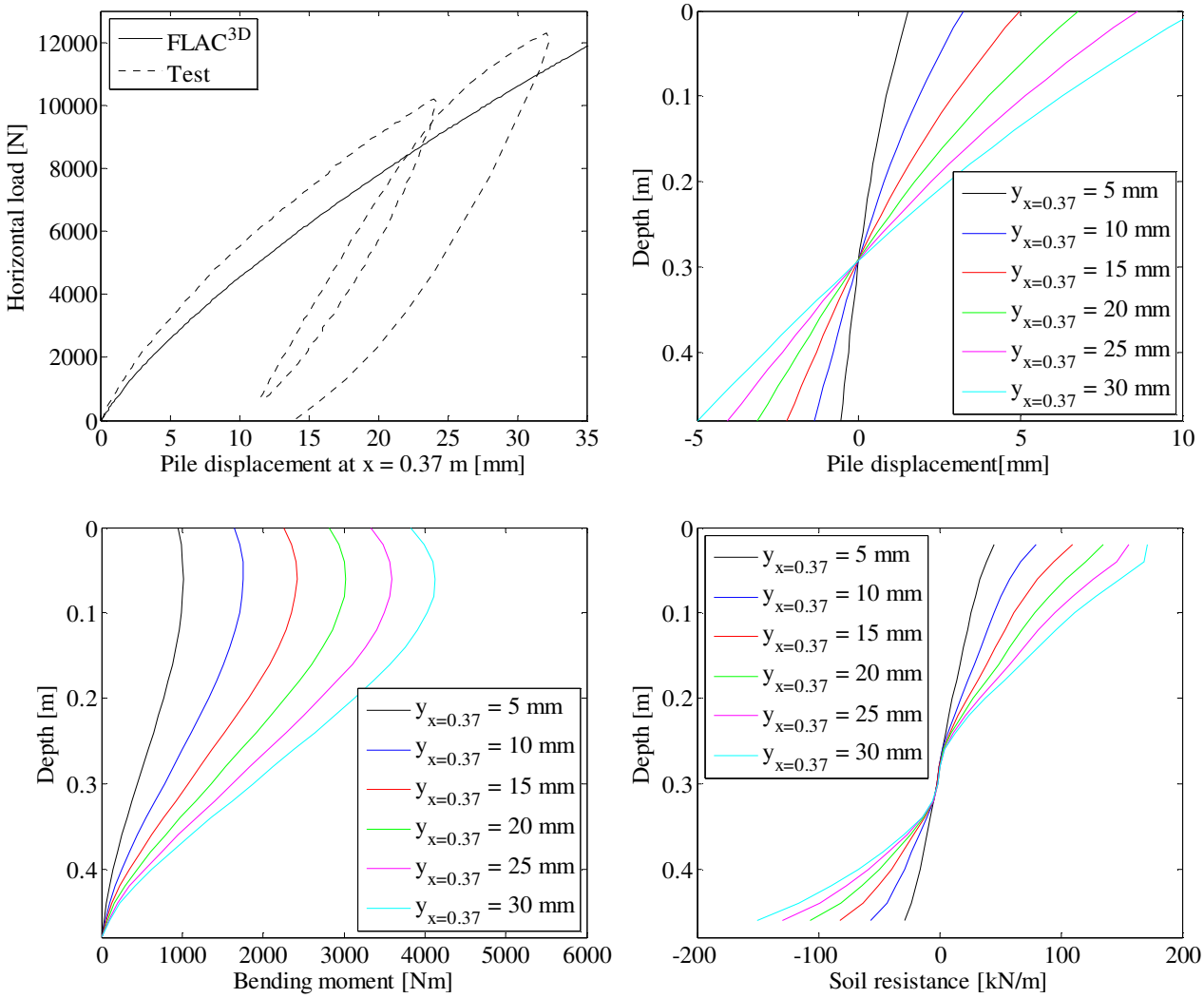

FIGURE 178. TOP LEFT: LOAD-DISPLACEMENT RELATIONSHIPS – TOP RIGHT: PILE DISPLACEMENT VERSUS DEPTH – BOTTOM LEFT: BENDING MOMENT VERSUS DEPTH – BOTTOM RIGHT: SOIL RESISTANCE VERSUS DEPTH.

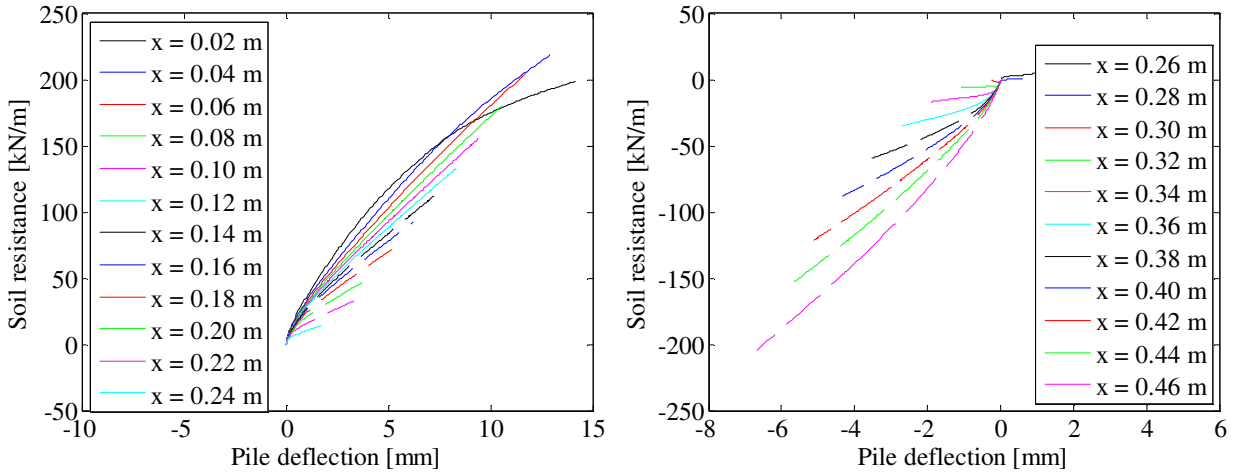

FIGURE 179. P-Y CURVES.

Test 26: D = 100 mm, L_p = 500 mm and P_0 = 0 kPa (Closed-ended)

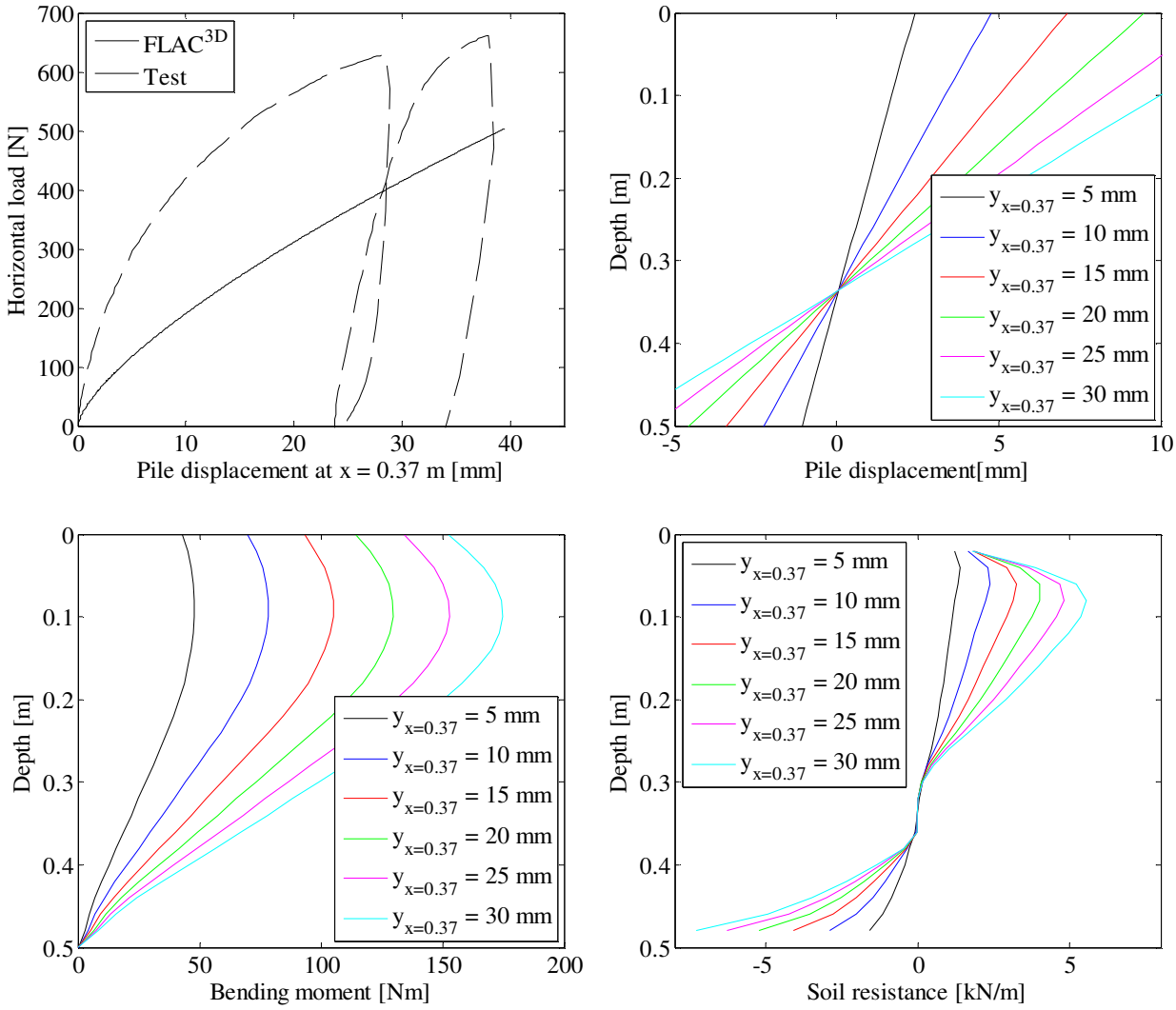

FIGURE 180. TOP LEFT: LOAD-DISPLACEMENT RELATIONSHIPS – TOP RIGHT: PILE DISPLACEMENT VERSUS DEPTH – BOTTOM LEFT: BENDING MOMENT VERSUS DEPTH – BOTTOM RIGHT: SOIL RESISTANCE VERSUS DEPTH.

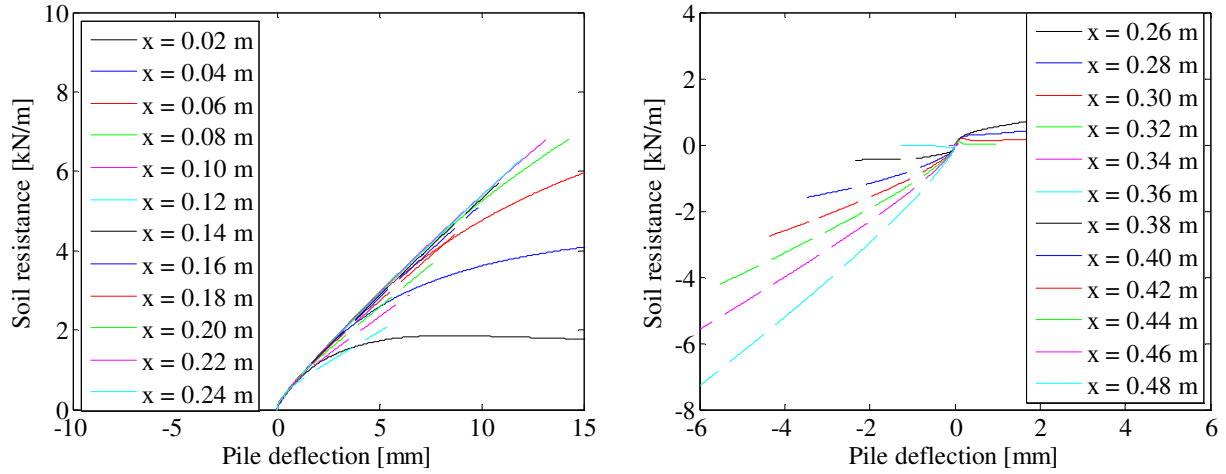

FIGURE 181. P-Y CURVES.

Test 27: D = 100 mm, L_p = 500 mm and P_0 = 50 kPa (Closed-ended)

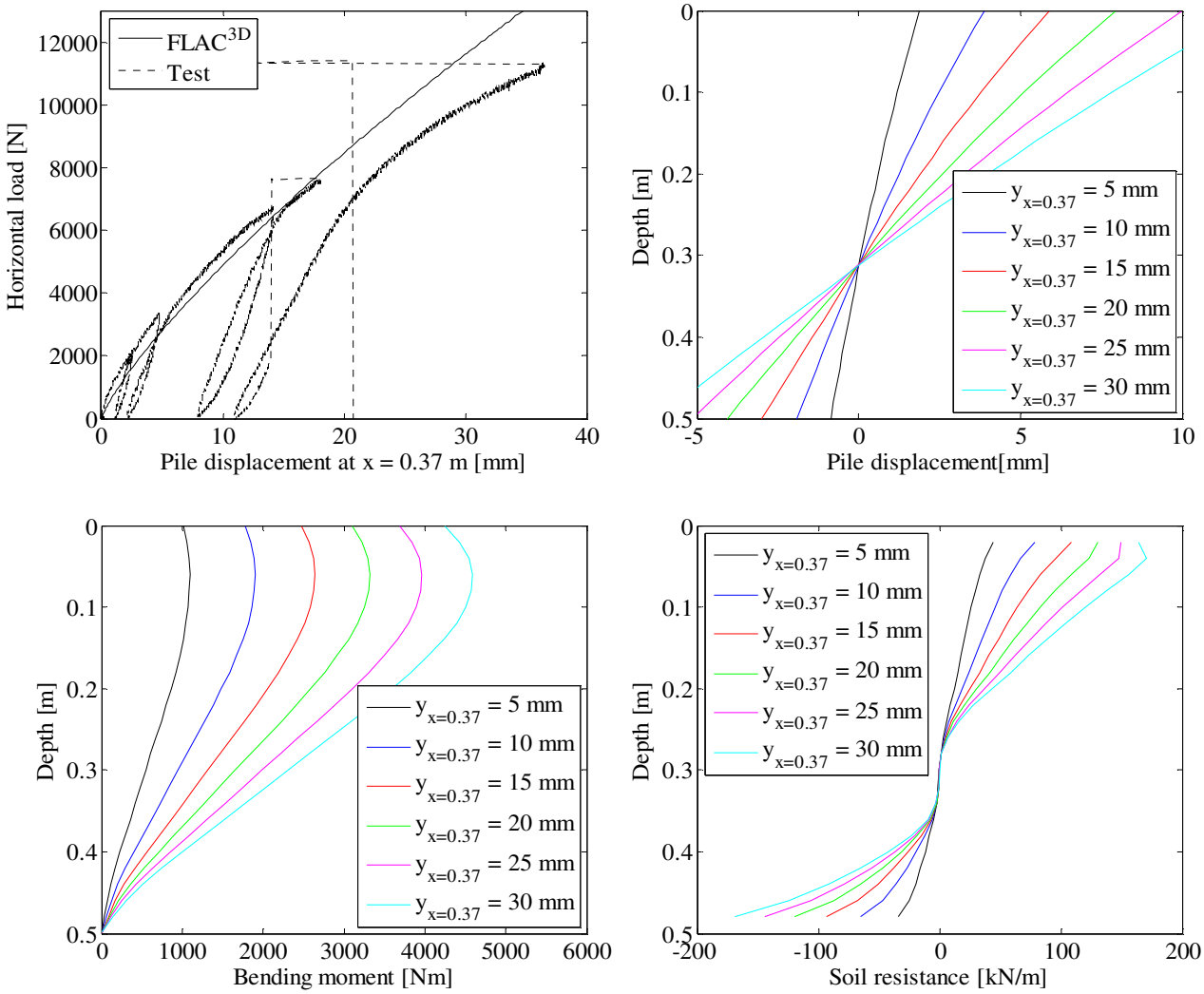

FIGURE 182. TOP LEFT: LOAD-DISPLACEMENT RELATIONSHIPS – TOP RIGHT: PILE DISPLACEMENT VERSUS DEPTH – BOTTOM LEFT: BENDING MOMENT VERSUS DEPTH – BOTTOM RIGHT: SOIL RESISTANCE VERSUS DEPTH.

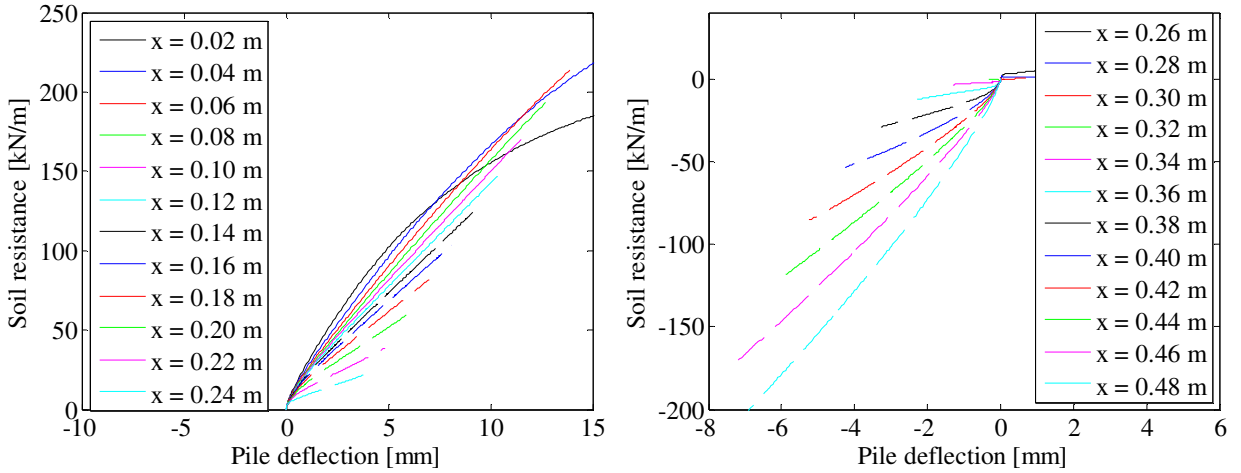

FIGURE 183. P-Y CURVES.

Test 28: D = 100 mm, L_p = 500 mm and P_0 = 50 kPa (Closed-ended)

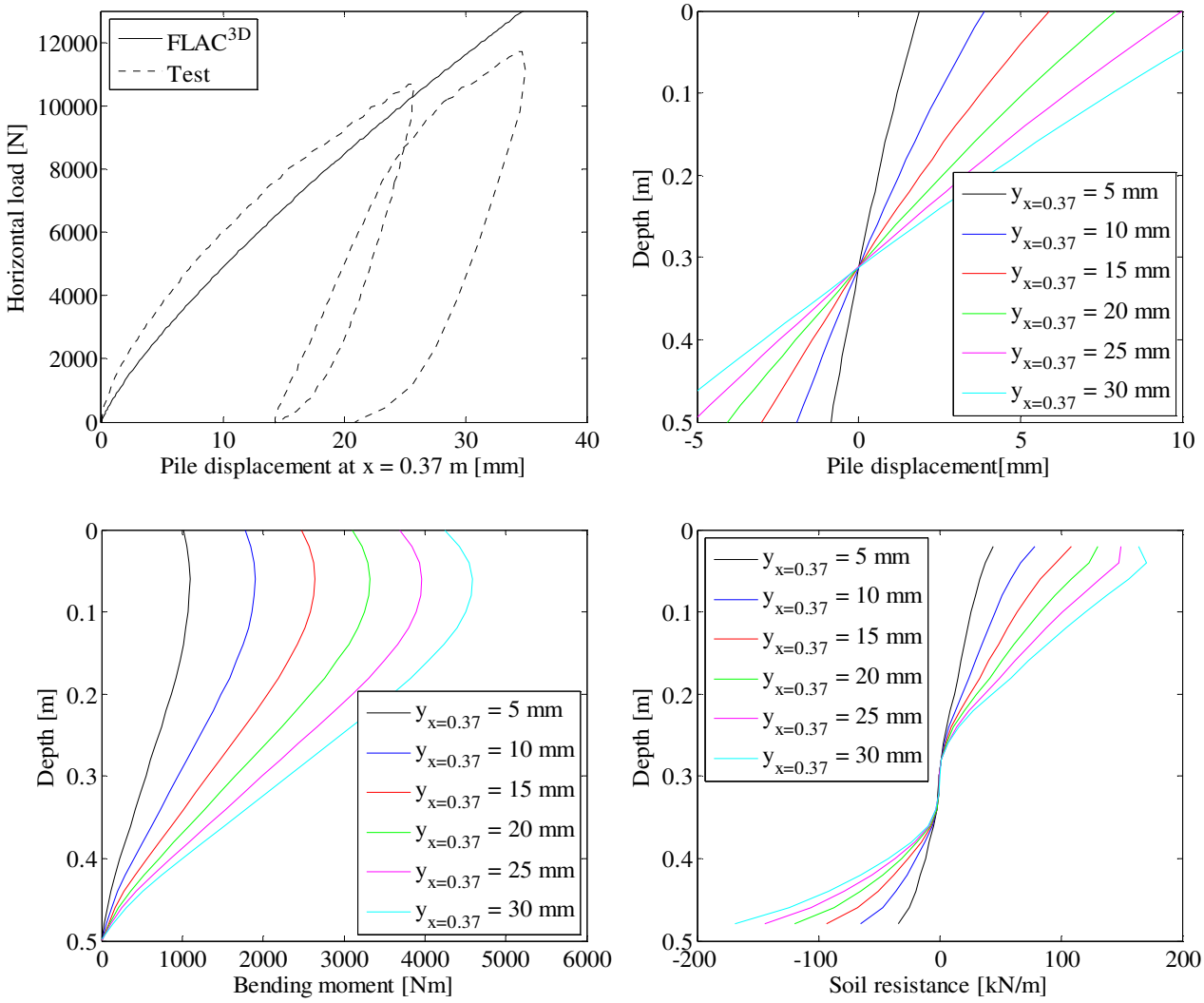

FIGURE 184. TOP LEFT: LOAD-DISPLACEMENT RELATIONSHIPS – TOP RIGHT: PILE DISPLACEMENT VERSUS DEPTH – BOTTOM LEFT: BENDING MOMENT VERSUS DEPTH – BOTTOM RIGHT: SOIL RESISTANCE VERSUS DEPTH.

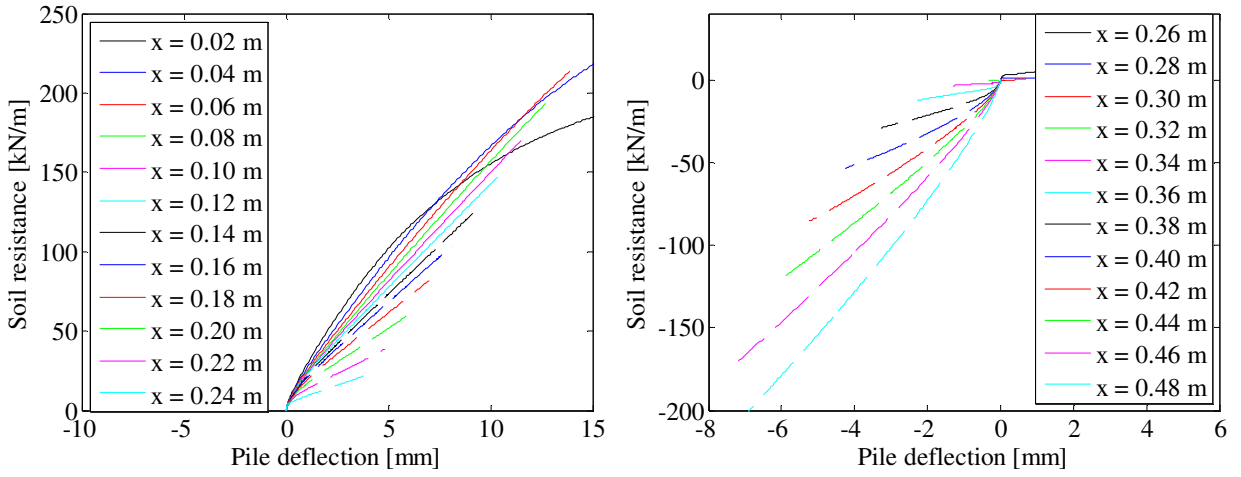

FIGURE 185. P-Y CURVES.

Test 29: D = 100 mm, L_p = 500 mm and P_0 = 100 kPa (Closed-ended)

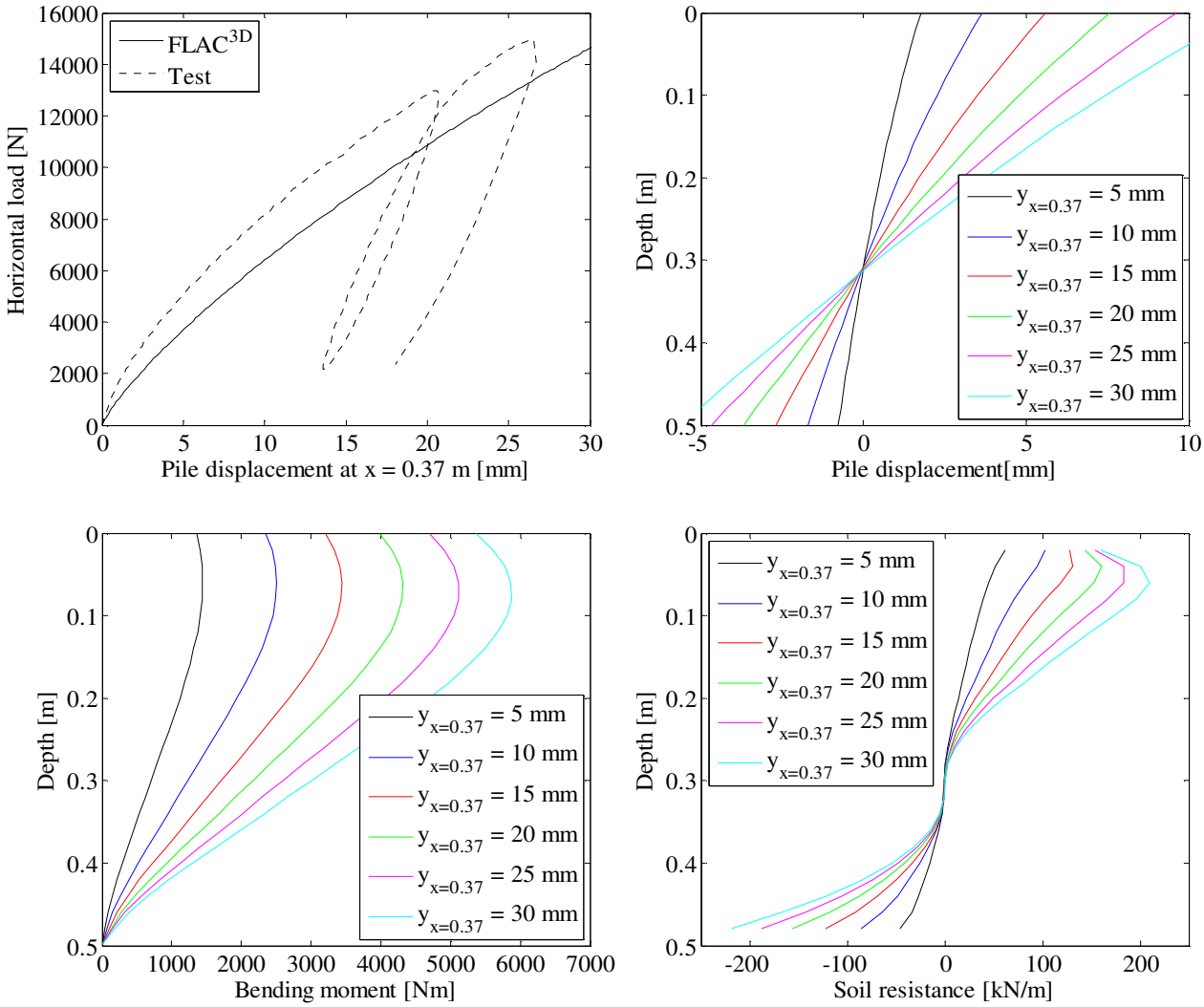

FIGURE 186. TOP LEFT: LOAD-DISPLACEMENT RELATIONSHIPS – TOP RIGHT: PILE DISPLACEMENT VERSUS DEPTH – BOTTOM LEFT: BENDING MOMENT VERSUS DEPTH – BOTTOM RIGHT: SOIL RESISTANCE VERSUS DEPTH.

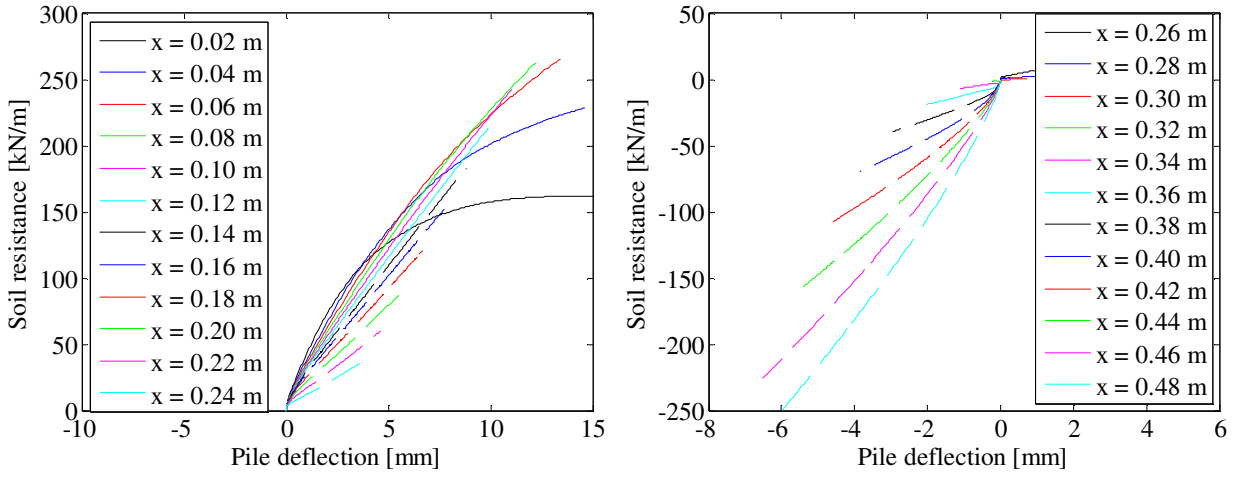

FIGURE 187. P-Y CURVES.

Acknowledgements

The experimental work has only been possible with the financial support from the Energy Research Programme administered by the Danish Energy Authority. The experimental work is associated with the ERP programme “Physical and numerical modelling of monopile for offshore wind turbines”, journal no. 033001/33033-0039. The funding is sincerely acknowledged. Appreciation is extended to Kristian T. Brødbæk, Martin Møller, Hanne R. Roesen, Kristina Thomassen, Alejandro B. Moreno, Linas Mikalauskas and Jose L. T. Diaz for helping with the experimental work. Furthermore, the authors would like to thank the staff at the laboratory at the Department of Civil Engineering, Aalborg University, for their immeasurable help with the test setup and Anders H. Augustesen, COWI A/S, and Christian LeBlanc and Morten Liingaard, DONG Energy A/S, for fruitful discussions.

Recent publications in the DCE Technical Report Series

Brødbæk K. T., Møller M., Sørensen S. P. H. & Augustesen A. H. 2009. Review of p-y relationships in cohesionless soil. *DCE Technical Report No.* 57*, Aalborg University, Denmark*.

Sørensen S. P. H., Møller M., Brødbæk K. T., Augustesen A. H. & Ibsen L. B. 2009. Evaluation of Load-Displacement Relationships for Non-Slender Monopiles in Sand. *DCE Technical Report No.* 79*, Aalborg University, Denmark*.

Sørensen S. P. H., Møller M., Brødbæk K. T., Augustesen A. H. & Ibsen L. B. 2009. Numerical Evaluation of Load-Displacement Relationships for Non-Slender Monopiles in Sand. *DCE Technical Report No.* 80*, Aalborg University, Denmark*.

Thomassen K., Roesen H. R., Ibsen L. B. & Sørensen S. P. H. 2010. Small-Scale Testing of Laterally Loaded Non-Slender Monopiles in Sand. *DCE Technical Report No.* 90*, Aalborg University, Denmark*.

Thomassen K., Roesen H. R., Ibsen L. B. & Sørensen S. P. H. 2010. Evaluation of Small-Scale Laterally Loaded Non-Slender Monopiles in Sand. *DCE Technical Report No.* 91*, Aalborg University, Denmark*.

ISSN 1901-726X
DCE Technical Report No. 112